A study of sulfur distribution, and minor and trace-element geochemistry of a high-volatile bituminous coal seam in northwestern New Mexico.

By

Abraham Araya

Submitted in partial fulfillment of the requirements of the degree of Doctor of Philosophy in Geology

New Mexico Institute of Mining and Technology

Socorro, New Mexico

August, 1993

Acknowledgments

I owe a deep debt of gratitude to the late Dr. Frederick J. Kuellmer of the New Mexico Institute of Mining and Technology (NMIMT). Dr. Kuellmer introduced me to the complex fields of coal and environmental sciences, and provided financial and academic support, and encouragement through the first 3-4 years of this study.

Dr. Allan Gutjahr (NMIMT) provided financial support that was necessary to complete this study. He also provided valuable advice regarding statistical analysis of multivariate data. The New Mexico Geological Society, and the R.A Matuszeski Graduate Research Fellowship (NMIMT) provided partial financial support. Lynn Brandvold, Jeanne Verploegh, and Barbara Popp of the New Mexico Bureau of Mines and Mineral Resources (NMBM&MR) contributed their time and expertise during the proximate and sulfur analyses. The NMBM&MR allowed me the use of the coal, x-ray, and rock preparation labs. Chris McKee (NMBM&MR) provided his time and expertise during XRD and XRF analyses. Gretchen Hoffman (NMBM&MR) critically reviewed this manuscript and provided much needed information regarding the coal geology of the study area.

I would also like to thank my advisor Dr. Peter Mozley, and my dissertation committee members Drs. Andrew Campbell, Philip Kyle, Fred Phillips, and Carl Popp of NMIMT, and Donald Hickmott of the Los Alamos National Laboratory for rendering their assistance at various stages of this study. Dr. Donald Wolberg (NMBM&MR) provided space for sample storage and offered his assistance during the course of this study. Dr. William Chavez (NMIMT) provided help during reflected microscopic analysis of polished samples. Dr. Michael Spilde (Univ. of New Mexico) did the electron microprobe

analysis. Dr. Robert Finkelman of the USGS provided some valuable advice and encouragement.

My thanks to the Santa Fe Pacific Coal Corporation for providing the personnel and equipment during sample collection at the Lee Ranch Mine. Brian Easterday, Quality Specialist at the mine, provided much needed help during the core drilling operation.

I also like to thank all my friends and fellow students who helped me during this study and provided their support and encouragement: Amare, Meseret, and Genet Abebe., Araya G.M., Jonathan, and Daniel W.M., Meseret S., Charles Mandevile IV., Zemen A., Terry P., Grazyna Z., Tesfaye (Sunny) T., Aman, Konjit, Muler, Meazah T., and Isaac S.

My special thanks is reserved for my family: my parents Araya Gebray and Zertihun Eyoab; my sisters Almaz, Asmeret, and the late Aster Araya; my nephews Yonas, and Ermias, and my niece Tsion. Thank you for all the love, support, and encouragement you have given me through the years.

Abstract

Major shifts in sulfur contents in the generally low-sulfur coals of the Menefee Formation (Cleary Coal Member) in the San Juan Basin of New Mexico were observed. Sulfur distribution within the coal seam studied varies both horizontally and vertically. Pyritic and organic sulfur are the dominant forms of sulfur (average = 0.39 and 0.49%, respectively) with sulfate sulfur occurring in negligible amounts (average = 0.07%). Relationships between the forms of sulfur suggest that variations in total sulfur in the coal samples are mainly due to variations in the amount of pyritic sulfur and, to a lesser extent, of organic sulfur. Three sulfur distribution patterns were recognized in the BB seam: (1) higher sulfur contents in coal samples adjacent to the seam margins and partings, and at certain stratigraphic levels, (2) higher sulfur contents toward the middle of the seam, and (3) distribution where the sulfur content in the coals varies slightly within the seam, but the maximum total sulfur content does not exceed 1% . Sulfur emplacement in the BB seam most likely occurred during two periods: a) during early stages of peat deposition mainly as organic sulfur (in the low-sulfur coal samples) and pyritic sulfur (in the high-sulfur coals in the second distribution pattern); and b) during and/or after cleat formation, mainly as pyritic sulfur near seam margins.

Trace-element ratios, and pyrite and siderite compositions were used to constrain the factors that may have caused the observed sulfur distributions. As/Se ratios in whole-coal samples from high- and low-sulfur coals show significant differences, with an average of 8.38 for high-sulfur samples and 0.63 for low-sulfur coal samples. The high As/Se ratios in the BB seam compare with values of around 10 observed in samples with marine and brackish overburden and may indicate marine or brackish water influence in the BB seam. In

contrast, siderite compositions in samples associated with both low- and high-sulfur coals suggest a predominantly fresh-water depositional setting with possible brackish-water influence.

Twenty-four elements were determined in whole coal, and associated non-coal samples. Some elements show large ranges in concentration (i.e., Ba, Fe, Co, Zn, As, Th, U, Sb, Cs, and Rb). Many of these elements may occur in sulfide, sulfate, carbonate, and phosphate minerals that may be concentrated in particular stratigraphic intervals. Other elements show relatively narrow ranges in concentration (i.e., Cr, Sc, La, Ce, Hf, Na, Se, Sr, Sm, Yb, Lu, Ta, and Tb). These elements may be associated with clay minerals and rare-earth element bearing minerals that are evenly distributed in the coal seam.

Comparison with average crustal concentrations (ACC) shows that Sb and Se are significantly enriched in the BB seam coals and associated clastic rocks suggesting high Se and Sb input into the swamp and that Se (and perhaps Sb) concentrated in the original plants was retained within the coal in sulfides and clay minerals. Enrichment factors scaled for equal La show that As, Ba, Sb, Se, and Sr are significantly enriched in the coals relative to associated claystones. These elements may be associated with diagenetic minerals such as iron sulfides and carbonates that formed in the peat. Cesium and Rb are depleted in the coals. The rest of the elements show enrichment factors close to one, but in general < 2, indicating a significant contribution from the detrital component in the coal.

The vertical distribution of trace elements in the BB seam generally exhibits a "C" shaped profile with high trace-element content in and near bounding lithologies and partings. In general, all elements except Se show higher concentrations in the non-coal lithologies. Higher trace-element

concentrations in the coals are in general associated with high-ash samples, and the presence of mineral phases such as pyrite and barite.

Comparison of trace-element contents of bright and dull coals shows that the dull coals contain more As, Cr, Fe, Se, and Sr than bright coals. Most of these elements may occur in association with sulfides, indicating that conditions that formed the dull coals favored sulfide precipitation.

Based on statistical analyses, calculation of theoretical partial concentrations, vertical distribution patterns, mineralogical composition (XRD) and direct evidence (electron microprobe and PIXE), the likely modes of occurrence of trace elements in the BB seam coals are: (1) in sulfides (As, Fe, Sb, Se, Sr, and Zn); (2) siderite and calcite (Fe, Sr); (3) in barite and celsian (Ba); (4) in feldspars and clay minerals (As, Ba, Cr, Cs, Fe, Hf, Na, Rb, Sb, Sc, Se, Sr, Th, U, Zn and the REEs; (5) in zircon, rutile, phosphates and other accessory minerals (Hf, Sc, Ta, Th, U, and the REEs; and (6) organically bound (Co).

Chondrite normalized REE patterns in the BB seam coals and associated lithologies are similar to NASC patterns, suggesting derivation of the REEs from sources with upper continental crust compositions. The majority of the elements in the BB seam exhibit strong correlations with ash and the REEs indicating that the original source for the bulk of these elements was detrital material. Comparison of trace-element concentrations of BB seam coals and associated claystones also supports a predominantly detrital origin for many of the trace elements.

Table of contents

List of Tables

List of tables in appendix

List of Figures

List of figures in appendix

1 - Introduction

1.1 General statements on coal

Coal is one of the basic sources of energy and an essential raw material for most metallurgical processing. Energy derived from coal comprises the largest of the world's available supplies of conventional energy, with over 60% of the total proven recoverable reserves and around 80% of the estimated additional resources (Ward, 1984).

The term "Coal" has been defined by many people in various ways each with its own problems. Schopf (1956), reviewed many of these definitions and came up with a definition that clearly differentiates coal from other rocks or rock material and states the essential attributes of coal. Schopf's definition is: " coal is a readily combustible rock containing more than 50% by weight and more than 70% by volume of carbonaceous material, formed from compaction or induration of variously altered plant remains similar to those of peaty deposits. Differences in the kind of plant (Type), in degree of metamorphism (Rank), and range of impurity (Grade), are characteristics of the varieties of coal." Depending on the purpose of the particular study, coal may be considered from different points of view. For example, it may be considered as an organic material with certain chemical and physical characteristics the combination of which determine the ways in which it is best able to be used. From the petrologic point of view, it may be viewed as a mildly metamorphosed sedimentary rock, with properties depending on both the nature of the original parent material and the degree of diagenesis or metamorphism to which it has been subjected. In this study the chemical, physical, and petrologic aspects of coal will be considered.

Coal seams usually originate from the diagenesis and coalification of peat deposited in swamps. The evolutionary development of the flora, the climate, and the geographical and structural position of the region are crucial factors in the formation of a peat swamp. Stach et al., (1982) discuss the effects of these factors in detail.

Coal is a heterogeneous substance that consists of various constituents of which macerals are the major components. Macerals are organic substances, or optically homogeneous aggregates of organic substances with distinct set of physical and chemical properties (Crelling and Dutcher, 1980). Macerals are to coal what minerals are to rocks. However, whereas minerals are characterized by a fairly well-defined chemical composition, by the uniformity of their substances, and by their crystallinity, coal macerals vary widely in their chemical composition and physical properties and are not crystalline. In addition to macerals, coal contains mineral matter. Elements other than organically derived and bound C, H, N, O, and S constitute mineral matter in coal. Mineral matter may consist of discrete minerals such as calcite, quartz, clays minerals, and pyrite, and /or organic compounds that contain organically bonded elements such as calcium and chlorine. Mineral matter and sulfur in coal are major contaminants that degrade its utility as a fuel (Stach et al., 1982; Cecil et al., 1982).

1.2 Purpose of study

Sulfur content is one of the chief factors governing the utilization of coal in either combustion or coke production. During coal combustion, sulfur is oxidized to SO_2 of which 0 to 7% (usually < 3%) is further oxidized to SO_3. The balance of the sulfur remains in the coal ash and slag (Tsai, 1982). This contributes to the formation of fire side boiler deposits that reduce boiler efficiency, creates

corrosion problems, and concentrates SO_2 in the flue gas vented to the air (Tsai, 1982; Walker and Hartner, 1966). The generation of acid water from pyrite (FeS_2) in waste piles and acid rain by atmospheric oxidation of SO_2 also creates problems in the utilization of coal.

The sulfur content of US coals ranges from less than 0.1% to over 10%, on a dry weight basis, with a typical total sulfur content in the range 0.5 to 5%. Western coals in general exhibit much lower sulfur content than mid-western or eastern coals. Many New Mexico coals, for example, average about 0.7% total sulfur, whereas coals of the Illinois Basin commonly lie in the range of 3 to 4% (Harvey et al, 1983).

Knowledge of the form in which sulfur occurs in coal is very important to the development of geochemical models explaining sulfur incorporation and enrichment in coal, and designing and development of improved sulfur removal methods. The sulfur in coal occurs in the following forms: (1) elemental sulfur which occurs in trace quantities and very infrequently (Smith and Batts, 1974); (2) metallic sulfates usually present as gypsum and occasionally as barite (Casagrande, 1987); (3) organic sulfur: perceived to occur in covalently bonded C-S compounds like thiophenes, thioethers, and bisthioethers (disulfides) and probably a coal-polysulfide complex (Narayan and Kullerud, 1988), and (4) Metallic sulfides: mostly as pyrite and/or marcasite and other sulfides (Casagrande, 1987).

Sulfur held in organic combinations generally cannot be separated from the coal substance by conventional cleaning and requires more expensive chemical treatment (Tsai, 1982). Sulfate and elemental sulfur are generally present in low concentrations and are usually of no great concern. Pyritic sulfur, a term generally applied to all forms of iron sulfide in coal, is easy to remove from coal by physical techniques involving a heavy media separation. Sulfur in coal is

not uniformly distributed and considerable variation can be seen within a province and in some cases even within a coal seam (Neavel, 1966; Casagrande, 1987). Many researchers have noted that coals from peats that were influenced by marine fluids during or following deposition exhibit significant enrichment in sulfur (Casagrande et al., 1977; Stach et al., 1982). Cecil et al., (1982) list the availability of dissolved calcium and carbonate ions that controlled pH in the ancestral peat environment, ionic strength of interstitial waters including the availability of iron and sulfate ions, and plant paleoecology as major factors to be considered in understanding the variations of ash and sulfur in coal currently being mined. Roof lithologies have been related to sulfur content in coal (Williams and Keith, 1963; Gluskoter and Simon, 1968) where marine derived shales are associated with coals having high sulfur content.

Most work done on the distribution of sulfur in coal is in high-sulfur coal provinces and little work has been done in low-sulfur western coals, especially New Mexico coals, which generally formed in fresh-water dominated depositional systems (Tabet et al., 1985; Beaumont, 1987).

With increase in coal consumption and use, the study of minor and trace elements in coal has also received attention. Among such studies are works by Gluskoter et al (1977), Finkelman (1980), Palmer (1983), Rimmer and Davis (1986), Goodarzi (1987,1988), Goodarzi and Van der Flier-Keller (1991), and Finkelman and Brown (1991). Kendrick (1985) and Baker (1989) examined trace- element distributions in selected New Mexico coals.

Knowledge of the nature and distribution of major, minor, and trace elements in coal and the degree of concentration of certain environmentally hazardous elements such as arsenic, cadmium, chromium, lead, sulfur, and selenium or industrially harmful elements such as sodium and sulfur is important in coal utilization. The production of an environmentally clean coal is dictated by

strict environmental standards set by coal users and governments (Goodarzi and Van der Flier-Keller, 1991). The mode of occurrence of trace elements in coal may influence their behavior during the cleaning , conversion, or combustion of coal, and during the weathering or leaching of the coal or its byproducts. In addition to environmental and industrial considerations, the modes of occurrence of trace elements in coal may provide information on the depositional environment of the coal, the conditions during diagenesis, the source of the trace elements and minerals in coal, and epigenetic processes (Palmer, 1983). Trace element concentrations and distribution patterns in coal may also be used as geochemical indicators for nearby mineralization (Finkelman and Brown, 1991) and as stratigraphic correlation tools (Bouska, 1981).

The principal objectives of this study are: (A) to investigate the distribution patterns and speciation of sulfur in a low-sulfur coal seam and evaluate the geological and geochemical factors that might control the observed distributions. In a few localities in the study area, seams of predominantly low-sulfur coal contain isolated occurrences of relatively high sulfur concentrations. Examination of these occurrences of high-sulfur zones in low-sulfur coal seams may help in the understanding of the mechanism(s) of sulfur incorporation and enrichment in low-sulfur coals; and (B) to document and investigate the distribution and modes of occurrence of minor and trace elements in the coals. The study of the distribution and modes of occurrence of the elements can help to understand the behavior of certain elements during beneficiation processes and utilization. It can also give clues to the original source of the trace elements in coal and to depositional and digenetic conditions that existed in the coal-forming system.

2- Location, geologic setting, and sampling

2.1 Location

The Lee Ranch Mine (Fig. 1) is located in the southeastern part of the San Juan Basin, in southeastern McKinley County, New Mexico, approximately 30 miles northeast of Grants . The following factors were considered in selecting the Lee Ranch Mine: (1) Low sulfur content of the coals (Kuellmer et al., 1987); (2) Presence of isolated occurrences of high-sulfur zones in this low-sulfur coal seam (Kuellmer, 1988, personal communication); (3) Availability of previous studies on the distribution of various minor and trace elements in the study area (Kuellmer et al., 1987; Baker,1989); and (4) Access to the mine.

2.2 Geologic setting

The Lee Ranch Mine area is located in a structural subdivision of the southern part of the San Juan Basin defined by Kelly (1950) as the Chaco Slope. The San Juan Basin is a late Cretaceous to early Tertiary structural depression located at the eastern margin of the Colorado plateau. The basin is strongly asymmetrical, with an axis trending northwest-southeast. The San Juan Basin contains sedimentary rocks ranging in age from Cambrian to Quaternary, with a maximum known thickness in excess of 4300 meters. Upper Cretaceous rocks are 1800 meters or more in thickness, and were deposited in environments ranging from fluvial to shallow marine (Fasset and Hinds, 1971).

Mesozoic sediments of the Western Interior apparently were deposited differentially and sporadically through time from the Middle Triassic to the Late Cretaceous in a north-south elongate geosynclinal trough which spanned the entire Western Interior of the continent. Sediment source areas lay west of the through in the Cordilleran orogenic belt, which formed along the tectonically active western edge of the North American plate (Green et al., 1991). During the

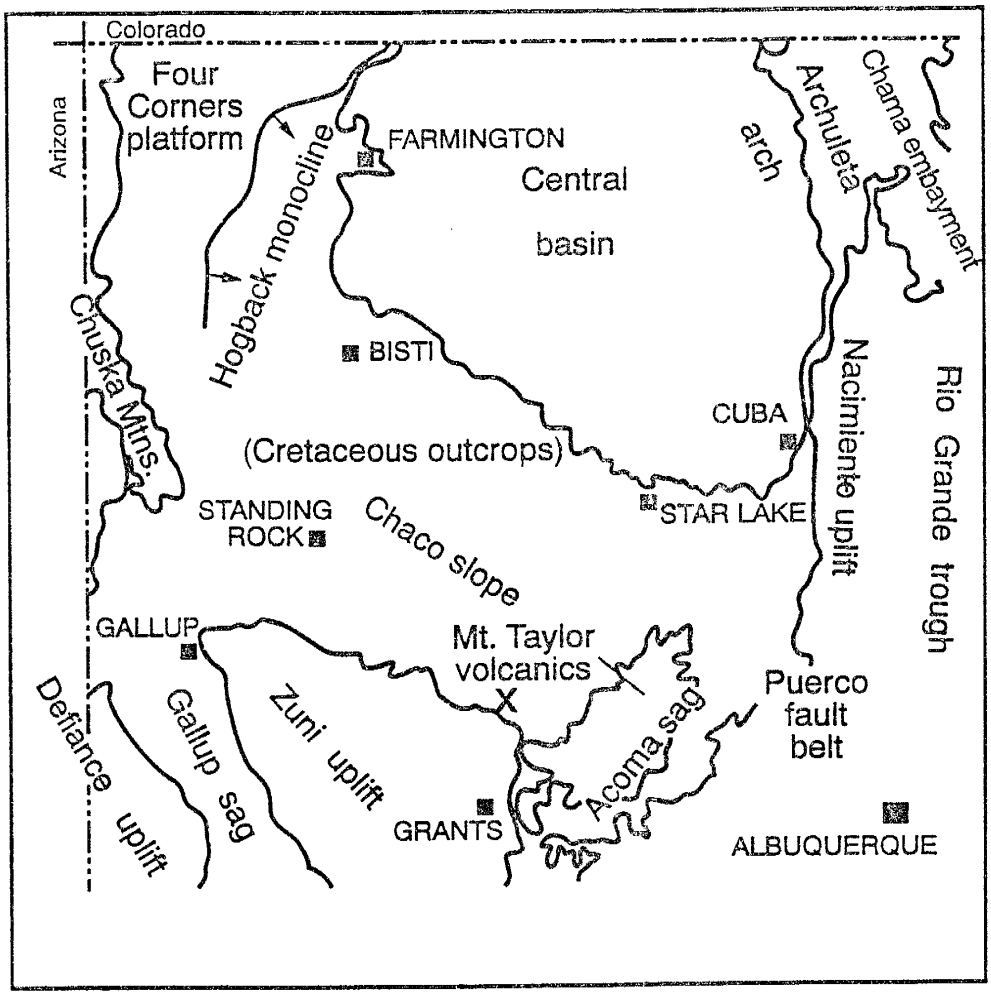

Figure 1. Tectonic map of the San Juan Basin, New Mexico (from Beaumont, 1982). X marks the approximate location of the Lee Ranch Mine.

Table 8. Summary of statistical analysis on total sulfur (%).

Group	No. of samples	mean total sulfur	standard deviation	% coeff. variation
DHS1	14	0.86	0.38	44.92
DHS2	13	1.40	1.63	117.75
DHS3	12	0.58	0.20	35.12
whole seam	39	0.95	1.00	106.31

probability of no difference between the mean values = 0.1218

Table 9. Summary of statistical analysis on organic sulfur (%).

Group	No. of samples	mean organic sulfur	standard deviation	% coeff. variation
DHS1	14	0.50	0.15	29.74
DHS2	13	0.54	0.25	45.64
DHS3	12	0.42	0.13	32.20
whole seam	39	0.49	0.19	38.77

probability of no difference between the mean values = 0.2591

Table 10. Summary of statistical analysis on pyritic sulfur (%).

Group	No. of samples	mean pyritic sulfur	standard deviation	% coeff. variation
DHS1	14	0.35	0.30	84.81
DHS2	13	0.66	1.04	157.00
DHS3	12	0.15	0.14	90.81
whole seam	39	0.39	0.65	166.67

probability of no difference between the mean values = 0.1362

4.2.1.5 Relationships among total, organic, and pyritic sulfur

The relationship among the various forms of sulfur and related coal characteristics, such as ash, can be examined by performing a correlation analysis on the variables and plotting each variable against the others. Correlation coefficients for the log-transformed values of the forms of sulfur are given in Table 11. Plots of organic and pyritic sulfur contents versus the total sulfur content, and forms of sulfur versus percent ash are shown in Figures 9 and 10, respectively.

Table 11 and Figure 9 (a and b) indicate a high correlation between pyritic and total sulfur, and organic and total sulfur. Variations in total sulfur in the BB seam seem to be due to variations in the amounts of pyritic sulfur and, to a lesser extent, of organic sulfur. Total sulfur and pyritic sulfur show little or no correlation with ash. Organic sulfur, on the other hand, shows a moderate negative ($r = -0.49$) correlation with ash. Figure 10 (a-c) shows these relationships.

The relationships among the various forms of sulfur may also be examined by comparing the pyritic to organic sulfur ratio and plotting this value against the total sulfur content. The pyritic to organic sulfur ratio (Py/Or) in the BB seam ranges from a minimum of 0.063 to a maximum of 4.7 (Fig. 11). Close to 77% of the samples analyzed have pyritic to organic ratios of less than 1. A plot of the Py/Or ratio versus the total sulfur (Fig. 12) shows a general increase in Py/Or ratio with increase in total sulfur ($r = 0.57$ for log-transformed data and 0.84 for raw data). This observation indicates increased importance of pyritic sulfur relative to organic sulfur in affecting the total sulfur content of the high-sulfur coals.

Table 11. Correlation matrix table for forms of sulfur and determined ash (%) content (n = 39). Log-transformed data used to calculate correlation coefficients.

	Total sulfur	Organic sulfur	Pyritic sulfur	Ash
Total sulfur	1			
Organic sulfur	0.74	1		
Pyritic sulfur	0.83	0.36	1	
Ash	-0.18	-0.49	0.07	1

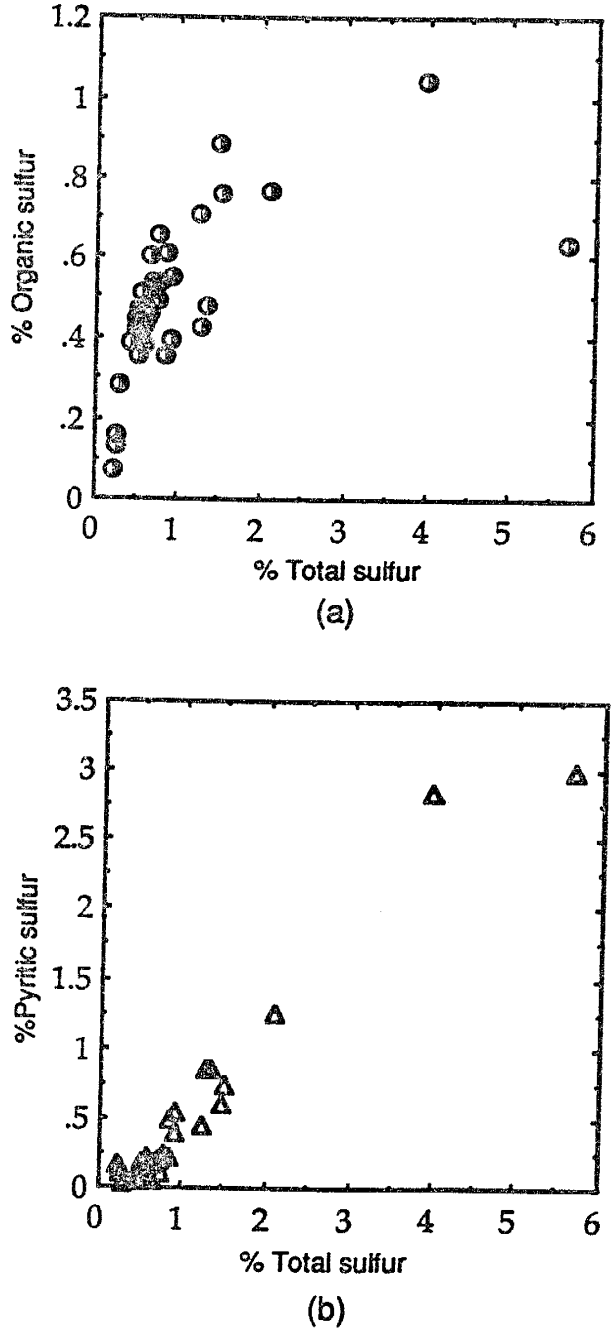

Figure 9. Total sulfur versus organic sulfur (a) and pyritic sulfur (b) in BB seam coals.

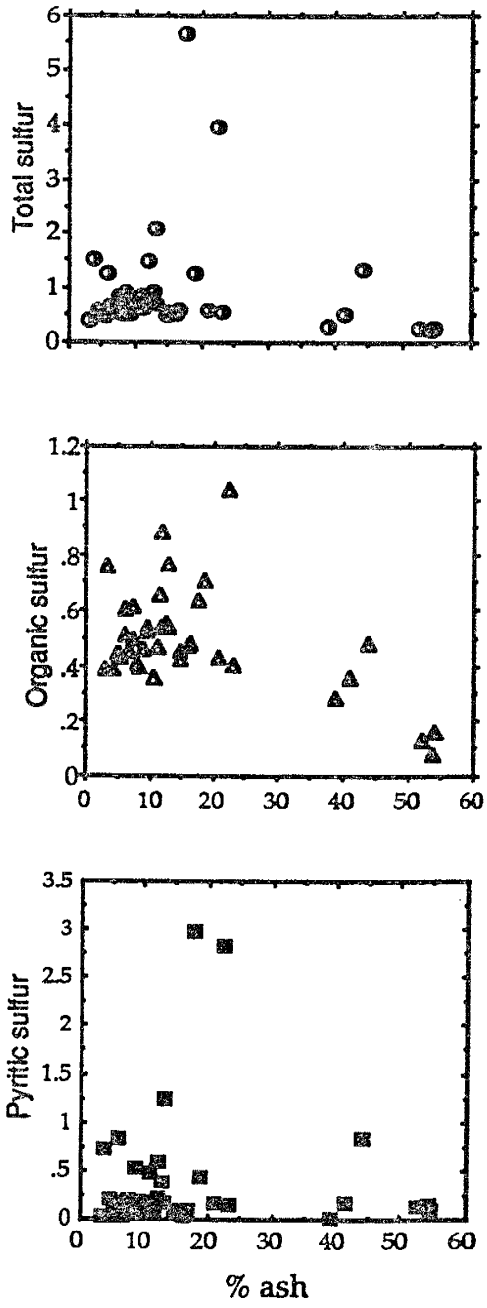

Figure 10. Forms of sulfur plotted against % ash in BB seam coals.

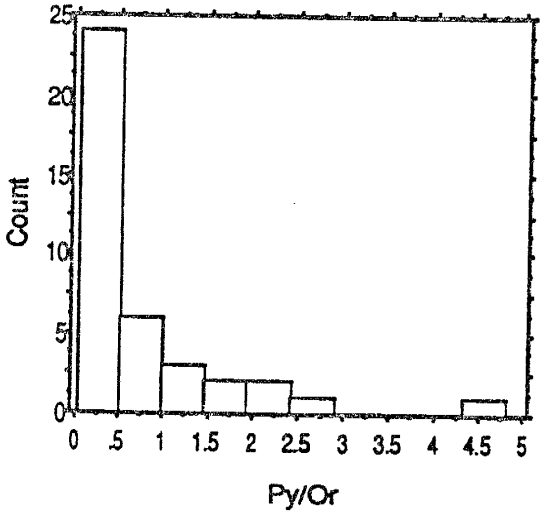

Figure 11. Pyritic to organic sulfur ratios in BB seam coals.

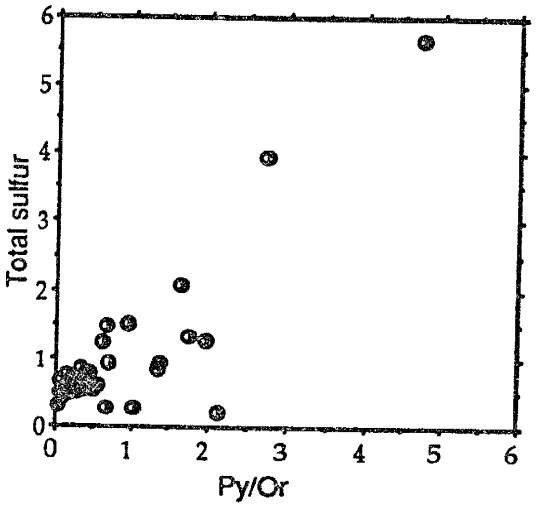

Figure 12. Total sulfur versus Pyritic to organic sulfur ratios in BB seam coals.

4.2.2 Vertical distribution of sulfur

The vertical variation of the sulfur forms in the three drill holes is shown in Figures 13, 14, and 15. The figures are constructed with distance from the base of the seam (in centimeters) plotted against percent sulfur content per sample. The thickness of each sample ranges from about 2 to 10 cm.

DHS1 (Fig. 13) shows a higher concentration of total, pyritic, and organic sulfur near the base and top of the seam, and adjacent to the parting. In addition, two samples, 80 and 88 cm above the base of the seam, also have high concentrations. The overlying and underlying claystones have the lowest sulfur content in all forms. Variations in total sulfur are accompanied by variations in pyritic and organic sulfur forms.

DHS2 (Fig. 14) shows distribution patterns significantly different from that in DHS1. As in DHS1, the bounding lithologies have the lowest sulfur content. Samples adjacent to the roof and floor contain more sulfur than the bounding lithologies. Toward the middle portion of the seam, in DHS2, there is a high-sulfur zone that is about 35 to 40 cm thick. Samples between the high-sulfur zone and the roof and floor show a relatively uniform sulfur distribution. Variations in total sulfur contents are accompanied by variations in pyritic and organic sulfur forms.

In DHS3 (Fig. 15), as in DHS1 and DHS2, the bounding lithologies have the lowest sulfur content. Samples adjacent to the roof and floor contain more sulfur than the bounding lithologies. The sulfur distribution in the coals vary slightly with some thin zones showing slight enrichments. The maximum total sulfur content doesnot exceed 1%.

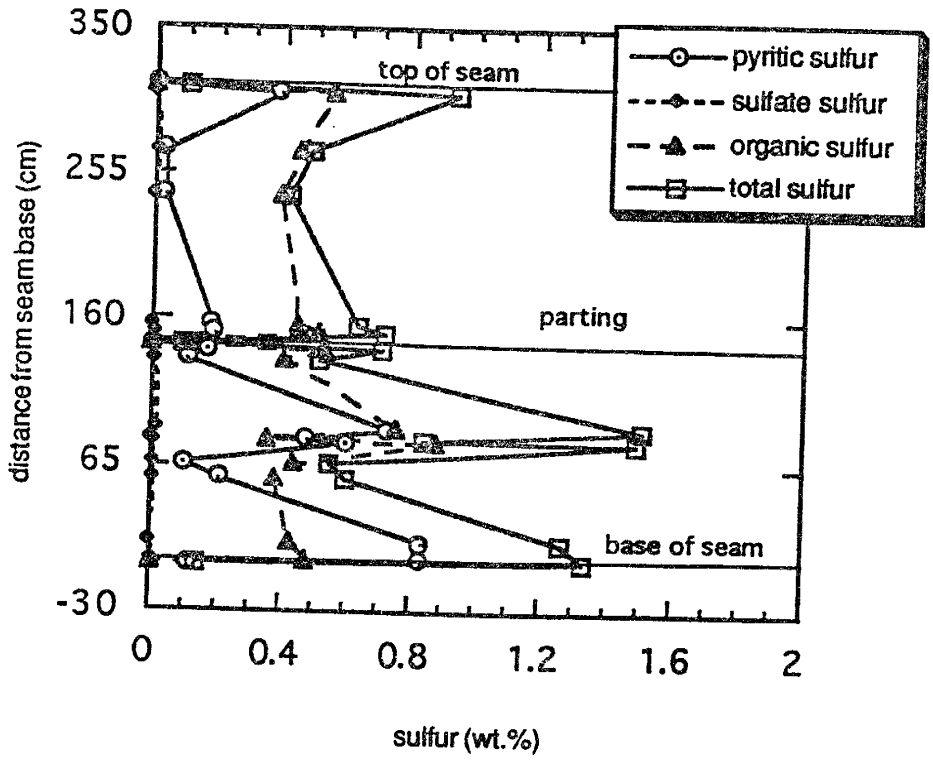

Figure 13. Vertical distribution of forms of sulfur in DHS1.

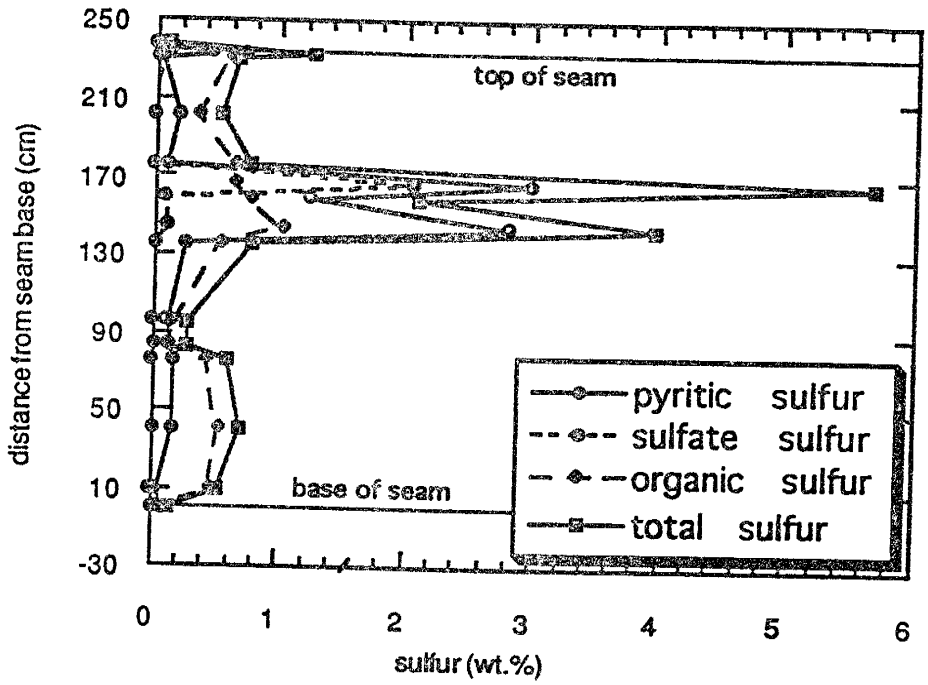

Figure 14. Vertical distribution of forms of sulfur in DHS2.

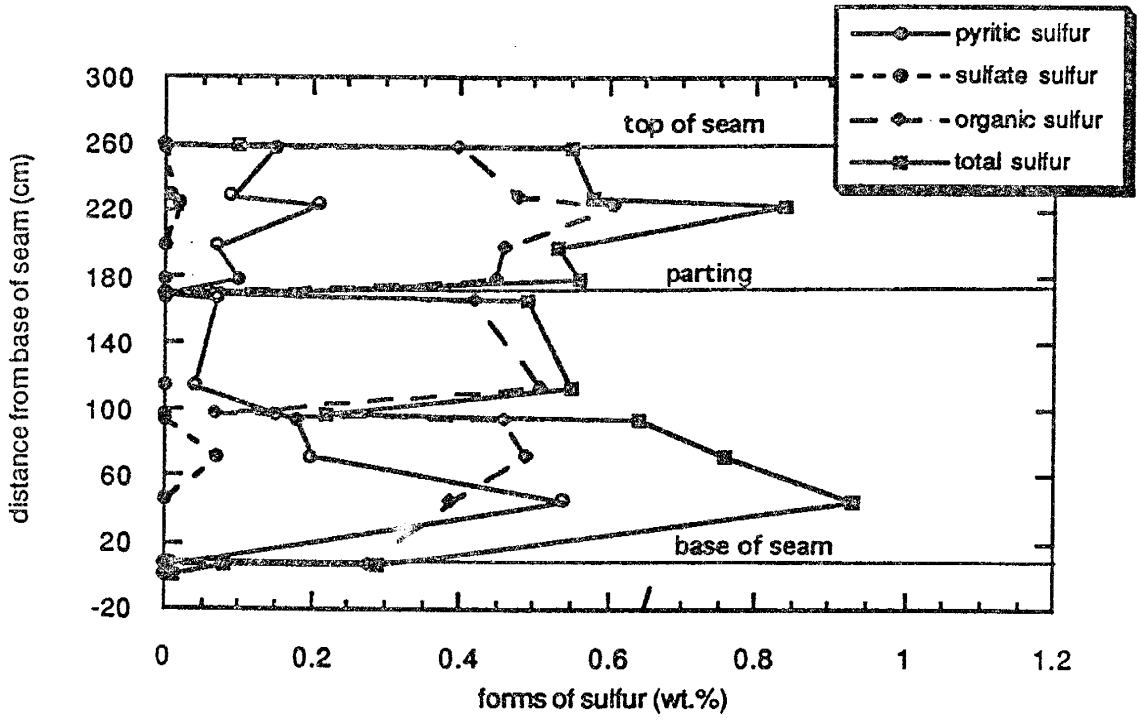

Figure 15. Vertical distribution of forms of sulfur in DHS3.

4.2.3 Iron sulfide occurrences

To document and evaluate iron sulfide occurrences and paragenetic sequences, eight samples were selected from the three drill holes for petrographic study. Five of these samples were from the dominantly low sulfur sites (DHS1 and DHS3), and the remaining three were from DHS2. The sulfur contents of these samples are given in Table 12.

4.2.3.1 Description of iron sulfides

Petrographic study of polished pellets indicates that iron sulfide occurrences in the BB seam are in the form of pyrite and marcasite. Marcasite occurs only in association with massive pyrite (Fig 16). Pyrite displays the following modes of occurrence:

(1) Pyrite framboids occurring in clusters or isolated, with diameters ranging from a few μm to 45 - 50 μm, (Fig. 17 A).

(2) Euhedral to subhedral crystals isolated or in clusters with sizes ranging from a few μm to 5 - 10 μm, (Fig. 17 B) and

(3) massive pyrite filling cellular structures and void spaces in inertinites, coating framboids and cementing pore spaces between clusters, and as cleat-filling (Figs. 18 A and B, and 19).

Framboids and euhedral pyrite crystals occur in minor amounts in the low- to medium- sulfur samples, whereas massive cleat-filling pyrite is relatively more abundant. Samples S2-18 and S2-21 contain abundant framboids and euhedral pyrite grains. Massive pyrite filling cellular structures and coating framboids and/or cementing pore spaces between framboids also occurs commonly in these samples. Massive cleat-filling pyrite is relatively minor in abundance in S2-18 and S2-21. Siderite, sometimes with pyrite inclusions, and calcite are present in some of these samples.

Table 12. Sulfur content and other relevant characteristics of the petrographic samples.

Sample number	Lithotype	Sample thickness	% ash	% total sulfur	% organic sulfur	% pyritic sulfur	% sulfate sulfur	Iron (ppm)[d]
S1-39[a]	Clarain	6.25 cm.	3.64	1.51	0.76	0.73	0.02	n.a.
S1-40[a]	Fusain	2.5 cm.	10.95	0.84	0.36	0.48	0.0	3658
S1-51[a]	Vitrain	7.5 cm.	5.86	1.27	0.43	0.84	0.0	7001
S2-18[b]	Vitrain	7.5 cm.	17.7	5.67	0.63	2.99	2.05	34157
S2-21[b]	Durain	8.75 cm.	22.41	3.96	1.04	2.82	0.1	23984
S2-40[b]	Vitrain	9.06 cm.	16.15	0.51	0.47	0.04	0.0	1017
S3-6[c]	Durain	8.91 cm.	23.27	0.55	0.40	0.15	0.0	5466
S3-35[c]	Vitrain	10.0 cm.	8.65	0.93	0.39	0.54	0.0	5144

a = sample from DHS1; b = sample from DHS2; c = sample from DHS3; n.a = not analyzed; d = iron concentration from INAA data.

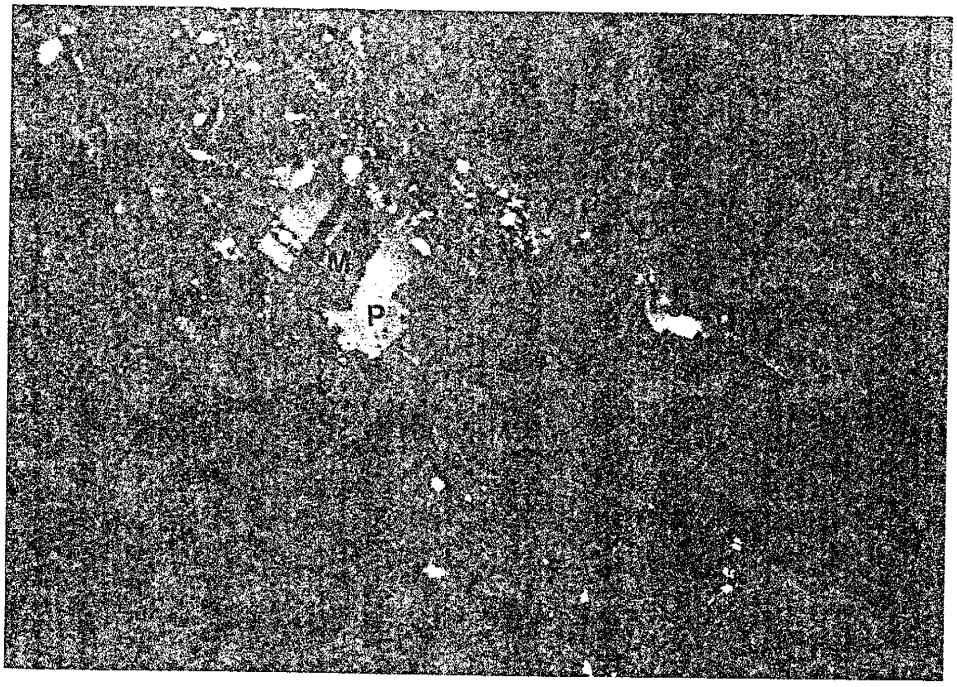

Figure16. An example of marcasite (M) association with massive pyrite (P) in sample S3-35. Grain dimension is about 200 μm. Reflected light, crossed nicols, 200 X.

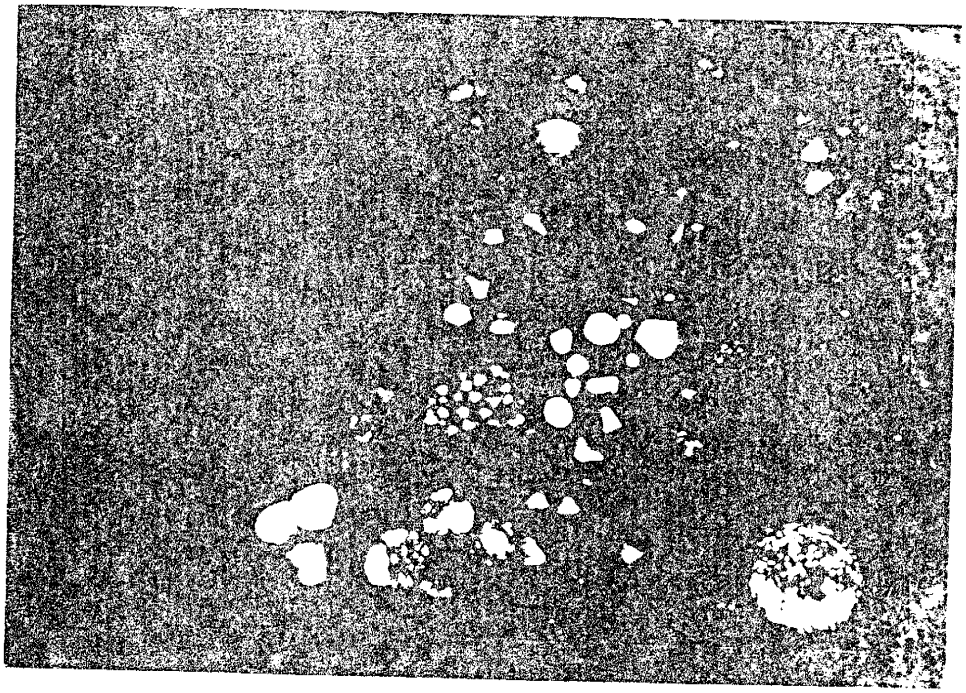

Figure 17A. An example of isolated pyrite framboid (lower right corner) in sample S2-21. The framboid is 20 μm across. Note the space between the crystallites within the framboid. Reflected light, ppl, 400 X.

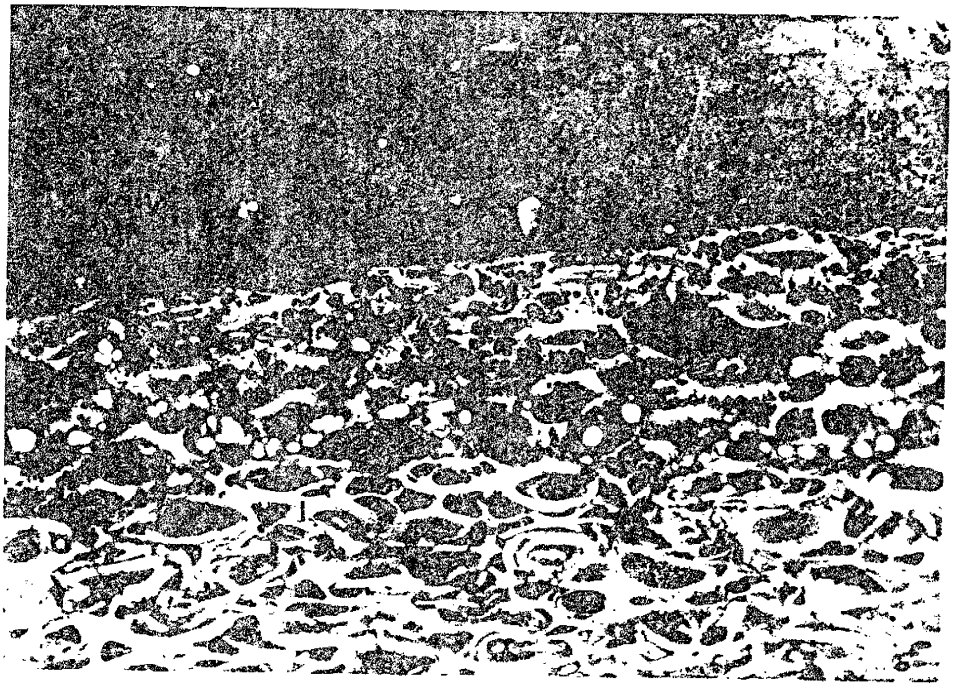

Figure 17B. An example of subhedral to euhedral pyrite crystals in vitrinite (V) and inertinite (I) in sample S2-18. Field of view is 325 µm across. Reflected light, ppl, 200 X.

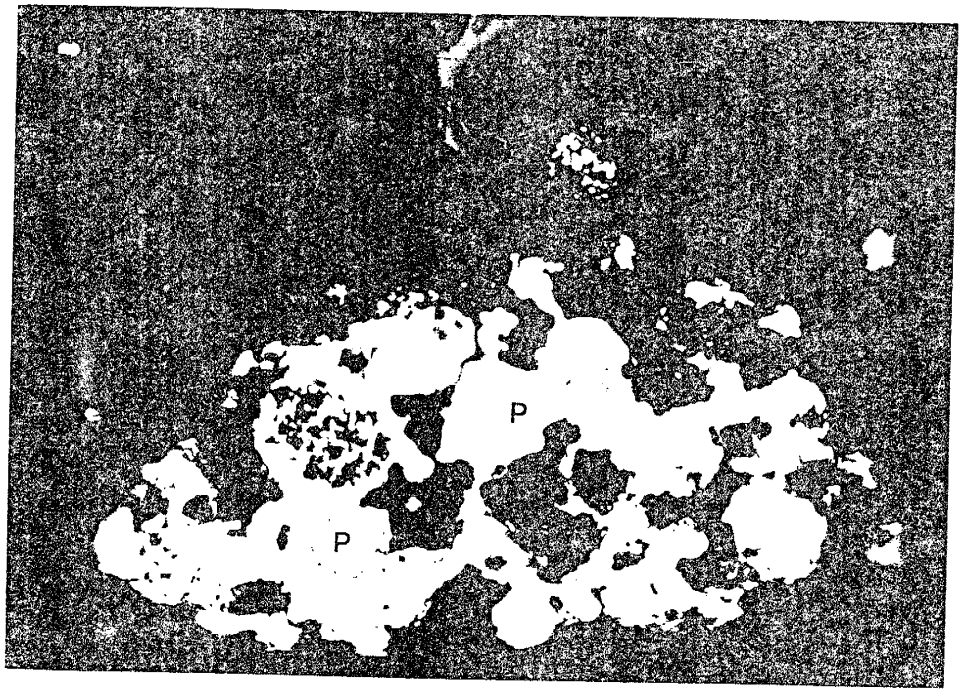

Figure 18A. An example of massive pyrite (P) coating framboids and cementing inter- and intra-framboid spaces in sample S2-18. Field of view is 138 µm across. Compare this with framboid in Figure I7A. Reflected light, ppl, 400 X.

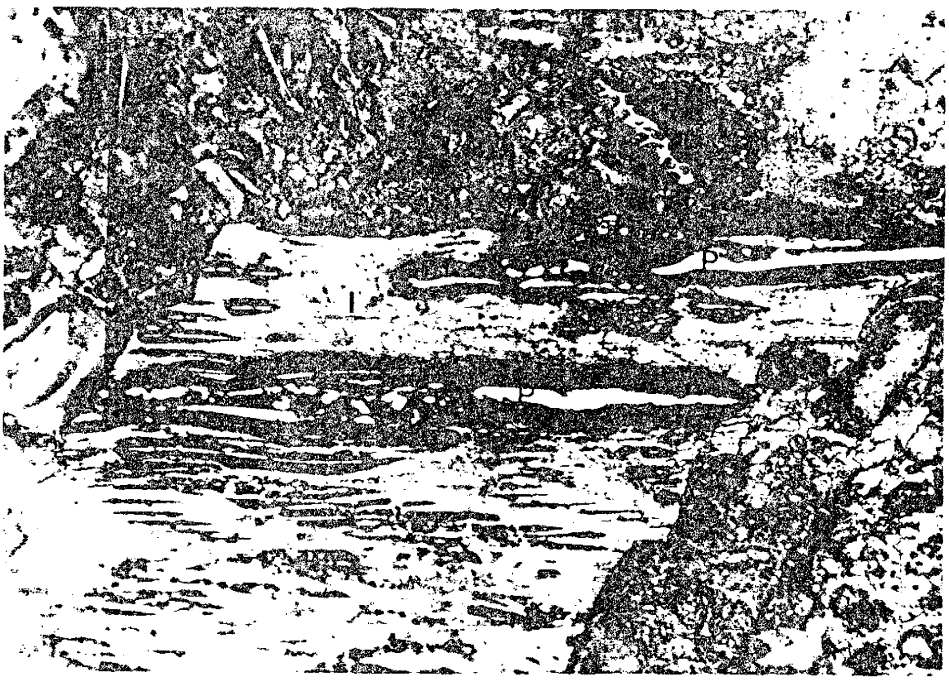

Figure 18B. An example of massive pyrite (P) filling cellular structures in inertinite (I) in sample S2-18. Field of view is 600 µm across. Reflected light, ppl, 100 X.

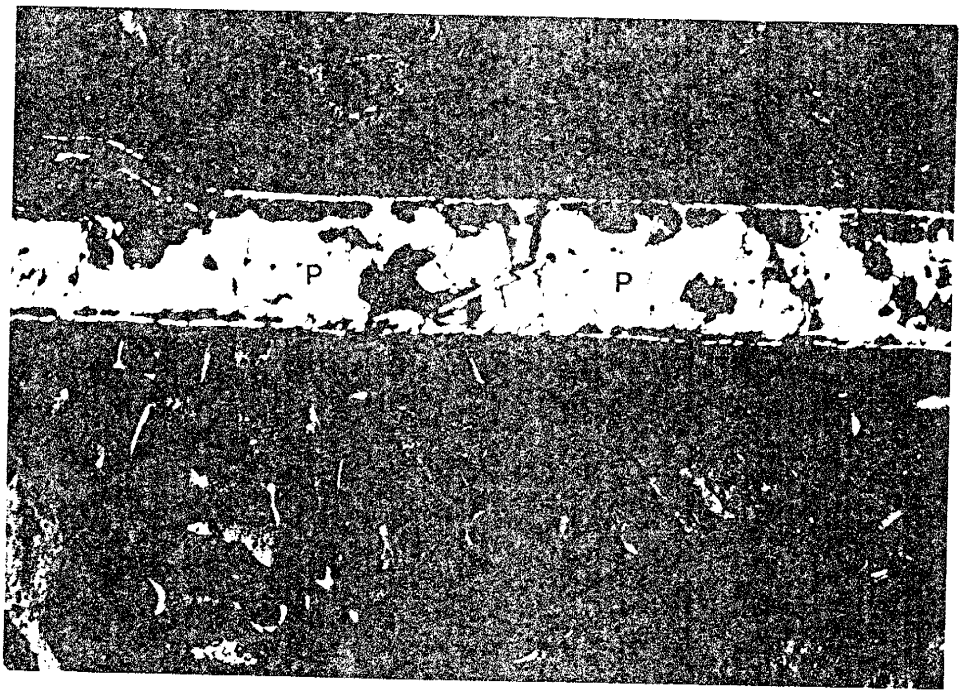

Figure 19. Massive cleat-filling pyrite (P) in sample S1-39. Field of view is 1.6 mm across. Reflected light, ppl, 50 X.

The different types of pyrite occurrences observed in the BB seam are similar to pyrite described from Alleghenian coals in the Seelyville Coal, Chinook Mine, Indiana (Boctor et al., 1976), Albian coals from the Maestrazgo Basin, southeastern Iberian Range, northeastern Spain (Querol et al., 1989), and Upper Paleozoic Ohio coals (Weise et al., 1986).

4.2.3.2 Precipitation stages

Minerals in coal are emplaced throughout the history of the coal bed. Two main stages of mineral emplacement are used to classify minerals occurring in coal according to their time of emplacement. These are : A) the syngenetic, and B) epigenetic stages (Renton, 1982).

According to this classification scheme, syngenetic minerals include those that were incorporated into coal from the earliest peat-accumulation stage up to the "early diagenetic stage of coalification." This stage of mineral emplacement is subdivided into two phases : A) the early syngenetic phase, and B) the late syngenetic phase. The syngenetic stage appears to end before major compaction and solidification of the coal and before the development of cleat. The early syngenetic phase takes place during the peatification stage and the later syngenetic phase of mineral emplacement begins after burial of the peat and during the humification-gelification stage (Renton, 1982). With burial, compaction, and continued geochemical gelification, porosity and permeability of the coal decrease with the dimension of pore spaces becoming reduced to those of a molecular sieve. This condition prevents hydrated ions, from which coal minerals could form, from entering the coal mass because of their molecular dimensions (Renton, 1982). The syngenetic stage of mineral emplacement ends at this point and is succeeded by the epigenetic stage of mineral emplacement following the development of cleats.

Following Renton's (1982) classification of mineralization stages in coal, and based on petrographic evidence, pyrite occurrences in the BB seam are classified as follows:

1) syngenetic stage iron sulfides- framboids, euhedral pyrite crystals, and massive forms of pyrite that coat framboids and cement inter-and intra-framboidal spaces; and

2) epigenetic stage iron sulfides- massive cleat-filling pyrite and associated marcasite.

The main petrographic criterion used to classify the iron sulfides into the two categories was their textural relationship with the coal macerals. Whereas iron sulfides that formed during the syngenetic stage (before cleat formation) are intimately associated with the coal macerals, the epigenetic iron sulfides cut across macerals suggesting emplacement after (or contemporaneous with) cleat formation. Marcasite associated with cleat-filling pyrite may be an overgrowth marcasite on pyrite and/or diagenetic product after the pyrite has formed.

Framboids and euhedral pyrite crystals have been documented to occur in plant cells, spores, and animal fragments in recent peats and sediments (Altschuler et al., 1983). Such morphologies have also been documented in coal and have been interpreted as forming during the syngenetic stage of mineral emplacement (Parratt and Kullerud, 1979; Querol et al., 1989). The petrographic relationship between massive pyrite-coated framboids and pyrite cementing inter-and intra-framboidal spaces indicate that the latter formed after the framboids during the syngenetic stage.

4.2.4 Interpretation

Recent peat forming systems including the Okefenokee swamp, Georgia and the Everglades swamp, Florida, have been proposed as suitable coal-forming models to understand the nature and origins of sulfur in coal (Davies and Raymond, 1983; Cohen et al., 1984; Casagrande, 1987).

Davies and Raymond (1983) in their studies of recent peats from the Florida Bay and coals from the Lower Kittanning coal seam (Pennsylvannia), recognized three periods of sulfur emplacement in the peat/coal cycle. The first period occurs during early stages of peat deposition when water circulation is unrestricted. During this period, organic sulfur is fixed, and depending on availability of iron and sulfur, small euhedral crystals and framboids of pyrite may also be incorporated within peats. Deposition in fresh-water environments may result in low organic sulfur contents and pyrite may be absent. Deposition in a marine environment could lead to higher organic sulfur contents, and higher pyritic sulfur contents, depending on iron availability. The second period is characterized by sulfur enrichment after peat deposition but before coalification. Permeation of previously deposited peat by marine waters enhances the organic and pyritic sulfur contents. During the third period recognized by Davies and Raymond (1983), sulfur emplacement occurs after coalification when permeability is restricted to joints and cleat fractures. The organic sulfur is not altered at this stage. Pyrite may be deposited as fracture and pore fillings depending on the availability of iron and sulfate ions.

Cohen et al., (1984) in their studies of peats from the Everglades-Mangrove region of Southern Florida, observed that marine to brackish peats contain more pyrite and total sulfur than fresh-water peats.

Casagrande (1987) studying peats from the fresh-water Minnie's Lake site in the Okefenokee swamp, and the marine-influenced Little Shark River area in

the Florida Everglades, reported differences in sulfur contents in these two areas. In the fresh-water peat the total sulfur content was low (0.17 - 0.21%) and changes little as a function of depth. Organic sulfur was the dominant form of sulfur. The total sulfur content in the marine-influenced peat , on the other hand, ranged from 1.29 to 10.11% on a dry peat basis. The pyritic sulfur in the marine-influenced peat (mean = 0.74%) was higher than that of the fresh water peat (mean = 0.0017%). In the marine-influenced peat the pyritic sulfur accounted for about 14% of the total sulfur as compared to about 1% in the fresh water peat.

Using sulfur distributions observed in peats, I attempt to explain the observed sulfur distribution patterns in the BB seam.

Based on the sulfur distribution in the three drill holes, three distribution patterns are recognized in the BB seam: 1) higher sulfur contents in the coal samples adjacent to the seam margins and parting, and at certain stratigraphic levels (DHS1); 2) higher sulfur content toward the middle of the seam (DHS2); and 3) distribution where the sulfur content in the coals varies slightly within the seam, but the maximum total sulfur content does not exceed 1%.

In the first distribution pattern, relatively low organic sulfur content, and higher pyritic sulfur contents adjacent to bounding claystones and parting (mainly in the form of cleat-filling pyrite and marcasite) suggest sulfur emplacement during two periods; a) during early stages of peat deposition mainly as organic sulfur (corresponding to the "first period" of Davies and Raymond (1983)), and b) sulfur emplacement, mainly as pyritic sulfur, during and/or after cleat formation ("third period" of Davies and Raymond (1983)). The organic sulfur in the low-sulfur samples may have resulted from plant sulfate assimilation with subsequent incorporation into the peat upon the death of the source plants (Casagrande, 1987). During the early stages of peat accumulation, sulfate ions in the peat may be reduced to hydrogen sulfide by anerobic sulfate reducing bacteria. The

ıydrogen sulfide could then react with coalifying peat components to form ɔrganic sulfur (Neavel, 1968; Casagrande, 1987). This process may explain the ncorporation of additional organic sulfur in the high-sulfur samples. The elatively low pyritic sulfur content may be partly due to a limited supply of iron hat could have reacted with the available sulfide to form iron sulfides. Neavel 1968) suggested that iron enters peat swamps adsorbed on clays. More iron nay thus be brought into the swamp during floodings which form partings and/or erminate the swamp. Iron is also relatively abundant in the basal claystones ınderlying peats (Neavel, 1968). During the early stages of peat accumulation, ·on derived from the underlying claystones may react with sulfides in the peat to ɔrm iron sulfides close to the coal-claystone boundaries. Iron brought into the wamp during flooding episodes may react with sulfides in the peat to form iron ulfides near partings and claystones overlying the peat.

In the second distribution pattern, the high-sulfur coal samples are haracterized by high pyritic sulfur, abundant framboidal and euhedral pyrite ·ystals, and massive void-filling pyrite. Cleat-filling pyrite is minor in these ɜmples. Organic sulfur in these samples is comparable to that observed in low-ılfur coal samples. These observations suggest that sulfur emplacement, ainly in the form of pyritic sulfur, occured during the early stages of peat ɜposition and compaction prior to coalification. The high sulfur content may be dicative of some brackish or marine water influence during the early stages of ɜat development. This sulfur emplacement period corresponds to the "second ·riod of sulfur emplacement" described by Davies and Raymond (1983). The ɜjor difference from the BB seam coals is that elevated organic contents were t observed to be associated with high total sulfur contents. High sulfur ntents adjacent to bounding claystones in the second pattern may have formed a similar manner as suggested for the first pattern. The high sulfur content

toward the middle of the seam may be indicative of ample supply of iron and sulfate ions in the swamp at the early stages of peat accumulation. In DHS3, the low total sulfur content and proportionally lower pyritic sulfur content suggests sulfur incorporation, mainly in the form of organic sulfur, at the early stages of peat accumulation. Although showing slight variations in each drill hole, the mean organic sulfur content in the three drill holes is similar (Table 12).

Bounding claystones and partings have the lowest sulfur content (< 0.1% total sulfur). These lithologies are believed to have been deposited from streams in fresh-water settings and thus may have contained little or no organic matter that may have acted as a sink for sulfur to form organic sulfur. Their fresh-water depositional setting suggests that sulfate supply may have been low. Also, as conditions during deposition of these clastic rocks were more oxidizing compared to the swamp environment, available sulfate would not be reduced to sulfide to react with the available iron to form iron sulfides. A combination of low organic and sulfate contents and oxidizing environments may have contributed to the low sulfur content of the bounding claystones and partings.

4.2.5 Sulfur variation with vitrinite content

In order to determine the variations in sulfur and ash contents that may exist between different coal lithotypes, ANOVA test was performed on the sulfur data. Samples were divided in to two groups: 1) bright coals (> or equal to 65% vitrinite); and 2) dull coals (< 65% vitrinite).

ANOVA results (Table 13) show that dull and bright coals have statistically significant differences in their total, and pyritic sulfur and ash contents. Dull coals have higher total sulfur, pyritic sulfur, and ash content than the bright coals. Organic sulfur values in the bright and dull coals are not statistically significantly different. Relationships between the forms of sulfur, ash, and macerals in bright and dull coals are summarized in Tables 14 and 15, respectively. Correlation coefficients are calculated using x-y pairs and log-transformed values.

Table 14 shows a negative relationship between inertinite and the forms of sulfur. Total sulfur and pyritic sulfur show more pronounced negative correlations to inertinite ($r = -0.63$ and -0.51, respectively) than organic sulfur ($r = -0.31$). Vitrinite shows a moderate correlation to total and pyritic sulfur ($r = 0.52$ and 0.46, respectively). Ash shows negative or poor correlation to the forms of sulfur.

In dull coals (Table 15), inertinite and exinite show moderate correlations with the forms of sulfur. Vitrinite shows moderate correlation with organic sulfur. As with bright coals, ash content in dull coals shows poor or moderate negative correlations with the forms of sulfur.

Table 13. Analysis of variance results for bright and dull coals.(90% confidence level).

Sulfur forms and ash (%)	Bright coal (n = 19) mean	s.d	Dull coal (n = 17) mean	s.d	ANOVA prob.*
total sulfur	0.67	0.29	1.31	1.44	0.06
organic sulfur	0.46	0.12	0.51	0.25	0.49
pyritic sulfur	0.20	0.22	0.66	0.9	0.04
Ash	13.70	13.20	21.9	15.5	0.09

* = probability of no difference between the means; s.d = standard deviation from the mean

Table 14 . Relationships among forms of sulfur, maceral groups and ash in bright coals.

	Ts	Os	Ps
Inertinite	-0.63	-0.31	-0.51
Vitrinite	0.52	0.28	0.46
Exinite	0.28	0.18	0.13
Ash	-0.47	-0.58	0.01

Ts = total sulfur; Os = organic sulfur; Ps = pyritic sulfur

Table 15. Relationships among forms of sulfur, maceral groups and ash in dull coals.

	Ts	Os	Ps
Inertinite	0.54	0.66	0.55
Vitrinite	0.32	0.60	0.18
Exinite	0.49	0.60	0.53
Ash	-0.32	-0.58	-0.19

Ts = total sulfur; Os = organic sulfur; Ps = pyritic sulfur

4.2.5.1 Discussion

Relationships between maceral types and contents, sulfur, and ash contents in coals may be explained by taking into account such factors as pH, Eh, sulfate ion and iron concentrations and availability, fluctuations in water table, and type of vegetation in the ancestral swamp. The effect of these factors is discussed in the following paragraphs.

Esterle and Ferm (1986) related bright and dull coals to arborescent vegetation and stunted, nutrient-deficient vegetation, respectively. Relatively low redox potentials (low Eh) were suggested to favor the formation of vitrinite precursors while under more aerobic conditions, oxidative biodegradation produces maceral precursors of the inertinite group (Stach et al., 1982; Roberts, 1988).

Cecil et al., (1982) suggested that coals derived from peats that formed in highly acidic environments (pH < 4.5) were low in sulfur (< 1%) and ash (<8 wt%). Coals derived from peats formed in less acidic environments (pH 4.5 - 7.5) tend to have a sulfur content more than 1% and a higher ash content. Highly acidic conditions would leach elements which tend to be soluble under such conditions. Acidic conditions also inhibit sulfate-reducing and fermentation microbial activities and peat degradation. At higher pH conditions, leaching of elements is minimal and sulfate-reducing activity is increased. These conditions would favor the concentration of mineral matter and increased sulfur contents.

Sulfate is the principal reactant for establishing pyritic and organic sulfur levels in peat and its concentration may be the key difference between fresh-water and marine influenced peats (Casagrande, 1987). Sulfate ion concentration in average river water is about 8 ppm as compared to 2710 ppm in sea water (Drever, 1982). Coals derived from peats that formed in a fresh-water

(low sulfate ion concentration) environment are believed to contain less sulfur than coals derived from peats influenced by marine water (Cecil et al., 1982).

Sulfate reducing bacteria reduce sulfate ions in the peat to form H_2S. The H_2S may be fixed as pyrite and/or organic sulfur. The formation of pyrite depends on the availability and reactivity of iron in the peat environment (Berner, 1984, Casagrande, 1987). Low pH and low sulfate conditions tend to reduce the activity of sulfate reducing bacteria (Cecil et al., 1982). This may result in low levels of H_2S and limited formation of pyrite and organic sulfur (Roberts, 1988).

The above discussion shows that various combinations of the different factors could produce different results. For instance a combination of low sulfate concentration, low pH, low Eh, and low detrital input would probably produce low-sulfur, low-ash, and vitrinite rich coal. A high pH, higher Eh (occasional oxidation), higher sulfate concentration and relatively higher detrital input into the peat could result in a high-sulfur, high-ash, and relatively inertinite-rich coal.

4.3 Pyrite and siderite chemistry

4.3.1 Pyrite trace element chemistry

Trace element chemistry of pyrites in coals and fine-grained sedimentary rocks may be used to identify trace constituents that may have environmental relevance (Raiswell and Plant, 1980; Pickhardt, 1989) and as a tracer of marine fluids in coal fields (Hickmott et al., 1992). Pickhardt (1989), studying trace elements in minerals of German bituminous coals, reported higher concentrations for Cd, Pb, and Zn in epigenetic pyrite compared to syngenetic pyrite cystals and framboids. The syngentic pyrites were enriched in Be, Co, Mo, Ni, Sr and V. Raiswell and Plant (1980) determined trace elements in marine biogenic pyrite from carbonate concretions in the Upper Lias (Lower Jurassic) of Yorkshire, England. They reported that Mn, Co, Ni, and Zn were concentrated in the framboidal pyrites whereas As, Mo, and possibly Cu were mainly associated with the euhedral forms. The difference in trace-element content between the two textural forms of pyrite was related to differences in their growth mechanism. The rapidly formed precipitates tend to incorporate trace elements mainly by occlusion and surface adsorption. The influence of crystallochemical and thermodynamic factors in selecting the most suitable elements for solid solution becomes more important as growth slows and precipitation occurs under near-equilibrium conditions. The fine-grained nature of the framboidal pyrite implies rapid growth, which would encourage the incorporation of large concentrations of Mn, Ni, Co, and Zn from a local iron oxide source by adsorption and occlusion (Raiswell and Plant, 1980). The later phase of euhedral pyrite is more crystalline, implying slower growth, perhaps controlled by the diffusion transport of iron from an external source via pore waters (Raiswell and Plant, 1980). The incorporation

of As and Mo in these pyrites may reflect the availabilty of these elements in the pore waters (Raiswell and Plant, 1980).

During coal cleaning, coarse-grained mineral matter is easily removed from the coal material by float-sink operations. However, the fine-grained mineral matter, framboidal pyrite grains for instance, may be very hard to remove and may be rafted with the coal. Trace elements contained in these grains could be released during coal combustion. For example, Hg and Se may reach the atmosphere in the vapor state and also associated with fine flyash particles (Swaine, 1990). Also, trace elements contained in pyrites, especially the framboidal pyrites because of their high reactivity, may be released from coal waste piles into the surrounding system upon oxidation of the pyrites. Caruccio (1973) has shown that framboidal pyrite was much more reactive and less stable than massive secondary pyrite.

Hickmott et al., (1992), examined iron sulfides from the Lower Kittanning coal of Western Pennsylvania and found that individual samples frequently show correlations between As and Se with As/Se ratios ranging from around 10 in samples with marine and brackish overburden down to < 1 in samples with fresh-water overburden. They suggested that the As/Se ratio of iron sulfides may be a diagnostic indicator of marine influences during sulfide growth, and may provide a useful tracer of marine fluids in coal fields.

Iron sulfide grains in six polished coal samples from the BB seam were analyzed for their trace-element composition. The electron microprobe analysis results are listed in Appendix 2 (Tables APP2-1 and APP2-2) and summarized in Table 16. Sulfur contents of the samples are also given for comparison.

Table 16. Electron microprobe analyses of iron sulfides in the BB seam (Concentrations in ppm unless noted otherwise).

Sample No.	Pb	Cd	Cu	Zn	Sr	Ni	Mn	% S*
S1-39	485** (182)*** n = 4	88 (42) n = 3	95 (41) n = 3	55 (11) n = 4	692 (189) n = 4	n.d	n.d	1.51 0.73 0.76
S1-40	470 (191) n = 6	65 (15) n = 4	63 (24) n = 4	n.d	446 (110) n = 4	n.d	n.d	0.84 0.48 0.36
S2-40	389 n = 1	n.d	n.d	n.d	400 n = 1	n.d	30 n = 1	0.51 0.04 0.47
S3-35	412 (126) n = 6	68 (3) n = 2	82 (41) n = 4	71 n = 1	470 (213) n = 6	n.d	n.d	0.93 0.54 0.39
S2-18	1207 (533) n = 16	60 (18) n = 3	162 (112) n = 11	58 (12) n = 2	392 (166) n = 9	65 n = 1	314 (352) n = 11	5.67 2.99 0.63
S2-21	1293 (852) n = 11	81 (20) n = 8	154 (114) n = 4	71 n = 1	505 (207) n = 8	174 n = 1	197 (156) n = 9	3.96 2.82 1.04
detection limit ****	200	40	40	35	200	25	25	

* = sulfur forms (total, pyritic, and organic in descending order); ** = average concentration (ppm); *** = standard deviation from the mean; **** = detection limit at 95% confidence limit; n = number of analyses; n.d = not detected (or below detection limit)

Two coal samples were analyzed using Proton-Induced X-ray Emission (PIXE) analysis. The PIXE microanalysis was done at the Los Alamos National Laboratory by Dr. Donald Hickmott. PIXE microanalysis is capable of standardless determination of trace-element abundances in coal macerals and sulfides using an internal normalization protocol. PIXE spectra are quantified using a least-squares data reduction protocol by normalization to iron determined by mineral stoichiometry in iron sulfides (Hickmott, personal comm.). Table 17 lists trace element concentrations in iron sulfides analyzed by PIXE.

Electron microprobe analysis of the iron sulfides in the BB seam coals shows a suite of trace elements in the sulfides. Lead is enriched in iron sulfides from the high-sulfur coals. Manganese is also detected primarily in the iron sulfides from the high-sulfur coals.

PIXE data (Table 17) shows a number of trace elements associated with the iron sulfides. The most notable difference between the two samples is that iron sulfides from the high-sulfur sample (S2-21) are enriched in trace elements whereas iron sulfides from the low-sulfur sample (S3-35) are almost barren of trace elements. The As/Se ratio in sample S2-21 is 10.72 and compares closely to the value of around 10 observed in samples with marine and brackish overburden (Hickmott et al., 1992). More analyses should be done on the iron sulfides to conclude that high As/Se ratios in the iron sulfides indicate marine and/or brackish water influences. Comparing the As/Se ratios in high- and low-sulfur coals (Table 18) from bulk coal samples shows that there is significant difference between these samples. The high-sulfur samples have significantly higher As/Se ratios (mean As/Se = 8.38) than samples with lower sulfur contents (mean As/Se = 0.63). Figures 20 and 21 show two populations with high As/Se ratios corresponding to high total and pyritic sulfur contents and low As/Se ratios associated with low total and pyritic sulfur contents. The high As/Se ratios

Table 17. Trace element data from PIXE analysis (Concentrations in ppm).

Sample No.	Pb	Cu	Zn	Sr	As	Se	Tl	Mo	Hg	Bi
S2-21	181[a] (52)[b] n = 2	194 n = 1	69 (6) n = 2	14 (7) n = 2	812 (733) n = 2	76 (50) n = 2	308 (221) n = 2	7 (1) n = 2	107 (92) n = 2	32 n = 1
S3-35	n.d	n.d	n.d	17 (16) n = 2	n.d	11 n = 1	31 n = 1	n.d	n.d	22 n = 1

a = mean values; b = one standard deviation of the mean values; n = number of analyses in the mean; n.d = not detected

Table 18. As/Se ratios (whole coal basis) for low-sulfur and high-sulfur coals in the BB seam.

parameter	low-sulfur n = 27	high-sulfur n = 3	ANOVA Prob.*	M-W. Prob **
Total sulfur	< 1.5 %	> 1.5%		
mean As/Se	0.63	8.38	0.01	0.005
std.dev	0.38	3.84		
range	0.11 - 1.81	5.64 - 12.77		

As/Se = arsenic to selenium ratio; Anova Prob.* = ANOVA probabilty of no difference; M-W. Prob ** = Mann-Whitney probabilty of no difference; std.dev = standard deviation from the mean

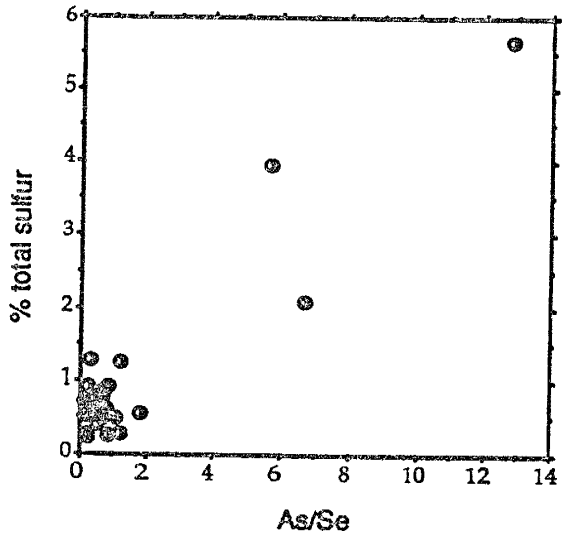

Figure 20. Total sulfur versus As/Se ratios in BB seam coals.

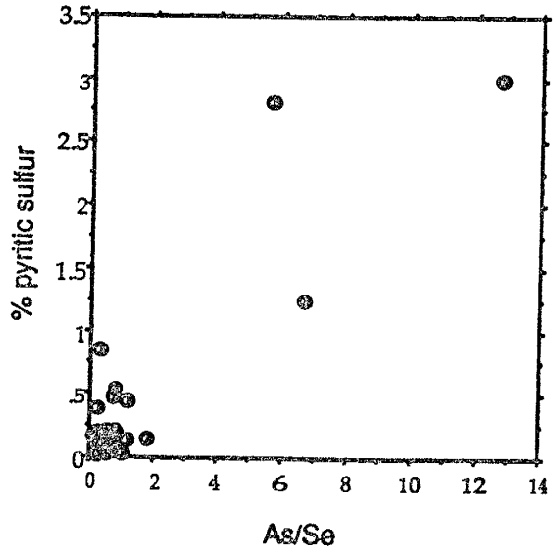

Figure 21. Pyritic sulfur versus As/Se ratios in BB seam coals.

associated with the high-sulfur coal samples may be indicative of some marine and/or brackish water influences in the BB seam.

The same pyrite grains were not analyzed by both PIXE and electron microprobe and thus results of these analyses could not be compared to each other.

To characterize the various iron sulfides observed in this study using their chemistry, the iron sulfides were divided into the following five groups: (1) marcasite, (2) cleat-filling pyrite, (3) framboids and euhedral/subhedral pyrite crystals, (4) replacement pyrite in inertinites, and (5) pyrite cementing inter- and intra-framboid spaces.

Tables 19 and 20 list the results of electron microprobe analyses of the iron sulfides. Indivdual analytical results are given in Appendix 2.

Results of the electron microprobe analyses (Tables 19 and 20) show that the iron sulfides analyzed have major element composition close to stoichiometric values for pyrite (S = 53.4 wt% and Fe = 46.6 wt%) and show very little variation in S/Fe weight ratios (stoichiometric S/Fe = 1.14). The most notable difference in trace-element composition of the various iron sulfides was that no manganese was detected in marcasite. Visual comparison shows that framboids and euhedral pyrite crystals, replacement pyrite in inertinites, and pyrite cementing framboids have more Pb than marcasite and cleat-filling pyrite. ANOVA probabilties of no difference using log wt.% values show that framboids and euhedral pyrite crystals contain more lead than marcasite and cleat-filling pyrite. ANOVA probabilties of no difference using log at.% values show that framboids and euhedral pyrite crystals contain more lead than marcasite, cleat-filling pyrite, and pyrite cementing framboids. When using at.%, the number of atoms (or moles) of the substance of interest is given as a percentage of the total number of atoms (or moles) in the sample. One mole of a substance always

Table 19. Electron microprobe analyses of iron sulfides in the BB seam (Concentration of Fe and S in wt%; concentration for the rest of the elements is given in ppm).

Group	Fe	S	Pb	Mn	Sr	Cd	Cu	S/Fe
marcasite	45.78* (0.25)** n = 11	54.65 (0.62) n = 11	500 (200) n = 6	n.d	500 (100) n = 8	100 (30) n = 4	100 (30) n = 6	1.19
cleat-filling pyrite	45.75 (0.98) n = 16	54.0 (1.14) n = 16	600 (400) n = 14	300 (200) n = 4	500 (200) n = 13	100 (20) n = 6	100 (100) n = 8	1.18
framboidal & euhedral pyrites	44.94 (0.89) n = 7	53.01 (0.67) n = 7	1900 (1200) n = 5	500 (500) n = 4	500 (300) n = 5	100 (15) n = 3	200 (100) n = 5	1.18
replacement pyrite in inertinite	45.01 (0.43) n = 7	54.85 (1.1) n = 7	1100 (300) n = 7	200 (200) n = 7	500 (200) n = 5	100 (20) n = 5	100 n = 1	1.22
pyrite cementing inter- and intra framboidal spaces	44.49 (0.27) n = 10	51.94 (0.68) n = 10	1000 (400) n = 10	100 (35) n = 6	400 (100) n = 6	100 (20) n = 3	100 (20) n = 6	1.15

* = mean values; ** = one standard deviation of mean values; n = number of analyses; n.d = not detected;

Table 20. Electron microprobe analyses of iron sulfides in the BB seam. Concentration in At.%.

Group	Fe	S	Fe : S
marcasite	32.46* (0.24)** n = 11	67.51 (0.24) n = 11	1: 2.08
cleat-filling pyrite	32.7 (0.35) n = 16	67.25 (0.34) n = 16	1: 2.06
framboidal & euhedral pyrites	32.71 (0.5) n = 7	67.21 (0.48) n = 7	1: 2.06
replacement pyrite in inertinite	32.0 (0.36) n = 7	67.94 (0.35) n = 7	1: 2.12
pyrite cementing inter- and intra framboidal spaces	32.89 (0.33) n = 10	67.01 (0.27) n = 10	1: 2.04

* = mean values; ** = one standard deviation of mean values; n = number of analyses;

contains a certain number of atoms regardless of the substance involved (Christian, 1986). Thus when comparing element concentrations, using at% helps to avoid differences that may be caused by differing atomic weights of the elements in consideration. As such, the statistical analyses based on at% values may be more reliable than those based on wt%.

In summary syngenetic pyrite is enriched in Pb relative to later formed (epigenetic) iron sulfides. This observation suggets that the early pore water was enriched in Pb. Probability analyses using both log wt.% and log at.% show that there are no differences in Mn, Sr, Cd, and Cu contents between the various forms of iron sulfides analyzed. Small amounts of Ni were detected in isolated framboids (65 -174 ppm) and pyrite cementing framboids (33 ppm) in samples S2-18 and S2-21, both high-sulfur samples.

4.3.2 Siderite chemistry

Siderite is a common authigenic iron mineral found in sediments. It forms as a result of reduction of ferric oxyhydroxides by organic matter in environments where there is an insufficient amount of sulfide to precipitate all the available reduced iron as FeS or pyrite (Postma, 1982). As such, siderite is widely regarded as a diagnostic indicator of methanic or post-oxic environments which contain little or no H_2S (Pye et al., 1990). However, Pye et al. (1990) suggested that siderite may form wherever the rate of iron reduction exceeds the rate of sulfate reduction, such that insufficient dissolved sulfide is available to precipitate all the available dissolved ferrous iron. Mozley and Wersin (1992) reported that siderite could form under slightly reducing conditions (suboxic zone) in marine environments that display relatively low concentration of organic matter and low sedimentation rates, and in nearshore and intertidal sediments which are subjected to alternating anoxic and oxic pore waters. Where iron reduction exceeds sulfate reduction, iron-rich authigenic carbonate minerals may be expected to co-precipitate with iron sulfide. Both sulfate reduction and iron reduction introduce HCO_3^- into the pore water system, thereby raising the likelihood of authigenic carbonate precipitation, particularly if H_2S escapes upwards to the surface (Coleman, 1985; Curtis, 1987).

Petrographic study of polished coal samples from the BB seam shows that siderite occurs as isolated massive crystals and associated with pyrite. Figures 22, 23, and 24 show some of the siderite occurrences and siderite-pyrite relationships in the samples. These occurrences are very similar to massive siderite occurrence reported in some Bulgarian coals (Kortenski, 1992. Plate IV, 2). Kortenski (1992) suggested that the siderite concretions formed under average to highly reducing conditions, high pH, and pore waters saturated with CO_2. The association of siderite with the coal material (Figure 24) suggests that

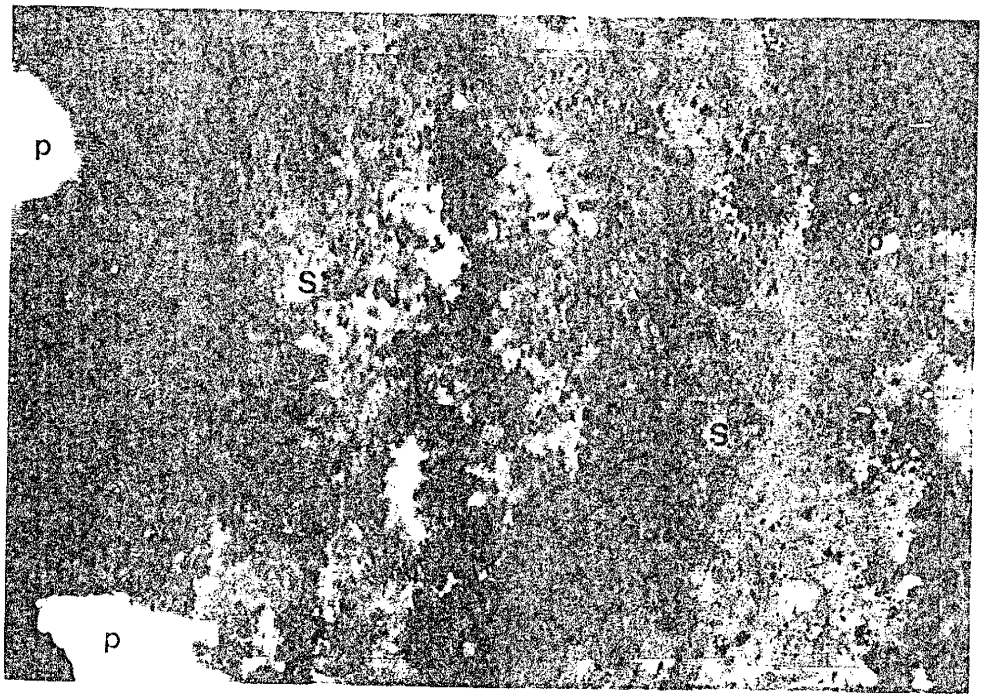

Figure 22. Siderite concretion (S) with pyrite inclusions (P) in sample S2-31. Note the porous nature of the siderite. Reflected light, ppl, 200 X.

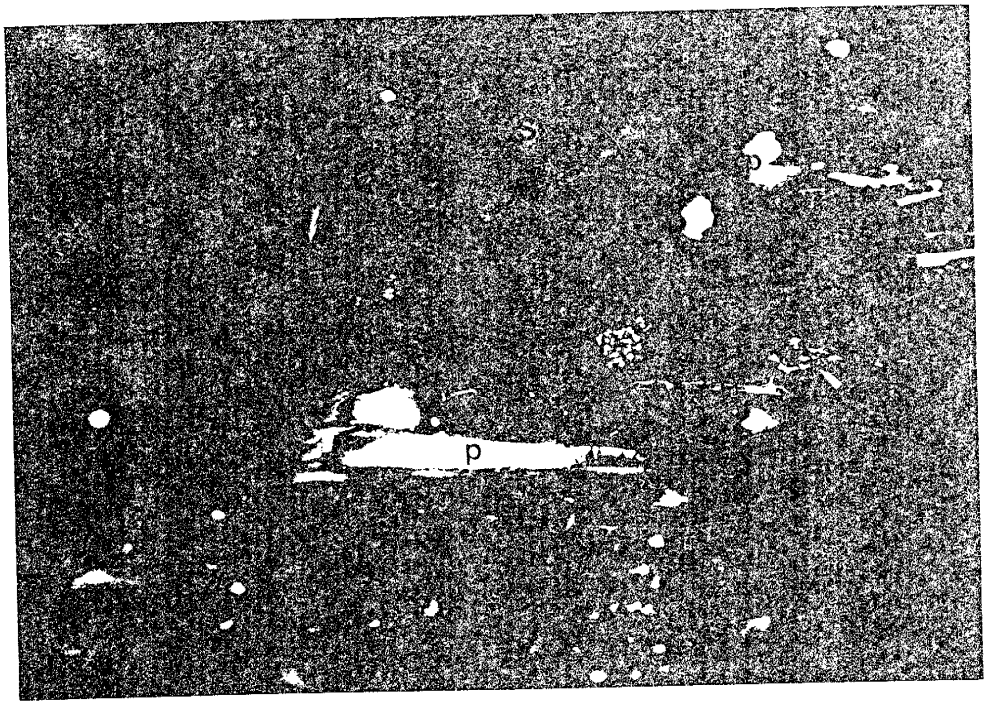

Figure 23. Siderite concretion (S), pyrite (P), and inertinite (I) association observed in sample S2-31. Reflected light, ppl, 200 X.

Figure 24. Siderite concretion (S), pyrite (P), and coal (C) association observed in sample S2-31. Note the deformation in the coal caused by the siderite. Reflected light, ppl, 200 X.

some of the siderite formed at the early stage of coal formation. The formation of siderite may have occurred in the following ways: 1) in the methanogenic zone, siderite precipitated after pyrite formation and depletion of sulfate ions, 2) in the sulfate reduction zone, pyrite precipitated first and then siderite precipitated between pyrite grains and other voids, or pyrite and siderite coprecipitated in the sulfate reduction zone in the presence of abundant iron, and 3) siderite precipitated in suboxic environment, where sulfate reduction and oxic conditions are juxtaposed producing oxidation of H_2S and concurrence of ferrous and ferric iron (Coleman, 1985).

Siderites from marine and fresh-water depositional environments are characterized by distinctive compositional trends; consequently elemental composition of early diagenetic siderites may be used to constrain depositional environment (Mozley, 1989). Siderites from fresh-water environments often have greater than 90 mol% $FeCO_3$ and commonly attain end-member composition and contain relatively more Ca and Mn versus Mg than marine siderites. Siderites from marine environments, on the other hand, are always extremely impure and generally have higher Mg/Ca ratios than fresh-water siderites.

Siderites associated with five low- and high-sulfur coal samples from the BB seam were analyzed for their chemistry. The electron microprobe analysis results for individual analyses are given in Appendix 2 (Table APP2-3). Plotting the composition (mol%) of the siderites on ternary diagrams in Figure 25 shows that these siderites are Fe-rich and plot toward the Fe end member. Comparison of these compositions with plots from Mozley (1989) show that the siderites from the BB seam plot (Figs. 26 and 27) in the area dominated by fresh-water siderites. The average elemental composition (mol%) of the siderites analyzed in this study and statistical results are listed in Table 21.

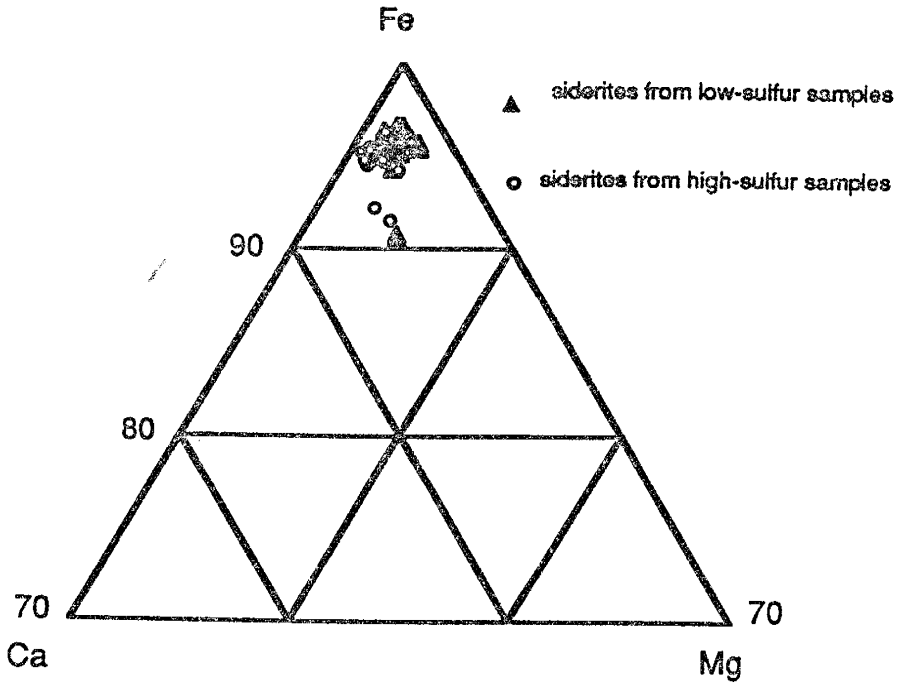

Figure 25. Ternary $CaCO_3$ - $MgCO_3$ - $FeCO_3$ plot for BB seam siderites analyzed by electron microprobe.

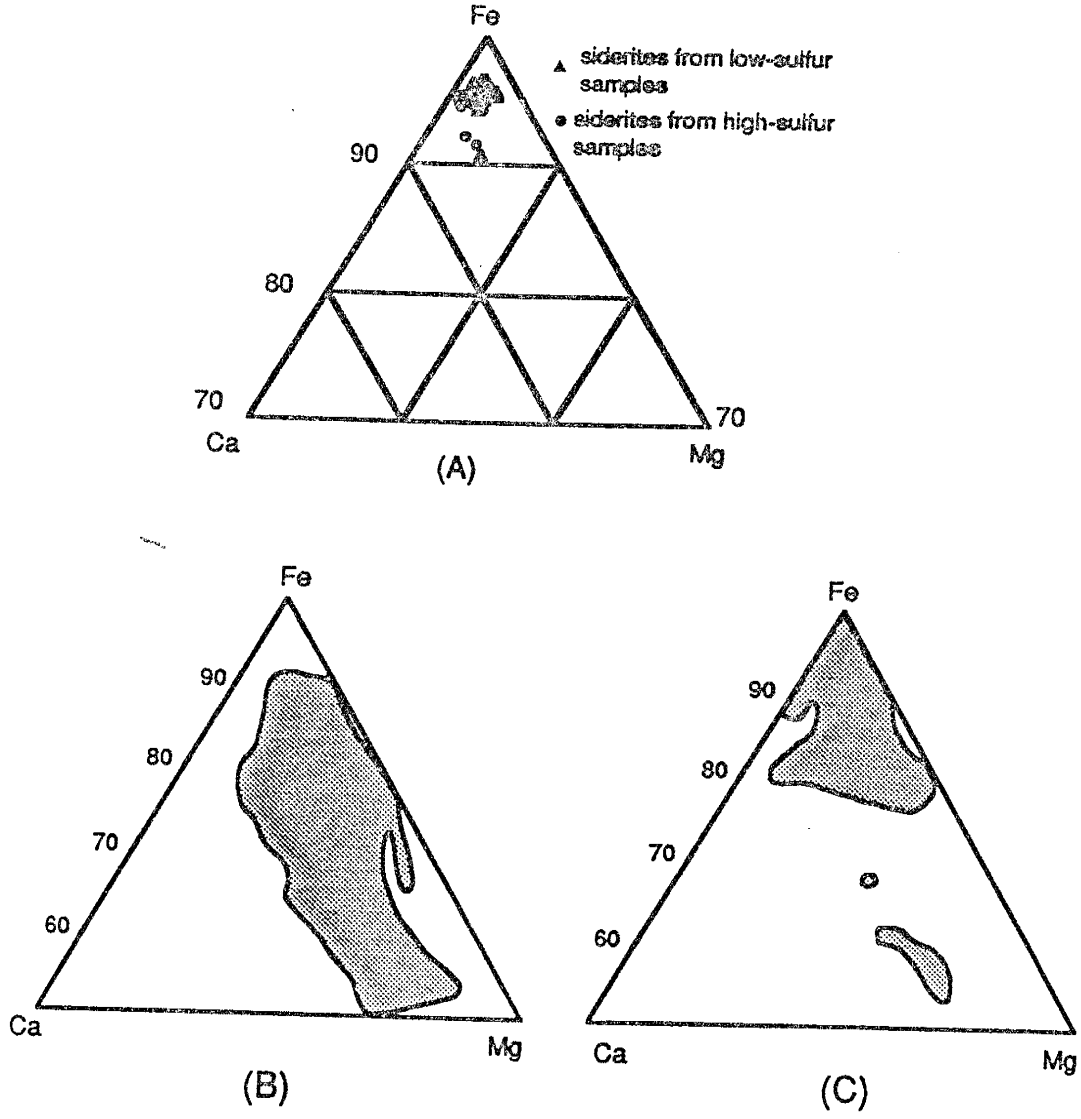

Figure 26. Ternary $CaCO_3$ - $MgCO_3$ - $FeCO_3$ plot for BB seam siderites (A) showing comparison with marine (B) and fresh-water siderites (C). Compositional fields for marine and fresh-water siderites from Mozley (1989).

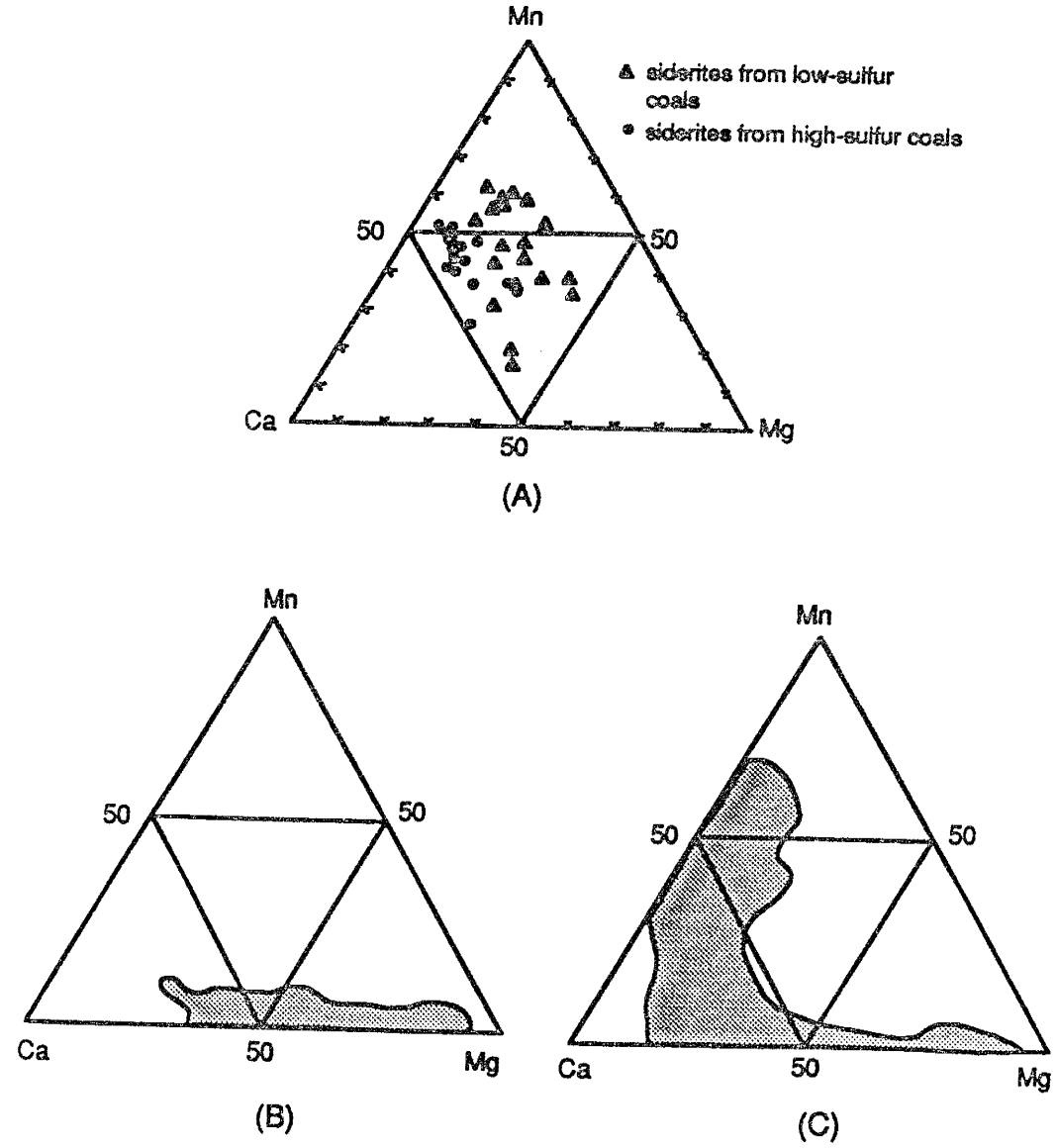

Figure 27. Ternary $CaCO_3$ - $MgCO_3$ - $MnCO_3$ plot for BB seam siderites (A) showing comparison with marine (B) and fresh-water (C) siderites. Compositional fields for marine and fresh-water from Mozley (1989).

Table 21. Element chemistry (mol %) of siderites and statistical results.

Element	high-sulfur samples (n = 21)	low-sulfur samples (n = 21)	ANOVA prob.*	M-W prob.**
Fe	89.68 (1.3)[a]	91.86 (2.44)	0.0009	0.0011
Mn	3.86 (0.65)	3.89 (1.25)	0.699	0.92
Mg	1.31 (0.74)	2.2 (0.87)	0.0001	0.0002
Ca	3.63 (0.51)	2.47 (0.95)	0.0001	0.0001
Mg/Ca	0.344 (0.15)	0.98 (0.45)	0.0001	0.0001

n = number of analyses; * = Analysis of variance probability of no difference at 90% significance level; ** = Mann-Whitney probability of no difference at 90% significance level; a = numbers in brackets indicate one standard deviation of the mean values

Table 21 shows that the siderites associated with the high-sulfur coal samples are characterized by higher Ca, and lower Mg and Fe contents. These siderites also have lower Mg/Ca ratios than the siderites associated with low-sulfur coal samples. The Mn content of siderites in both low- and high-sulfur samples is comparable.

4.4 Discussion and conclusions on sulfur distribution

Sulfur distribution within the BB seam varies both horizontally and vertically. Pyritic and organic sulfur are the dominant forms of sulfur with sulfate sulfur occurring in negligible amounts. Pyritic sulfur correlates strongly with total sulfur ($r = 0.83$). Organic sulfur shows slightly lower correlation with total sulfur ($r = 0.74$). There is a general increase in the pyritic/organic sulfur ratio with increase in total sulfur. These relationships suggest that variations in total sulfur in the coal samples seem to be mainly due to variations in the amounts of pyritic sulfur and, to a lesser extent, of organic sulfur. Total sulfur and pyritic sulfur show no correlation with ash ($r = -0.18$ for total sulfur-ash, and 0.07 for pyritic sulfur-ash pairs). The poor correlations suggest that whereas sulfides contribute strongly to the total sulfur content, their contribution to the ash content of the coal is insignificant. Organic sulfur shows a negative correlation ($r = -0.49$) with ash. Even though this correlation is not very strong, the negative relationship is expected. An increase in ash content implies an increase in the amount of mineral matter, with an associated decrease in the amount of organic matter that could act as a sink for the available sulfur.

Based on the sulfur distribution in the three drill holes, three distribution patterns are recognized in the BB seam: 1) higher sulfur contents in the coal samples adjacent to the seam margins and parting, and at certain stratigraphic levels (DHS1); 2) higher sulfur content toward the middle of the seam (DHS2);

and 3) distribution where the sulfur content in the coals varies slightly within the seam, but the maximum total sulfur content does not exceed 1%.

The distribution patterns indicate sulfur incorporation during two periods; a) during the early stages of peat deposition mainly as organic sulfur in DHS1 and DHS3 and mainly as pyritic sulfur in DHS2, and b) sulfur incorporation, mainly as pyritic sulfur, during and/or after cleat formation. The organic sulfur in the low-sulfur samples may have resulted from plant sulfate assimilation with susequent incorporation into the peat upon the death of the source plants (Casagrande, 1987). Additional organic sulfur may be incorporated into the peat by the reaction of excess hydrogen sulfide ions with coalifying peat components during the early stages of peat accumulation (Neavel, 1968; Casagrande, 1987). Low pyritic-sulfur contents in the low-sulfur coal samples may be partly due to a limited supply of iron that could have reacted with the available sulfide to form iron sulfides. During the early stages of peat accumulation, iron derived from the underlying claystones may react with sulfides in the peat to form iron sulfides close to the coal-claystone boundaries. Also, iron brought into the swamp during flooding episodes may react with sulfides in the peat to form iron sulfides near partings and claystones overlying the peat. These processes may explain the relatively high pyritic sulfur contents and thus higher total sulfur contents adjacent to seam margins and partings.

The high sulfur contents in DHS2 suggest that there was an abundant supply of sulfate ions during the accumulation of the peat at site 2 indicating perhaps the peat at this stage of accumulation may have been influenced by marine or brackish water sources. The extent of this influence may have been aerially limited as samples from DHS3 (about 250 meters laterally from DHS2) do not show such elevated sulfur concentrations at any level within the seam at that area. Occasional sea sprays, and high tides (that may have flooded the ancient

swamp locally) may have been the sources of the high-sulfate water. After flooding, when the tide retreated, the salt water that covered relatively higher areas in the swamp could have been flushed by fresh waters, whereas in relatively low lying areas of the swamp, some of the sea water may have been left to react with the peat thus enhancing the level of sulfur concentration in localized areas. There is no direct proof showing that there was a difference in elevation between DHS2 and DHS3. However, high-sulfur occurrences in predominantly low-sulfur areas are not uncommon in the Menefee Formation. Hoffman (1991) reported high-sulfur occurrences in the Monero coals (Menefee Formation coals) and suggested a back-barrier swamp environment where the swamp deposits were subjected to periodic invasions by the sea.

As/Se ratios in high- and low-sulfur coals from the BB seam show significant differences with an average of 8.38 for high-sulfur samples and 0.63 for low-sulfur coal samples. The As/Se ratio of pyrite in one high-sulfur coal sample was 10.72. The high As/Se ratios in the high-sulfur BB seam coals compare with values of around 10 observed in samples with marine and brackish overburden (Hickmott et al., 1992). These high As/Se values may be indicative of some marine or brackish water influence in the BB seam. More analyses of the iron sulfides associated with the low- and high-sulfur coals need to be done to strengthen this observation.

While As/Se ratios indicate some brackish or marine influence in the BB seam, siderite compositions in samples associated with both low- and high-sulfur coals suggest fresh-water depositional settings. However, as Mozley (1989) sampled only fresh and marine end members, composition of the siderites associated with high-sulfur BB seam coals may represent brackish environments. The siderite compositions suggest that the pore water composition was not of normal marine composition.

The fresh-water composition of the siderites may be explained as follows: 1) there was no marine or brackish water influence in the peat, in which case factors other than high-sulfate concentration are needed to explain the high sulfur contents observed. Such factors include unusual activity by sulfate reducing bacteria, and high fluid flux of low-sulfate fluid (Hickmott, personal comm.), or 2) there was a brackish water influence at the early stage that was diluted by fresh-water, folowed by siderite formation with fresh-water signature.

The following models are proposed to explain sulfur distributions in the BB seam coals:

	conditions	results
A)	low pH, low sulfate concentration, ample supply of iron, limited oxidation of peat and low detrital input	low-sulfur, low-ash, and relatively vitrinite-rich coal (bright coal); sulfur mainly as organic sulfur with some pyrite framboids and euhedral crystals.
B)	low pH, low sulfate concentration, ample supply of iron, limited oxidation of peat and low detrital input, some post-coalification sulfur addition	low- to medium-sulfur, low-ash, and relatively vitrinite-rich coal (bright coal); sulfur mainly in the form of organic and pyritic sulfur; some pyrite framboids and euhedral crystals, and cleat-filling pyrite close to seam margins.

C) relatively higher pH, high sulfate concentration (or high fluid flux of low-sulfate fluid), unusual activity by sulfate reducing bacteria, ample supply of iron, relatively high oxidation and/or relatively high detrital input

high-sulfur, high-ash, and relatively inertinite rich coal (dull coal); pyritic sulfur dominant; framboids, euhedral pyrite crystals, and void-filling massive pyrite abundant.

5- Major, minor and trace element geochemistry

5.1 Introduction

Source (origin), geochemical affinity or chemical (or mineral) associations, and geochemical processes may be used to classify elements occurring in coal (Palmer, 1983). Based on source (origin) and processes, inorganic constituents in coal are generally classified into four groups (Stach et al.,1982, Bouska, 1981):

(1) inorganic constituents from the original plant,

(2) inorganic-organic complexes and minerals which formed during the early stage of the coalification process, or were introduced into the early coal-forming environment by water and wind-transported detrital material, volcanic eruptions, and cosmic dust,

(3) minerals deposited by ascending or descending solutions in cracks and fissures or cavities, or by alteration of clastic material. This occurs after consolidation and coalification of the peat, and

(4) elements attached to coal at the contact with igneous intrusions as a result of exhalations or hydrothermal activity.

Minerals which have formed together with the coal or have been introduced into the swamp during the early stage of coalification are, in general, fine grained and intimately intergrown with the coal (Stach et al., 1982). Materials brought into the swamp by water, wind, or other external agents, commonly form ashy layers in the coal seam that are laterally continuous in many cases. Minerals that formed at a later stage of the coalification process are relatively coarse-grained and are not intimately intergrown with the coal because most of these were deposited in cracks and fissures (Stach et al., 1982).

The terms "inorganic constituents", "mineral matter", and "minerals" have been used interchangeably in some studies (Finkelman, 1980). Finkelman

(1980) made a distinction between these terms. He used the terms "mineral matter" and "minerals" for those species which are naturally occurring homogeneous solids formed inorganically and have a definite chemical composition and ordered atomic arrangements. The term "inorganic constituents" was used for all elements regardless of their mode of occurrence in the coal, except for carbon, oxygen, nitrogen, hydrogen, and organic sulfur. Palmer (1983) used the term "inorganic constituents" to include those species such as microbially generated pyrite, which, although organically formed, are physically identical to other minerals in coal. The above distinction between "inorganic constituents" and "mineral matter", or "minerals" is followed in this study.

Elements found in coal occur partly associated with the organic fraction and partly associated with the inorganic fraction (Swaine, 1990). Organic association includes: (1) elements that form organometallic complexs or chelates, and (2) inorganic constituents fixed by adsorption, or ion exchange on functional groups such as acid groups (-COOH), or phenolic groups (-OH). Elements in the inorganic fraction (mineral matter) can occur as discrete minerals, as replacement ions in minerals, and adsorbed on mineral surfaces (Swaine, 1990).

Various researchers have used different methods and approaches to identify and characterize the modes of occurrence and distributions of minor and trace elements in coal. Palmer (1983) noted that the elements in coal are primarily chalcophile (associated with sulfides), lithophile (associated with silicates and oxides), and biophile (associated with organic matter). By using plots of element contents in coal and coal ash against the ash content, Nicholls (1968) described elements in coal as being : 1) associated with the organic fraction (high organic affinity), 2) associated with the inorganic fraction (high

inorganic affinity), and 3) associated with both the organic and inorganic fractions. Solari et al., (1989) discussed an approach (basically an extension of Nicholls' (1968) approach) to the characterization of trace elements in coal based on a model that uses analyzed elemental concentrations in coal or coal ash as a function of the ash content of the coal to calculate elemental concentrations in the organic and inorganic components. Gluskoter et al., (1977) calculated an index of "organic affinity" of the elements from washability curves of the data determined on specific gravity fractions of the washed coals. On the basis of the value of the "organic affinity" index, they classified the elements as "organic" (Ge, Be, B, Sb), "intermediate organic" , "intermediate inorganic", and "inorganic" (Zn, Cd, Mn, As, Mo, and Fe). Finkelman (1980) used scanning electron microscopy (SEM) and energy-dispersive-x-ray detection to identify modes of occurrences of trace elements in coal. Palmer and Filby (1984) used a combination of analytical techniques such as x-ray flouresence spectroscopy (XRF), SEM, and INAA to study the correlation of trace elements with major minerals and the role of minor minerals in the mode of occurrence of trace elements in size and density separates of low temperature ashed coals. Coal demineralization (Kuhn et al., 1980), and ion-exchange studies (Miller and Given, 1978) have also been used to determine organic and inorganic association of elements in coal. Finkelman et al., (1990) used leaching and combustion experiments to establish modes of occurrences of some trace elements. Statistical analyses have been used to characterize the variability of element content in coal and establish the organic/inorganic affinities of trace elements in coal (Glick and Davis, 1987, Mukherjee et al., 1988). For a review of the literature on the various approaches and analytical techniques that have been used to characterize trace element occurrence in coal, the reader is refereed to Finkelman (1980), and Swaine (1990).

Due to a limited budget and time, such analytical techniques as Scanning electron microscopy (SEM), and experiments involving leaching ,combustion, and ion-exchange were not used in this study. Only a few analytical techniques including instrumental neutron activation analysis (INAA), x-ray diffraction analysis (XRD), electron microprobe analysis (EMP), proton-induced x-ray emission analysis (PIXE) , and x-ray fluoresence analysis (XRF) and statistical analyses (correlation analysis, principal component analysis, cluster analysis etc.) were used to characterize trace-element distributions and identify their modes of occurrence.

5.2 - Major oxide chemistry and mineralogy

5.2.1 - Major oxide chemistry

Coal ash compositions provide valuable information on mineralogical and elemental composition of coal, and aid in the evaluation of slagging properties, ash fusion temperatures, and corrosive potentials (Valkovic, 1983). For instance, the "base to acid ratio" is used to estimate slag viscosity (Sage and McIlroy, 1959). As this ratio increases to 1, the viscosity of the slag decreases. The "base to acid ratio" is defined by the following equation:

$$\text{Base/acid} = \frac{Fe_2O_3 + CaO + MgO + Na_2O + K_2O}{SiO_2 + Al_2O_3 + TiO_2}$$

The major oxides give clues to what minerals may be present in the coal. Aluminium is a major constituent of clays and feldspars. Silica is a major component in quartz and clay minerals. Phosphorus is a major element in phosphates. Potassium is associated with illite, mixed layer clays, and feldspars. Calcium may be associated with calcite, gypsum, illite, mixed layer clays, and

minor quantities of silicates and phosphates. Sodium is primarily asociated with clay minerals. Titanium occurs in rutile, anatase, and also as a major constituent in mixed layer clays. Manganese is present in pyrite, calcite and other carbonates, and clay minerals. Iron occurs in sulfides, siderite, ankerite, and illite. Magnesium may indicate the presence of carbonate minerals (Palmer, 1983).

The silicate minerals, mainly alumino-silicates and quartz, constitute between 60 to 90% of the total mineral matter in most bituminous coals (Raask, 1985). The alumino-silicate minerals are present largely in the form of clays in the coal and associated strata. The most common alumino-silicate species are muscovite and illite (potassium-alumino silicates), mixed layer illite-montmorillonite, and kaolinite.

The approximate amounts of quartz, potassium-alumino silicates, and kaolinite species in the mineral matter may be calculated using the concentrations of SiO_2, Al_2O_3, and K_2O in the coal ashes (Raask, 1985). Coal ash and finely-ground claystone and sandstone samples were analyzed for major-oxide content (Table 22). Approximate amounts of quartz, potassium-alumino silicates, and kaolinite in BB seam coals and associated lithologies are calculated and listed in Table 23. The following equations from Raask (1985) were used to calculate the approximate amounts of quartz, potassium-alumino silicates, and kaolinite:

(1) $SiO_{2(Q)} = SiO_{2(T)} - 1.5\ (Al_2O_3)$

(2) $K_{(Al\ -\ Sil)} = 9.1\ K_2O$

(3) $\text{Kaolinite} = (SiO_{2(T)} + Al_2O_3 + K_2O) - (SiO_{2(Q)} + K_{(Al\ -\ Sil)})$

where $SiO_{2(T)}$, Al_2O_3 and K_2O are wt% values from XRF analyses, and $SiO_{2(Q)}$ and $K_{(Al\ -\ Sil)}$ are approximate quartz and potassium-alumino silicate contents (in %), respectively.

Average values of major oxides in BB seam coals and associated lithologies are listed in Table 24. Major-oxide content of BB seam coals are compared with major-oxide contents in coals from the Rocky Mountain province and the San Juan River region (Table 25). Table 25 also shows a range of major-oxide compositon of coal ash compiled by Valkovic (1983).

The average SiO_2 content in BB seam coal ash is lower than that of the associated claystones and sandstones (Table 26). This is probably due to a reduced quartz input into the swamp. The calculated quartz content in the coal ash is comparable to that of the claystones but lower than that of the sandstones. A higher proportion of kaolinite relative to illite (potassium-alumino silicates) may also result in lower SiO_2 content of the coals (Spears and Martinez-Tarazona, 1993). The kaolinite to potassium-alumino silicate ratio in the coal ash is higher than that of the associated claystones and sandstones.

The average Al_2O_3 content of the coal ash is comparable to that of the claystones and greater than the sandstones. The higher Al_2O_3 content of the coal ash and claystones relative to that of the sandstones is probably due to a higher proportion of kaolinite in the coal ash and claystones relative to their potassium-alumino silicate content.

Average contents of CaO, MgO, Fe_2O_3, and MnO in the coal ash are higher than those of the claystones and sandstones. The high Fe_2O_3 content in the coal ash is suggested to be due to the presence of diagenetic pyrite and iron-rich carbonates (siderites for example) in the coals.

Table 22. Major-oxide content of selected coal samples and associated lithologies.

Sample No.	lithology	Distance	SiO2	TiO2	Al2O3	Fe2O3	MnO	MgO	CaO	Na2O	K2O	P2O5	Total %
S3-5	Claystone	258.89	54.94	0.632	16.616	20.279	0.508	2.041	1.014	0.489	2.789	0.105	99.41
S3-6	Durain	257.64	62.849	1.007	19.814	4.401	0.126	3.065	5.703	1.156	1.664	0.055	99.84
S3-17	Vitrain	177.95	50.251	1.011	27.811	14.124	0.34	3.214	2.714	1.342	0.571	0.067	101.44
S3-18	Claystone parting	169.51	53.624	0.97	40.285	3.03	0.067	0.246	0.354	0.139	0.162	0.031	98.91
S3-28	Durain	97.33	37.903	0.651	11.632	41.2	1.524	4.04	1.711	1.898	0.893	0.06	101.52
S3-40	Durain/carb.shale	7.34	70.395	1.438	22.245	1.046	0.019	0.778	1.346	0.294	1.452	0.054	99.07
S3-42	Claystone	0	72.054	0.977	21.044	1.876	0.014	1.451	0.632	0.213	2.129	0.037	100.43
S1-31	Claystone parting	143.43	56.174	0.916	41.632	0.521	0.013	0.433	0.341	0.114	0.122	0.035	100.5
S1-54	Claystone	0	70.969	0.898	23.415	1.426	0.015	1.302	0.54	0.172	2.376	0.054	101.16
S2-2	Sandstone	268.25	79.206	0.512	14.044	1.318	0.035	0.433	0.913	1.589	3.064	0.145	101.26
S2-5	Claystone	238.25	61.591	0.787	19.724	9.161	0.258	1.537	0.799	0.612	3.367	0.136	97.97
S2-8	Durain	233.25	58.507	1.132	22.345	7.762	0.041	3.001	2.177	1.35	1.804	0.058	98.18
S2-11	Durain	201.38	65.639	0.95	25.864	2.601	0.024	1.194	1.264	0.212	1.774	0.052	99.57
S2-21	Durain	144.05	45.65	1.029	26.44	20.177	0.113	2.287	2.981	1.429	0.15	0.046	100.3
S2-43	Sandstone	-18	79.388	0.681	15.893	1.838	0.039	0.475	0.324	0.261	2.478	0.035	101.41

Table 23. Approximate quartz, potassium-alumino silicate, and kaoilinte concentrations in BB seam coals and associated lithologies.

	% quartz	% $K_{(Al - Sil)}$	% kaolinite	% Total	$K/K_{(Al - Sil)}$
coal (n=7)	22.41	10.83	46.14	79.38	4.26
claystone (n=6)	20.83	16.56	53.14	90.53	3.21
sandstone (n=2)	58.84	25.21	13.0	97.05	0.51

n = number of samples; $K_{(Al - Sil)}$ = potassium-alumino silicates; $K/K_{(Al - Sil)}$ = kaolinite to potassium-alumino silicate ratio; % Total = total amount of silicate minerals (approximated by the sum of quatz, kaolinite and potassium-alumino silicates) contributing to the mineral matter content of the coals

Table 24. Major-oxide content in BB seam coals and associated lithologies (mean concentration in %).

major oxides	coal ash n = 7	sandstone n = 2	claystone n = 6
SiO_2	55.88 (11.70)*	79.30 (0.13)	61.56 (8.18)
Al_2O_3	22.31 (5.48)	14.97 (1.31)	27.15 (11.0)
CaO	2.56 (1.53)	0.62 (0.42)	0.61 (0.26)
MgO	2.51 (1.17)	0.45 (0.03)	1.17 (0.69)
Na_2O	1.10 (0.62)	0.92 (0.94)	0.29 (0.21)
K_2O	1.19 (0.65)	2.77 (0.41)	1.82 (1.37)
Fe_2O_3	13.04 (14.14)	1.58 (0.37)	6.05 (7.62)
MnO	0.31 (0.54)	0.04 (0.003)	0.14 (0.20)
TiO_2	1.03 (0.23)	0.60 (0.12)	0.86 (0.13)
P_2O_5	0.06 (0.007)	0.09 (0.08)	0.07 (0.04)

n = number of samples; * = number in parenthesis are values of the standard deviation

Table 25. Comparison of major-oxide content in ash from BB seam coals with other coals (mean concentration of coal ash in %).

major oxides (%)	BB seam coal ash n = 7	Rocky mountain * n = 295	San Juan River* n = 79	Range of oxides in coal ash ***
SiO_2	55.88 (11.70)**	46	54	30 - 60
Al_2O_3	22.31 (5.48)	21	24	10 - 40
CaO	2.56 (1.53)	8.9	4.9	2 - 20
MgO	2.51 (1.17)	1.63	0.88	0.5 - 4
Na_2O	1.10 (0.62)	1.39	1.56	1 - 4****
K_2O	1.19 (0.65)	0.65	0.61	****
Fe_2O_3	13.04 (14.14)	7.6	3.8	5 - 30
MnO	0.31 (0.54)	0.049	0.022	n.a
TiO_2	1.03 (0.23)	0.89	1.0	0.5 - 3
P_2O_5	0.06 (0.007)	n.a	n.a	n.a

n = number of samples; * = Rocky Mountain province and San Juan River region coal samples ashed at 525 ^{0}C (from Hatch and Swanson, 1976) ; ** = standard deviation ; *** = typical values for oxides in coal ash from Valkovic (1983); **** = $Na_2O + K_2O$ reported as alkalies; n.a = data not available

The relatively higher CaO, MgO, and MnO content in the coal ash is probably due to the presence of carbonates including calcite and siderite in the coals in a relatively higher concentrations than in the claystones and sandstones.

Average Na_2O content of the coal ash is comparable to that of the sandstones and higher than that of the claystones. The higher Na_2O content of the coal ash and the sandstones may be due to a relatively higher feldspar content. Average K_2O, TiO_2, and P_2O_5 contents in coal ash, claystone, and sandstone are similar.

Major-oxide composition of coal ash in the BB seam falls within ranges given for typical values for oxides in coal ash (Table 25). Average SiO_2, Al_2O_3, MgO, Na_2O, K_2O, and TiO_2, concentrations in BB seam coal ash are similar to those reported for Rocky Mountain Province and San Juan River region coals. The San Juan River Region coals occur in the Rocky Mountain Province and include coals from northwestern New Mexico and southeastern Colorado (Hatch and Swanson, 1976). The average CaO concentration in BB seam coal ash is lower while the average Fe_2O_3 content is higher compared to Rocky Mountain Province and San Juan River region coals.

Ash fusion charcteristics are one of the more important properties of coal for use in pulverized fuel bolers. Coals that have low ash fusion temperatures are likely to cause slag deposits to form on the boiler surfaces (Ward, 1984). Schmidt (1976) gives a list of parameters regarding fouling and slagging properties of coals. Even though most of the emperical relationships were formulated for eastern coals, they could be used to gain some insight into the fouling and/or slagging behavior of some western coals. Coal ash from the BB seam coals has an average base/acid ratio of 0.29 (s.d = 0.31). This value gives an estimated ash fusion temperature 2600 ^{0}F at 250 poises when plotted on the viscosity vs. base-to-acid ratio diagram of Sage and McIlroy (1959). This

value compares with ash fusion temperatures of 2700 ^{0}F and 2800 ^{0}F reported for Standing Rock and San Mateo coal fields (in New Mexico) respectively (Campbell and Roybal, 1987). The high ash fusion temperature of the BB seam coals indicates a low slagging potential of the coals according to Scmidt's (1976) classification.

5.2.2 - Mineralogy

Minerals identified in coal include clay minerals, sulfides, carbonates, oxides, hydroxides, phosphates, sulfates, silicates, and salts (Stach et al., 1982). Quartz, kaolinite, siderite, and pyrite are fairly common. Minerals such as Kyanite occur very rarely. Finkelman (1980) compiled a fairly extensive list of minerals that occur in coals. Identification of major and accessory minerals in coal is important, as they can give insight into source rocks, and behavior of coals in beneficiation processes (Swaine, 1990). These minerals can also be hosts to trace elements in coal. For instance, pyrite may host Sb, Co, and Zn; and clay minerals may contain such trace elements as Cr, Cs, Th, Ti, U, and V as trace constituents (Martin and Cavaroc, 1991).

In the BB seam, pyrite and calcite were observed in handspecimen. Electron microprobe analyses have also shown the presence of these minerals and quartz in the coal samples. Petrographic analyses have shown the presence of pyrite, marcasite, and siderite in the coals. X-ray diffraction analysis of non-coal lithologies and low temperature ash (LTA) of coal samples shows a variety of minerals occurring in the BB seam. The minerals identified in the BB seam are listed in Table 26.

In gerneral, quartz and kaolinite are the dominant minerals in BB seam coals and bounding lithologies. The approximate concentrations of quartz, and kaolinite in BB seam coals and associated claystones and sandstones are listed in Table 23. Pyrite, siderite, bassanite, feldspars, and illite are fairly common.

The bassanite may have formed as a result of oxidation of sulfide minerals during the low temperature ashing process (Renton, 1982) and thus may not be an original coal mineral. Barite and celsian occur rarely. Calcite was detected in few samples during x-ray diffraction analyses.

Table 26. Minerals identified in BB seam coals and associated lithologies.

Sample	Lithology	Q	K	M	P	S	SP	B	F	I	C	BA	CE
S1-4	claystone	xx	x	tr					x	tr			
S1-5	coal	xx	x					x	tr				
S1-30	coal	x	xx		tr			x	x				
S1-31	claystone	x	xx	tr									
S1-32	coal	x	x		x			x	x				
S1-40	coal	xx	x					x					
S1-45	coal	x	x		x			tr	x			tr	tr
S1-51	coal	xx	x		x		tr	tr			x		
S1-54	claystone	xx	x	tr					tr				
S2-2	sandstone	xx	x	tr					x				
S2-3	claystone	xx	x	tr					x	x			
S2-5	coal	xx	x	x		tr			x	tr			
S2-11	coal	xx	x		tr								
S2-18	coal	xx	x		x	tr							
S2-19	coal	xx	x		x	tr	tr	tr			x		
S2-21	coal	xx	x		x	tr							
S2-29	coal	xx	x								tr		
S2-31	coal	xx	x			x				tr			
S2-40	coal	xx	x		tr			x	x				
S2-41	claystone	xx	x							tr			
S2-42	claystone	xx	x	tr		tr			tr				
S2-43	sandstone	xx	x	tr					x				
S3-5	coal	xx	x			x			tr	tr			
S3-6	coal	xx	x					tr		tr			x
S3-17	coal	xx	x					tr			tr		
S3-18	claystone	x	xx										
S3-19	coal	xx	x	x		tr							
S3-28	coal	x	x	tr		xx				tr			
S3-41	claystone	xx	x	tr						tr			
S3-42	claystone	xx	x	tr					tr				

XX = relatively high concentration; X = 3 or more peaks identified; tr = 2 peaks identified;
Q = quartz; K = kaolinite; M = micas; P = pyrite; S = siderite; SP = sphalerite; B = bassanite;
F = feldspars; I = illite; C = calcite; BA = barite; CE = celsian ($BaAl_2Si_2O_8$)

5.3 - Trace and minor elements in the BB seam

A total of 43 samples, including 30 coal and 13 non-coal samples, from 3 drill holes penetrating the BB seam were analyzed using instrumental neutron activation analysis (INAA). The 24 elements determined in whole coal samples, the bounding lithologies (claystones and sandstones), and claystone partings, include: arsenic (As), barium (Ba), cerium (Ce), cobalt (Co), chromium (Cr), cesium (Cs), europium (Eu), iron (Fe), hafnium (Hf), lanthanum (La), lutetium (Lu), sodium (Na), rubidium (Rb), antimony (Sb), scandium (Sc), selenium (Se), samarium (Sm), strontium (Sr), tantalum (Ta), terbium (Tb), thorium (Th), uranium (U), ytterbium (Yb), and zinc (Zn).

Trace-element concentrations in drill holes DHS1, DHS2, and DHS3 are given in Appendix 3. Average trace-element concentration in whole coal (average of the three drill holes) is given in Table 27. Comparisons of average element contents in whole coal, claystone and sandstone samples (from the BB seam) with average concentration in the earth's crust (ACC) (Taylor, 1964), average concentrations in shales and sandstones (Turekian and Wedepohl, 1961), and other coals (Hatch and Swanson, 1976, Gluskoter et al., 1977) are given in Tables 28, 29, and 30, respectively. Enrichment factors are calculated for each element by dividing the geometric mean values in the whole coal by the ACC, and average concentrations in shales and sandstones respectively.

Table 27 shows two groups of elements:

1) elements that have relatively large ranges (2 orders of magnitude or greater) and coefficients of variation > 100% include As, Ba, Co, Cs, Fe, Rb, Sb, Th, U, and Zn; and 2) elements that have relatively low coefficients of variation (<100%) and distribution ranges of less than 2 orders of magnitude. This group includes Ce, Cr, Eu, Hf, La, Lu, Na, Sc, Se, Sm, Sr, Yb, Ta, and Tb.

Table 27. Trace element concentrations in BB seam coals (concentrations in ppm unless noted otherwise).

Element	Mean[a]	S.D	Co.Va	GM	Range	OM	N
As	5	11	236	1.8	.50 - 55	2	30
Ba	337	811	241	105	5 - 4120	3	30
Ce	19	16	86	14	3 - 60	1	30
Co	5	12	215	2	.40 - 65	2	30
Cr	13	10	83	10	3 - 47	1	30
Cs	2	3	130	1	0 - 10	2	18
Eu	.34	.20	60	.3	0 - .82	1	30
Fe (%)	1.2	2.53	213	.43	.06-12.8	2	30
Hf	2	1	71	1	.3 - 5	1	30
La	10	8	87	7	2 - 32	1	30
Lu	.12	.08	62	.1	0 - 0.3	1	30
Na	238	143	60	200	76 - 580	1	30
Rb	17	19	112	7	1 - 61	2	16
Sb	2	3	116	1	1 - 10	2	23
Sc	3	2	71	3	1 - 9	1	30
Se	3	2	57	3	1 - 9	1	30
Sm	2	1	66	1	.2 - 4	1	30
Sr	112	58	52	96	37 - 230	1	30
Ta	.35	.24	67	.26	.04 - .80	1	30
Tb	0.25	0.16	64	0.2	0.04 - 0.54	1	30
Th	7	10	141	4	.5 - 54	2	30
U	3	3	100	2	.2 - 15	2	30
Yb	.90	.54	63	.70	.1 - 2	1	30
Zn	20	37	184	11	3.5 - 199	2	30

a = arithmetic mean; S.D = standard deviation between the arithmetic means; Co.Va = coefficient of variation; GM = geometric mean; OM = order of magnitude difference between maximum and minimum concentrations; N = number of samples

The distribution of minor and trace elements in BB seam coals show that 2/3 of the elements have log normal (or close to log normal) distributions. Elements with this distribution include As, Ba, Ce, Co, Cr, Cs, Fe, La, Rb, Sb, Sc, Se, Tb, Th, U, and Zn. The other 1/3 of the elements, Eu, Hf, Lu, Na, Sm, Sr, Ta, and Yb, have normal distributions.

Table 28 shows that the BB seam coals are depleted in the following elements relative to ACC; Na, Sc, Cr, Fe, Co, Zn, Sr, Ba, La, Ce, Sm, Eu, Yb, Lu, Hf, Ta, Th, U, Rb, and Cs. Arsenic values are close to ACC. Antimony shows slight enrichment in the coals (5 times ACC). Selenium is the only element that is highly enriched (60 times ACC) in the coal samples.

Table 29 shows that claystones associated with the BB seam are depleted in Ba, Co, Eu, Fe, Lu, Na, Rb, Sc, Sm, Sr, Ta, Yb, and Zn relative to ACC. As, Ce, Hf, La, Th, and U concentrations are close to ACC. Cesium is slightly enriched in the claystones while Sb and Se show significant enrichments relative to ACC. Cerium, Cs, Hf, Se, Ta, Th, and U concentrations in the BB seam claystones are close to concentrations in average shales (Turekian and Wedepohl, 1961). The rest of the elements are depleted in the claystones relative to their concentration in average shales.

Trace element concentrations in two sandstone samples overlying the BB seam at DHS2 are compared with ACC of the elements and element concentrations in sandstones (Table 30). Table 30 shows that the sandstones associated with the BB seam are depleted in Cr, Sc, Na, Sr, La, Ce, Sm, Eu, Yb, Lu, Ta, and Tb relative to ACC. Cobalt, Cs, Rb, Th, U, and Zn concentrations are close to ACC. Arsenic and Hf are slightly enriched whereas Se and Sb are significantly enriched in the BB seam sandstones relative ACC. Compared to average sandstone concentrations (Turekian and Wedephol, 1961), the BB seam sandstones are depleted in Ce, Cr, Eu, La, Lu, Na, Sm, and Yb. Iron, Hf, and Rb

Table 28. Comparison of average trace-element concentration in BB seam whole coal samples with average crustal concentration (ACC) (concentrations in ppm unless noted otherwise).

Element	BB seam geometric mean	ACC	EF 1	n
As	1.8	1.8	1.0	30
Ba	105	425	.25	30
Ce	14	60	. 23	30
Co	2	25	.08	30
Cr	10	100	.1	30
Cs	1	3	.33	18
Eu	0.3	1.2	.25	30
Fe (%)	0.43	5.63	.08	30
Hf	1	3	.33	30
La	7	30	.23	30
Lu	0.1	.5	.20	30
Na (%)	.02	2.36	.01	30
Rb	7	90	.08	16
Sb	1	0.2	5	23
Sc	3	22	.14	30
Se	3	.05	60	30
Sm	1	6	.17	30
Sr	96	375	.26	30
Ta	0.26	2	.13	30
Tb	0.20	0.9	0.22	30
Th	4	9.6	.42	30
U	2	2.7	.74	30
Yb	0.7	3	.23	30
Zn	11	70	.16	30

EF 1 = enrichment factor relative to ACC; n = number of samples; ACC values from Taylor (1964)

Table 29. Comparison of average trace-element concentration in BB seam claystones with average crustal concentration (ACC) and average concentration of the elements in shale (concentrations in ppm unless noted otherwise) .

Element	BB seam geometric mean	ACC	Average in shales	EF 1	EF 2	n
As	3	1.8	13	1.67	.23	11
Ba	232	425	580	.55	.4	11
Ce	63	60	59	1.05	1.07	11
Co	6.4	25	19	.26	.34	11
Cr	29	100	90	.29	.32	11
Cs	11	3	5	3.67	2.2	8
Eu	.9	1.2	1	.75	.9	11
Fe (%)	1.63	5.63	4.72	.29	.34	11
Hf	6	3	2.8	2	2.1	11
La	34	30	92	1.13	.37	11
Lu	.3	.5	.7	.6	.43	11
Na (%)	.09	2.36	0.96	.04	.09	11
Rb	77	90	140	.85	.55	8
Sb	1.3	0.2	1.5	6.5	.87	11
Sc	9	22	13	0.41	0.7	11
Se	1.5	.05	.6	30	2.5	11
Sm	4.4	6	6.4	.73	.69	11
Sr	139	375	300	.37	.46	11
Ta	1.4	2	0.8	.7	1.75	11
Tb	.7	0.9	1.0	0.78	.7	11
Th	13	9.6	12	1.35	1.08	11
U	5	2.7	3.7	1.85	1.35	11
Yb	2	3	2.6	.67	.77	11
Zn	45	70	95	.64	.47	11

EF 1= enrichment factor relative to ACC; EF 2= enrichment factor relative to average concentration in shales; n = number of samples; ACC values from Taylor (1964); average concentration in shales from Turekian and Wedepohl (1961)

Table 30. Comparison of average trace element concentration in BB seam sandstones with average crustal concentrations (ACC) and average concentration of the elements in sandstones (concentrations in ppm unless noted otherwise).

Element	BB seam geometric mean (n = 2)	ACC	Average in sandstones	EF 1	EF 2
As	7.5	1.8	1.0	4.16	7.5
Ba	562	425	x0. *	1.32	n.a.
Ce	45	60	92	0.75	0.49
Co	30	25	0.3	1.2	101.21
Cr	26	100	35	0.26	0.74
Cs	3.4	3	0.x *	1.13	n.a.
Eu	0.8	1.2	1.6	0.67	.5
Fe (%)	1	5.63	0.98	0.18	1.02
Hf	7.5	3	3.9	2.5	1.92
La	22	30	30	0.73	0.73
Lu	0.33	.5	1.2	0.66	0.28
Na (%)	0.29	2.36	0.33	0.12	0.88
Rb	91	90	60	1.01	1.52
Sb**	2.3	0.2	0.0x *	11.5	n.a.
Sc	7	22	1.0	0.32	7
Se	0.43	.05	0.05	8.6	8.6
Sm	3.6	6	10	.6	0.36
Sr	105	375	20.0	0.28	5.25
Ta	1.3	2	0.0x *	0.65	n.a.
Tb	0.55	0.9	1.6	0.61	0.34
Th	10	9.6	1.7	1.04	5.88
U	3	2.7	.45	1.11	6.67
Yb	2.35	3	4	0.78	0.59
Zn	81	70	16	1.16	5.06

* = only order of magnitude given; n.a. = concentration comparison can't be done quantitatively as values are given as order of magnitudes only; ** = only one sample; ACC values from Taylor (1964); average concentrations in sandstone from Turekian and Wedepohl (1961)

concentrations are close to average sandstone concentrations. Even though only order of magnitudes are given for concentration values for Ba, Cs, Sb, and Ta, these elements appear to be enriched in the BB seam sandstones relative to the average sandstone concentrations. Elements that show significant enrichment in the BB seam sandstones relative to average concentrations in sandstone (Turekian and Wedephol, 1961) are As, Co, Sc, Se, Sr, Th, U, and Zn. Cobalt shows the highest enrichment (about 100 times).

Trace-element concentrations in the BB seam coals are compared to average concentrations in the associated claystones (Table 31). The enrichment factors (EF) in coal (Table 31) show that all the elements except Se are depleted in the coal relative to concentrations in the claystones. Using La as a predominantly detrital element, the enrichment factors were normalized to La to reduce the effects of variation in detrital geochemistry (Spears and Martinez-Tarazona, 1993). Lanthanum was selected as a normalizing element because: 1) it has good analytics (INAA data), and 2) as a REE it is coherent during transportation and deposition and thus may be transfered nearly in bulk from source to sediment (Taylor and McLennan, 1985). The enrichment factors scaled for equal La (Table 31) show that As, Ba, Sb, Se, and Sr are significantly enriched ($EF_{La} > 2$) in the coals. Cesium and Rb are significantly depleted in the coals and the rest of the elements show EF_{La} values close to one, but in general < 2.

Trace element concentrations in the BB seam were also compared with element concentration in coals from the San Juan River region, Rocky Mountain Province and Eastern US coals (Table 32). Compared to San Juan River Region coals, the BB seam has lower concentrations of Ba, Na, and U, and higher concentrations of Cr, Sb, and Se. Arsenic, Co, Fe, Sc, Sr, Th, Yb, and Zn concentrations are about equal in the BB seam and San Juan River Region

Table 31. Comparison of trace-element concentrations in BB seam whole coal samples with concentrations in the associated claystones (concentrations in ppm unless noted otherwise).

Element	coal mean[a] (n=30)*	claystone mean[a] (n=11)	EF	EF_{La}
As	1.8	3	.6	2.9
Ba	105	232	.45	2.14
Ce	14	63	.22	1.05
Co	2	6.4	.31	1.5
Cr	10	29	.34	1.6
Cs	1	11	.09	.43
Eu	0.3	.9	.33	1.6
Fe (%)	0.43	1.63	.26	1.24
Hf	1	6	.17	.81
La	7	34	.21	1.0
Lu	.1	.3	.33	1.6
Na	200	900	.22	1.05
Rb	7	77	.09	.43
Sb	1	1.3	.78	3.71
Sc	3	9	.33	1.6
Se	3	1.5	2	9.5
Sm	1	4.4	.23	1.1
Sr	96	139	0.69	3.3
Ta	.26	1.4	.19	.9
Tb	.2	.7	.28	1.3
Th	4	13	.31	1.5
U	2	5	.4	1.9
Yb	.7	2	.35	1.7
Zn	11	45	.24	1.14

a = geometric mean; n = number of samples (n = 16 for Rb, 23 for Sb, and 18 for Cs in the coals); EF = enrichment factor in coal; EF_{La}= enrichment factor in coal scaled for equal lanthanum

Table 32. Comparison of average concentration of elements in the BB seam (whole coal basis) with other coals (concentrations in ppm unless noted otherwise).

Element	BB seam (N = 30) GM	Rocky Mountain [1] (N = 295) GM	San Juan River [1] (N = 79) GM	Eastern US[2] GM
As	1.8	2.0	2.0	15 *
Ba	105	150	300	170 **
Ce	14	n.a	n.a	23 **
Co	2	1.5	2.0	7.6 *
Cr	10	5.0	5.0	18 *
Cs	1 (N = 18)	n.a		1.6 **
Eu	0.3	n.a	n.a	0.47 **
Fe (%)	0.43	0.34	0.48	1.3 *
Hf	1	n.a	n.a	1.1 **
La	7	n.a	n.a	14 **
Lu	0.1	n.a	n.a	0.18 **
Na(%)	.02	.055	0.203	0.03 *
Rb	7 (N =16)	n.a		19 **
Sb	1 (N = 23)	0.3	0.4	1.1 *
Sc	3	1.5	3.0	4.5 **
Se	3	1.2	1.9	3.4 *
Sm	1	n.a	n.a	2.4 **
Sr	96	100	100	100 **
Ta	0.26	n.a	n.a	0.26 **
Tb	0.25	n.a	n.a	0.28
Th	4	2.9	4.3	4.0 **
U	2	1.1	2.2	1.3 **
Yb	.7	0.5	0.7	0.73 **
Zn	11	6.8	11.1	19 *
% Ash	12.5 (N = 41)	10.9	19.4	12 *

n.a = data not available; GM = geometric mean; N = number of samples; * = N=23; ** = N = 14
1 = Rocky Mountain Province and San Juan River Region data from Hatch and Swanson (1976);
2 = data from Gluskoter et al (1977)

Coals. Barium, and Na occur in lower concentrations compared to Rocky Mountain Province Coals. Cobalt, Cr, Fe, Sb, Sc, Se, Th, U, and Zn concentrations are higher in the BB seam. Arsenic, Sr, and Yb concentrations are comparable in the BB seam and San Juan River Region coals. Caution should be taken when comparing the concentrations as the number of samples analyzed is much higher in the case of Rocky Mountain Province and San Juan River Region Coals. Comparison with Eastern US. coals shows that the BB seam has lower concentrations in many elements. These elements include As, Ba, Ce, Co, Cr, Cs, Eu, Fe, La, Lu, Na, Rb, Sc, Se, Sm, and Zn. Hafnium, Sb, Sr, Ta, Tb, Th, U and Yb concentrations are comparable.

5.3.1 Discussion

Elements that have relatively large ranges and standard deviations larger than their arithimetic means (i.e coefficients of variation > 100%), have been suggested to occur in discrete mineral phases such as sulfides, sulfates, and phosphates (Gluskoter et al., 1977; Ruch et al., 1977). In BB seam coals, elements that show these characteristics are As, Ba, Co, Cs, Fe, Rb, Sb, Sb, Th, U, and Zn. Arsenic, Ba, Co, Fe, Sb, Sb, and Zn in BB seam coals may occur in sulfide, sulfate and carbonate minerals such as pyrite, sphalerite, barite, and siderite. Thorium, and U may be concentrated in phosphates. The relatively large ranges of Cs and Rb may be due to relatively high concentration of clay minerals and feldspars which may be concentrated in particular stratigraphic intervals as opposed to being evenly distributed in the coal seam. Elements that showed relatively narrow distribution ranges are thought to be in part associated with the organic material and with silicate minerals (Gluskoter et al., 1977; Ruch et al., 1977). In BB seam coals, elements that show narrow distribution ranges are Ce, Cr, Eu, Hf, La, Lu, Na, Sc, Se, Sm, Sr, Yb, Ta, and Tb. These elements

may occur in clay minerals and rare-earth element bearing minerals that are evenly distributed in the coal seam.

Comparison of trace-element concentrations in coal with their average crustal concentrations (ACC) may give an indication of the efficacy of the coal-forming processes in fixing various elements in coal (Gluskoter et al., 1977). Selenium is the only element that is significantly enriched (60 times) in the BB seam coals relative to its ACC. Antimony in the coals is enriched about 5 times its ACC. In the claystones and sandstones associated with the BB seam, Sb and Se are significantly enriched (Tables 29 and 30) relative to their ACC. Selenium enrichments have been reported in coals (Gluskoter et al., 1977; Coleman et al., 1987). Gluskoter et al., (1977) reported that Se was enriched in eastern and western US, and Illinois Basin coals by a factor of 68, 26, and 40, respectively, relative to ACC. Coleman et al., (1987) reported Se enrichment in coal by about a factor of 4 when compared to crustal abundances. Selenium in coal may be inherited directly from the Se concentrated by plants in the original coal swamp (Valkovic, 1983). When present in soluble forms Se is readily absorbed by plants. In plants Se partly resembles sulfur in its biochemical properties and is able to replace sulfur in amino acids as well as in several biological processes (Pendias and Pendias, 1984). Cameron et al., (1989) reported an average of 1.49 ppm Se from a peat deposit along the Batang Hari river in Sumatra. As suggested by Gluskoter et al., (1977), Se enrichment in the BB seam coals and associated lithologies may represent a contribution from the plants that formed the coals. It is suggested that the Se concentrated in the original plants was retained within the coal - forming system fixed in sulfides and clay minerals. However, inorder for the plants to assimilate Se from the peat waters, the amount of Se that entered the peat environment had to have been high originally. During chemical weathering of rocks Se is easily oxidized and the state of its oxidation,

as well as its solubility, are controlled by the oxidation-reduction regime and by pH of the environment. Selenite ions resulting from oxidation processes are stable and able to migrate until they are adsorbed on minerals or organic particles. In consequence, the Se level is increased in several coals, as well as in clay sediments (Pendias and Pendias, 1984). The Sb enrichment in the BB seam coals and associated lithologies may be due to high Sb input into the basin and susequent fixation in the peat forming environment. Even though the reactions of Sb during weathering are not well known, its common occurrence in waters, its concentration in coals, and its association with Fe hydroxides indicate mobility in the soil environment (Pendias and Pendias, 1984). Antimony is considered a nonessential metal and is known to be easily taken up by plants if present in soluble forms. Concentrations of up to 7 to 50 ppm (dry weight) of Sb have been reported from trees and shrubs growing in mineralized zones (Pendias and Pendias, 1984).

Claystones and sandstones associated with the BB seam show variable depletions and enrichments in trace-element concentrations (Tables 29 and 30) relative to average shale and sandstone compositions, respectively. Depletions or enrichments of certain trace elements in the BB seam claystones and sandstones may be indicative of the relative amount of minerals (depleted or enriched in particular trace elements) in the detrital material brought into the coal-forming environment. Assuming that the detrital component is dominant in the claystones, the claystone composition may enable the detrital background concentrations of trace elements to be established (Spears and Martinez-Tarazona, 1993). This comparison helps to demonstrate enrichment or depletion of the elements in coal above the background detrital concentrations. The enrichment factors scaled for equal La (Table 31) show that As, Ba, Sb, Se, and Sr are significantly enriched ($EF_{La} > 2$) in the coals. These elements may

be associated with diagenetic minerals such as iron sulfides and carbonates that formed in the peat. Cesium and Rb are significantly depleted in the coals and the rest of the elements show EF_{La} values close to one, but in general < 2. These elements may indicate significant contribution from the detrital component in the coal.

Comparison of trace-element concentrations in BB seam coals with other coals (Table 32) shows variable depletion and enrichment trends suggesting that even though some generalization could be made for particular coal fields or provinces, trace-element content of coals is highly variable within a coal province and between basins. The BB seam coals have comparable ash contents with eastern coals (Table 32), but have lower concentrations in several trace elements. This observation may be indicative of differences in the mineralogy and geochemistry of the source rocks in the two regions.

5.4 - Vertical distribution of minor and trace elements

The vertical distribution patterns of trace elements in the BB seam show that, in general, high trace element concentrations are associated with the bounding lithologies and/or partings forming a "C" type profile. Only Se shows relatively high concentrations in the coal samples. The vertical distribution patterns of trace elements in the three drill holes are shown in Figures A4-2 to A4-25 in Appendix 4. The vertical profile of ash content is shown in Figure A4-1 for comparison.

Trace element profiles in the BB seam can be grouped into 3 types:

Type 1 - higher trace element concentrations in the coals are associated with high-ash samples. Elements that display this profile include Cr, Cs, Fe, Hf, Rb, Sc,Se, Sr, Ta, Th, U, Zn, and the REEs. Several of these elements show significant correlation with ash content (Appendix 5).

Type 2 - higher trace element concentrations in the coals are associated with the presence of such minerals as pyrite and barite at certain stratigraphic positions. Elements that show this distribution pattern include As, Ba, Co, Fe, Sb, and Se.

Type 3 - trace element concentration in the coals does not show any variation related to the presence of certain mineral phases or the ash content. This profile is a flat "C" shaped curve. Only Na displays this profile.

Some elements show high concentrations in coal samples adjacent to one or both seam margins relative to interior coal samples. Elements showing this behavior include As, Ba, Co, Sb, Se, and Zn.

In DHS1, the parting is depleted in As, Ba, Co, Cr, , Sb, Sc, Se, Sr, Th, and the REEs relative to one or both of the adjacent coal samples. The parting in DHS1 is enriched in Fe, Hf, and Ta relative to both adjacent coal samples.

In DHS3, the parting is depleted in As, Ba, Cr, Cs, Fe, Rb, Sb, Sc, Sr, Tb, Th, U, Yb, and Lu relative to one or both of the adjacent coal samples. The parting in DHS3 is enriched in Hf, Se, Ta, U, La, and Ce relative to both adjacent coal samples.

Nicholls (1968) suggested that enrichments of elements in the margins of coal seams may be explained by transport and deposition of elements by ground water. Drever et al., (1977), suggested that the marginal enrichments of the trace elements may be explained by changes in redox conditions and leaching of trace elements from zones of high permeability. They suggested that the overburden-coal interface may have been a redox interface in the ground water system and trace elements could have been leached from either the coal or surrounding sediments and redeposited close to the interface. As coal is a relatively permeable aquifer, it is possible that trace elements originally distributed through out the coal could have been leached out and transported away by the ground water. The margins would then represent low permeability areas which have not been leached (Drever et al., 1977). Goodarzi (1987) related the concentration of elements near boundary sediments overlying and/or underlying coal seams to the transportation of elements in solution from the sediments into the coal seams. Such "C" shaped distribution profiles observed in some coal seams may also be related to trace-element profiles in the original peats. Sillanpaa (1972), studying two peat profiles in Finland, observed a notable concentration of elements in the surface horizon, followed by a decrease which reaches minimum in the the midprofile, and a strong increase in the peat/mineral soil transition zone, reaching a maximum in the mineral soil.

Sillanpaa (1972) considered the trace elements as originating from the mineral soil underlying the peat. Plants growing and decaying, first on the mineral soil and later on the peat, derive trace elements from further below and, upon dying accumulate on the surface layer, thus translocating elements upwards. With increased growth of the peat layer, the bulk of the plant roots do not touch the mineral soil and the most recent generations of plants lift up the elements from the peaty parts of the peat. This "element-lifting" activity results in decreased trace element content in the peat profile with increasing peat thickness. Shotyk (1988) reported that the vertical distribution of mineral matter through peat profiles generally exhibits a C-shape and that the abundance of mineral matter in the basal and upper surfaces of peats reflects the supply of detrital materials during the early stages of peat land development and during the demise of the peat by sediment cover.

The following factors are suggested to explain the observed vertical distribution patterns of trace elements in the BB seam:

(1) ash related variations - the increase in trace element content with increase in ash content indicates that those elements that show strong positive correlation with ash are associated with the inorganic fraction. The ash content of the seam is influenced by both regional and local conditions in the depositional basin. Increased detrital input into the peat forming system due to uplift and erosion of the source area, for instance, may result in the formation of a clastic parting or the demise of the peat. Trace elements associated with minerals will thus show higher concentrations in these layers relative to the vegetation-dominated peat. The ancestral peats were accumulating in nearshore swamps and back barrier lagoons (Pierce and Shomaker, 1971) that may have been prone to ocassional influx of detrital material. The lenticular and discontinous nature of the sandstone beds associated with the coals (Beaumont, 1987) also

suggests periodic influx of detrital material into the peat forming system was not uncommon. Ocassional degradation (or oxidation) of the peat material that may result due to lower water table conditions, could result in ash-rich layers within the peat. Such ash related variations may explain the Type 1 profile observed in the BB seam.

(2) geochemical and hydrological factors - Geochemical factors, such as Eh and pH of the peat environment as well as the environment during and subsequent to coal formation, can have dramatic effect on the inorganic element content (Lindahl and Finkelman, 1986). In the BB seam, elements that display Type 2 distribution profile are mainly chalcophile elements and may have formed from the alteration of non-sulfide minerals and subsequent deposition in a reducing (low Eh) environment as sulfides or selenides. Redistriution of some elements by leaching (by acidic waters) from the bounding clastic sediments and redeposition in the nearby peaty material (coal precursor) due to changing geochemical conditions such as lowered Eh may explain trace element enrichments in coal samples adjacent to the seam margins or partings. Where as the above described processes operate during the compaction of the peat and the early stages of coalification, transport and deposition of metals by ground water can also happen after coalification. In the BB seam, this is evidenced by the presence of cleat-filling pyrite and calcite. This epigentic mineralization can affect trace element concentration in the coal seam. In contrast to epigenetic mineralization, some elements may be leached from the peat by circulating ground water and removed from the system. This process may explain the Type 3 distribution profile displayed by Na.

5.5 - Lithotype control of trace element concentrations

Variations in minor- and trace-element concentrations in bright and dull coals are discussed in this section.

Average values of minor and trace element concentrations and ash contents for bright and dull coals and results of statistical analyses are listed in Table 33. Comparison of mean concentrations in bright versus dull coals (Table 33) shows that dull coals have higher average concentrations of ash, As, Ba, Ce, Co, Cr, Fe, Hf, La, Na, Sc, Se, Sm, Sr, Th, U, Yb, and Zn. Bright coals have relatively higher concentrations of Cs, Rb, and Sb. Europium, Lu, and Ta concentrations in bright and dull coals are comparable.

Analysis of variance (ANOVA) was performed on log-transformed data and Mann-Whitney probabilities were calculated using the raw trace-element data. Statistical analysis (Table 33) shows that bright and dull coals have comparable concentrations in many trace elements. Statistically significant differences were seen only in As, Cr, Fe, Se, and Sr concentrations. These elements, with the exception of Cr, may be concentrated in sulfide and carbonate minerals. Dull coals contain higher concentrations of these elements than bright coals. Ash content is also statistically different and higher in dull coals. ANOVA results show that Hf is highly concentrated in the dull coals while Mann-Whitney probability of no difference suggests that there is no statistically significant difference in Hf concentration between bright and dull coals.

Table 33. Element concentration in bright and dull coals (concentrations in ppm unless noted otherwise).

Element	Bright coals[n]		Dull coals[n]		ANOVA	M-W
	mean	S.D	mean	S.D	prob.*	prob.**
As	1.3	1	9	16	0.015	0.011
Ba	149	226	560	1148	0.168	0.237
Ce	19	18	21	17	0.44	0.328
Co	3	4	4	5	0.638	0.837
Cr	10	9	16	12	0.074	0.035
Cs	3	4	2	2	0.93	1.0
Eu	0.3	0.2	0.4	0.2	0.376	0.504
Fe	4113	3502	21408	35045	0.025	0.051
Hf	1.4	1	2	1	0.07	0.136
La	9.5	9.2	11	8	0.334	0.217
Lu	0.1	0.1	0.1	0.1	0.219	0.227
Na	210	172	250	125	0.237	0.217
Rb	27	29	16	16	0.72	0.48
Sb	2.4	2.9	2	2	0.74	0.89
Sc	3	3	4	2	0.18	0.217
Se	2.4	1.03	4	2	0.036	0.057
Sm	1.54	1.2	2	1	0.389	0.382
Sr	91	63	128	54	0.065	0.072
Ta	0.35	0.28	0.4	0.2	0.22	0.487
Th	6	6	10	13	0.124	0.165
U	3	3	4	4	0.114	0.165
Yb	0.8	0.6	1	0.5	0.19	0.237
Zn	12	12	30	52	0.252	0.28
% Ash	15	16	22	16	0.101	0.083

* = ANOVA probability of "no difference" at 90% significance level; ** = Mann-Whitney probability of no difference at 90% significance level; n = number of samples; n=12 for bright coals except for Cs (n=5), Rb (n=4), and Sb (n=11); n = 14 for dull coals except for Cs, Rb, and Sb (n=10)

5.6 - Organic-Inorganic affinity of the elements

Several researchers have used different methods and approaches to predict the organic and/or inorganic affinity of elements present in coal. One of these approaches originally proposed by Nicholls (1968) was a qualitative method that looked at the effect of ash content on element concentration in the coal and the ash. A modified and expanded version of this approach was proposed by Solari et al., (1989) to quantitatively describe the distribution of trace elements in various coal fractions. According to this proposed model, element concentration in the organic matter, and the sulfide and non-sulfide fractions of the inorganic matter of coal may be calculated using the following equation:

$$C = (C_{ns} - C_o)\, W_i + (C_s - C_{ns})\, W_s + C_o \qquad \text{(eqn. 1)}$$

Where C is the elemental concentration in a coal sample, W_i and W_s are the weight fractions of the inorganic matter and sulfide minerals respectively, and C_s, C_{ns}, and C_o are the elemental concentrations in the sulfide, non-sulfide, and organic fractions, respectively. C_s, C_{ns}, and C_o are obtained by doing multiple regression analysis with C as the dependent variable and W_i and W_s as independent variables. The sulfide fraction (W_s) is estimated using the following relationship:

$W_s = 1.9\, S_p$ where S_p = % pyritic sulfur content of the coal.

The above equation is based on the relationship that pyritic sulfur is combined with iron in sulfide with the weight ratio of FeS_2 to S of 1.9:1 (Raask, 1985). The average ash content of the coal samples is taken to be equal to the weight fraction of the inorganic matter (W_i). In its simplest form the model assumes that the trace elements are generally present in variable concentrations

in the organic and inorganic components of coal and that the concentration of the trace elements in the inorganic fraction is homogeneously distributed throughout the mineral components. This simplified model can be written as:

$$C = (1-W_i)\, C_o + W_i C_i \qquad \text{(eqn. 2)}$$

where C = element concentration in whole coal, C_i = element concentration in the inorganic fraction, C_o = element concentration in the organic fraction, and W_i = weight fraction of the inorganic fraction.

Solari et al., (1989) also proposed a scale of relative organic affinity of the elements in the coal defined as:

$$I_o = C_o / C_i$$

I_o values greater than one indicate preferential concentration in the organic fraction (high organic affinity) and values less than one indicate preferential concentration in the inorganic fraction (high inorganic affinity).

The model proposed by Solari et al., (1989) was applied with some success by Pires and Teixeira (1992) to characterize the geochemical distribution of some Brazilian coals. This model is also used and tested in this study to determine the organic and/or inorganic affinity of the trace elements in the BB seam. Results of simple and multiple regression analyses, calculated partial concentrations of elements, I_o values, and comparison of calculated and measured trace element concentrations are given in Tables 34 and 35.

Table 34. Measured and calculated (using equation 2) trace element concentrations in BB seam coals (concentrations in ppm unless noted otherwise).

Element	C_o	C_i	I_o	R	F	C_c	C_m mean	S.D
As	3.9	9	0.44	0.07	0.12	5	5	11
Ba	323	398.568	0.81	0.01	0.005	336	337	811
Ce	7	74.82	0.09	0.64	19.35	18	19	16
Co	6	2.677	2.28	0.04	0.05	6	5	12
Cr	4	52.335	0.08	0.69	25.59	12	13	10
Cs	-0.8*	11.955	<0	0.72	17.22	2	2	3
Eu	0.2	1.166	0.14	0.72	30.84	0.33	0.34	0.2
Fe (%)	0.54	4.19	0.13	0.22	1.38	1.1	1.2	2.53
Hf	0.8	5.5	0.14	0.61	17.03	2	2	1
La	3.4	39	0.09	0.63	18.88	9	10	8
Lu	0.06	0.4	0.16	0.66	22.1	0.12	0.12	0.08
Na	1284	754	0.17	0.66	21.31	232	238	143
Rb	-3.4*	76	<0	0.69	12.67	13	17	19
Sb	2	3	0.6	0.09	0.16	2	2	3
Sc	1.3	13	0.09	0.76	38.18	3	3	2
Se	2	6	0.35	0.36	4.3	3	3	2
Sm	.7	6	0.11	0.75	35.16	1	2	1
Sr	70	308	0.23	0.62	17.56	109	112	58
Ta	0.2	1	0.14	0.66	22.1	0.33	0.35	0.24
Tb	0.13	0.65	0.20	0.62	17.59	0.22	0.25	0.16
Th	5	17	0.31	0.17	0.83	7	7	10
U	2	8	0.23	0.29	2.58	3	3	3
Yb	0.4	3	0.15	0.66	22.1	0.8	.9	.5
Zn	10	68	0.15	0.23	1.61	19	20	37

C_o = concentration in the organic fraction; C_i = concentration in the inorganic fraction; I_o = scale of relative organic affinity; F = test of regression significance; R = coefficient of simple or multiple regression; C_c = concentration in whole coal calculated; C_m = concentration in whole coal measured; S.D = standard deviation from the mean; *= considered as zero for calculations.

Table 35. Measured and calculated (using equation 1) partial trace element concentrations in DB seam coals (concentrations in ppm unless noted otherwise).

Element	C_o	C_{ns}	C_s	R	F	C_c	C_m mean	S.D
As	-3	7	782	0.95	107.31	5	5	11
Ba	384	4	-3546	0.06	0.046	289	337	811
Ce	8	67	-100	0.64	8.56	17	19	16
Co	7	-4	-102	0.13	0.21	4	5	12
Cr	5	48	-126	0.71	12.59	11	13	10
Cs	-0.4	12	-29	0.73	7.26	1.5	2	3
Eu	0.2	1	-1.6	0.74	14.88	0.3	0.34	0.2
Fe (%)	0.38	3.6	27	0.06	0.86	1.13	1.2	2.53
Hf	1	4	0.4	0.6	7.23	1.5	2	1
La	4	34	-59	0.4	8.39	9	10	8
Lu	0.1	0.3	-0.7	0.46	10.82	0.11	0.12	0.08
Na	107	653	746	0.49	12.03	204	238	143
Rb	2	71	-244	0.7	5.27	12	17	19
Sb	1.4	2	126	0.19	0.37	2.5	2	3
Sc	1.4	12	-27	0.78	19.54	3	3	2
Se	2	4	36	0.46	3.39	3	3	2
Sm	1	5	-7	0.57	16.34	1	2	1
Sr	65	250	-85	0.43	9.37	95	112	58
Ta	0.2	1	2	0.44	10.02	0.33	0.35	0.24
Tb	0.1	0.7	-2	0.65	8.97	0.21	0.25	0.16
Th	6	10	-25	0.02	0.32	6	7	10
U	2	6	-12	0.08	1.11	3	3	3
Yb	0.5	2	-5	0.46	10.78	0.7	.9	.5
Zn	11	56	-76	0.05	0.68	18	20	37

C_o = concentration in organic fraction; C_{ns} = concentration in non-sulfide inorganic fraction; C_s = concentration in sulfide fraction; F = test of regression significance; R = coefficient of simple or multiple regression; C_c = concentration in whole coal calculated; C_m = concentration in whole coal measured; S.D = standard deviation from the mean

Comparison of the values of the relative organic affinity scale (I_o) in Table 34 shows that most of the elements have I_o values less than 1 suggesting that these elements are inorganically bound. Cobalt is the only element that has an I_o value greater than 1 suggesting that Co is in organic combination. Barium has an I_o value of 0.81 suggesting that it might be present organically as well as inorganically. Rubidium and Cs have I_o values less than zero suggesting that these two elements solely occur associated with the inorganic constituents. Comparison of the calculated and measured mean concentrations shows that the average concentration of all the elements can be predicted using equation 2. However, analysis of the results of the test of regression significance and correlation coefficients (F and R values in Table 34) indicate that As, Ba, Co, Fe, Sb, Th, U, and Zn do not show any significant linear trend with ash and that this model may not be a good predictor for these elements. The concentration of many elements including As is predicted well using equation 1 (Table 35). However, as was the case for equation 2, analysis of the results of the test of regression significance and correlation coefficients for Ba, Co, Fe, Sb, Th, U, and Zn shows that equation 1 may not be a good predictive model for these elements.

Using C_o, C_s, and C_{ns} values from this study, and W_s and W_i values from Baker (1989), element concentrations for the BB seam were calculated. These calculated values (Table 36) were compared with values determined by Baker (1989) for the BB seam from two drill holes. Using equation 1, the only elements not predicted well by the model were As, Ba, Rb, Sr, and Tb. The calculated concentrations of As, and Sr were lower than the measured values while those of Ba, Rb, and Tb were higher. Calculated concentrations for Cs, and Zn are higher than measured values but within a standard deviation of the measured values.

Table 36. Comparison of measured and calculated trace element concentrations (in ppm unless noted) in BB seam coals using data from Baker (1989) to test the Solari et al., (1989) model.

Element	C_{c1}	C_{c2}	C_m mean	S.D
As	-1	5	1.4	1.4
Ba	333	333	66	43
Ce	16	16	17	12
Co	6	6	7	3
Cr	11	10	7	5
Cs	1	1	0.45	1
Eu	0.28	0.3	0.29	0.13
Fe (%)	0.82	1.02	0.8	0.94
Hf	1.34	1.41	1.48	1.15
La	8	8	8	6
Lu	0.1	0.11	0.12	0.07
Na	179	211	179	61
Rb	11	7	2	5
Sb	1	2	3	4
Sc	3	3	3	1
Se	2	3	2	1
Sm	1.3	1.4	1.3	0.6
Sr	89	102	108	24
Ta	0.28	0.30	0.31	0.2
Tb	0.44	0.20	0.23	0.12
Th	6	7	7	9
U	3	3	3	3
Yb	0.71	0.75	0.77	0.44
Zn	17	18	13	9

C_{c1} = element concentration in whole coal calculated using equation 1*; C_{c2} = element concentration in whole coal calculated using equation 2*; C_m = element concentration in whole coal measured. Data from Baker (1989); * = to calculate these concentrations, $W_s = 0.0003$ and $W_i = 0.1321$ (from Baker, 1989) and C_o, C_s, and C_{ns} values from this study were used

Calculated concentration for Sb is lower than the measured value but within a standard deviation of it. Using equation 2, calculated concentrations of As, and Ba are found to be higher than measured values. All other calculated element concentrations are within one standard deviation of the measured values. The comparison between trace-calculated element concentrations and values determined by Baker (1989) suggests that, given W_s and W_i values, the concentration of several of the trace elements in the BB seam coals may be predicted at a given location using C_o, C_s, and C_{ns} values calculated in this study.

5.7 - Principal Component Analysis

Principal Component Analysis (PCA) was done on log-transformed element concentration data from 24 samples on a whole coal basis. The PCA method is described in detail in Appendix 6 (section 2.5). PCA results are given in Tables 37 and 38. Cesium, Rb, and Sb were not included in the analysis due to missing values.

Table 37 shows that 89% of the variance can be explained by 5 components. The first component contains strong positive loadings for the elements Ce, Cr, Eu, Hf, La, Lu, Na, Sc, Se, Sm, Sr, Ta, Tb, Th, U, Yb, Zn, and ash. This component also contains moderate positive loadings for Fe, and Co, and a negative loading for organic sulfur. The elements that show strong loadings in this component are those that tend to be associated with aluminosilicates and accessory minerals that contain rare-earth elements. The positive loadings for the chalcophile elements Fe, Co, and Zn may suggest that these elements are associated with clay minerals. The presence of ash in this component and the negative loading on organic sulfur indicates that the elements in component 1 are associated with the inorganic fraction.

The second component contains strong positive loadings for As, total sulfur, pyritic sulfur, and organic sulfur. Iron shows a moderate positive loading. This component indicates that arsenic may be associated with iron sulfides in the coals.

The third component is dominated by Na, Sr, and Zn. Ash, Fe, and Cr show low positive loadings whereas the elements Se, Th, U, and the forms of sulfur have low negative loadings. This component contains elements that may be present in association with clay minerals.

Cobalt dominates the fourth component. Terbium and organic sulfur show low positive loading. The fifth component is dominated by Ba. Organic sulfur

Table 37. Unrotated principal component matrix for BB seam coals (whole coal basis).

Element	comp*. 1	comp. 2	comp. 3	comp.4	comp.5	commu**
As	0.35	0.83	0.11	-0.25	-0.06	0.9
Ba	0.39	0.17	0.13	0.21	0.79	0.86
Ce	0.84	-0.15	-0.29	-0.23	-0.07	0.87
Co	0.49	-0.04	-0.09	0.72	-0.12	0.79
Cr	0.81	-0.10	0.39	-0.16	0.10	0.85
Eu	0.90	-0.12	-0.12	0.28	-0.12	0.94
Fe	0.55	0.48	0.24	-0.31	-0.26	0.75
Hf	0.89	-0.05	-0.22	-0.22	0.06	0.90
La	0.82	-0.14	-0.24	-0.37	0.003	0.88
Lu	0.91	-0.05	0.03	0.32	-0.11	0.95
Na	0.70	0.22	0.57	0.03	-0.07	0.87
Sc	0.96	-0.06	0.12	0.10	0.04	0.95
Se	0.74	0.20	-0.43	-0.12	0.21	0.84
Sm	0.91	-0.13	-0.17	0.15	-0.14	0.92
Sr	0.61	0.18	0.65	0.01	-0.03	0.83
Ta	0.86	0.02	-0.19	-0.11	-0.06	0.79
Tb	0.86	-0.12	-0.01	0.42	-0.1	0.95
Th	0.81	-0.03	-0.47	-0.22	0.16	0.94
U	0.83	-0.01	-0.41	-0.14	0.17	0.91
Yb	0.91	-0.05	0.03	0.32	-0.12	0.94
Zn	0.65	0.18	0.54	-0.04	0.37	0.88
Ash	0.90	-0.01	0.23	-0.18	-0.17	0.92
Org. Sul	-0.29	0.61	-0.27	0.39	0.22	0.73
Pyr. Sul	0.02	0.86	-0.21	-0.02	-0.17	0.82
Tot. Sul	-0.15	0.93	-0.25	0.16	-0.09	0.97
% variance	54	13	10	7	5	
cumulative % variance	54	67	77	84	89	

* Comp. = component; ** Comm. = communality. This indicates what proportion of the variability of any particular variable has been explained by the components shown. It can be approximated by adding the square of each component; for example for arsenic the communality is = (0.36^2 + 0.82^2 + 0.11^2 + -0.28^2 + -0.03^2) = 0.89; % variance refers to the proportionate variance contribution by each respective component

and Zn show low positive loading. Ash shows low negative loadings in both components 4 and 5. Components 4 and 5 may suggest organic association of Co, Ba, and some Zn.

The component matrix produced by rotation on five components is given in Table 38. Rotation on five components produced a similar structure. The first rotated component contains strong positive loadings for Sc, Se, La, Ce, Sm, Eu, Hf, Ta, Th, U, and ash. Moderate loadings are observed for Cr, Yb, Lu, and Tb. Organic sulfur has a low negative loading. The second rotated component contains As, Fe, and the forms of sulfur. This component clearly shows the association of As predominantly with iron sulfides. The third rotated component contains strong positive loadings for Cr, Fe, Sc, Zn, As, Sr, Na, and ash. Lu, and Yb have moderate positive loadings. Organic sulfur has a low negative loading in this component. The fourth rotated component contains Co, Eu, Yb, Lu, and Tb. Moderate loadings are observed for Sc, and Sm. Rotated component five is dominated by Ba with moderate loadings for Zn and organic sulfur. The rotated components show some correlation between them. Rotated component 1 has correlation coefficients of $r = 0.72$ and 0.70 with rotated components 3 and 4, respectively. Rotated component 3 has a correlation coefficient of $r = 0.63$ with rotated component 4. Rotated components 2 and 5 do not correlate with any other component or each other. Rotated components 1, 3, and 4 contain elements that occur in association with the inorganic fraction. Rotated component 2 contains elements associated with sulfides, and rotated component 5 contains elements that may be associated with the organic fraction. The presence of some elements in more than one component suggests occurrence in more than one phase.

Table 38. Rotated Principal component matrix for BB seam coals (whole coal basis).

Element	comp. 1	comp. 2	comp. 3	comp.4	comp.5	commu.
As	0.26	0.75	0.48	-0.19	0.03	0.9
Ba	0.17	0.06	0.21	0.12	0.88	0.86
Ce	0.89	-0.11	0.18	0.16	-0.05	0.87
Co	0.16	0.06	0.06	0.86	0.09	0.79
Cr	0.50	-0.23	0.70	0.13	0.19	0.85
Eu	0.67	-0.07	0.28	0.64	0.03	0.94
Fe	0.38	0.41	0.64	-0.08	-0.18	0.76
Hf	0.89	-0.04	0.26	0.14	0.09	0.90
La	0.90	-0.13	0.22	0.01	-0.01	0.88
Lu	0.58	-0.02	0.42	0.66	0.07	0.95
Na	0.24	0.08	0.87	0.24	0.09	0.87
Sc	0.65	-0.09	0.53	0.45	0.18	0.95
Se	0.84	0.24	0.03	0.12	0.26	0.84
Sm	0.75	-0.07	0.27	0.53	-0.02	0.92
Sr	0.15	0.03	0.88	0.17	0.11	0.83
Ta	0.80	0.04	0.29	0.25	0.02	0.79
Tb	0.53	-0.07	0.33	0.74	0.09	0.95
Th	0.95	0.02	0.01	0.10	0.17	0.94
U	0.91	0.03	0.06	0.17	0.21	0.91
Yb	0.58	-0.02	0.42	0.66	0.06	0.94
Zn	0.25	-0.01	0.76	0.07	0.49	0.88
Ash	0.65	-0.07	0.67	0.20	-0.08	0.92
Org. Sul	-0.26	0.67	-0.32	0.12	0.31	0.73
Pyr. Sul	0.06	0.90	0.03	-0.03	-0.08	0.82
Tot. Sul	-0.10	0.97	-0.11	0.001	0.001	0.97
% variance	41	14	22	16	6	
cumulative % variance	41	55	77	93	99	

commu. = communality

5.8 - Cluster analysis

Hierarchical clustering using log-transformed element data on whole coal basis was performed to group elements according to their mutual correlations. The statistical procedure is discussed in Appendix 6 (section 2.4). All the analyzed elements (with the exception of Sb, Rb, and Cs (excluded due to missing values)), ash, organic sulfur, pyritic sulfur and total sulfur were used in the cluster analysis. Figure 28 shows the resulting dendrogram.

The following four groupings are identified from the cluster diagram:

Cluster A) pyritic sulfur, As, and Fe,

Cluster B) La, Ce, U, Th, Hf, Ta, Se, ash, Cr, Lu, Yb, Eu, Sm, and Sc,

Cluster C) Na, Sr, and Zn, and

Cluster D) organic sulfur, Ba, and Co.

Cluster A suggests that As may be occurring in association with iron sulfides. This cluster will be refered to as the sulfide cluster. Cluster B may be subdivided into three: cluster B1 showing clustering of the element pairs La-Ce, U-Th, Hf-Ta, and Se; cluster B2 including ash and Cr, and cluster B3 including element pairs Lu-Yb, Eu-Sm, and Sc. The common factor among the elements in cluster B is that all the elements show significant correlation with ash. This suggests that the elements in this cluster occur in association with the mineral matter. Even though Se clusters with cluster B elements, the relationship is not strong as indicated by the relatively large distance of clustering (Fig. 28). With the exception of Cr and Se, all the elements in cluster B are either REEs or elements that are chemically similar to REEs. It is suggested that the clustering of Cr and Se with these elements is due to their common correlation with ash. Chromium may occur in aluminosilicates such as clay minerals. The clustering of the REE, U, Th, Hf, Ta, and Sc together suggests a similar mode of occurrence

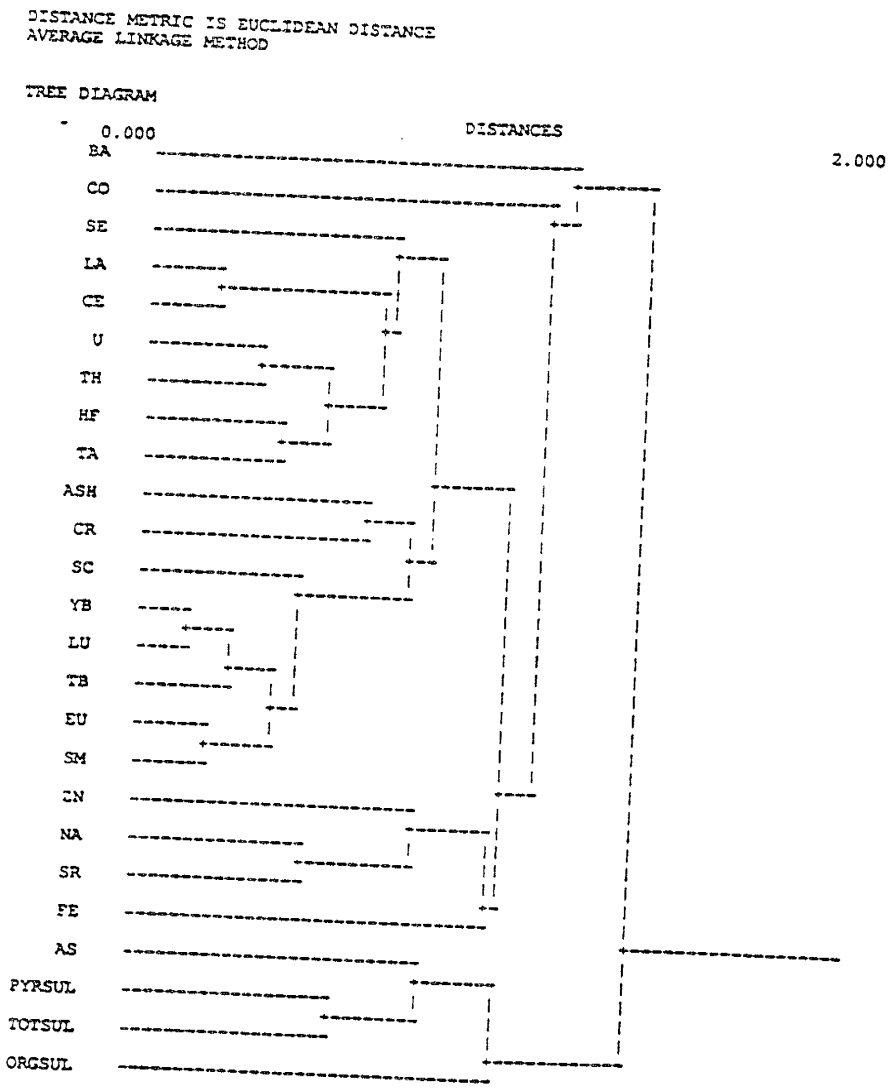

Figure 28. Dendrogram (from cluster analysis) showing the grouping of elements in BB seam coals.

or origin for these elements. These elements possibly occur in accessory minerals such as zircon or may have been derived from such minerals. Cluster B1 indicates that U, Th, Hf, and Ta may behave chemically close to the LREEs La and Ce. Cluster B3 suggests for Sc a chemically similar behavior to the intermediate and heavy REEs. Cluster C that includes Na and Sr suggests common occurrence in or common origin from such minerals as feldspars. Cluster D includes elements that did not cluster with the other elements. The reason that organic sulfur and the other elements do not cluster with the other elements could be that they are associated with the organic fraction. In the case of Ba, Co, and Zn, another explanation is that they occur in minerals that do not contribute much to the ash content of the coal.

6 - Mode of occurrence of trace elements

It is attempted in this section to determine the likely modes of occurrence of trace elements in the BB seam using the following approaches: 1) element distribution in the coal in relation to the ash content and calculation of a relative scale of organic/inorganic affinity (I_o) , 2) direct analysis of iron sulfides and carbonate minerals using electron microprobe analysis and PIXE, 3) distribution of elements in the coals and associated lithologies, 4) mineralogical composition (from XRD analyses) and 5) statistical techniques including correlation, principal component, and cluster analyses. In the following discussion, mean (average) values refer to arithmetic means.

Arsenic (As)

Swaine (1990) gives the range of As concentration in most coals between 0.5 - 80 ppm with US coals averaging 14 ppm. The mean value of As in the BB seam is 5 ppm. This value is lower than the US average, but falls in the range reported for most coals.

Various modes of occurrences of As in coal have been reported including association with sulfides (for example pyrite, arsenopyrite), and clay minerals (Finkelman, 1980; Palmer, 1983; Eskenazy, 1989). Coleman and Bragg (1989) suggested that low levels (< 5 ppm) of As may be associated with the organic matter. Organic association of As has also been suggested by Leutwein and Rosler (1956), Bogdanov (1965), Filby et al., (1977), Kryukov et al., (1985), Goodarzi (1987) and Demir et al., (1990).

The vertical distribution patterns in DHS1 and DHS3, show that the bounding claystones have relatively higher As concentrations than the coal samples. The claystones and coals in these drill holes have low pyritic sulfur

(and total sulfur) contents, and relatively high As contents do not coincide with high pyritic sulfur contents. This suggests that As in low-sulfur coal samples in DHS1 and DHS3 and the associated claystones occurs in clay minerals. In DHS2, high As concentrations in coal samples are associated with samples with high pyritic sulfur contents indicating As association with iron sulfides in these high-sulfur coals. An average of 811 ppm As was detected by PIXE in pyrite from a high-sulfur coal sample. Calculated partial concentrations for As (Table 35) suggest that As occurs predominantly associated with the sulfide fraction. The low correlation ($r = 0.41$) of As to ash indicates that As-bearing minerals (such as pyrite) do not contribute much to the ash content of the coal samples. Principal component and cluster analyses also suggest As association with iron sulfides.

Barium (Ba)

Most coals have Ba concentrations ranging between 20 and 1000 ppm and mean values of 70 to 300 ppm (Swaine, 1990). Swanson et al., (1976) report a mean value of 150 ppm for Ba in coal. The mean value of Ba in the BB seam is 337 ppm. The average Ba concentration in the BB seam coals falls with in the range of mean values reported for most coals.

Barium may occur associated with both the organic and inorganic fractions in coal. Gluskoter et al., (1977), and Kuhn et al., (1978) reported organic affinity for Ba. Nicholls (1968), Filby et al., (1977), Finkelman (1980), and Palmer (1983) suggested predominant inorganic association for Ba in coal. Barium containing minerals found in coal include barite, witherite, barytocalcite, alstonite, Ba-bearing feldspars, ankerite, barytocelestine, clay minerals, gorceixite and other Ba-bearing crandalite group minerals (Finkelman, 1980., Palmer, 1983., Swaine, 1990).

The vertical distribution patterns for Ba show higher concentrations in the bounding lithologies suggesting inorganic association in these lithologies. X-ray diffraction analyses have shown that the bounding lithologies contain feldspars and illite which may host Ba. Localized high Ba concentration are found in the BB seam. The minerals celsian and barite are identified in the high-Ba coal samples. Barium concentration in the coals shows no significant correlation with the ash content. The low correlation with ash results because Ba is not evenly distributed in the inorganic fraction but rather concentrated in a few grains of Ba-bearing minerals.

Cobalt (Co)

Cobalt concentrations in coal range from 0.5 - 30 ppm with a mean of 4-8 ppm (Swaine, 1990). Swanson (1976) gives a mean value of 7 ppm for Co in coal. The mean value of Co in the BB seam is 5 ppm. This value is slightly lower than the average Co concentration in coals, but falls in the range reported for coal.

Gluskoter et al., (1977), and Pickhardt (1989) reported predominant association of Co with the organic fraction in coal. Inorganic association has been suggested by Leutwein and Rosler (1956), Nicholls (1968), and Filby et al., (1977) among others. Cobalt in coal may occur associated with sulfides (perhaps in some solid solution with pyrite), linnaeite-group minerals, and clay minerals (Finkelman, 1980; Palmer, 1983; Finkelman et al., 1990).

The vertical distribution patterns for Co show that bounding lithologies have higher concentrations than the coal samples. Even though analyses of test of regression significance and coefficient of simple or multiple regression (Tables 34 and 35) suggest that the Solari et al., (1989) model was not a good predictive model for Co, the calculated values of Co agree well with the measured values.

Cobalt is the only element that has an organic affinity value of greater than 1 and partial concentration values show that Co is associated with the organic fraction. Localized high Co concentrations in the BB seam may suggest Co occurrence in some accessory minerals not identified by x-ray diffraction analyses in this study. Cobalt in the bounding lithologies may be associated with the clay minerals. Electron microprobe and PIXE analyses of pyrites in selected BB seam coals did not detect Co in the samples analyzed.

Chromium (Cr)

The range of Cr concentrations in coal is between 0.5 and 60 ppm with a general mean around 20 ppm (Swaine, 1990). Swanson et al., (1976) give the mean value for Cr concentration in coals at 15 ppm. The mean concentration of Cr in BB seam coals is 13 ppm. This value is slightly lower than the average Cr concentration in coals, but falls with in the range reported for coals.

A wide range of organic associations have been noted for Cr in coal (Horton and Aubrey, 1950., Otte, 1953., Leutwein and Rosler, 1956., Zubovic et al., 1961). Inorganic association for Cr has also been suggested by several people including Bogdanov (1965), Nicholls (1968), Schultz et al., (1975), and Ford (1977). Finkelman (1980), Palmer (1983), and Finkelman et al. (1990) suggested Cr association with silicate minerals, sulfides, oxides such as chromite, and clay minerals.

The vertical distribution patterns of Cr show high Cr concentrations in the bounding lithologies. In theses lithologies, Cr may be associated with the silicate minerals (feldspars, micas, and illite) identified by x-ray diffraction analysis. In the coal samples, high concentrations of Cr are associated with high-ash samples. Trace amounts of illite have been identified in these samples. Chromium also shows significant correlation ($r = 0.8$) with the ash content of the

coals indicating association of Cr with the inorganic fraction. Calculated partial concentrations and an I_o value of 0.08 also suggest predominant association of Cr with the inorganic fraction. Principal component and cluster analyses show Cr association with ash and several elements including the REEs, Sc Th, U, and Hf. PCA also shows a negative relationship of Cr to organic sulfur indicating inorganic association. It is suggested that Cr in the coals occurs associated with clay minerals and perhaps with heavy minerals.

Cesium (Cs)

The range of concentration for Cs in coal is between 0.3 - 5 ppm with a mean of around 1 - 2 ppm (Swaine, 1990). The average Cs concentration in the BB seam is 2 ppm. This value is falls with in the range reported for coals and is comparable to the average Cs concentration in coals.

Inorganic association has been suggested to be the primary mode of occurrence of Cs in coals (Gluskoter et al., 1977., Filby et al., 1977, Finkelman, 1980). Finkelamn (1980), Palmer (1983), Palmer and Filby (1984) and Swaine (1990) noted that Cs was very likely to be associated with K-rich minerals including some clays, micas and feldspars. Based on an inverse relationship with ash, an organic association was suggested for Cs in brown coals from the Dnieper Basin, Russia (Razdorozhniy and Petrus, 1975).

The vertical distributions of Cs show that concentrations are high in bounding lithologies compared to the coals. High Cs concentrations in the coal samples are associated with high-ash samples. Cesium shows a moderate ($r = 0.68$) correlation with ash and has an organic affinity (I_o) value of less than zero suggesting inorganic association. Calculation of partial concentrations for Cs indicate strong association with the non-sulfide inorganic fraction. It is suggested

that Cs occurs in K-bearing minerals, including feldspars, micas, and clay minerals.

Iron (Fe)

Iron shows a relatively wide range of concentration in coals. Gluskoter et al., (1977) give a mean value of 0.53% and 1.5% Fe for western and eastern US coals, respectively. The mean Fe concentration in the BB seam is 1.2%.

Iron is a major element in coal and occurs in a number of minerals including sulfides, carbonates, oxides, hydrous oxides, and sulfates (Valkovic, 1983). Palmer (1983) and Finkelman et al., (1990) reported varied modes of occurrence for Fe, including occurrence in exchangeable sites in clays and in the organic matter, sulfates, sulfides, oxides, carbonates, chelates, and Fe-bearing silicate minerals.

Vertical distribution patterns show that coal samples in the BB seam contain lower Fe concentrations than the bounding lithologies. High Fe concentrations in the coals are related to samples with high pyritic sulfur and siderite (from x-ray diffraction analyses) contents. Iron shows moderate ($r = 0.57$) correlation with ash and has an I_o value of 0.13 indicating association with the inorganic fraction. Calculation of partial concentrations suggest Fe association predominantly with the sulfide fraction and to a lesser extent with the non-sulfide fraction of the inorganic matter. Principal component analysis shows that Fe is correlated to several trace elements (that show good correlation with ash) and forms of sulfur and As. Cluster analysis shows Fe association with Zn, Na and Sr. Electron microprobe and PIXE analyses show Fe association with pyrite, siderite, and calcite. In addition to the above minerals, Fe may occur in association with clay minerals and REE-bearing accessory minerals.

Hafnium (Hf)

Hafnium concentration in most coals falls in the range 0.4 - 5 ppm (Swaine, 1990). The average Hf concentration in the BB seam is 2 ppm. This value falls with in the range reported for most coals.

As zircon is a common accessory phase in coal, and because of similarity in chemical properties with Zr, it has been suggested that the bulk of the Hf in coals is associated with zircon (Goldschmidt, 1954; Finkelman, 1980; Palmer, 1983; Finkelman et al., 1990). Palmer (1983) suggested that Hf may be associated with clays. Eskenazy (1987) reported that Hf was mainly associated with the organic fraction in some Bulgarian coals, and that organically bound Hf dominated in some low-ash coals.

Vertical distribution patterns show that Hf concentration in the bounding lithologies is higher than that of the coals. High Hf concentrations in the coals occur in samples with high ash contents. The correlation between Hf and ash is strong ($r = 0.80$) and together with the low organic affinity index ($I_o = 0.14$) of Hf suggests inorganic association. Calculated partial concentrations show that Hf is predominantly associated with the non-sulfide fraction. Principal component and cluster analyses show Hf association with Ta, REEs and several other trace elements that show high correlations with ash. No Hf-bearing phase was identified in this study. It is speculated here that Hf very likely occurs in association with zircon, and perhaps with other accessory minerals and clays minerals.

Sodium (Na)

Gluskoter et al., (1977) reported mean concentrations of 0.05%, 0.04%, and 0.14% Na in Illinois Basin, eastern US, and western US coals, respectively. Demir et al., (1990) reported that coal beds in the Illinois Basin contain as much

as 0.4% Na. Lovblad (1977) reported a mean value of 0.076% (range = 0.006 - 0.182%) for Na in coals from seven countries. The mean Na concentration in the BB seam is 238 ppm. This value is lower than average Na concentrations in western and eastern US, and Illinois Basin coals.

Sodium may be present as NaCl and Na_2SO_4 (Palmer, 1983; Valkovic, 1983). Palmer (1983) and Demir et al., (1990) suggested that Na occurs adsorbed on and in exchangeable sites in clay minerals. Finkelman et al., (1990) reported that Na may occur in ion-exchangeable sites, particularly in low-rank coals, where it is likely to be associated with the organic constituents.

Vertical distribution patterns show that coal samples have lower Na contents than bounding lithologies. Sodium shows strong correlation ($r = 0.74$) with ash and has an I_o value of 0.17 suggesting inorganic association. Calculation of partial concentrations for Na show that it occurs associated with both the sulfide and non-sulfide fractions of the mineral matter. However, Na was not detected during electron microprobe and PIXE analyses of iron sulfides. Principal component analysis shows Na association with ash and a suite of elements including REE, Sc, Cr, Fe, Zn, Se, Sr, Ta, Th, and U. Cluster analysis shows Na association with Sr. No Na-rich minerals were identified in this study. It is suggested that Na in the BB seam occurs in association with clay minerals and feldspars.

Rubidium (Rb)

Swanson et al., (1976) reported Rb concentration in US sub-bituminous coals at 5.3 ppm. Swaine (1990) gives Rb concentration in most coals in the range of 2 to 50 ppm. The average Rb concentration in the BB seam is 17 ppm. This value is higher than the average Rb concentration reported for US sub-bituminous coals and falls with in the range reported for most coals.

Association of Rb with the inorganic fraction has been suggested by Gluskoter et al., (1977) and Filby et al., (1977) among others. Finkelman (1980), Palmer (1983), and Palmer and Filby (1984) suggested that substantial amounts of Rb in coal are associated with K-rich minerals, including clays and feldspars. Razdorozhny and Petrus (1975), in their study of coals from the Dnieper and Donets Basins (Russia), observed an inverse relationship between Rb and ash contents and concluded that Rb was associated with the organic fraction in those coals.

In the BB seam, Rb concentrations are high in bounding lithologies compared to the coals. High Rb concentrations in the coal samples are associated with high ash samples. Rubidium shows a moderate ($r = 0.66$) correlation with ash and has an organic affinity (I_o) value of less than zero suggesting inorganic association. Calculation of partial concentrations for Rb indicate strong association with the non-sulfide inorganic fraction. It is suggested that Rb occurs in the K-bearing minerals, identified in the BB seam, including feldspars, micas, and clay minerals. Rubidium shows very strong correlation ($r = 0.99$) to Cs indicating that these two elements have very similar modes of occurrence.

Antimony (Sb)

Swaine (1990) gives Sb concentration for most coals in the range 0.05 - 10 ppm. Swanson et al., (1976) give mean Sb concentration of 1.4 ppm in bituminous coals and an average value of 1.1 ppm for US. coals (of different ranks). The mean Sb concentration in the BB seam is 2 ppm. This value falls in the range reported for most coals and is slightly higher than average Sb concentrations reported for bituminous coals.

Gluskoter et al., (1977) and Swaine (1990) reported organic association of Sb in coal. Finkelman (1980) reported that Sb was concentrated in the sink fractions in Waynesburg and Upper Freeport coals and suggested that a substantial amount of the Sb in these coals may occur in minute grains of stibnite (Sb_2S_3) dispersed throughout the organic matrix and that this mode of occurrence may account for the apparent organic affinity by Sb in some sink float experiments. Palmer (1983) noted that Sb was associated with the clay minerals and to some extent with pyrite.

Vertical distribution patterns show that bounding lithologies are in general enriched in Sb relative to the coals. Antimony shows moderate correlation (r = 0.43) with ash and has an I_o value of 0.6 indicating inorganic affinity. Calculated partial concentrations suggest that Sb is predominantly associated with the sulfide fraction. Antimony was not detected in iron sulfides in the samples analyzed. This could perhaps be due to the low concentration of Sb in the iron sulfides analyzed. Possible modes of occurence of Sb in the BB seam include association with sulfides, and clay minerals.

Scandium (Sc)

Swaine (1990) gives a range of Sc concentration in coals between 1 and 10 ppm, with a mean of about 4 ppm. Swanson et al., (1976) give a mean value of 3 ppm Sc for US coals. The average Sc concentration in the BB seam is 3 ppm. This value falls with in the range and is comparable to the mean Sc concentration reported for coal.

Scandium appears to be associated with both the mineral matter and organic matter in coals. Swaine (1964) reported that between 40 - 95% of the Sc in Australian bituminous coal was organically bound. Swaine (1964), Palmer (1983), Singh et al., (1983), Finkelman (1980), and Finkelman et al., (1990)

reported Sc occurrences in coal in association with siderite, calcite, kaolinite (and other clay and silicate minerals), aluminum phosphates, and zircons.

Vertical distribution patterns show that Sc concentrations in bounding lithologies are higher than those in the coal samples. High Sc concentrations in the coals are associated with high-ash samples. Scandium shows strong correlation ($r = 0.83$) with ash and has an I_o value of 0.09 suggesting strong inorganic affinity. Calculated partial concentrations for Sc show predomonant association with the non-sulfide inorganic fraction. Principal component and cluster analyses show Sc association with the REEs and ash. Scandium in the BB seam probably occurs in clay minerals and REE-bearing accessory minerals.

Selenium (Se)

Swaine (1990) gives a range of concentration between 0.5 and 4 ppm Se for US coals. The mean Se concentartion in the BB seam is 3 ppm. This value falls with in the range reported for US coals.

Selenium may be present in both organic and inorganic combinations in coal. It has been suggested that at least a portion of the Se in coal may be inherited directly from the Se concentrated by plants in the original coal swamp (Valkovic, 1983). Finkelman et al., (1990), and Swaine (1990) reported organic association of Se in coals. Finkelman (1980), Palmer (1983), and Swaine (1990) reported that Se occurrence in coal in association with pyrite and other sulfides such as galena, clay minerals and as lead selenide .

Vertical distribution patterns show that except for the parting in DHS3 which has higher Se concentration than the coals (in DHS3), Se concentration in the coals is higher than that in the bounding lithologies. Selenium is the only element in the BB seam that shows this relationship. Coal samples with high pyritic sulfur content have high Se concentrations. Correlation with ash is

moderate (r = 0.61) and Se has an I_o value of 0.35 suggesting inorganic affinity. Partial concentrations calculated for Se show predominant association with the sulfide fraction. Principal component and cluster analyses show Se association with ash, and REEs and several trace elements that show positive correlations with ash suggesting inorganic affinity for Se. Selenium was detected during PIXE analysis of iron sulfides from two coal samples supporting the sulfide association. The parting in DHS3 has the highest Se content in this drill hole. The pyritic sulfur (and total sulfur) content of this parting is low. This may suggest that in addition to occurring in sulfides, Se in the BB seam also occurs in association with clay minerals.

Strontium (Sr)

Most coals have Sr concentrations in the range of 15 to 500 ppm with a mean of about 100 ppm (Swaine, 1990). The average Sr concentration in the BB seam is 112 ppm. This value falls with in the range and is comparable to the mean Sr concentration reported for coal.

Finkelman (1980), Finkelman et al., (1990), and Swaine (1990) suggested that substantial amounts of Sr in coal can occur associated with the organic fraction and that organically associated Sr may predominate in most low-rank coals. Finkelman (1980) and Palmer (1983) reported the occurrence of Sr in several minerals including crandallite group minerals, barite, celestite, Sr-bearing rare earth phosphates, calcite, strontianite, and Sr-bearing clays.

Vertical distribution patterns show that bounding lithologies have higher Sr concentration than coal samples. High Sr concentrations in the coals are associated with high-ash coal samples. Strontium has an I_o value of 0.23 and shows moderate correlation (r = 0.68) with ash suggesting inorganic association. Principal component analysis shows Sr with the REEs, Cr, Fe, Sc, Zn, As, Na,

and ash. Cluster analysis shows Sr association with Na, Zn, and Fe. Calculated partial concentrations for Sr show predominant association with the non-sulfide fraction and none with the sulfide fraction. Electron microprobe analysis shows Sr in calcite, siderte and iron sulfides (up to 0.05 wt%). PIXE analysis showed 14 to 17 ppm of Sr in iron sulfides. The bounding lithologies have high Sr concentrations , but have low pyritic sulfur (and total sulfur), and carbonate contents. This suggests that the Sr in these lithologies may occur in clay minerals and feldspars.

Tantalum (Ta)

Swaine (1990) gives Ta concentration in most coals in the range of about 0.1 and 1.0 ppm with a mean value of about 0.3 ppm. The average Ta content of the BB seam is 0.35 ppm. This value falls in the range given for coals and compares with the mean value reported for coals.

Solodov et al., (1975), Gluskoter et al., (1977), Palmer and Filby (1984) and Finkelman et al., (1990), among others, have suggested inorganic association for Ta in coal. Palmer (1983) reported Ta association with rutile, other heavy oxides and possibly clays. Gluskoter et al., (1977) reported Hf/Ta ratios of 3.6, 3.64, and 5.2 for Illinois Basin, Eastern US, and Western US coals respectively. Finkelman (1980) reported that Hf/Ta ratios in Waynesburg coals (ranging from 2.6 - 4.6 with a mean of 3.7) compare with a ratio of 3 that would be expected from a granitic source. He concluded that Ta appears to be primarily associated with the detrital inorganic matter in coal. Finkelman et al., (1990) reported that Ta in some coals may occur in organic association.

Vertical distribution patterns show that Ta concentration in bounding lithologies is higher than that in coals. An I_o value of 0.14 and strong correlation ($r = 0.77$) with ash suggest inorganic association for Ta. Calculated partial

concentrations indicateTa concentration predominantly in association with the sulfide and non-sulfide fractions of the mineral matter. However, Ta was not detected in iron sulfides during electron microprobe and PIXE analyses. Principal component and cluster analyses show Ta association with ash, the REEs, Hf, and several other trace elements that correlate with ash. Tantalum shows strong correlation (r = 0.92) with Hf. The average Hf/Ta ratio of 5.01 (range= 2.03 - 10.09) in the BB seam coals compares to that reported for western US coals (Hf/Ta = 5.2) by Gluskoter et al., (1977). Tantalum in the BB seam may occur in accessory heavy minerals such as rutile and in clay minerals.

Thorium (Th)

Swaine (1990) gives a range of concentration of 0.5 - 10 ppm Th for most coals. Swanson et al., (1976) give a mean value of 4.7 ppm Th in US coals. The average concentration of Th in the BB seam is 7 ppm. This value falls in the range reported for coal, and slightly higher than the mean value reported for US coals.

Gluskoter et al., (1977) and Filby et al., (1977) suggested strong inorganic affinity for Th in coal. Kuhn et al., (1978) suggested organic affinity for Th, despite the fact thatTh was relatively enriched in the heavier specific gravity fractions. Assuming that Th occurs in association with monazite and that there is a difference in the Th content of detrital versus authigenic monazites in coal, Finkelman (1980) suggested that the seemingly contradictory results of Gluskoter et al., (1977) and Kuhn et al., (1978) may be a reflection of different behavior of authigenic and detrital monazites. The detrital Th-rich grains would be concentrated in the ash-rich zones, readily sinking to the heavier specific gravity fractions, whereas the Th-poor authigenic monazites would be enmeshed in the organic fraction and float. Finkelman (1980), Palmer (1983), Palmer and Filby

(1984), Finkelman et al., (1990), and Swaine (1990), reported Th association with monazite, zircon, xenotime, iron oxides, and clay minerals. Finkelman et al., (1990) reported that some of the Th in their samples may occur in organic association.

In the BB seam, bounding lithologies show higher concentrations of Th than coal samples. High Th concentrations in the coals are associated with ash-rich samples. Thorium shows moderate correlation ($r = 0.66$) with ash and has an I_o value of 0.31 suggesting inorganic association. Calculated partial concentrations indicate Th association predominantly with the non-sulfide fraction of the mineral matter. Principal component and cluster analyses show Th association with ash, the REEs, U, and several trace elements that show positive correlation with ash. Thorium shows strong correlations with Hf ($r = 0.93$) and U ($r = 0.97$). Thorium in the BB seam possibly occurs in accessory minerals such as zircon, and monazite, and clay minerals.

Uranium (U)

Swaine (1990) gives a range of concentration between 0.5 - 10 ppm U for most coals with a mean of about 2 ppm. The average U concentration in the BB seam is 3 ppm. This value falls in the range reported for coals and is slightlly higher than the mean concentration for coals.

The literature on the occurrence of U in coals is fairly extensive. Summaries and reviews of various studies on U in coal can be found in Finkelman (1980), Valkovic (1983), and Swaine (1990).

Finkelman (1980) suggested that although there is strong evidence to indicate that the bulk of the U in coal is organically bound, inorganically bound U may be significant in some coals. Finkelman (1980), Palmer (1983), Van der Flier and Fyfe (1985), and Swaine (1990) reported that U may be associated with

zircon, rare earth-phosphates, uraninite, coffinite, autunite, torbernite, carnotite rutile, calcite, and clay minerals.

Vertical distribution patterns show that bounding lithologies show higher concentrations of U than coal samples. High U concentrations in the coals are associated with ash-rich samples. Uranium shows moderate correlation ($r = 0.68$) with ash and has an I_o value of 0.23 suggesting inorganic association. Calculated partial concentrations indicate U association predominantly with the non-sulfide fraction of the mineral matter. Principal component and cluster analyses show U association with ash, the REEs, Th, and several trace elements that show positive correlation with ash. Uranium shows strong correlations with Hf ($r = 0.90$) and Th ($r = 0.97$). Uranium in the BB seam possibly occurs in accessory minerals such as zircon and monazite, and clay minerals.

Zinc (Zn)

Zinc concentration in most coals ranges between 5 - 300 ppm (Swaine, 1990). Swanson et al., (1976) reported a mean value of 39 ppm for Zn concentration in US coals. The average Zn concentration in the BB seam is 20 ppm. This value falls in the range and is lower than the mean reported for coals.

Gluskoter et al., (1977) and Kuhn et al., (1978) suggested inorganic association of Zn in coal. Nicholls (1968), Finkelman (1980), Palmer (1983), Finkelman et al., (1990) and Swaine (1990) reported Zn occurrence in coal associated with sphalerite, and other sulfides including pyrite, and carbonates. Leutwein and Rosler (1956), Bogdanov (1965), Finkelman (1980) and Swaine (1990) suggested that Zn may be organically bound in some coals.

Vertical distribution patterns show that bounding lithologies have higher Zn concentrations than the coals. Moderate correlation ($r = 0.65$) with ash and an I_o value of 0.15 suggest inorganic association for Zn. Calculated partial

concentrations for Zn indicate association predominantly with the non-sulfide fraction and no association with the sulfide fraction. However, an average of about 70 ppm Zn was determined by electron microprobe and PIXE analyses of iron sulfides in some coal samples. This observation indicates that the Solari et al., (1989) model was not a good predictive model for Zn. Principal component and cluster analyses show Zn association with Fe, Na, and Sr. This association and relatively high Zn concentrations in the bounding lithologies,which have very low pyritic sulfur contents, may be indicative of Zn occurrence in clay minerals. It is suggested that Zn in BB seam coals and associated lithologies occurs in sulfides and clay minerals.

Rare Earth Elements (REEs)

The rare earth elements (REEs) are a group of 15 elements (lanthanum to lutetium) with atomic numbers ranging from 57 (La) to 71 (Lu), 14 of which occur naturally (Wilson, 1989). In this study the REEs La, Ce, Sm, Eu, Tb, Yb, and Lu were determined in whole coal samples and associated lithologies. Swaine (1990) gives approximate values (in ppm) for ranges for most coals as 1 -40 (La), 2 - 70(Ce), 0.5 - 6 (Sm), 0.1 - 2 (Eu), 0.1 - 1.0 (Tb), 0.3 - 3.0 (Yb), and 0.03 - 1.0 (Lu). The average REE concentrations in the BB seam coals and associated lithologies are given in Table 39.

REEs show both inorganic and organic affinities in coal. Gluskoter et al., (1977) reported strong inorganic affinities for Ce and Sm. Europium showed intermediate affinities, whereas La, Yb, and Lu showed varied associations ranging from organic to inorganic. Other studies reporting inorganic association of REEs in coal include Filby et al., (1977), Bogdanov (1965), Tsui et al., (1979), Eskenazy (1978) and Goodarzi and Van der Flier-Keller (1988). Finkelman (1980) suggested a mineralogical control for the occurrence of REEs in coal.

Table 39. Comparison of average rare earth element concentrations in BB seam coals with concentrations in the associated claystones and sandstones, and NASC. Concentrations are in ppm.

Element	coal (n = 30)	all claystones (n = 11)	bounding claystones (n = 9)	parting (n = 2)	sandstone (n = 2)	NASC[a]
La	9.58	37.03	39.47	26.03	22.5	32
Ce	18.62	71.95	77.61	46.50	45.05	73
Sm	1.60	5.51	6.32	1.89	3.65	5.7
Eu	0.34	1.09	1.26	0.35	0.79	1.24
Tb	0.25	0.69	0.81	0.14	0.55	0.85
Yb	0.86	2.35	2.75	0.56	2.35	3.1
Lu	0.12	0.36	0.42	0.08	0.33	0.48
Eu/Eu*	0.70	0.69	0.68	0.75	0.72	0.72
LREE/HREE	27.67	41.56	29.67	95.05	21.94	24.99

n = number of samples; a = NASC composition from Haskin et al., (1968); "all claystones" includes the bounding claystones and partings; Eu/Eu* = europium anomaly. the size of the europium anomaly was estimated by comparing the chondrite normalized Eu value on the REE pattern curve with its interpolated value between Sm and Tb; LREE = sum of La, Ce, and Sm; HREE = sum of Tb, Yb, and Lu. The mean values are arthimetic averages of individual samples.

He indicated that the REEs occur in the RE-phosphates, monazite, and xenotime. Chou (1982) suggested that the REEs in coal are associated with clays. Leaching experiments (Finkelman et al., 1990) showed that REEs were predominantly associated with phosphate minerals and that in the low-rank samples the REEs may occur as chelate compounds. Kuellmer et al., (1987) suggested that a small portion of the REEs may be occurring in organic association.

As REEs may be transferred nearly in bulk from source to sediment (Taylor and McLennan, 1985), the REE patterns in coal and associated lithologies may resemble REE distribution patterns in cratonic shales. REE abundances in BB seam coals, partings, and bounding claystones and sandstones are compared with REE abundances of North American Paleozoic Shales (NASC) which is a composite of 40 North American shales (Taylor and McLennan, 1985). The NASC is believed to be reasonably representative in REE distribution of the average composition of detrital materials being delivered by rivers to the oceans (Condie, 1990). Comparison of the absolute abundances (Table 39) shows that the coals are depleted in REEs relative to the associated claystones and sandstones, and NASC. The claystones are enriched in LREEs relative to the sandstones. The claystone partings are depleted in HREEs compared to the coals, and the bounding claystones and sandstones. This depletion may be due to preferential removal of the HREEs in the acidic swamp environment. All lithologies are enriched in LREEs relative to the HREEs, and the size of the Eu anomaly is comparable to that of NASC.

In order to eliminate the Oddo-Harkins effect, which is the existence of higher concentrations of elements with even atomic numbers as compared to those with odd atomic numbers, and to smoothe out the concentration variations from element to element, the concentration of each REE was normalized to its

abundance in chondritic meteorites. Chondritic REE normalizing factors used are from Haskin et al., (1968).

Chondrite normalized REE patterns in whole coal are compared with those of NASC (Figure 29). The REE patterns of all BB seam coals fall between patterns of samples S2-29 and S1-17 that represent the maximum and minimum limits in the coal samples, respectively. The REE patterns in the coals are very similar to NASC pattern but depleted. Sample S2-29 has a high ash content (54.3%) and plots closer to the NASC pattern than sample S1-17 that has a low ash content (3.18%). The REEs in the coal samples also show significant correlations with the determined ash contents and show inorganic affinity ($I_o < 1$) indicating that these elements are associated with the mineral matter. This suggests that the depleted pattern in Figure 29 is due to the dilution effect of the organic fraction. In order to compensate for the dilution effect by the organic matter, the REE abundances in the whole coal are normalized to the determined ash content (i.e. each abundance is divided by the ash fraction) before chondrite normalization. Figure 30 shows the REE patterns on an ash basis. In Figure 30, samples S3-17 and S3-28 represent the range of REE abundances on an ash basis. Most of the samples show enriched REE patterns relative to NASC reaffirming the above suggestion that the depleted REE pattern (Figure 29) in the coals is due to the dilution effect of the organic matter. Samples S2-29 and S3-28 have very similar ash contents (54.3% and 54.1% respectively) and the shapes of their REE patterns are very similar. However, sample S3-28 shows a more depleted pattern than S2-29. Comparison of the mineralogy of these samples (from XRD analysis) shows that whereas the mineralogy of sample S2-29 is dominated by quartz and kaolinite with traces of illite, the mineralogy of sample S3-28 is dominated by siderite with fair amount of quartz and kaolinite and traces of illite and micas. This comparison suggests that even though the

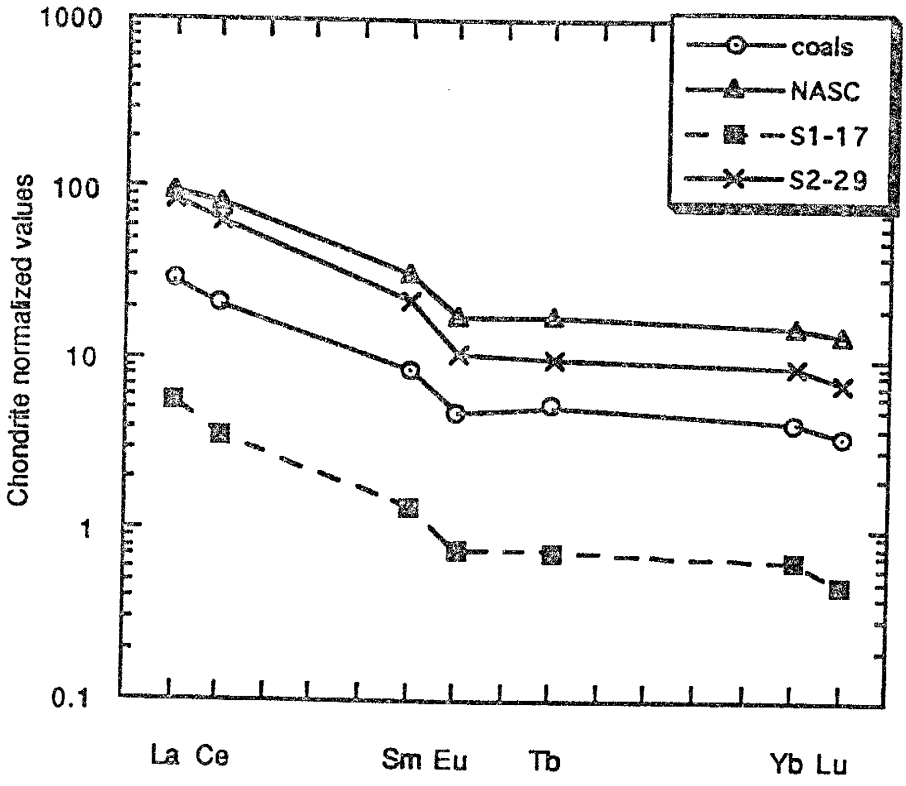

Figure 29. REE pattern of BB seam coals; coals = pattern of the average REE concentration of 30 coal samples (on whole-coal basis). S1-17 and S1-29 represent the minimum and maximum limits in the coals, respectively.

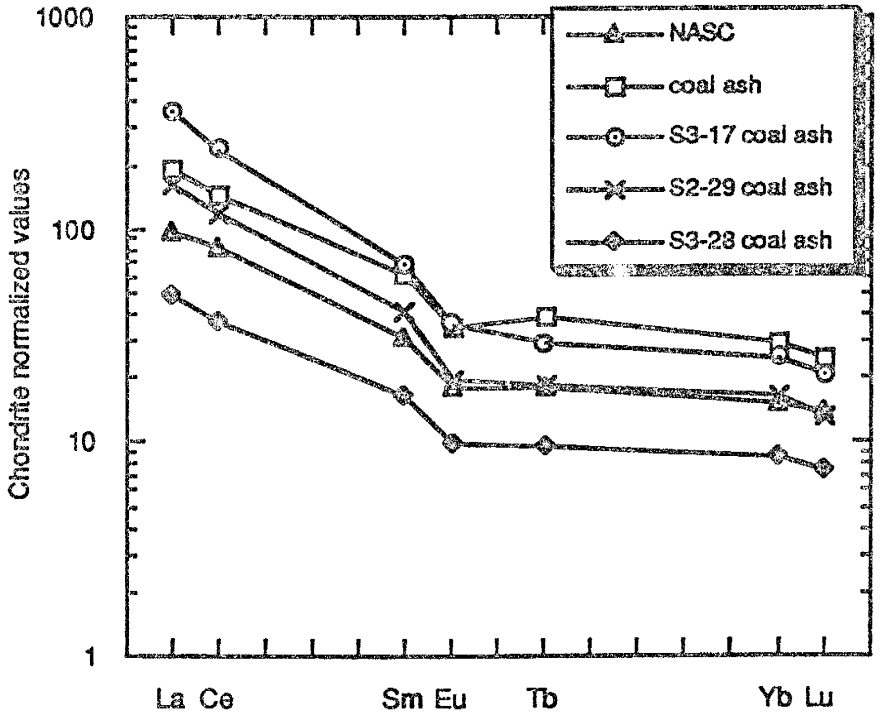

Figure 30. REE pattern of BB seam on an ash basis; coal ash = REE pattern representing the average of 30 coal samples; S3-28 and S3-17 represent minimum and maximum limits of REE patterns in the coals (on an ash basis), respectively. NASC = North American Shale Composite.

REE abundance in the coals may be related to the amount of inorganic material, the composition of the inorganic material may be of great importance in governing the abundance and occurrence of the REEs. Siderite in sample S3-28 may be acting as a dilutant. Carbonates take very low concentrations of REEs (up to 2 orders of magnitude less than clays) (Condie, 1993, personal comm.).

Bounding claystones show very similar REE pattern to NASC (Figure 31). In Figure 31, samples S2-3 and S2-41 define the range of REE patterns of the claystones. The average chondrite normalized pattern of the claystones is almost identical to the NASC pattern. This suggests that the bulk of the REEs in these rocks were derived from detrital material with an average crustal REE pattern.

The REE patterns of the sandstones (Figure 32) show similar but depleted pattern as NASC. The relatively low REE abundance in the sandstones may be due to sedimentary sorting. Factors associated with sedimentary sorting such as grain size contrast, general mineralogy, and heavy mineral fractionation may affect REE patterns in sediments (Taylor and McLennan, 1985). The bulk of the REEs are believed to reside in the silt and clay size fraction suggesting that the trivalent REEs may be readily accommodated in most clay minerals (Taylor and McLennan, 1985). Quartz contains very low concentrations of REEs and enrichments of quartz in sands and silts result in a dilution effect. Sand fractions tend to have the lowest REE abundances compared to silt and clay fractions and commonly display lower La/Yb ratios than finer grain sizes (Taylor and McLennan, 1985). La/Yb ratios calculated for sandstones (La/Yb = 9.55) and claystones (La/Yb = 15.76) associated with the BB seam are consistent with the above statement. Enrichment in HREEs in sandstones may be a result of the heavy mineral content (Taylor and McLennan, 1985). This may explain the

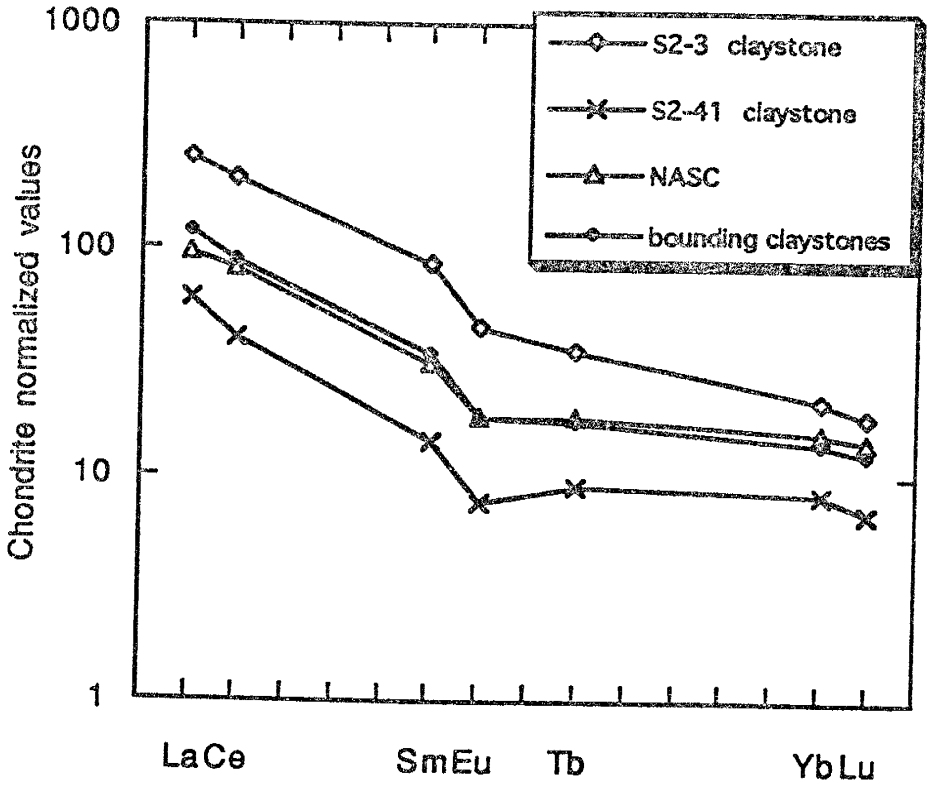

Figure 31. REE patterns in bounding claystones in the BB seam; bounding claystones = pattern for the average REE concentration in the claystones. S2-41 and S2-3 represent the minimum and maximum limits, respectively, of the REE patterns in the claystones. NASC = North American Shale Composite.

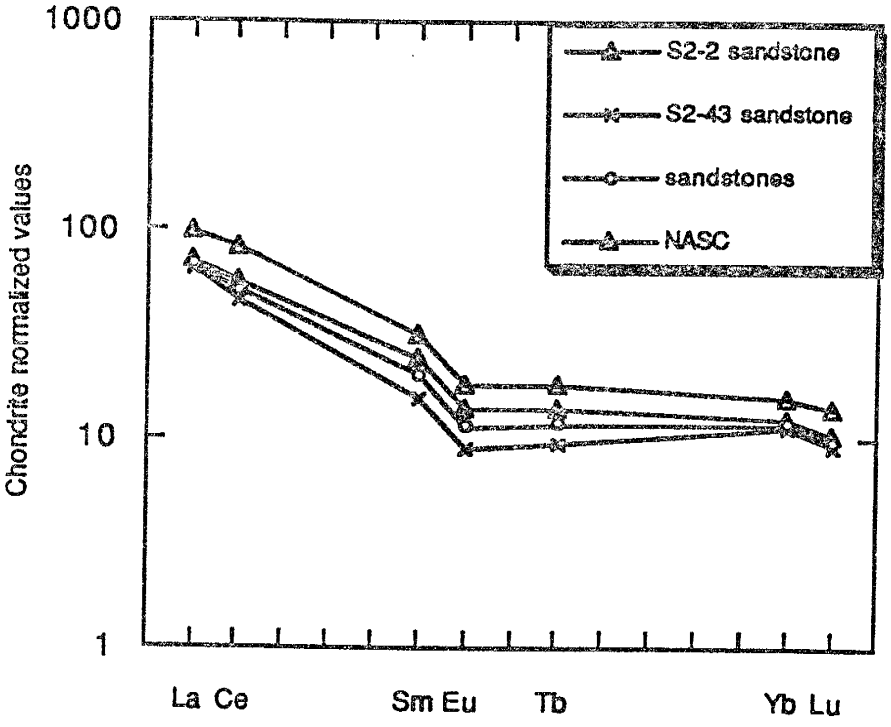

Figure 32. REE patterns in bounding sandstones; "sandstones" represents pattern for the average REE concentration in the sandstone samples. NASC = North American Shale Composite.

comparable abundance of Yb and Lu in the sandstones and claystones (Figure 33).

The average chondrite normalized REE abundances in the different lithologies are plotted in Figure 33. The similarity in patterns suggests that the REEs associated with the coal and bounding lithologies were derived from clastics with an average crustal REE pattern. Eskenazy (1978) observed that REE distribution patterns in some high-ash coals from Bulgaria approached that for shales. Tsui et al., (1979) reported REE distributions in Illinois coals that were nearly identical to that of shale. Finkelman (1980) found that the distribution of chondrite normalized REE abundances in the ash of Waynesburg and Upper Freeport coals was nearly identical to that of NASC.

To evaluate any possible fractionation or remobilization in the coal forming environment, REE patterns of partings and bounding claystones are compared with REE patterns of adjacent coal samples. The chondrite normalized NASC REE pattern is also plotted for comparison. In DHS1 (Figure 34) sample S1-30, overlying the parting, is depleted in La, Ce, Sm and Eu, and slightly enriched in Tb relative to the parting. This sample has comparable abundances of Yb, and Lu. Sample S1-32, underlying the parting, is enriched in REEs relative to the parting especially in the heavy REEs (HREEs). In DHS3 (Figure 35), the overlying coal sample (S3-17) is depleted in light REEs (LREEs) La and Ce, and slightly enriched in Yb. Samarium, Eu, Tb, and Lu abundances in this sample are comparable to that of the parting. The underlying coal sample (S3-19) in DHS3 is depleted in light and middle REEs (LREEs and MREEs) and enriched in the HREEs Yb, and Lu relative to the parting. In both drill holes (DHS1 and DHS3), the partings and adjacent coals are depleted in REEs relative to NASC. The depleted patterns in coal samples adjacent to partings may reflect the original REE distribution pattern where higher concentrations may be expected in

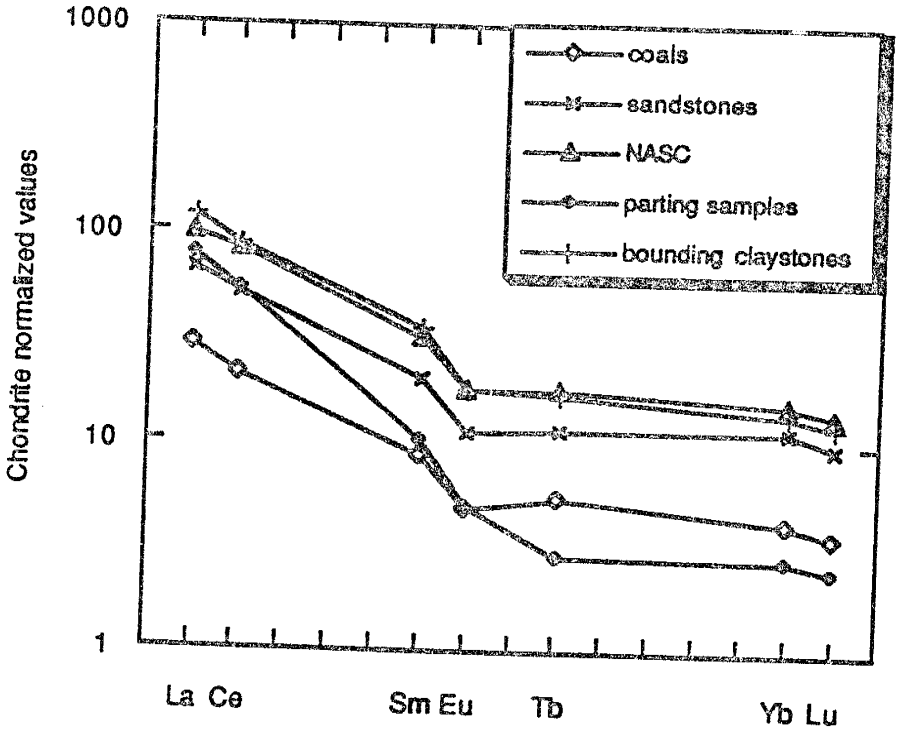

Figure 33. Comparison of REE patterns in BB seam coals and associated lithologies; coals = pattern representing the average REE concentration of 30 coal samples; sandstone = average of 2 sandstone samples; parting samples = average of 2 partings; bounding claystones = average of 8 bounding claystones. NASC = North American Shale Composite.

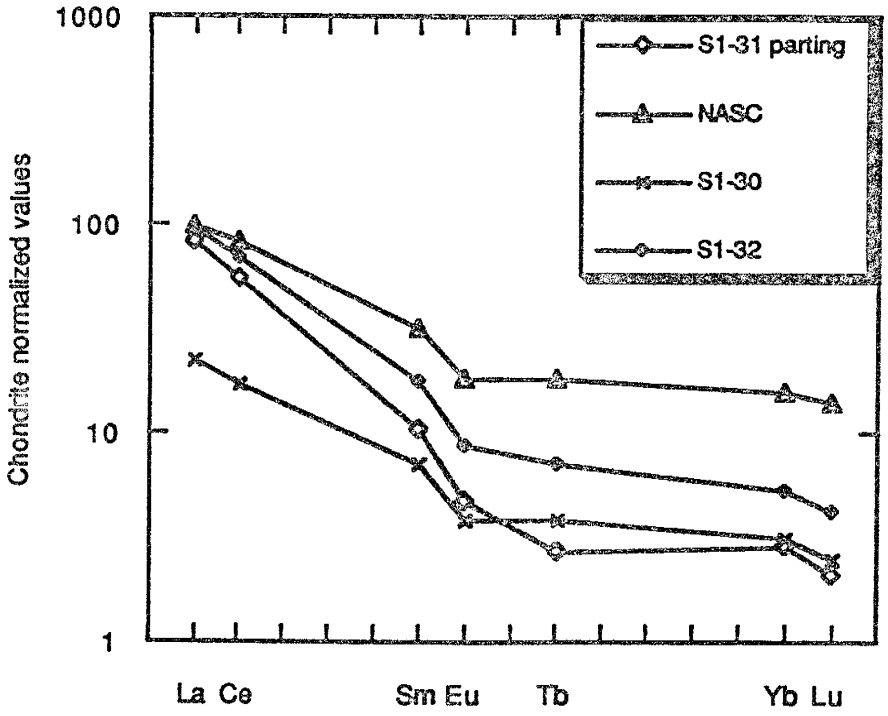

Figure 34. Comparison of REE patterns of parting (S1-31) and adjacent coals (S1-30 and S1-32) in DHS1. NASC = North American Shale Composite.

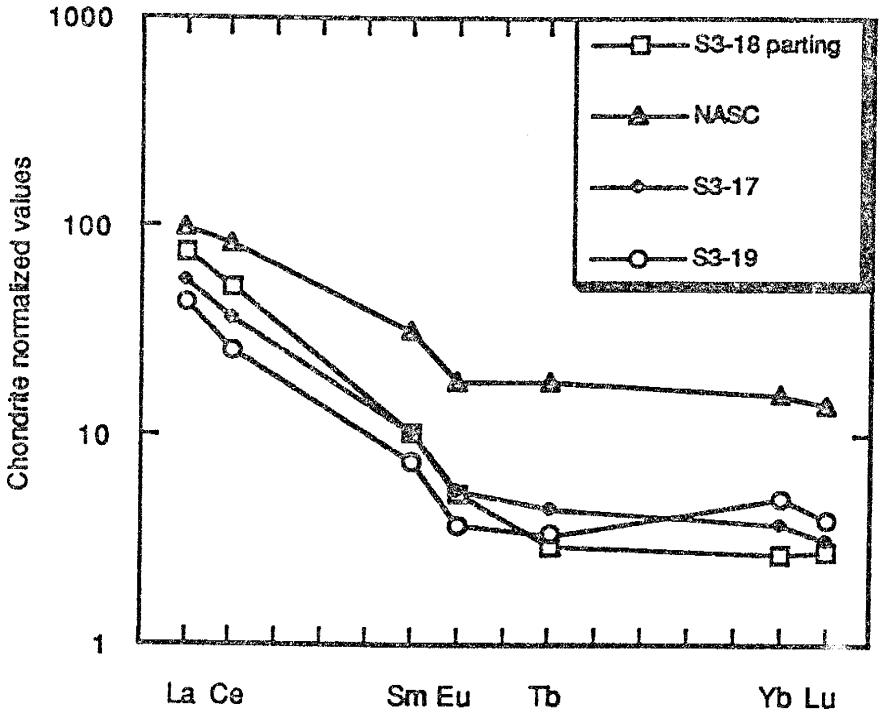

Figure 35. Comparison of REE patterns of parting (S3-18) and adjacent coal samples (S3-17 and S3-19) in DHS3. NASC = North American Shale Composite.

the clastic rocks. The REE enrichment in the adjacent coals could be the result of localized mobilization of the REEs from the parting in acidic swamp environment. Rare earth elements can be leached from clastic rocks associated with coal seams by acidic swamp water and adsorbed by the coal in the early stages of coalification (Birk and White, 1991).

To evaluate any possible remobilization of the REEs from the seam margins, REE patterns of bounding claystones and adjacent coal samples were compared. Figures 36, 37, and 38 show these comparisons in DHS1, DHS2, and DHS3, respectively. In general, coal samples situated adjacent to the bounding claystones do not show enrichment in REEs relative to the claystone suggesting very little or no mobilization of the REEs from the bounding claystones.

Source of REEs in the BB seam

Immobile elements such as Th, Zr, Nb, Sc, Co, and Ti can be used for provenance and tectonic setting determinations (Bhatia and Crook, 1986). These elements have relatively low mobility during sedimentary processes and low residence time in sea water. These elements are transferred quantitatively into clastic sedimentary rocks during weathering and transportation and thus would reflect the signature of the parent material (McLennan et al., 1983). Scandium appears to behave similarly to the REEs during sedimentary processes and the average Sc abundances in sedimentary rocks can be related to the abundances in the upper continental crust. Thorium also behaves coherently with the REEs such that Th/Sc ratios are fairly constant in shales at about 1.0 (McLennan, 1989). Thorium is the most incompatible and Sc the most compatible in igneous differentiation processes (Taylor and McLennan, 1985). Thus it might be

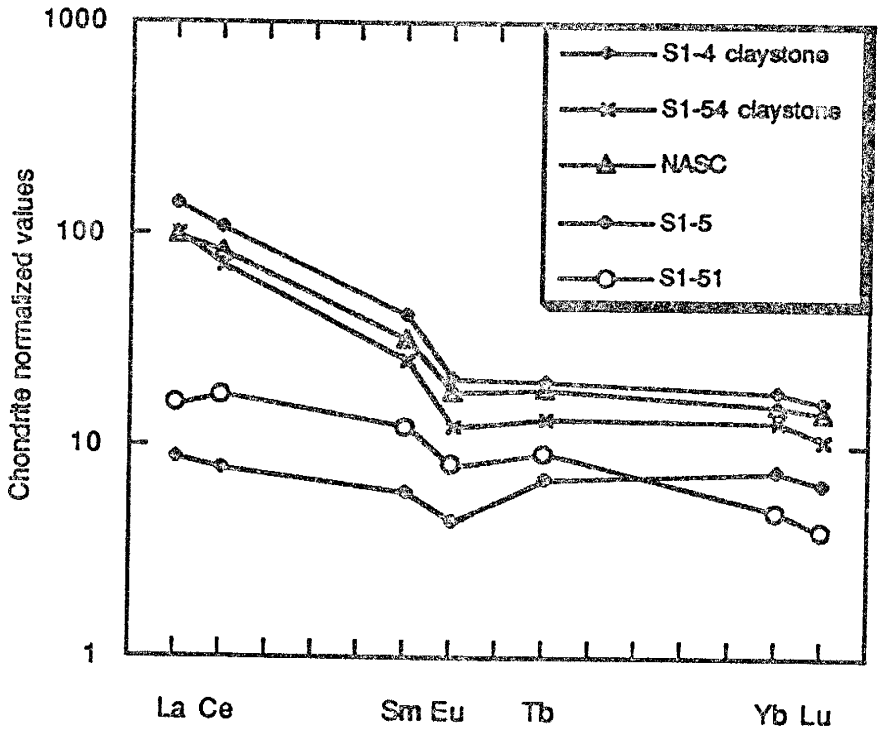

Figure 36. Comparison of REE patterns of bounding claystones (S1-4 and S1-54) and adjacent coal samples (S1-5 and S1-51) in DHS1. NASC = North American Shale Composite.

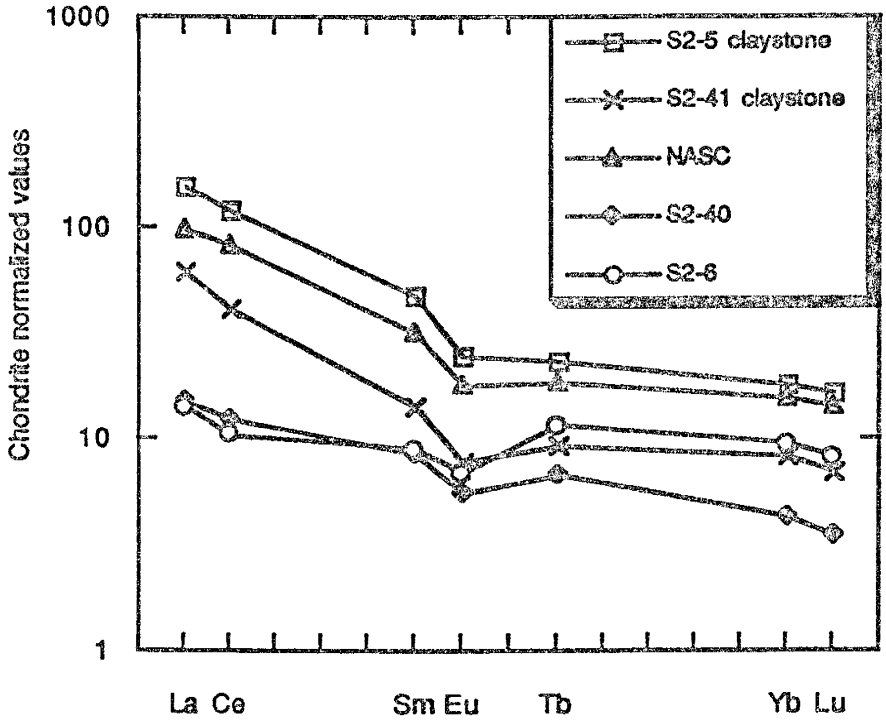

Figure 37. Comparison of REE patterns of bounding claystones (S2-5 and S2-41) and adjacent coal samples (S2-6 and S2-40) in DHS2. NASC = North American Shale Composite.

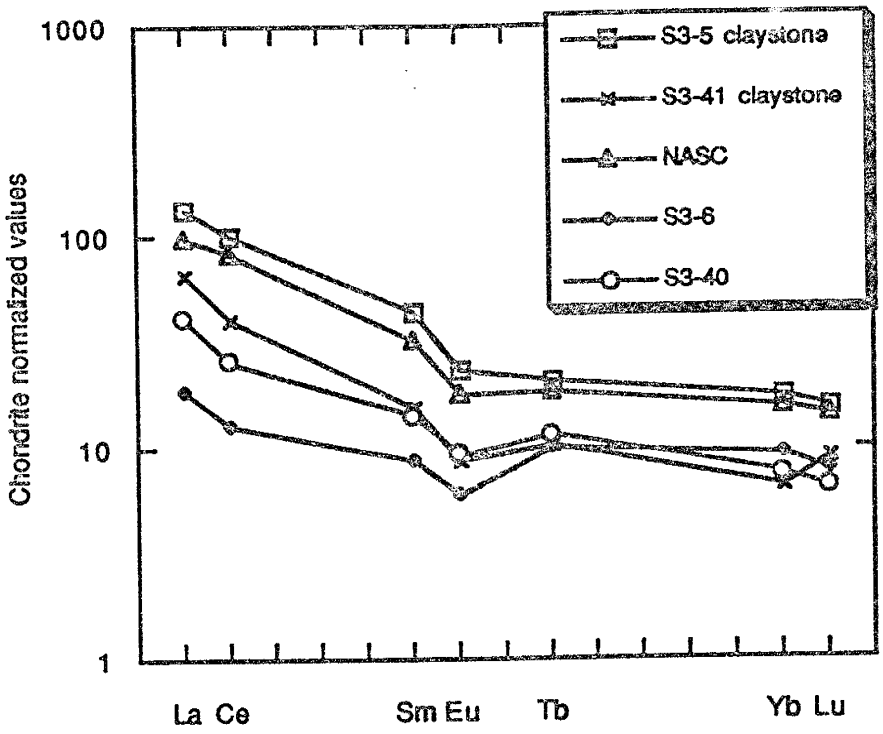

Figure 38. Comparison of REE patterns of bounding claystones (S3-5 and S3-41) and adjacent coal samples (S3-6 and S3-40) in DHS3. NASC = North American Shale Composite.

expected that a ratio of these elements would be the most sensitive index of overall chemical composition (i.e. mafic vs. felsic).

In the BB seam, several trace elements including Th and Sc show statistically significant positive correlations with ash content and the REEs (Appendix 5). The relationship between these elements and the REEs suggests that ratios of elements such as Th/Sc, La/Sc, and La/Th would reflect upper continental crust compositions. Th/Sc, La/Sc, and La/Th ratios in the BB seam coals and associated non-coal lithology are plotted in Figures 39, 40, and 41, and compared with post Archean fine-grained sedimentary rocks (Table 40). Table 40 shows that coal, sandstone, and bounding claystone samples have very similar ratios to post Archean shales. Parting samples show similar La/Th ratios as post Archean shales, but have higher Th/Sc and La/Sc ratios. These higher ratios may be indicative of Sc remobilzation and loss from the partings in the acidic environment. The vertical distribution patterns of La, Sc, and Th suggest that there has been some mobilization of these elements in the acidic swamp. The high Th/Sc and La/Sc ratios may thus result if removal of Sc from the partings was relatively higher than that of La and Th.

In general, the element ratios suggest that the REEs and associated elements were derived from rocks with upper continental crust composition. Comparison of average La/Th ratios in the BB seam (Table 40) with averages for granites (2.35) and basalts (4.54) (Taylor, 1964), suggest derivation from predominantly granitic sources. Finkelman (1980) reported that, in the coal samples he studied, trace element ratios obtained from coal ash were identical to those of detrital sedimentary rocks, and elements such as Zr, Ta, Nb, Hf, and the REEs were generally associated with the more resistive minerals.

Cecil et al., (1982) suggested that plant inorganic matter in conjunction with ion exchange can be considered to be the dominant source of elements including the REEs, Zr, Cs, Rb, Hf, Pb, Cu, Cd, Se, and Sc among others in the coals they studied. They reported that their interpretation was consitent with (a) moderate ash content of the coals (8 - 15 wt%), (b) positive correlation of those elements with coal macerals (vitrinite, fusinite, semifusinite), and (c) positive correlation of these elements and macerals with ash content. In the BB seam coals there is poor or negative correlation between macerals and ash (section 4.2.5). Staistical analysis (section 5.5) also shows that bright (> 65% vitrinite) and dull (< 65% vitrinite) coals have comparable concentrations in several trace elements suggesting that there is no strong correlation between the trace element concentrations and coal macerals in the BB seam. Even though some trace elements could be derived from the plant inorganic matter, the results from this study suggest that the majority of the elements in the BB seam coals may have been derived predominantly from the detrital material that was brought into the swamp.

Table 40. Ratios of relatively immobile elements in BB seam coals and associated lithologies.

Lithollogy	Th/Sc	La/Sc	La/Th
parting claystones n =2	3.92 * 2.53** 1.03 - 5.75***	12.25 0.99 11.55 - 12.95	2.17 0.37 1.91 - 2.60
sandstones n = 2	1.44 0.12 1.36 - 1.52	3.18 0.40 2.9 - 3.46	2.21 0.10 2.14 - 2.28
claystones n = 9	1.08 0.17 0.86 - 1.39	3.03 1.23 1.78 - 5.56	2.72 0.75 1.91 - 4.0
whole cooal n = 30	2.20 2.56 0.31 12.86	3.11 1.57 0.58 - 7.50	2.19 1.49 0.52 - 7.91
post Archean shales****	0.91 (1.1)	2.4 (4.0)	2.6 (3.6)

n = number of samples; * = mean; ** = standard deviation; *** = range; **** = values from Taylor and McLennan (1985); numbers in parentheses are from Krauskopf (1967).

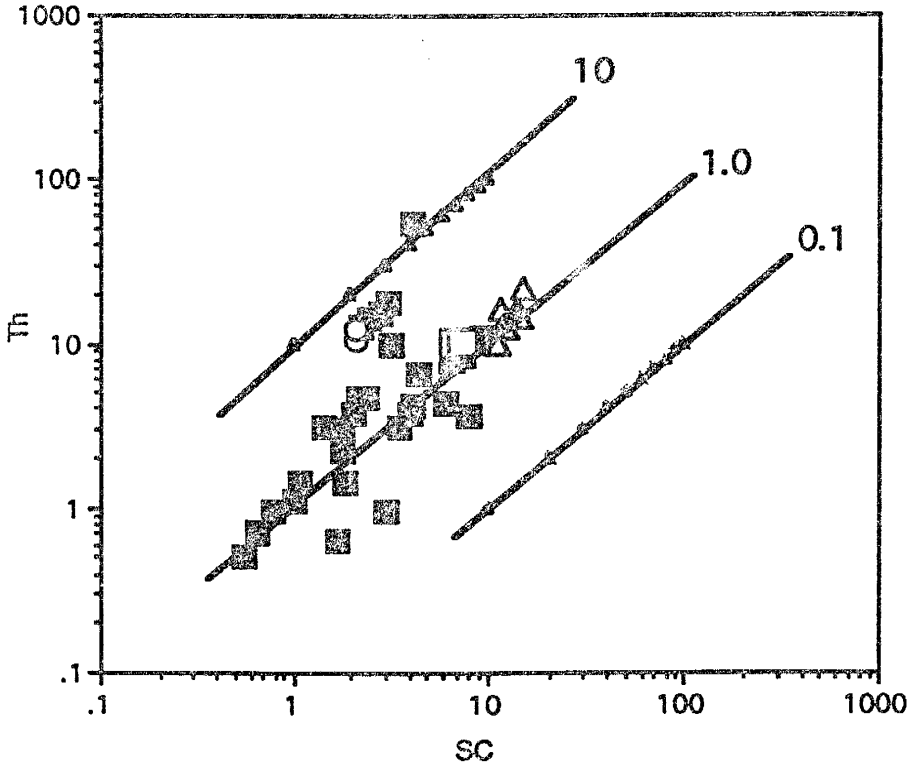

Figure 39. Th/Sc ratios in BB seam coals and associated lithologies; ■ = coal, ○ = partings, Δ = bounding claystones, □ = sandstones. Line numbers refer to Th/Sc ratios.

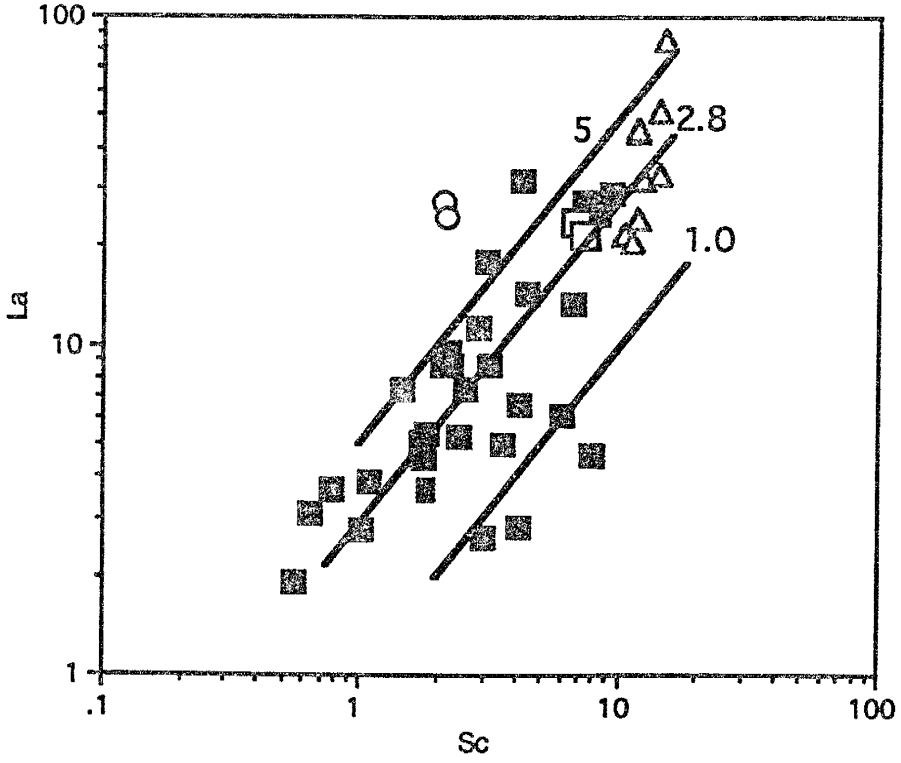

Figure 40. La/Sc ratios in BB seam coals and associated lithologies; ■ = coal, O = partings, Δ = bounding claystones, □ = sandstones. Line numbers refer to La/Sc ratios.

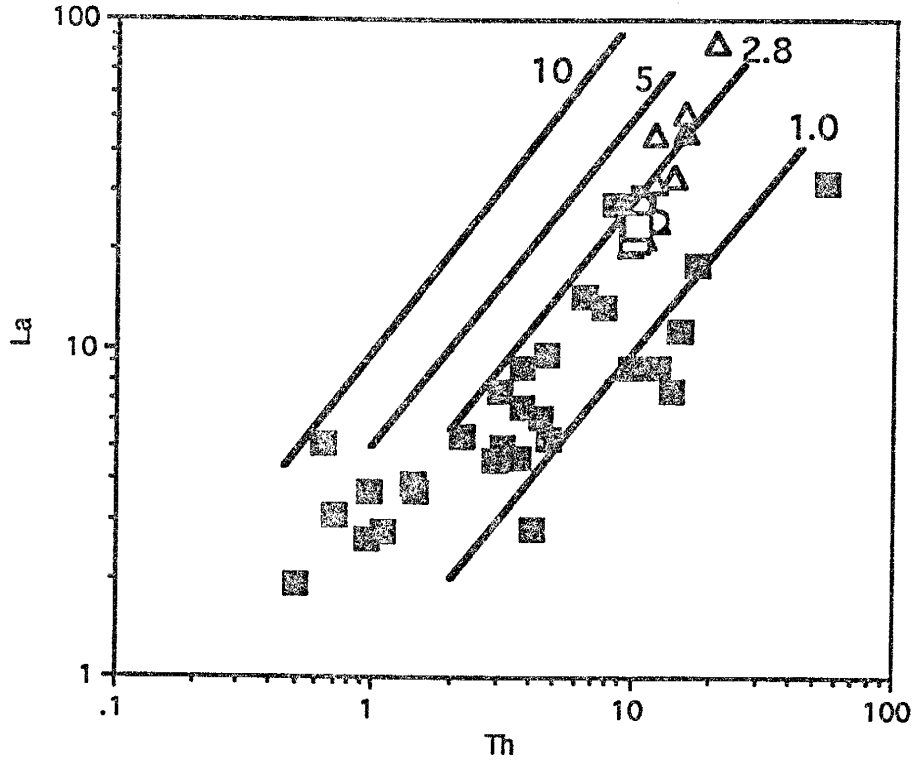

Figure 41. La/Th ratios in BB seam coals and associated lithologies; ■ = coal, ○ = partings, Δ = bounding claystones, □ = sandstones. Line numbers refer to La/Th ratios.

Mineralogical control on REEs

In the absence of direct evidence, mineralogical control of REEs may be constrained from linear coefficients between REEs and other elements, and major oxides (Condie, 1990). Correlation coefficients between REEs, Hf, and selected major oxides in BB seam coals and claystones are given in Tables 41 and 42.

Table 41 shows poor or non existent correlation of the REEs to P_2O_5 and Al_2O_3 suggesting that the distribution of the REEs is not controlled by either the clay minerals or phosphate minerals (such as apatite or monazite) but perhaps by a combination of these minerals and other REE-bearing minerals. Because of similarity in chemical properties with Zr, it has been suggested that Hf is primarily associated with zircon (Swaine, 1990). Thus, the strong positive correlation of the REEs to Hf may indirectly suggest that at least part of the REEs are associated with zircon. The LREEs are more strongly associated with Hf than the HREEs. As zircons invariably have high HREE/LREE ratios (Hickmott, 1993 personal comm.) the reason for this relationship is not readily apparent.

In the claystones (Table 42), the REEs show strong positive correlation to P_2O_5 and negative correlation to Al_2O_3 suggesting that the REEs are primarily associated with phosphate minerals. The negative correlation of REEs to Hf suggests that zircon may not be a primary source of REEs in these claystones.

Table 41. Correlation between REEs and Hf, and major oxides in BB seam coals (REE and Hf, and major oxide concentrations from whole coal and coal ash, respectively).

	La	Ce	Sm	Eu	Tb	Yb	Lu
P_2O_5 *	0.07	0.04	0.05	0.14	0.09	0.06	0.07
Al_2O_3 *	0.37	0.34	0.22	0.08	-0.07	-0.09	-0.13
Hf **	0.84	0.81	0.72	0.67	0.59	0.68	0.68

* = 8 samples; ** = 30 samples

Table 42. Correlation between REEs and Hf, and major oxides in claystones (REE and Hf, and major oxide concentrations from whole coal and coal ash, respectively).

	La	Ce	Sm	Eu	Tb	Yb	Lu
P_2O_5 *	0.99	0.99	0.98	0.98	0.94	0.87	0.89
Al_2O_3 *	-0.62	-0.62	-0.77	-0.77	-0.86	-0.94	-0.93
Hf **	-0.86	-0.85	-0.94	-0.94	-0.91	-0.88	-0.86

* = 6 samples; ** = 30 samples

7 - Summary and conclusions

Chemical and petrographic analyses of whole coal samples and associated non-coal lithologies in the BB seam have been made in this study. This study has generated information concerning the nature, occurrence and distribution of sulfur, and minor and trace elements in coal. Major shifts in sulfur contents in the generally low-sulfur coals of the Menefee Formation (San Juan Basin, New Mexico) and the highest total sulfur content in Menfee Formation coals (Cleary Coal Member) observed to date are documented in this study. This is the first study that makes use of trace-element concentration of pyrite, and siderite chemical compositions in an attempt to constrain the processes that may have contributed to the observed sulfur distributions in Menefee coals, New Mexico. This study is also the most detailed examination of trace-element geochemistry of Menefee coals in the San Juan Basin of New Mexico. The organic/inorganic affinity of trace-elements and their likely modes of occurrence in the coals, the relationships between minerals and trace elements, and source of trace elements in the coals are treated in more detail than previous studies on Menefee coals (Kuellmer et al., 1987, Baker, 1989).

7.1 - Sulfur distribution

Sulfur distribution within the BB seam varies both horizontally and vertically. Pyritic and organic sulfur are the dominant forms of sulfur with sulfate sulfur occurring in negligible amounts (average = 0.07%). The total sulfur content of the coals ranges from 0.22% to 5.67% with an average of 0.95% for the BB seam. The average pyritic and organic sulfur contents are 0.39%, and 0.49%, respectively. Relationships between the forms of sulfur suggest that variations in total sulfur in the coal samples seem to be mainly due to variations in the amount of pyritic sulfur and, to a lesser extent, of organic sulfur. Poor

correlations of total and pyritic sulfur to ash are observed. Negative correlation of organic sulfur with ash indicates that an increase in ash content due to increase in the amount of mineral matter, via detritus input into the peat and/or extreme degradation in the peat will result in a decrease in the amount of organic matter that could act as a sink for the available sulfur.

Iron sulfides (mainly marcasite and pyrite) in the BB seam occur as: a) framboids and euhedral crystals, b) massive forms filling voids, and c) cleat-filling. Marcasite occurs only in association with cleat-filling pyrite.

Based on sulfur distribution in the three drill holes, three distribution patterns were recognized in the BB seam: (1) higher sulfur contents in coal samples adjacent to the seam margins and parting, and at certain stratigraphic levels (DHS1); (2) higher sulfur content toward the middle of the seam (DHS2); and (3) distribution pattern where the sulfur content in the coals varies slightly within the seam, but the maximum total sulfur content does not exceed 1%.

The distribution patterns indicate sulfur incorporation during two periods: (a) during the early stages of peat deposition - mainly as organic sulfur in the low-sulfur coal samples, and mainly as pyritic sulfur in the high-sulfur coal samples (DHS2), and (b) during and/or after cleat formation - mainly as pyritic sulfur near seam margins. The high sulfur contents in DHS2 suggest aerially limited brackish or marine water influence during the early stages of peat accumulation. Occasional sea sprays, and high tides that may have flodded the ancient swamp locally may have been the source of the high-sulfate water.

As/Se ratios in whole coal samples from high- and low-sulfur coals show significant differences with an average of 8.38 for high-sulfur samples and 0.63 for low-sulfur coal samples. The high As/Se ratios in the BB seam compare with values of around 10 observed in coals with marine and brackish overburden. These high As/Se values may be indicative of some marine or brackish water

influence in the BB seam. In contrast to marine/brackish water influence indicated by As/Se ratios, siderite compositions in samples associated with both low- and high-sulfur coals suggest fresh-water depositional settings and probably some brackish-water influence.

Various combinations of such factors as Fe and sulfate ion availabilty, Eh - pH conditions, and detritus input are used to explain the relationships of sulfur content with ash and vitrinite content in the BB seam. Low pH, low sulfate concentrations, limited supply of reactive Fe, reducing conditions in the peat and low detrital input into the peat may result in coal that has low sulfur and low ash contents, and relatively rich in vitrinite. Relatively higher pH, ample supply of Fe, and sulfate ions (due to influence of sulfate-rich waters or high fluid flux of low-sulfate waters), and relatively higher oxidation and detrital input may result in inertinite-rich coal with high sulfur and ash contents.

7.2 - Minor and trace element geochemistry

Quartz and kaolinite are the most abundant minerals in the BB seam coals and associated lithologies. Other identified minerals include, pyrite, siderite, bassanite, feldspars, mica, illite, calcite, barite, and celsian.

Twenty four elements were determined in whole coal, and associated non-coal samples. Statistical analyses show :

1) most elements show log normal distribution,

2) the elements Ba, Fe, Co, Zn, As, Th, U, Sb, Cs, and Rb have relatively large ranges (2 or more orders of maginitude) and high coefficients of variation,

3) the elements Na, Sc, Cr, Fe, Co, Zn, Sr, Ba, La, Ce, Sm, Eu, Yb, Lu, Hf, Ta, Tb, Th, U, Rb, and Cs are depleted in the coals relative to their average crustal concentrations (ACC). Average As content in the coals is close to ACC. Antimony and Se are enriched in the coals relative to their ACC,

4) many elements in the claystones and sandstones are depleted relative to ACC. Antimony and Se are enriched in the claystones and sandstones relative to their ACC. Claystones and sandstones associated with the BB seam show variable depletions and enrichments in trace-element concentrations relative to average shale and sandstone compositions, respectively, and 5) variable depletion and enrichments are observed in the BB seam relative to San Juan River Region and Rocky Mountain coals. Compared to Eastern US coals, the BB seam is depleted in As, Ba, Ce, Co, Cr, Cs, Eu, Fe, La, Lu, Na, Rb, Sc, Se, Sm, and Zn.

The elements that have relatively large ranges and standard deviations larger than their arithimetic means (i.e coefficients of variation > 100%), may occur in sulfide, sulfate, carbonate, silicates and phosphate minerals such as pyrite, sphalerite, barite, siderite, zircon and apatite. The relatively large ranges of Cs and Rb may be due to relatively high concentration of clay minerals and feldspars which may be concentrated in particular stratigraphic intervals as opposed to being evenly distributed in the coal seam. Elements that showed relatively narrow distribution ranges are thought to be in part associated with clay minerals and rare-earth element bearing minerals that are evenly distributed in the coal seam.

Antimony and Se enrichments (relative to ACC) in the BB seam coals and associated clastic rocks suggest that Sb and Se input into the swamp was high and that the Sb and Se concentrated in the original plants were retained within the coal - forming system fixed in sulfides and clay minerals. Depletions or enrichments of certain trace elements in the BB seam claystones and sandstones may be indicative of the relative amount of minerals (depleted or enriched in particular trace elements) in the detrital material brought into the coal-forming environment. Enrichment factors scaled for equal lanthanum show that

As, Ba, Sb, Se, and Sr are significantly enriched in the coals. These elements may be associated with diagenetic minerals such as iron sulfides and carbonates that formed in the peat and/or after coalification and development of cleats. Cesium and Rb are depleted in the coals and the rest of the elements show EF_{La} values close to one, but in general < 2. These elements indicate significant contribution from the detrital component in the coal.

Comparison of trace-element concentrations in BB seam coals with other coals shows variable depletion and enrichment trends. The trends indicate that even though it may be possible to make some generalizations, trace element concentrations within a coal province or between basins are highly variable. The BB seam coals have comparable ash contents with eastern US coals (Table 32) but have lower concentrations in several trace elements. This observation suggests differences in the mineralogy and/or geochemistry of the source rocks and perhaps differences in the local depositional regimes in the two regions.

The vertical distribution of trace elements in the BB seam generally exhibits a "C" shaped profile with high-trace element content in and near bounding lithologies and partings. In general, all elements except Se show higher concentrations in the non-coal lithologies. Selenium concentration in the coals is generally higher than that in the non-coal samples. Higher trace-element concentrations in the coals are in general associated with ash-rich samples and the presence of mineral phases such as pyrite and barite. The majority of elements in the BB seam show significant correlation with the ash content. Arsenic, and Fe show relatively lower correlation with ash while Ba and Co show poor correlation with the ash content. The poor correlation of Co with ash may be explained by predominant association with the organic matter. The low correlations of As, Ba, and Fe with the ash content result due to the the presence of mineral phases which occur in certain zones and are rich in these

elements but do not contribute much to the ash content of the coal. The high correlations with ash suggest that the majority of the trace elements are associated with mineral matter (rich in these elements) admixtured with the organic matter.

The vertical distribution of trace elements in the BB seam may be explained by the following factors: 1) ash related variations - the increase in trace element content with increase in ash content indicates that those elements that show strong positive correlation with ash are associated with the inorganic fraction. Increased detrital input into the peat forming system may result in the formation of a clastic parting or the demise of the peat. Trace elements associated with minerals will thus show higher concentrations in these layers (bounding lithologies and partings) relative to the vegetation- dominated peat. Ocassional degradation (or oxidation) of the peat material that may result due to lower water table conditions, could result in ash-rich layers within the peat. Such ash related variations may explain the Type 1 profile observed in the BB seam.

(2) geochemical and hydrological factors - Redistriution of some elements by leaching (by acidic waters) from the bounding clastic sediments and redeposition in the nearby peaty material (coal precursor) due to changing geochemical conditions such as lowered Eh may explain trace element enrichments in coal samples adjacent to the seam margins or partings. In the BB seam, elements that display Type 2 distribution profile are mainly chalcophile elements and may have formed from the alteration of non-sulfide minerals and subsequent deposition in a reducing (low Eh) environment as sulfides or selenides. Where as the above described processes may operate during the compaction of the peat and the early stages of coalification, transport and deposition of metals by ground water can also happen after coalification. In the BB seam, this is evidenced by the presence of cleat-filling pyrite and calcite. This

epigentic mineralization can affect trace element concentration in the coal seam. In contrast to enrichment by epigenetic mineralization, some elements may be leached from the peat by circulating ground water and removed from the system. This process may explain the Type 3 distribution profile displayed by Na.

Comparison of trace-element contents of bright and dull coals shows that dull coal contains more As, Cr, Fe, Se, and Sr than bright coals. Most of these elements may occur in association with sulfides, indicating that conditions that formed the dull coals favored sulfide precipitation. Such conditions include ample supply of Fe and relatively high pH and low Eh conditions.

Results of the geochemical distribution of trace elements calculated by a theoretical model (Solari et al., 1989) show that the elements As, Fe, Sb, and Se are predominantly associated with the sulfide fraction. The REEs and Cr, Cs, Hf, Rb, Sc, Sr, Th, U, and Zn are predominantly associated with the non-sulfide inorganic fraction. I_o values show that Co occurs exclusively in association with the organic fraction, and Ba may be partly associated with the organic matter. Sodium, and Ta showed association with both the sulfide and non-sulfide fractions.

Principal component and cluster analyses show that the elements may be grouped in to the following groups:

1) elements that may be associated with the non-sulfide inorganic fraction. This group includes the REEs, Cr, Hf, Na, Sc, Se, Sr, Ta, Th, and U.,

2) elements that may be associated with sulfides. Arsenic and Fe fall into this group., and

3) elements that may be associated with the organic fraction. This group includes Ba, Co, and Zn.

There are slight differnces between the results obtained using the Solari et al., (1989) model , and principal component and cluster analyses. These

differences may be due to the nature of the procedures applied. Whereas the Soalri et al., (1989) model uses only the relation between element concentration and ash (and sulfide)content, The principal component and cluster analyses take into consideration the relationship among all the trace elements and ash content of the samples.

Based on statistical analyses, calculation of theoretical partial concentrations, vertical distribution patterns, mineralogical composition (from XRD analysis) and direct evidence (electron microprobe and PIXE), the likely modes of occurrence of trace elements in the BB seam coals are belived to be as follows:

As - in iron sulfides and possibly in clay minerals

Ba - in barite and celsian, and possibly in feldspars and illite

Co - probably associated with the organic fraction, or accessory heavy mineral phases in the coal matrix

Cr - probably in clay minerals and accessory heavy minerals

Cs and Rb - possibly in potassium - bearing phases including feldspars, micas and illite (all identified in the BB seam)

Fe - in pyrite, marcasite, siderite, and calcite, and possibly in clay minerals and heavy accessory minerals

Hf - possibly in clay minerals and heavy accessory minerals such as zircon

Na - possibly in clay minerals and feldspars

Sb - possibly in sulfides and clay minerals

Sc - possibly in clay minerals and REE - bearing accessory minerals

Se - in sulfides, and possibly in clay minerals

Sr - in calcite, siderite, iron sulfides, and possibly in clay minerals

Ta - possibly in accessory minerals such as rutile, and clay minerals

Th and U - possibly in clay minerals and heavy accessory minerals such as zircon

Zn - in sulfides, and possibly clay minerals

REEs - possibly in phosphate minerals (such as apatite and monazite), zircon, and clay minerals.

REE patterns in the BB seam coals suggest derivation from sources with upper continental crust compositions (possibly predominantly granitic). The majority of elements in the BB seam exhibit strong correlations with ash and the REEs indicating that the original source for the bulk of these elements was the detrital material brought into the swamp. Comparison of trace-element concentrations of BB seam coals and associated claystones also support a predominantly detrital origin for many of the trace elements.

References cited

Altschuler, Z.S., Schnepfe, M.M., Silber, C.C., and Simon, F.O., 1983. Sulfur diagenesis in Everglades peat and origin of pyrite in coal. Science vol. 221, 221-227.

Augustithis, S.S., 1983. The significance of trace elements in solving petrogenetic problems and controversies. Theophrastus Publications S.A.

American Society for Testing and Materials, 1990. Annual book of ASTM standards section 5, volume 05.05, gaseous fuels; coal and coke: American Society for Testing and materials, Philadelphia, PA, 213-512.

Baker, L.A., 1989. Vertical distribution of trace elements in coal seams from the San Juan and Raton Basins. New Mexico. New Mexico Institute of Mining and Technology (unpublished MS. Thesis), Socorro, New Mexico.

Beaumont, E.C., 1982. Geology of New Mexico coal deposits and settings for field trips: In Coal-bearing Sequences- Modern Geological Concepts for Exploration and Development; Amer. Asso. Petr. Geol., Short Course Notes, March 1982, Figure 3.

Beaumont, E.C., 1987. Geology and mining activity in the Lee Ranch Mine area, McKinley County, New Mexico. New Mexico Bureau of Mines and Mineral Resources Bulletin 121, 37-40.

Bence, A.E., and Albee, A.L., 1968. Empirical correction factors for the electron microanalysis of silicates and oxides. Jour. of Geology. vol. 76, pp. 382-403.

Berner, R.A., 1984. Sedimentary pyrite formation: an update. Geochimica et Cosmochimica Acta. vol. 48, 605-615.

Bhatia, M. R., and Crook, K. A. W., 1986. Trace element characteristics of graywackes and tectonic setting discrimination of sedimentary basins. Contrib. Mineralogy and Petrology, vol. 92, pp. 181 - 193.

Birk, D., and White, J.C., 1991. Rare earth elements in bituminous coals and underclays of the Sydney basin, Nova Scotia: element sites, distribution, mineralogy. International Journal of Coal Geology. vol. 19, pp. 219-251.

Boctor, N.Z., Kullerud, G., and Sweany, J.L., 1976. Sulfide minerals in Seelyville Coal, Chinook Mine, Indiana. Mineralium Deposita, 11, pp. 249-266.

Bogdanov, V. V., 1965. Zur genese der mikroelemente in den kohlefuhrenden sammelwerk: Materialy K 9. Ssovest. Rabotn. geol. organ., Leningrad 7, pp. 90 - 94 (cited in Finkelman, 1980).

Bouska, V., 1981. Geochemistry of coal. Amsterdam, Elsevier, 248 p.

Brookes, C.J., Betteley, I.G., and Loxston, S.M., 1966. Mathematics and Statistics for Chemists, Wiley, New York.

Campbell, F. W., and Roybal, G. H., 1987. Characterization of New Mexico coals, Menefee and Crevasse Canyon Formations. New Mexico Bureau of Mines and Mineral Resources, Bulletin 121, pp. 41 - 48.

Cameron, C.C., Esterle, J.S., and Palmer, C.A., 1989. The Geology, botany and chemistry of selected peat-forming environments from temperate and tropical latitudes. International Journal of Coal Geology. vol. 12, pp. 105 - 156.

Caruccio, F.T., 1973. Estimating the acid potential of coal mine refuse: In The ecology of resource degradation and renewal, Chadwick and Goodman (editors), Blackwell Scientific Publications.

Casagrande, D.J., 1987. Sulfur in peat and coal. In Coal and coal-bearing strata, Recent advances, Geological Society special

publication no. 32, 87-105.

Casagrande, D.J., Siefert, K., Berschinski, C., and Sutton, N., 1977. Sulfur in peat forming systems of the Okefenokee Swamp, and Florida Everglades: Origins of sulfur in coal. Geochimica et Cosmochimica Acta. vol. 41, 161-167.

Cecil, C.B., Stanton, R.W., Dulong, F.T., and Renton, J.J., 1982. Geologic factors that control mineral matter in coal. In Atomic and Nuclear Methods in Fuel Fossil Energy Research (eds. R.H. Filby, B.S. Carpenter and R.C. Ragaini). New York: Plenum, 323-335.

Chambers, W. F., and Doyle, J. H., 1990. SANDIA TASK 8, Version C: A subroutined electron microprobe automation system. Sandia Report SAND 90 - 1703, Sandia National Laboratory, Albuquerque, NM, 166 p.

Choen, A.D., Spackman, W., and Dolson, P., 1984. Occurrence and distribution of sulfur in peat-forming environments of southern Florida. Int. Jour. Coal Geology, vol.4, pp73-96.

Chou, C. -L., 1982. Geol. Soc. America abstracts, north central Section, vol. 14, No. 5, pp. 256 - 257.

Coleman, M.L., 1985. Geochemistry of diagenetic non-silicate minerals: kinetic considerations. Phil. Trans. R. Soc. A, 286, pp. 353-372.

Coleman, S. L., and Bragg, L. J., 1990. Distribution and mode of occurrence of arsenic in coal. in Recent advances in coal geochemistry, Chyi, L. L., and Chou, C. -L., editors, Geological Society of America, Special Paper 248, pp. 13 - 26.

Condie, K. C., 1990. Another look at rare earth elements in shales. Geochim. Cosmochim. Acta. vol, 55, pp. 2527 - 2531.

Crelling, J.C., and Dutcher, R.R., 1980. Principles and Applications of Coal Petrology. SEPM Short Course Notes No. 8, 127 p.

Curtis, C.D., 1987. Mineralogical consequences of organic matter degradation in sediments: inorganic/organic diagenesis. In Marine clastic sedimentology, Leggett, J.K. and Zuffa, G.G. editors, Graham and Trotman, London. pp. 108-123.

Davies, T.D., and Raymond, R. Jr., 1983. Sulfur as a reflection of depositional environments in peats and coals. In Raymond, R. Jr., and Andrejko, M.J. (eds.). Mineral matter in peat: its occurrence, form and distribution. Los Alamos Natl. Lab., Earth and Space Sci. Div., Los Alamos, New Mexico. 123-139.

Davis, J. C., 1986. Statistics and Data Analysis in Geology. 2nd. edition, John Wiley and Sons.

Demir, I., Chou, C. -L., and Chaven, C., 1990. Abundances and leachabilities of sodium and chlorine in lithotypes of Illinois Basin coals, in Recent Advances in Coal Geochemistry, Chyi, L. L., and Chou, C. -L., editors, Geological Society of America, Special Paper 248, pp. 73 - 85.

Drever, J. I., 1982. The Geochemistry of Natural Waters. Englewood Cliffs, New Jersey, Prentice -Hall, Inc., 388 p.

Drever, J. I., Murphy, J. W., and Surdam, R. C., 1977. The distribution of As, Be, Cd, Hg, Mo, Pb, and U associated with the Wyodak coal seam, Powder River Basin, Wyoming. Contrib. Geology, University of Wyoming, vol. 15, No.2, pp. 93 - 101.

Duran, B. J., and Odell, P. L., 1974. Cluster analysis - a survey. lecture notes in economics and mathematical systems, Vol. 100.

Elifson, K. W., Runyon, R. P., and Haber, A., 1990. Fundamentals of Social Statistics. 2nd edition. McGraw Hill.

Eskenazy, G. M, 1978. Rare earth elements in some coal basins of Bulgaria. Geological Balcanica, vol.8, No. 2, pp. 81 - 88 (cited in Finkelman, 1980)

Eskenazy, G. M, 1987. Zirconium and hafnium in Bulgarian coals. Fuel, vol. 66, pp.1652 - 1657.

Eskenazy, G. M, 1989. Modes of occurrences of trace elements in Bulgarian coals. Jour. of Coal Quality, vol. 8, No. 3 - 4, pp. 102 - 109.

Esterle, J. S., and Ferm, J. C., 1986. Relationship between petrographic and chemical properties and coal seam geometry, Hance Seam, Breathitt Formation, southeastern Kentucky. Int. Jour. Coal Geology, vol. 6, pp. 199 - 214.

Fassett, J.E., and Hinds, J.S., 1971. Geology and fuel resources of the Fruitland Formation and Kirtland Shale of the San Juan Basin, New Mexico and Colorado. U.S. Geological survey Professional Paper 676, 76 p.

Feldman, D., Gagnon, J., Hofmann, R., and Simpson, J., 1988. StatView SE + Graphics, the solution for data analysis and presentation graphics. Abacus Concepts, Inc.

Filby, R. H., Shah, K. R., and Sautter, C. A., 1977. A study of trace element distribution in the Solvent Refined Coal (SRC) process using neutron activation analysis. Jour. Radioanalytical Chemistry, vol. 37, pp. 693 - 704.

Finkelman, R. B., 1980. Modes of occurrence of trace elements in coal (Ph.D. Dissertation) University of Maryland, 301 p.

Finkelman, R. B., and Brown, R. D. Jr., 1990. Coal as a host and as an indicator of mineral resources. in Geology in coal resource utilization, C. P. Douglas, editor, Tech Books, pp. 471 - 481.

Finkelman, R. B., Palmer, C. A., Krasnow, M. R., Aruscavage, P. J., Sellers, G. A., and Dulong, F. T., 1990. Combustion and leaching behavior of elements in the Argonne Premium coal samples. Energy and Fuels, vol. 4, pp. 755 -766.

Ford, C. T., 1977. Coal cleaning to remove trace elements prior to utilization, in 4th symposium on coal utilization, Louisville, Kentucky, October 1977, pp. 146 - 191.

Gladney, E. S., Burns, C. E., Perrin, D. R., Roelandts, I., and Gills, T. E., 1982. Compilation of elemental concentration data for NBS biological, geological, and environmental standard reference materials. NBS Special Publication 260 - 88, 200 p.

Glick, D. C., and Davis, A., 1987. Variabilty in the inorganic element content of US coals including results of cluster analysis. Organic Geochemistry, vol. 11, No. 5, pp. 331 - 342.

Gluskoter, H.J., and Simon, J.A., 1968. Sulfur in Illinois coals. Illinois State Geological Survey Circular 432, 28 P.

Gluskoter, H. J., Ruch, R. R., Miller, W. G., Cahill, R. A., Dreher, G. B., and Kuhn, J. K., 1977. Trace elements in coal: occurrence and distribution. Illinois State Geological Survey, Circular No. 499, 154 p.

Goldschmidt, V. M., 1954. Geochemistry. Oxford Press, London, 730 p.

Goodarzi, F., 1987. Concentration of elements in lacustrine coals from Zone A Hat Creek Deposit No. 1, British Columbia, Canada. Int. Jour. Coal Geology, vol. 8, pp. 247 - 268.

Goodarzi, F., 1988. Elemental distribution in coal seams at the Fording coal mine, British Columbia, Canada. Chem. Geol., vol. 68, pp. 129 - 154.

Goodarzi, F., and Van der Flier-Jeller, E., 1988. Distribution of major, minor and trace elements in Hat Creek Deposit No. 2, British Columbia, Canada. Chem. Geol., vol. 75, pp. 313 - 333.

Goodarzi, F., and Van der Flier-Jeller, E., 1989. Geological controls and constraints on the concentration of elements in western Canadian coals. in Geology in Coal Resource Utilization, C. P. Douglas, editor, Tech Books, pp. 389 - 412.

Green, M.W., Mytton, J.W., Sandberg, D.T., and Gardner, N.K., 1991. Geologic framework and major coal-bearing formations of the San Juan Basin. US Geol. Survey Bulletin 1972, pp 3-14.

Green, P. E., 1978. Analyzing multivariate data. The Dryden Press.

Harvey, R.D., Cahill, R.A., Chou, C.-L., and Steele, J.D., 1983. Mineral matter and trace elements in the Herrin and Springfield coals, Illinois Basin Coal Field. Illinois State Geological Survey Contract/Grant Report No.1983-4. Illinois State Geological Survey, Champaign, Illinois. 106 p.

Haskin, L. A., Haskin, M. A., Frey, F. A., and Wildeman, T. R., 1968. Relative and absolute abundances of the rare earth elements. in Origin and Distribution of the Elements, pp. 889 - 912. Pergamon Press.

Hatch, J. R., and Swanson, V. E., 1976. Trace elements in Rocky Mountain coals, in Proceedings of the 1976 symposium on the geology of Rocky mountain coal, D. K. Murray, editor, pp. 143 - 163.

Hickmott, D.D., Baldridge, W.S., and Raymond, R., 1992. Proton-induced x-ray emission microanalysis of coal macerals and sulfides: application to the Lower Kittanning coal of western Pennsylvania. Unpublished report submitted to Economic Geology.

Hoffman, G.K., 1991. Geology ad coal quality of Menefee Formation

coals, Monero coal field, Rio Arriba County, New Mexico. New Mexico Geology, vol. 13, no.1, 1-8.

Horton, L., and Aubrey, K. V., 1950. Distribution of minor elements in vitrain: three vitrains from the Barnsley seam. Jour. Soc. Chem. Industry (Supplement No. 1), pp. 541 - 548.

Jacobs, J. W., Korotev, R.L., Blanchard, D. P., and Haskin, L. A., 1977. A well tested procedure for instrumental neutron activation analysis of silicate rocks and minerals. Jour. Radioanalytical Chemistry, vol. 40, pp. 93 - 114.

Kelly, V.C., 1950. Regional Structure of the San Juan Basin. In: Guide book of the San Juan Basin, New Mexico and Colorado. New Mexico Geological Society guide book 1, 101-108.

Kendrick, D.T., 1985. Vertical distribution of selected trace elements within the Fruitland number eight coal seam, near Farmington, New Mexico. New Mexico Institute of Mining and Technology (unpublished MS. Thesis), Socorro, New Mexico.

Kendrick, D. T., Kyle, P. R., and Kuellmer, F. J., 1988. Analysis of NBS coal standard reference materials 1632A and 1635 by instrumental neutron activation analysis. Geostandards Newsletter, vol. 12, No. 2, pp. 375 - 377.

Kim, Jae-on., and Mueller, C. W., 1978a. Introduction to factor analysis - what it is and how to do it- Quantitative applications in the social sciences, series No. 07 - 013. Sage Publications.

Kim, Jae-on., and Mueller, C. W., 1978b. Factor analysis - statistical methods and practical issues. Quantitative applications in the social sciences, series No. 07 - 014. Sage Publications.

Kortenski, J., 1992. Carbonate minerals in Bulgarian coals with different degrees of coalification. Int. Jour. Coal Geology, Vol. 20, pp. 225 - 242.

Krauskopf, K. B., 1967. Introduction to Geochemistry. McGraw Hill.

Krauskopf, K. B., 1979. Introduction to Geochemistry. McGraw Hill.

Kryukova, V. N., Kindeeva, V. P., Baskova, L. V., and Latyshev, V. P., 1985. Arsenic in coal of eastern Siberia. Solid Fuel Chemistry, vol. 19, pp. 120 - 123.

Kuhn, J. K., Fiene, F., and Harvey, R., 1978. Geochemical evaluation and characterization of a Pittsburgh No. 8 and a Rosebud seam coal. Department of Energy, Morgantown Energy Technology Center. Document METC/CR - 78/8, 40 Xiii p. (cited in Finkelman, 1980).

Kuhn, J. K., Fiene, F. L., Cahill, R. A., Gluskoter, H. J., and Shimp, N. F., 1980. Abundance of trace and minor elements in organic and mined fractions of coal. Environmental Geol. notes., Illinois State Geological Survey, No. 88, 67 p.

Kuellmer, F.J., Kendrick, D.T., and Baker, L., 1987. Trace element distributions in some New Mexico coals: final technical report. New Mexico Research and Development Institute. NMERDI report no. 2-74-4321. 252 p.

Leutwein, F., and Rosler, H. J., 1956. Geochemical investigations of Paleozoic and Mesozoic coals from central and east Germany. Freiburg. Forschungsh., C 19, pp. 1 - 196 (cited in Swaine, 1990).

Lindahl, P.C., and Finkelman, R.B., 1986. Factors influencing major, minor, and trace element variations in US coals. In : Vorres, K.S., ed., Mineral Matter and Ash in Coal. ACS Symposium Series 301, pp 61-69.

Lindstrom, D. J., and Korotev, R. L., 1982. TEABAGS: computer programs for instrumental neutron activation analysis. Jour. Radioanalytical Chemistry, vol. 70, No. 1 - 2, pp. 439 - 458.

Loevblad, G., 1977. Trace element concentrations in some coal samples possible emissions from coal combustion in Sweden, Rep. IVL - B - 358 (cited in Valkovic, 1983).

Mack, M., and Spielberg, N., 1958. Statistical factors in X-ray intensity measurements. Spectrochimica Acta, vol. 12, pp. 169 - 178.

Martin, J. W., and Cavaroc, V., 1991. Lithotype control of trace element concentrations in some southeastern West Virginia coals. in Geology in Coal Resources Utilization C. P. Douglas, editor, Tech Books, pp. 427-450.

Mastalerz, M., and Smyth, M., 1988. Petrography and depositional conditions of the 64/65 coal seam in the Intrasudetic basin, SW Poland. Int. Jour. Coal Geology, vol. 10, pp. 309 - 336.

McLennan, S. M., 1989. Rare earth elements in sedimentary rocks: influence of provenance and sedimentary processes. Rev. Mineralogy, vol. 21, pp. 170 - 199.

McLennan, S. M., Nance, W. B., and Taylor, S. R., 1980. Rare earth element - thorium correlations in sedimentary rocks and the composition of the continental crust. Geochim. Cosmochim. Acta. vol. 44, pp. 1833 - 1839.

Miller, R. N., 1977. A geochemical study of the inorganic constituents in some low-rank coals (Ph.D. Dissertation) Pennsylvania State University, 301 p.

Miller, R. N., and Given, P. H., 1978. A geochemical study of the inorganic constituents in some low-rank coals. Technical Report 1, US Department of Energy Report FE - 2494 - TR - 1, 314 p.

Molenaar, C.M., 1983. Major depositional cycles and regional correlations of Upper Cretaceous rocks, southern Colorado Plateau and adjacent areas, In : Reynolds, M.W., and Dolly, E.D., eds., Mesozoic Paleogeography of the West-Central United States. Denver, Colo., Rocky Mountain Section, SEPM, pp 201-224.

Mozley, P. S., 1989. Relation between depositional environment and the elemental composition of early diagenetic siderite. Geology, vol. 17, pp. 704 - 706.

Mozely, P.S., and Wersin, P., 1992. Isotopic composition of siderite as an indicator of depositional environment. Geology, vol. 20, pp. 817-820.

Mukherjee, K. N., Dutta, N. R., Chandra, D., Pandalai, H. S., and Singh, M. P., 1988. A statistical approach to the study of the distribution of trace elements and their organic/inorganic affinity in Lower Gondwana coals of India. Int. Jour. Coal Geology, vol. 10, pp. 99 - 108.

Narayan, R., and Kullerud, G., 1988. A new perspective on the nature of "organic" sulfur in coal. Third chemical congress of North America, Abstracts of papers. p 3.

Neavel, R.C., 1966. Sulfur in coal: Its distribution in the seam and mine products. ph.D. Thesis, The Pennsylvania State University, University Park. 188-190.

Nicholls, G. D., 1968. The geochemistry of coal-bearing strata, in Coal and Coal-Bearing strata. Murchison, D., and Westoll, T.S. editors, pp. 269 - 307.

Norrish, K., and Hutton, J.T., 1969. An accurate x-ray spectrographic method for the analysis of a wide range of geological samples. Geochim. Cosmochim. Acta, vol. 33, pp. 431-453.

Otte, M. U., 1953. Trace elements in some German hard coals. Chem. Erde, 16, pp. 239 - 294 (cited in Swaine, 1990).

Palmer, C. A., 1983. the distribution of trace elements in minerals found in coal (Ph.D. Dissertation) Washington State University, 214 p.

Palmer, C. A., and Filby, R. H., 1984. Distribution of trace elements in coal from the Powhatan No. 6 mine , Ohio. Fuel, vol. 63, pp. 318 - 328.

Palmer, J.J., and Scott, A.J., 1984. Stacked shoreline shelf sandstone of La Ventana Tongue (Campanian), northwestern New Mexico. Amer. Assoc. Petr. Geol. Bull. Vol. 68, No. 1, pp. 74-91.

Parratt, R.L., and Kullerud, G., 1979. Sulfide minerals in Coal Bed V, Minnehaha Mine, Sullivan County, Indiana. Mineralium Deposita, 14, 195-206.

Pendias, A.K., and Pendias, H., 1984. Trace elements in Soils and Plants. CRC Press, Inc., 315 p.

Pickhardt, W., 1989. Trace elements in minerals of German bituminous coals. Int. Jour. Coal Geology, vol. 14, pp. 137 - 153.

Pierce, W.H., and Shomaker, J.W., 1971. Strippable coal resources of San Mateo Menefee area. In Shomaker, J.W., Beaumont, E.C., and Kottlowski, F.E., eds., Strippable low-sulfur coal resources of the San Juan Basin in New Mexico and Colorado: New Mexico Bureau of Mines and Mineral resources. Memoir 25, 64-68.

Pires, M., and Teixeira, E. C., 1992. Geochemical distribution of trace elements in Leao coal, Brazil. Fuel, vol. 71, pp. 1093 - 1096.

Postma, D., 1982. Pyrite and siderite formation in brackish and fresh water swamp sediments. Amer. Jour. Science, vol. 282, pp. 1151 - 1183.

Pye, K., Dickson, J. A. D., Schiavon, N., Coleman, M. L., and Cox, M., 1990. Formation of siderite - Mg-calcite - iron sulfide concretions in intertidal marsh and sandflat sediments, north Norfolk, England. Sedimentology, vol. 37, pp. 325 - 343.

Querol, X., Chinchon, S., and Lopez-Soler, A., 1989. Iron sulfide precipitation sequence in Albian coals from the Maestrazgo Basin, southeastern Iberian Range, northeastern Spain. International Journal of Coal Geology. vol. 11, 171-189.

Raask, E., 1985. The mode of occurrence and concentration of trace elements in coal. Prog. Energy Combust. Sci., vol. 11, pp. 97 - 118.

Raiswell, R., and Plant, J., 1980. The incorporation of trace elements into pyrite during diagenesis of blakshales, Yorkshire, England. Economic Geology, vol. 75, pp 684 - 699.

Razdorozhniy, V. F., and Petrus, A. G., 1975. Rare alkalies in coals of the Dnieper and Donets Basins. Chemical Abstracts, vol. 82, No. 88336r.

Reeves, R.D., and Brooks, R.R., 1978. Trace element analysis of geological materials. John Wiley and Sons., pp. 374-408.

Renton, J.J., and Hidalgo, R.V., 1975. Some geochemical considerations of coal. West Virginia Geologic and Economic Survey Circular No. 4, 35p.

Renton, J.J., 1979. The mineral content of coal. In: Donaldson, A.C., Presley, M.W., and Renton, J.J. (editors), Carboniferous Coal. W. Va. Geological Survey., 1, 191-207.

Renton, J.J., 1982. Mineral matter in coal. In: R.A. Meyers (ed), Coal Structure. Academic Press, New York, NY., pp. 283-324.

Reyes-Navarro, J., and Davis, A., 1976. Pyrite in coal. Its forms and distribution as related to the environments of coal deposition in three selected coals from Western Pennsylvania. Special Research Report SR-110, Coal Reasearch Section, the Pennsylvania State University, 141p.

Rimmer, S. M., and Davis, A., 1986. Geologic controls on the inorganic composition of the Lower Kittanning coal, in Mineral Matter and Ash in

Coal, K. S. Vorres, editor, American Chemical Society Symposium Series 301, pp. 41 - 52.

Roberts, D. L., 1988. The relationship between macerals and sulphur contents of some South African Permian coals. Int. Jour. Coal Geology, vol. 10, pp. 399 - 410.

Roybal, G.H., Campbell, F. W., Beaumont, E.C., Cohen, A.D., Kuellmer, F.J., Kottlowski, F.E., and Cook, K.H., 1987. Quality assessment of strippable coals in New Mexico, Year 2, phase 2, Fruitland, Menefee, and Crevasse Canyon Formation coals in the San Juan Basin of northwestern New Mexico. New Mexico Research and Development Institute report 2-74-4331, 101 p.

Roybal , G.H., 1989. Coal characteristics of major coal-bearing sequences, Gallup field, northwestern New Mexico. New Mexico Geological Society Guidebook, 40th field conference, south eastern Colorado Plateau, 309-315.

Sage, W. L., and McIlroy, J. B., 1959. Relationship of coal ash viscosity to chemical composition. Combustion, vol. 31, No. 5, pp. 41 - 48.

Schmidt, R.A., 1979. Coal in America: An Encyclopedia of Reserves, Production, and Use. McGraw Hill Publications., pp 50-57.

Schopf, J. M., 1956. A definition of coal. Economic Geology, Vol. 51, No. 6, pp.

Schultz, H., Hattman, E. A., and Booher, W. B., 1975. The fate of some trace elements during coal pretretment and combustion, in Trace elements in Fuel, S. P., Babu, editor, American Chemical Society, Advances in Chemistry Series 141, chapter 11, pp. 139 - 153.

Shotyk, W., 1988. Review of the inorganic geochemistry of peats and peatland waters. Earth Science Reviews, vol. 25, pp. 95 - 176.

Siegel, S., 1956. Nonparametric statistics for the behavioral sciences. McGraw Hill.

Siemers, C.T., 1978. Generation of a simplified working depositional model for repetitive coal-bearing sequence using field data: an example from the Upper Cretaceous Menefee Formation (Mesa Verde Group), Northwestern New Mexico. In Proceedings of the 2nd symposium on the geology of Rocky Mountain coal, 1977., H.E. Hodgson (ed). Colorado Geological Survey Resource series 4, 1-22.

Sillanpaa, M., 1972. Distribution of trace elements in peat profiles. Proc. 4th int. peat cogr., Otaniemi, Finland, vol. 5, pp. 185 - 191.

Singh, R. M., Singh, M. P., and Chandra, D., 1983. Occurrence, distribution and probable source of the trace elements in Ghugas coals, Wardha Valley, districts Chandrapur and Yeotmal, Maharashtra, India. Int. Jour. Coal Geology, vol. 2, pp. 371 - 381.

Smith, J.W., and Batts, B.D., 1974. The distribution and isotopic composition of sulfur in coal. Geochimica et Cosmochimica Acta. vol. 38, 121-133.

Solari, J. A., Fiedler, H., and Schneider, C. L., 1989. Modelling of the distribution of trace elements in coal. Fuel, vol. 68, pp. 536 - 539.

Solodov, N. A., Kostin, Yu., Mertov, E.S, Bel'kov, V. I., Zyroyanov, A. P., and Pankov, E. N., 1975. Cesium and tantalum in mined coals of the USSR. Chemical Abstracts, vol. 83, pp. 154, no. 166700s.

Spears, D.A., and Martinez-Tarazona, M.R., 1993. Geochemical and mineralogical characteristics of a power station feed-coal, Eggborough, England. Int. Jour. Coal Geology, vol 22, pp 1-20.

Stach, E., Mackowsky, M.-Th., Teichmuller, M., Taylor, G.H., Chandra,

D., and Teichmuller, R., 1982. Stach's Textbook of Coal Petrology. Gebruder Borntrager, Berlin.

Swaine, D. J., 1964. Scandium in Australian coals and related materials. Amer. Chem. Soc., Div. Fuel Chemistry, preprint, vol. 8, No. 3, pp. 172 - 177.

Swaine, D. J., 1990. Trace Elements in Coal. Butterworths, 278 p.

Swanson, V. E., Medlin, J. H., Hatch, J. R., Coleman, S. L., Wood, G. H. Jr., Woodruff, S. D., and Hildebrand, R. T., 1976. Collection, chemical analysis, and evaluation of coal samples in 1975. US Geological Survey, open - file report 76 - 468, 503 p.

Tabet, D.E., Frost, S.J., and Kottlowski, F.E., 1985. Depositional environments for Menefee Formation low-sulfur coals in southeast San Juan Basin of New Mexico. In: Cross, A.T. (ed), 9th International Congress on Carboniferous Startigraphy and Geology. vol. 4, 321-328. Washington and Champaign-Urbana, May 17-26, 1979.

Taylor, S. R., 1964. Abundances of chemical elements in the continental crust: a new table. Geochim. Cosmochim. Acta, vol. 28, pp. 1273 - 1285.

Taylor, S. R., and McLennan, S. M., 1985. The Continental Crust: Its Composition and Evolution. Blackwell, pp. 9 - 56.

Tsai, S.C., 1982. Coal Science and Technology 2: Fundamentals of coal beneficiation and utilization. Elsevier, Amsterdam.

Tsui, F. F., Cahill, R. A., and Frost, J. K., 1979. Concentrations of rare earth elements in coals of the Illinois Basin. 9th international congress of Carboniferous Startigraphy and Geology, Urbana, Illinois, may 1979: Carbondale, Illinois, Southern Illinois University Press, pp. 218.

Turekian, K. K., and Wedepohl, K. H., 1961. Distribution of the elements in some major units of the earth's crust. Bull. Geol. Soc. America, vol. 72,

pp. 175 - 192.

Valkovic, V., 1983. Trace elements in coal Vol. 1, Boca Raton, Florida, CRC Press Inc., 210 p.

Van der Flier-Keller, E., and Fyfe, W. S., 1985. Uranium - thorium systematics of two Canadian coals. Int. Jour. Coal Geology, vol. 4, pp. 335 - 353.

Walker, F.E., and Hartner, F.E., 1966. Forms of sulfur in U.S. coals. U.S. Bureau of mines Information Circular 8301.

Ward, C. R., 1984. Coal geology and coal technology. Blackwell Scientific Publications, pp. 1 - 3.

Weise, R.G., and Fyfe, W.S., 1986. Occurrence of Iron sulfides in Ohio coals. International Journal of Coal Geology. vol. 6, 251-276.

Wilkinson, L., 1989. SYSTAT: The system for statistics. Evanston, IL, Systat, Inc.

Williams, E.G., and Keith, M.L., 1963. Relationship between sulfur in coals and the occurrence of marine roof beds. Economic Geology. vol. 58, 720-729.

Wilson, M., 1989. Igneous petrogenesis; A global tectonic approach.

Wood, G. H., Kehn, T. M., Carter, M. D., and Culbertson, W. C., 1983. Coal Resources Classification System of the USGS. US Geological Survey Circular 891.

Appendix 1. Description of stratigraphic sections

Table APP1-1. Description of measured stratgraphic column in drill hole S1 (DHS1), BB seam, Lee Ranch Mine.

Thcikness (cm)		Sample number	Lithotype*/Lithology
Total	unit		
390.89	37.5	S1-1 to S1-4 (top of core)	Claystone; lightgray, V. thinly laminated
353.39	28.25	S1-5 to S1-9 (top of coal seam)	Clarain; cleat filling pyrite toward the bottom V. thin fusain bands.
325.14	2.5	S1-10	Vitrain; some pyrite flakes
322.64	25.62	S1-11 to S1-14	Vitrain; V. thin and sparse bands fusain, cleat pyrite, resin blebs present sporadically
297.02	2.5	S1-15	Vitrain; V.thin bands of durain, some pyrite and resin present
294.52	23.75	S1-16 to S1-18	Clarain; V. thin fusain band at the bottom, resin blebs and cleat pyrite toward the top.
270.77	2.5	S1-19	Clarain; cleat filling pyrite and calcite present
268.27	17.97	S1-20 and S1-21	Clarain; vertcal fractures filled with pyrite and calcite, few resin blebs
250.30	27.5	S1-22 to S1-25	Clarain; cleat filling pyrite and calcite, resin blebs abundant toward top
222.8	34.06	S1-26 to S1-30	Clarain; few pyrite filled cleats, V.thin bands of fusain, resin fragments toward bottom
188.74	3.91	S1-31 (parting)	Claystone; light gray, coaly fragments present, sharp contacts with overlying and coal

Table APP1-1. continued

Thcikness (cm)		Sample number	Lithotype*/Lithology
Total	unit		
184.83	28.59	S1-31 to S1-35	Clarain; resin blebs, cleat filling pyrite and calcite
156.24	28.75	S1-36 to S1-39	Clarain; calcite and pyrite filled cleats, resin fragments
127.49	2.5	S1-40	Fusain
124.99	23.75	S1-41 to S1-44	Clarain; calcite and pyrite in cleats, resin fragments
101.24	53.43	S1-45 to S1-52	Vitrain; very brittle toward top, pyrite and calcite filled cleats, resin fragments
47.81	2.5	S1-53 (base of coal seam)	Carbonaceous shale (Durain ?); vitrain fragments, some pyrite
45.31	45.31	S1-54 to S1-58 (base of core)	Claystone; dark gray, some coaly fragments

Table APP1-2. Description of measured stratgraphic column in drill hole S2 (DHS2), BB seam, Lee Ranch Mine.

Thcikness (cm)		Sample number	Lithotype*/Lithology
Total	unit		
324.50	15.0	S2-1(top of core) & S2-2	Sandstone; gr. wht., fine- to-med. grd., moderately sorted., moderately indurated
309.50	30.0	S2-3 to S2-5	Dark gray calystone
279.50	2.50	S2-6 (top of coal seam)	Durain with thin vitrain bands and fusain fragments; few resin fragments
277.0	29.37	S2-7 to S2-10	Vitrain; few resin fragments and pyrite
247.63	27.02	S2-11 to S2-15	Durain; fairly abundant resin fragments in the lower half; disseminated pyrite; thin vitrain bands and some fusain fragments
220.61	15.62	S2-16 to S2-18	Vitrain; few resin fragments
204.99	23.44	S2-19 to S2-21	Durain; thin vitrain and fusain bands; fairly abundant resin fragments; minor pyrite
181.55	37.81	S2-22 to S2-27	Clarain; thin alternating bands of vitrain, durain, and minor fusain; fairly abundant resin fragments, and cleat-filling and disseminated pyrite
143.74	2.5	S2-28	Clarain; very thin bands of alternating vitrain, durain, and fusain bands; sparse disseminated pyrite and resin fragments
141.24	19.69	S2-29 to S2-31	Durain; vitrain and fusain fragments; resin fragments fairly abundant; disseminated pyrite
121.55	41.24	S2-32 to S2-36	Vitrain; abundant resin fragments; cleat-filling and disseminated pyrite
80.31	34.06	S2-37 to S2-40 (base of coal seam)	Vitrain; thin durain bands; abundant resin toward the top; cleat-filling pyrite
46.25	17.81	S2-41 & S2-42	Claystone; dark gray; some coaly fragments
28.44	28.44	S2-43 & S2-44 (base of core)	Sandstone; light gray; medium-grained

Table APP1-3. Description of measured stratgraphic column in drill hole S3 (DHS3), BB seam, Lee Ranch Mine.

Thcikness (cm)		Sample number	Lithotype*/Lithology
Total	unit		
331.86	41.25	S3-1 (top of core) to S3-5	claystone; dark gray; few coaly fragments
290.61	34.38	S3-6 (top of coal seam) to S3-10	Durain; thin vitrain and fusain bands; fairly abundant resin fragments; cleat-filling calcite toward the top
256.23	53.75	S3-11 to S3-17	Vitain; cleat-filling and disseminated pyrite; few resin fragments
202.48	3.59	S3-18	Claystone parting; dark gray; some coaly fragments
198.89	54.53	S3-19 to S3-25	Vitrain; cleat-filling and disseminated pyrite; few resin fragments
144.36	14.06	S3-26 & S3-27	Vitrain; sparse pyrite; fairly abundant resin fragments
130.30	3.12	S3-28	Durain; few thin vitrain bands; siderite(?) nodules
127.18	12.50	S3-29	Vitrain; fairly abundant resin fragments
114.68	18.75	S3-30 & S3-31	Vitrain; resin fragments; disseminated pyrite
95.93	11.56	S3-32 & S3-33	Vitrain; few resin fragments
84.37	6.25	S3-34	Vitrain; abundant resin fragments; few fusain fragments and pyrite
78.12	37.81	S3-35 to S3-39	Vitrain; abundant resin fragmentsfairly abundant pyrite; cleat-filling calcite; some durain fragments
40.31	7.34	S3-40 & S3-41 (base of coal seam)	Durain/carbonaceous shale(?); few resin fragments
32.97	32.97	S3-40 & S3-41 (base of core)	Claystone; light gray., some coaly fragments and resins toward the top

Appendix 2. Results of electron microprobe analysis of iron sulfides and carbonates

Table APP2-1. Electron microprobe analysis results (wt%) of iron sulfides.

Sample no.	Iron sulfide type	wt% Fe	wt% S	Pb	Mn	Sr	Cd	Cu	Zn	Co	Ni	S/Fe
S2-40	framboids	45.56	53.51	n.d	30	n.d	n.d	n.d	n.d	n.d	n.d	1.17
S1-39	marcasite	45.70	55.18	553	n.d	n.d	n.d	n.d	n.d	n.d	n.d	1.21
S1-39	marcasite	45.78	53.43	n.d	n.d	433	128	n.d	n.d	n.d	n.d	1.17
S1-39	cleat-filling	46.35	55.08	711	n.d	887	44	n.d	n.d	n.d	n.d	1.19
S1-39	cleat-filling	46.53	54.38	n.d	n.d	393	n.d	49	63	n.d	n.d	1.17
S1-39	cleat-filling	46.27	54.55	313	n.d	715	n.d	129	n.d	n.d	n.d	1.18
S1-39	cleat-filling	46.65	54.05	n.d	n.d	n.d	n.d	n.d	48	n.d	n.d	1.16
S1-39	cleat-filling	46.36	53.73	364	n.d	732	n.d	107	n.d	n.d	n.d	1.16
S2-18	framboids	44.16	52.54	2024	1159	n.d	54	196	n.d	n.d	n.d	1.19
S2-18	framboids	44.31	52.82	1138	226	260	63	102	n.d	n.d	n.d	1.19
S2-18	pyrite cementing framboids	44.36	51.74	973	43	359	57	103	n.d	n.d	n.d	1.17
S2-18	pyrite cementing framboids	44.83	51.52	1371	66	280	n.d	82	n.d	n.d	n.d	1.15
S2-18	pyrite cementing framboids	43.97	50.77	1300	70	n.d	n.d	105	n.d	n.d	n.d	1.16
S2-18	pyrite cementing framboids	44.46	52.68	1103	106	496	77	n.d	n.d	n.d	n.d	1.18
S2-18	pyrite cementing framboids	44.29	51.89	1313	133	354	n.d	n.d	n.d	n.d	33	1.17
S2-18	pyrite cementing framboids	44.79	53.02	428	n.d	n.d	n.d	n.d	n.d	n.d	n.d	1.18
S2-18	pyrite cementing framboids	44.55	52.47	542	n.d	n.d	n.d	n.d	n.d	n.d	n.d	1.18
S2-18	pyrite cementing framboids	44.48	52.24	1425	50	348	n.d	58	n.d	n.d	n.d	1.17
S2-18	framboids	45.57	53.69	2306	n.d	588	n.d	n.d	n.d	n.d	n.d	1.18
S2-18	framboids	44.17	52.27	n.d	676	261	n.d	285	n.d	n.d	65	1.18
S2-18	cleat-filling	43.93	51.83	1452	430	n.d	n.d	391	67	n.d	n.d	1.18
S2-18	cleat-filling	43.65	52.55	1087	495	692	n.d	290	50	40	n.d	1.20
S2-18	pyrite cementing framboids	44.34	51.83	250	n.d	385	n.d	75	n.d	n.d	n.d	1.17
S2-18	pyrite cementing framboids	44.78	51.23	1011	n.d	n.d	41	100	n.d	n.d	n.d	1.14
S3-35	marcasite	45.80	55.24	560	n.d	n.d	n.d	97	n.d	n.d	n.d	1.21
S3-35	marcasite	45.95	54.69	n.d	n.d	798	70	n.d	n.d	n.d	n.d	1.19
S3-35	marcasite	46.16	54.50	n.d	n.d	n.d	n.d	48	n.d	n.d	n.d	1.18
S3-35	marcasite	46.15	55.73	373	n.d	475	n.d	133	71	n.d	n.d	1.21
S3-35	cleat-filling	45.97	54.53	294	n.d	238	n.d	n.d	n.d	n.d	n.d	1.19
S3-35	cleat-filling	46.26	55.24	563	n.d	311	n.d	n.d	n.d	n.d	n.d	1.19
S3-35	cleat-filling	46.63	54.95	410	n.d	358	66	n.d	n.d	n.d	n.d	1.17
S3-35	cleat-filling	46.08	55.97	271	n.d	639	n.d	51	n.d	n.d	n.d	1.22
S1-40	marcasite	45.60	54.62	n.d	n.d	668	66	45	n.d	n.d	n.d	1.20
S1-40	marcasite	45.92	54.38	390	n.d	334	n.d	n.d	n.d	n.d	n.d	1.18
S1-40	cleat-filling	46.33	54.28	295	n.d	370	49	47	n.d	n.d	n.d	1.17
S1-40	cleat-filling	45.39	53.32	489	n.d	476	n.d	n.d	n.d	n.d	n.d	1.18
S1-40	cleat-filling	45.70	53.69	456	n.d	334	84	n.d	n.d	n.d	n.d	1.18
S1-40	marcasite	45.42	54.30	358	n.d	486	n.d	62	n.d	n.d	n.d	1.20
S1-40	marcasite	45.43	54.14	833	n.d	478	n.d	97	n.d	n.d	n.d	1.19
S1-40	marcasite	45.69	54.99	n.d	n.d	419	60	n.d	n.d	n.d	n.d	1.20
S2-21	cleat-filling	45.28	52.08	888	38	471	98	n.d	n.d	n.d	n.d	1.15
S2-21	framboids	44.42	53.88	368	n.d	266	83	322	n.d	n.d	174	1.21
S2-21	cleat-filling	44.38	53.83	1190	239	n.d	75	119	n.d	n.d	n.d	1.21
S2-21	replacement pyrite	45.74	55.26	1057	38	506	n.d	n.d	49	n.d	n.d	1.21
S2-21	replacement pyrite	44.85	53.50	1195	233	n.d	70	n.d	n.d	n.d	n.d	1.19
S2-21	replacement pyrite	45.02	55.08	888	481	474	58	n.d	n.d	n.d	n.d	1.22
S2-21	replacement pyrite	45.26	55.45	630	393	728	53	72	n.d	n.d	n.d	1.23
S2-21	replacement pyrite	45.11	56.68	1066	126	412	98	n.d	n.d	n.d	n.d	1.26
S2-21	framboids	46.40	52.34	571	n.d	880	n.d	102	n.d	n.d	n.d	1.13
S2-21	replacement pyrite	44.64	53.86	1407	86	n.d	110	n.d	n.d	n.d	n.d	1.21
S2-21	replacement pyrite	44.44	54.15	1652	141	302	n.d	n.d	47	n.d	n.d	1.22

Table APP2-2. Electron microprobe analysis results (at%) of iron sulfides.

Sample no	Iron sulfide type	At% Fe	At% S	S/Fe ratio
S2-40	framboids	32.82	67.15	2.05
S1-39	marcasite	32.22	67.77	2.10
S1-39	marcasite	32.96	67.01	2.03
S1-39	cleat-filling	32.55	67.38	2.07
S1-39	cleat-filling	32.93	67.04	2.04
S1-39	cleat-filling	32.73	67.22	2.05
S1-39	cleat-filling	33.13	66.85	2.02
S1-39	cleat-filling	33.11	66.84	2.02
S2-18	framboids	32.50	67.36	2.07
S2-18	framboids	32.48	67.45	2.08
S2-18	pyrite cementing framboids	32.96	66.99	2.07
S2-18	pyrite cementing framboids	33.29	66.65	2.00
S2-18	pyrite cementing framboids	33.19	66.76	2.01
S2-18	pyrite cementing framboids	32.63	67.31	2.06
S2-18	pyrite cementing framboids	32.86	67.08	2.04
S2-18	pyrite cementing framboids	32.65	67.34	2.06
S2-18	pyrite cementing framboids	32.76	67.22	2.05
S2-18	pyrite cementing framboids	32.81	67.13	2.05
S2-18	framboids	32.73	67.19	2.05
S2-18	framboids	32.63	67.28	2.06
S2-18	cleat-filling	32.69	67.18	2.06
S2-18	cleat-filling	32.25	67.64	2.10
S2-18	pyrite cementing framboids	32.93	67.04	2.04
S2-18	pyrite cementing framboids	33.40	66.56	1.99
S3-35	marcasite	32.24	67.73	2.10
S3-35	marcasite	32.52	67.43	2.07

Table APP2-2. continued

Sample no.	Iron sulfide type	At% Fe	At% S	S/Fe ratio
S3-35	marcasite	32.71	67.28	2.06
S3-35	marcasite	32.21	67.75	2.10
S3-35	cleat-filling	32.60	67.38	2.07
S3-35	cleat-filling	32.46	67.52	2.08
S3-35	cleat-filling	32.84	67.13	2.04
S3-35	cleat-filling	32.08	67.88	2.12
S1-40	marcasite	32.39	67.58	2.09
S1-40	marcasite	32.64	67.33	2.06
S1-40	cleat-filling	32.88	67.10	2.04
S1-40	cleat-filling	32.81	67.15	2.05
S1-40	cleat-filling	32.81	67.16	2.05
S1-40	marcasite	32.43	67.53	2.08
S1-40	marcasite	32.49	67.46	2.08
S1-40	marcasite	32.28	67.69	2.10
S2-21	cleat-filling	33.27	66.68	2.00
S2-21	framboids	32.08	67.80	2.11
S2-21	cleat-filling	32.10	67.84	2.11
S2-21	replacement pyrite	32.20	67.76	2.11
S2-21	replacement pyrite	32.47	67.47	2.08
S2-21	replacement pyrite	31.91	68.01	2.13
S2-21	replacement pyrite	31.88	68.05	2.13
S2-21	replacement pyrite	31.34	68.60	2.19
S2-21	framboids	33.71	66.23	1.97
S2-21	replacement pyrite	32.22	67.73	2.10
S2-21	replacement pyrite	32.00	67.93	2.12

Table APP2-3. Composition of siderites associated with BB seam coals.

Sample no.	siderite association	Mg/Ca ratio	Mol % Fe	Mol % Mn	Mol % Mg	Mol % Ca
S2-31	low-sulfur coal	0.91	93.95	2.85	2.31	2.54
S2-31	low-sulfur coal	1.95	94.80	2.44	3.08	1.58
S2-31	low-sulfur coal	1.00	92.08	3.13	2.03	2.03
S2-31	low-sulfur coal	0.89	86.55	2.22	4.16	4.65
S2-31	low-sulfur coal	0.69	92.98	2.55	2.29	3.33
S2-31	low-sulfur coal	1.94	94.28	2.67	2.80	1.44
S2-31	low-sulfur coal	1.31	94.31	2.62	2.34	1.79
S2-31	low-sulfur coal	0.91	90.19	1.76	4.45	4.86
S3-28	low-sulfur coal	0.63	88.55	5.41	1.56	2.49
S3-28	low-sulfur coal	0.99	90.52	3.65	2.00	2.02
S3-28	low-sulfur coal	0.69	94.22	3.97	1.83	2.64
S3-28	low-sulfur coal	1.06	90.50	4.52	1.64	1.55
S3-28	low-sulfur coal	0.52	88.19	5.79	1.53	2.95
S3-28	low-sulfur coal	0.65	94.49	3.75	2.01	3.10
S3-28	low-sulfur coal	1.45	91.35	4.40	2.34	1.61
S3-28	low-sulfur coal	1.37	95.07	4.41	2.41	1.76
S3-28	low-sulfur coal	0.39	90.50	4.92	1.20	3.17
S3-28	low-sulfur coal	0.40	90.80	5.56	0.99	2.46
S3-28	low-sulfur coal	0.76	92.31	5.07	1.42	1.87
S3-28	low-sulfur coal	0.60	89.79	5.49	1.43	2.40
S3-28	low-sulfur coal	1.48	93.62	4.52	2.45	1.65
S2-19	high-sulfur coal	0.54	88.10	2.62	2.57	4.79
S2-19	high-sulfur coal	0.73	89.88	2.95	2.64	2.81
S2-19	high-sulfur coal	0.64	86.65	4.79	3.59	4.41
S2-19	high-sulfur coal	0.34	89.47	3.28	1.26	3.68
S2-19	high-sulfur coal	0.39	89.33	3.54	1.35	3.41
S2-19	high-sulfur coal	0.28	89.36	3.62	1.15	4.07
S2-19	high-sulfur coal	0.25	89.84	4.36	0.94	3.68
S2-19	high-sulfur coal	0.23	88.83	4.43	0.79	3.41
S2-19	high-sulfur coal	0.30	88.02	4.04	1.09	3.63
S2-19	high-sulfur coal	0.19	88.77	4.56	0.73	3.82
S2-18	high-sulfur coal	0.34	90.44	3.90	1.15	3.38
S2-18	high-sulfur coal	0.50	90.16	2.90	1.65	3.31
S2-18	high-sulfur coal	0.31	90.58	3.29	1.02	3.27
S2-18	high-sulfur coal	0.45	92.02	3.27	1.10	2.46
S2-18	high-sulfur coal	0.30	89.92	3.94	1.13	3.80
S2-18	high-sulfur coal	0.27	89.70	3.94	0.98	3.57
S2-18	high-sulfur coal	0.32	89.44	3.82	1.07	3.32
S2-21	high-sulfur coal	0.27	89.58	4.09	1.03	3.80
S2-21	high-sulfur coal	0.13	92.35	4.93	0.54	4.07
S2-21	high-sulfur coal	0.20	89.30	4.73	0.82	4.00
S2-21	high-sulfur coal	0.24	91.39	4.11	0.85	3.59

Appendix 3. Trace element concentrations in DHS1,DHS2, and DHS3.

Table APP3-1. Trace-element concentrations (ppm) in DHS1.

Sample No.	lithology	Distance	Cr	Ba	Fe	Sc	Na	Co	Zn	As	Se
S1-4	Claystone	313.08	49	604	14924	12	6223	10	109	4.79	2.40
S1-5	Clarain	308.08	7	21	3424	4	147	14	4	0.65	2.59
S1-12	Vitrain	269.83	5	14	582	1	100	1	4	1.01	0.94
S1-17	Clarain	240.46	3	5	568	1	91	0	4	0.49	0.91
S1-29	Clarain	156.55	5	72	1862	1	98	1	7	1.00	2.82
S1-30	Clarain	150.93	5	239	1824	3	104	2	8	0.75	3.38
S1-31	Claystone parting	143.43	4	41	2719	2	136	1	5	0.48	3.80
S1-32	Clarain	139.52	11	493	1500	4	98	18	5	0.93	8.55
S1-33	Clarain	135.43	7	297	1261	3	96	2	6	1.03	4.15
S1-40	Fusain	82.18	17	17	3658	2	121	0	10	2.10	2.79
S1-43	Clarain	65.93	4	287	1036	1	111	1	6	0.84	1.47
S1-45	Vitrain	55.93	4	834	1857	1	97	1	11	1.30	1.64
S1-51	Vitrain	14.37	4	61	7001	2	76	6	4	0.76	2.34
S1-54	Claystone	0	48	288	9344	15	510	4	37	2.15	1.20

Table APP3-1. Trace-element concentrations (ppm) in DHS1.

Sr	La	Ce	Sm	Eu	Yb	Lu	Hf	Ta	Th	U	Sb	Tb
110	45	92	7.00	1.00	4.00	0.60	11.00	1.40	16	5.00	1.33	1.00
47	3	7	1.00	0.30	1.00	0.20	1.00	0.55	4	2.00	10.00	0.33
37	4	7	0.60	0.10	0.30	0.04	1.00	0.10	1	0.40	0.10	0.07
39	2	3	0.20	0.05	0.10	0.02	0.30	0.05	1	0.20	0.10	0.04
43	7	15	1.00	0.20	0.30	0.10	1.00	0.21	3	1.40	1.30	0.15
42	7	15	1.00	0.30	0.60	0.10	2.00	0.60	14	7.00	2.40	0.20
21	27	48	2.00	0.30	0.60	0.10	7.00	3.40	11	11.00	0.80	0.10
41	32	61	3.00	0.60	1.00	0.10	5.00	0.51	54	15.00	1.70	0.33
52	11	26	2.00	0.40	1.00	0.10	2.50	0.40	15	6.00	2.00	0.24
54	9	15	1.00	0.10	0.50	0.10	2.00	0.33	5	1.40	0.30	0.10
54	4	7	0.40	0.10	0.10	0.02	0.34	0.07	1	0.50	0.20	0.05
56	3	5	0.40	0.10	0.10	0.02	0.30	0.05	1	0.30	0.23	0.04
50	5	15	2.00	0.60	1.00	0.10	0.33	0.05	1	0.40	4.00	0.43
108	33	63	4.00	1.00	3.00	0.40	5.00	1.20	14	5.30	1.40	0.60

Table APP3-2. Trace-element concentrations (ppm) in DHS2.

Sample No.	Lithology	Distance	Cr	Ba	Fe	Sc	Na	Co	Zn	As	Se	Sr
S2-2	Sandstone	268.25	20	653	8671	7	10522	26	80	6	0	123
S2-3	Claystone	263.25	55	563	19694	15	5052	22	173	9	1	230
S2-5	Claystone	238.25	37	428	49033	14	2506	13	109	6	2	238
S2-6	Durain	233.25	29	4121	7714	8	490	6	199	5	4	179
S2-10	Vitrain	207.63	12	77	1786	4	413	3	13	1	2	139
S2-11	Durain	201.38	25	108	7598	3	580	4	28	4	5	203
S2-15	Durain	176.08	5	41	1338	2	332	65	8	1	2	132
S2-18	Vitrain	166.24	8	69	34157	2	264	2	13	55	4	94
S2-19	Durain	158.74	8	37	11552	2	265	1	8	13	2	113
S2-21	Durain	144.05	7	106	23985	2	283	2	13	34	6	121
S2-28	Clarain	97.49	8	62	2287	3	265	3	8	1	1	149
S2-29	Durain	94.99	31	156	9342	9	521	3	42	2	3	203
S2-31	Durain	82.8	27	109	61538	7	436	4	31	3	3	172
S2-36	Vitrain	40.31	10	68	4123	2	264	2	21	1	2	131
S2-40	Vitrain	9.06	16	74	1018	4	264	4	7	1	2	108
S2-41	Claystone	0	47	179	9405	11	568	7	70	2	2	194
S2-42	Claystone	-17.81	49	303	44712	13	641	9	38	4		158
S2-43	Sandstone	-18	33	484	11490	7	798	36	82	10		91

Table APP3-2. Trace-element concentrations (ppm) in DHS2.

La	Ce	Sm	Eu	Yb	Lu	Hf	Ta	Th	U	Sb	Cs	Rb	Ta
24	49	4	1	2	0.3	7	1	10	3		3	68	0.6
84	179	16	3	4	0.6	7	1	21	7	2	13	146	1.7
52	104	9	2	4	0.6	4	1	16	4	1	15	144	1
5	9	2	0.5	2	0.3	1	0.3	4	2		2	18	0.5
7	13	2	0.4	1	0.1	1	0.3	4	3	•	1	8	0.3
25	48	3	0.6	1	0.2	3	0.8	10	6	•	6	41	0.4
5	10	1	0.3	1	0.1	1	0.5	3	1	•	0.1	•	0.2
9	17	1	0.2	0.6	0.1	1	0.3	4	1	•	0.6	4	0.1
5	10	1	0.2	0.6	0.1	1	0.3	5	2	•	0.4	2	0.1
9	17	1	0.2	0.6	0.1	3	0.8	13	5	•	0.3	2	0.1
3	7	1	0.3	0.8	0.1	0	0.04	1	1	2	0.2	1	0.3
29	57	4	0.8	2	0.2	3	0.8	11	3	1	10	61	0.5
27	55	4	0.8	2	0.2	3	0.6	8	3	1	7	48	0.5
5	9	1	0.1	0.4	0.06	1	0.2	2	1	0.3	0.05	•	0.1
5	11	2	0.4	0.9	0.1	2	0.3	3	1	5	0.2	1	0.3
20	36	3	0.5	2	0.2	4	0.9	10	3	4	16	75	0.4
32	61	5	1	2	0.3	6	0.9	12	3	2	10	87	0.7
21	41	3	1	2	0.3	8	1	10	3	2	4	84	0.4

Table APP3-3. Trace-element concentrations (ppm) in DHS3.

Sample No.	lithology	Distance	Cr	Ba	Fe	Sc	Na	Co	Zn	As	Se	Sr
S3-5	Claystone	258.89	30	381	89386	12	1415	12	103	9	1	228
S3-6	Duraln	257.64	19	2029	5466	6	349	8	82	5	3	231
S3-11	Vitrain	223.26	5	131	3667	2	181	4	4	1	1	158
S3-17	Vitrain	177.95	7	136	10164	3	184	2	10	1	3	130
S3-18	Claystone parting	169.51	4	61	16729	2	267	2	11	1	6	109
S3-19	Vitrain	165.92	24	213	128415	4	262	1	16	2	3	153
S3-28	Duraln	97.33	11	38	8632	3	166	3	15	1	5	132
S3-35	Vitrain	45.15	6	75	5141	1	138	2	4	1	2	135
S3-40	Duraln/carb.shale	7.34	47	114	3028	7	352	3	17	1	5	163
S3-41	Carb.shale/Duraln	6.09	54	193	8508	10	481	7	25	2	2	200
S3-42	Claystone	0	52	256	11242	12	571	5	52	2	1	185

Table APP3-3. Trace-element concentrations (ppm) in DHS3.

La	Ce	Sm	Eu	Yb	Lu	Hf	Ta	Th	U	Sb	Cs	Rb	Tb
44	87	8	2	3	0.5	3	1	12	3	1	12	115	1
6	11	2	0.4	2	0.3	2	0.33	4	3	8	2.4	19	0.5
4	9	1	0.31	1	0.1	1	0.1	1	1	2	0.1	1	0.23
18	32	2	0.4	1	0.1	2	0.5	18	9	3	1	5	0.21
25	45	2	0.4	1	0.1	8	4	12	10	0.3	1.6	9	0.1
14	22	1	0.26	1	0.1	2	0.5	7	2	0.5	4	31	0.2
9	18	2	0.4	1	0.1	2	0.4	10	7	1	0.25	2	0.25
3	4	0	0.07	0	0.02	1	0.1	1	0	0.34	•	•	0.04
13	22	3	0.64	2	0.22	3	0.7	8	3	5	3.6	28	0.5
22	36	3	0.6	1	0.3	5	1	11	4	2.5	18	80	0.5
24	41	3	0.5	2	0.3	6	1	13	3	1.6	16	106	0.4

Appendix 4 - vertical distribution patterns of minor and trace elements in the BB seam.

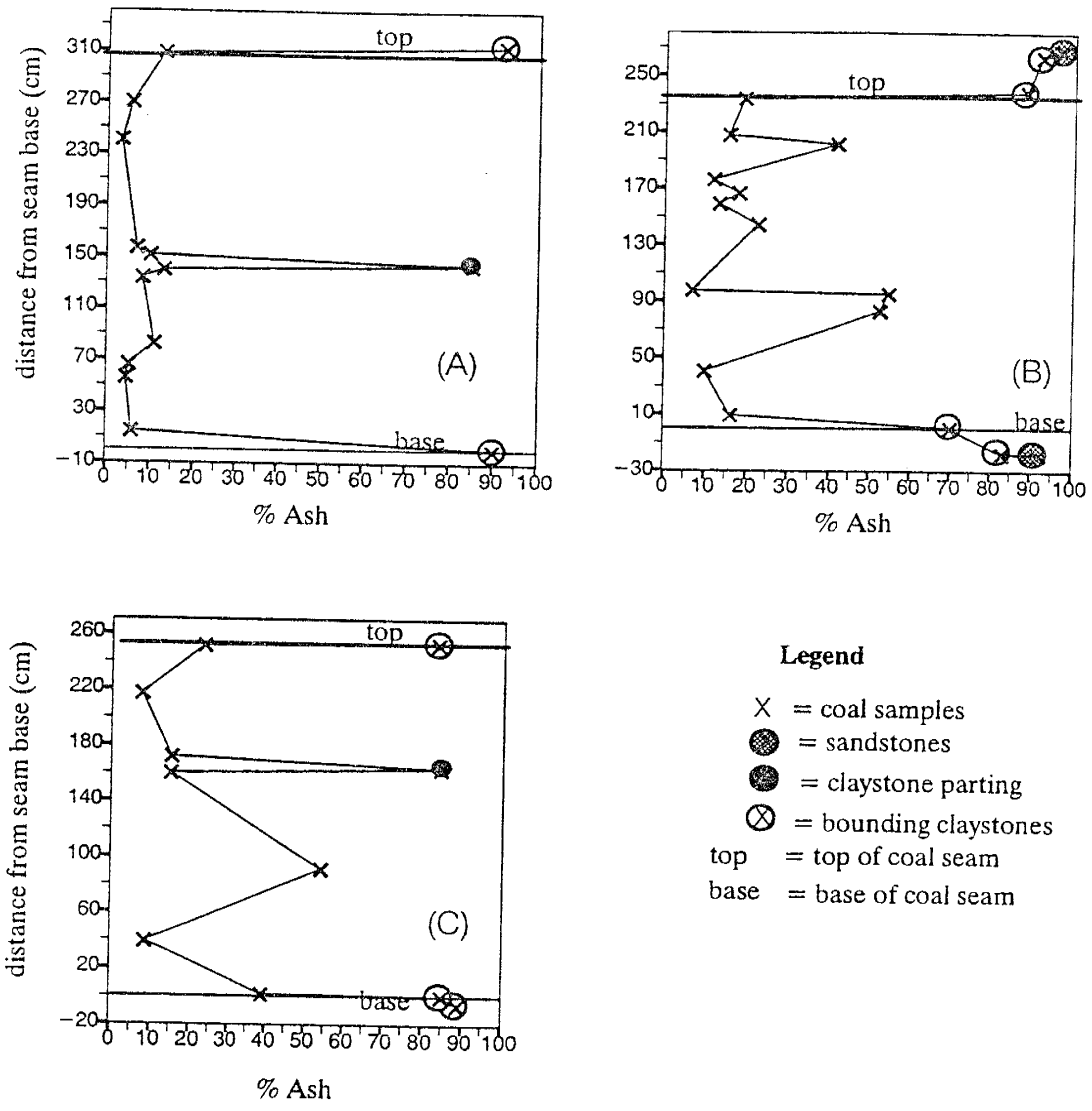

Figure A4-1. Vertical distribution of ash content in the BB seam; (A) in DHS1, (B) in DHS2, and (C) in DHS3.

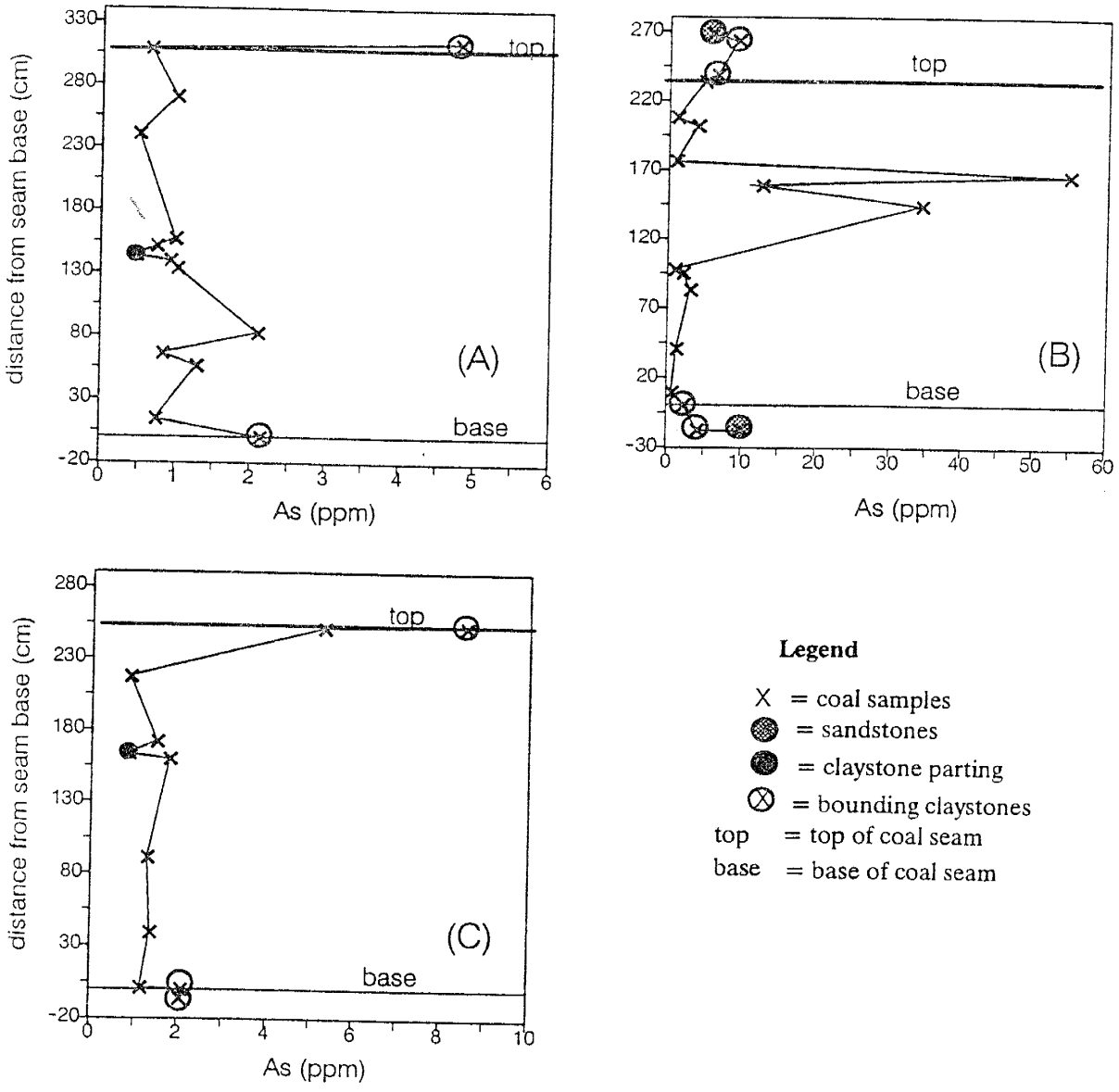

Figure A4-2. Vertical distribution of arsenic in the BB seam; (A) in DHS1, (B) in DHS2, and (C) in DHS3.

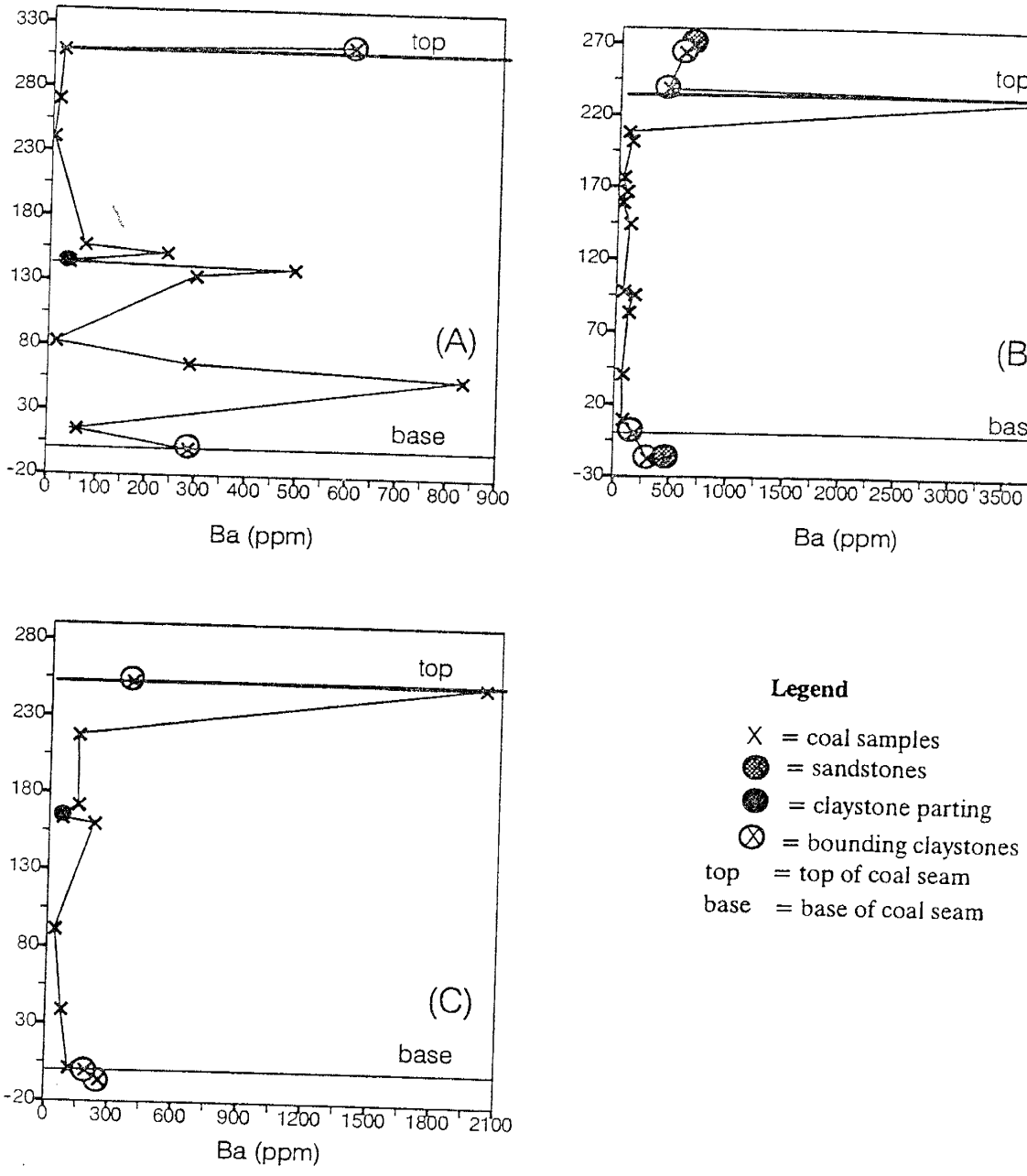

Figure A4-3. Vertical distribution of barium in the BB seam; (A) in DHS1, (B) in DHS2, and (C) in DHS3.

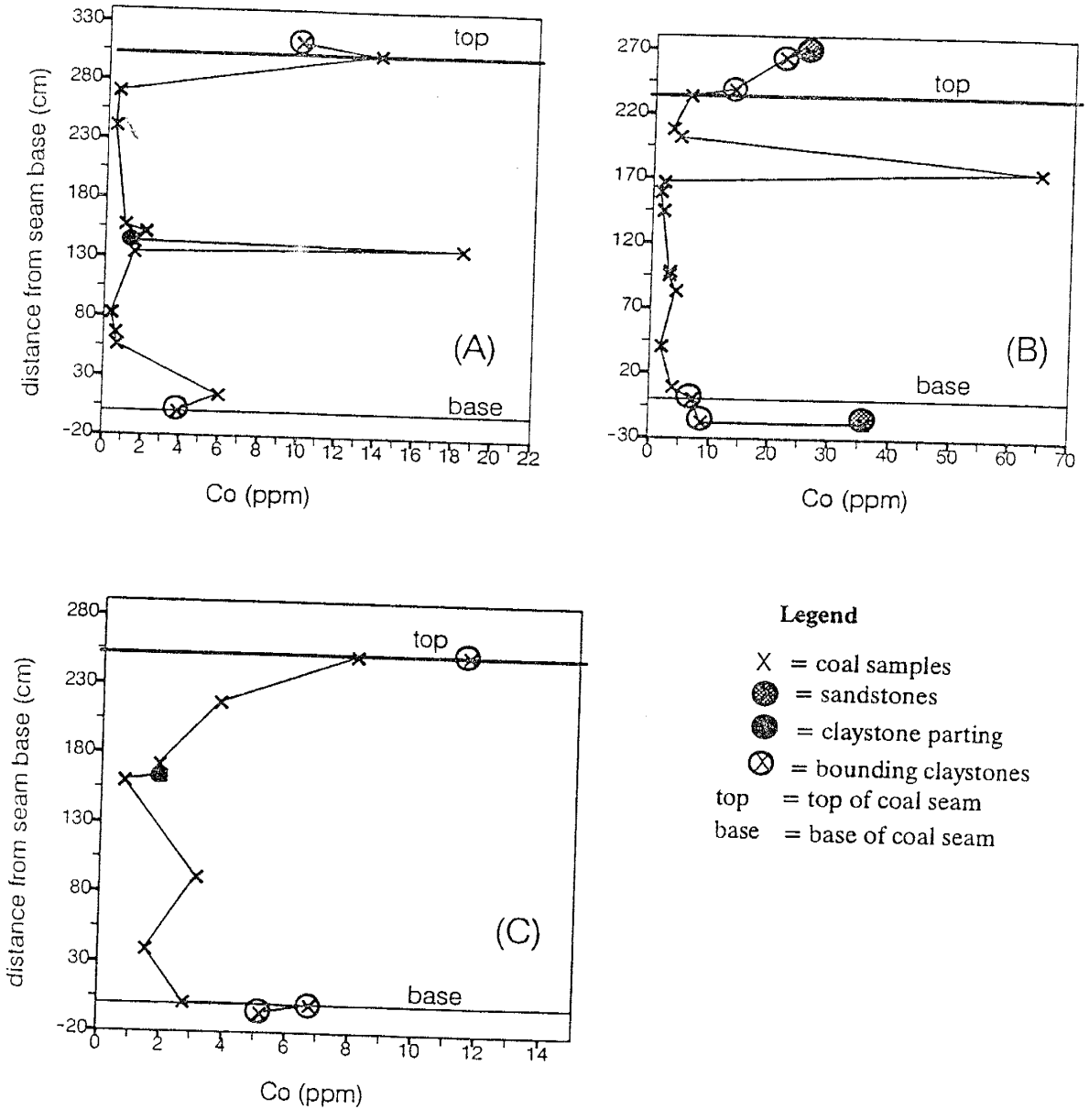

Figure A4-4. Vertical distribution of cobalt in the BB seam; (A) in DHS1, (B) in DHS2, and (C) in DHS3.

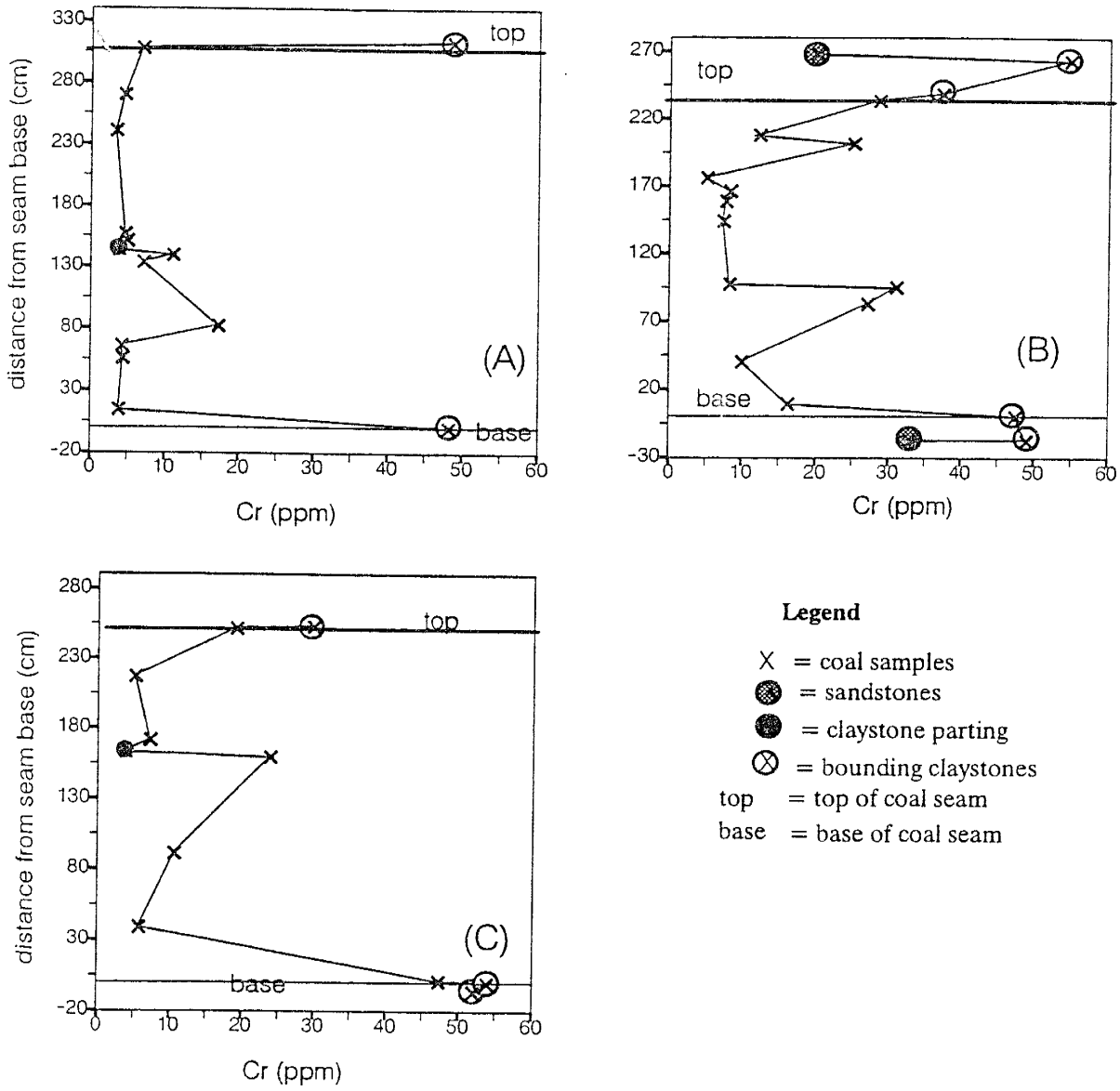

Figure A4-5. Vertical distribution of chromium in the BB seam; (A) in DHS1, (B) in DHS2, and (C) in DHS3.

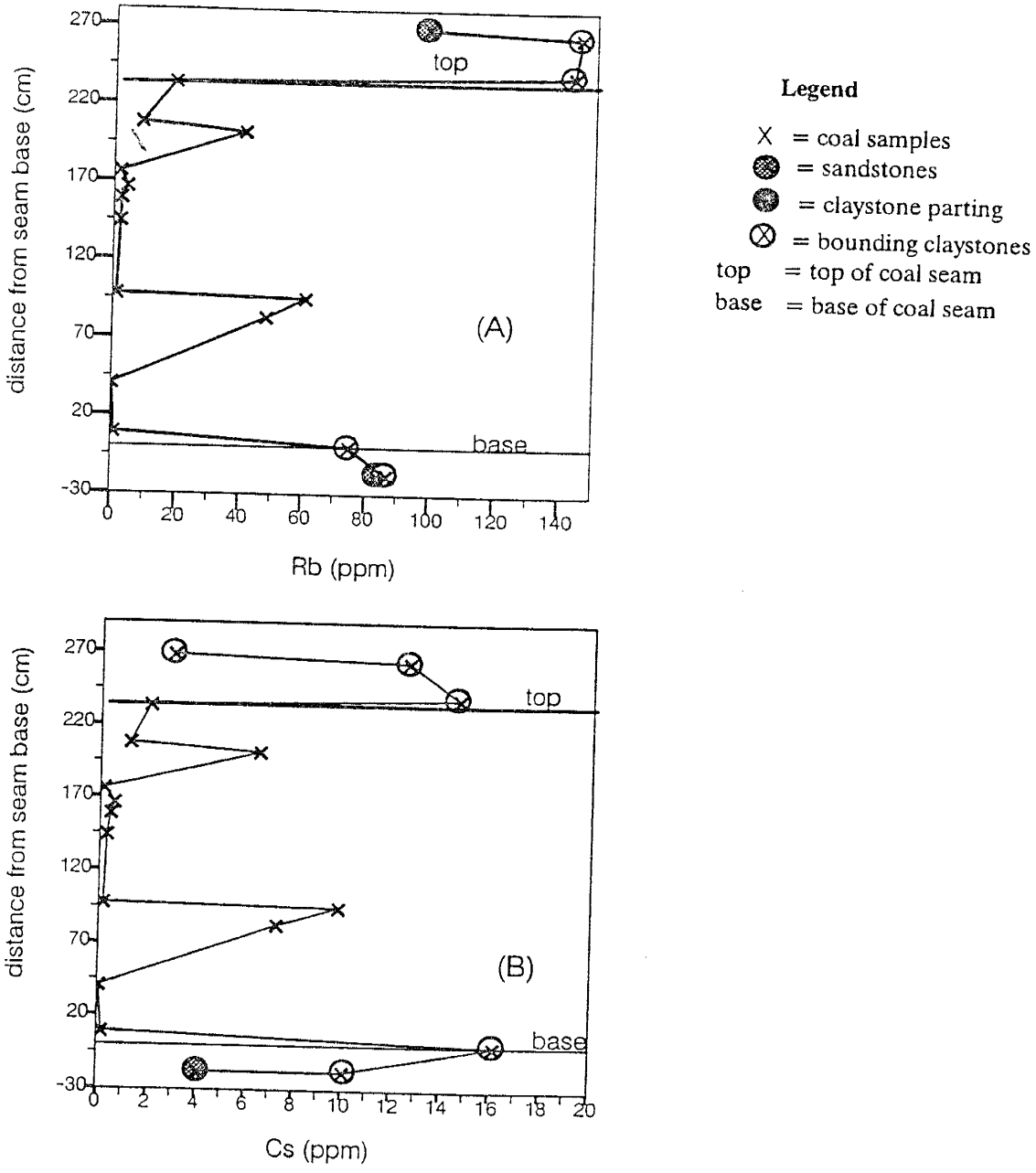

Figure A4-6. Vertical distribution of rubidium (A) and cesium (B) in the BB seam (DHS2).

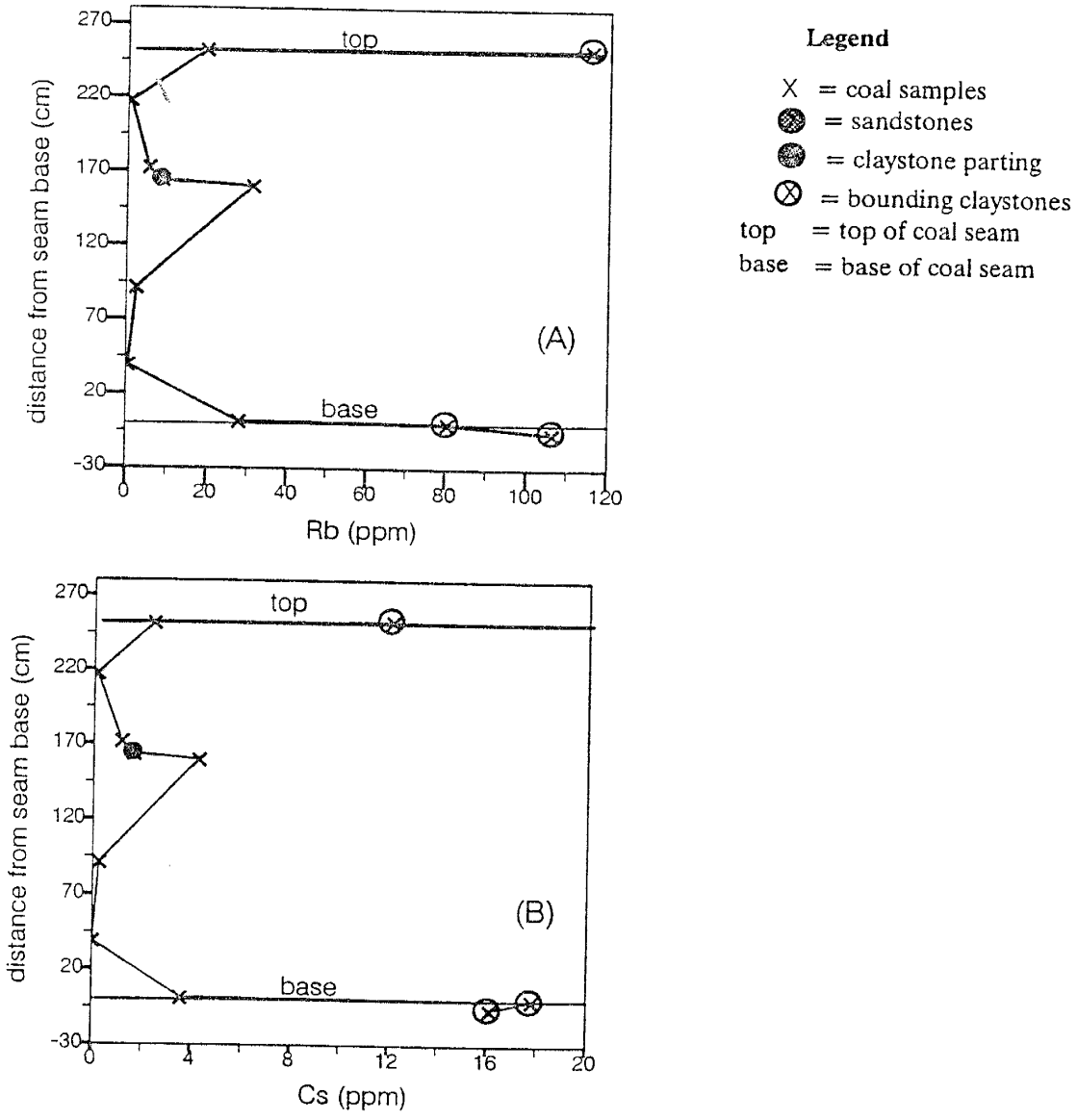

Figure A4-7. Vertical distribution of rubidium (A) and cesium (B) in the BB seam (DHS3).

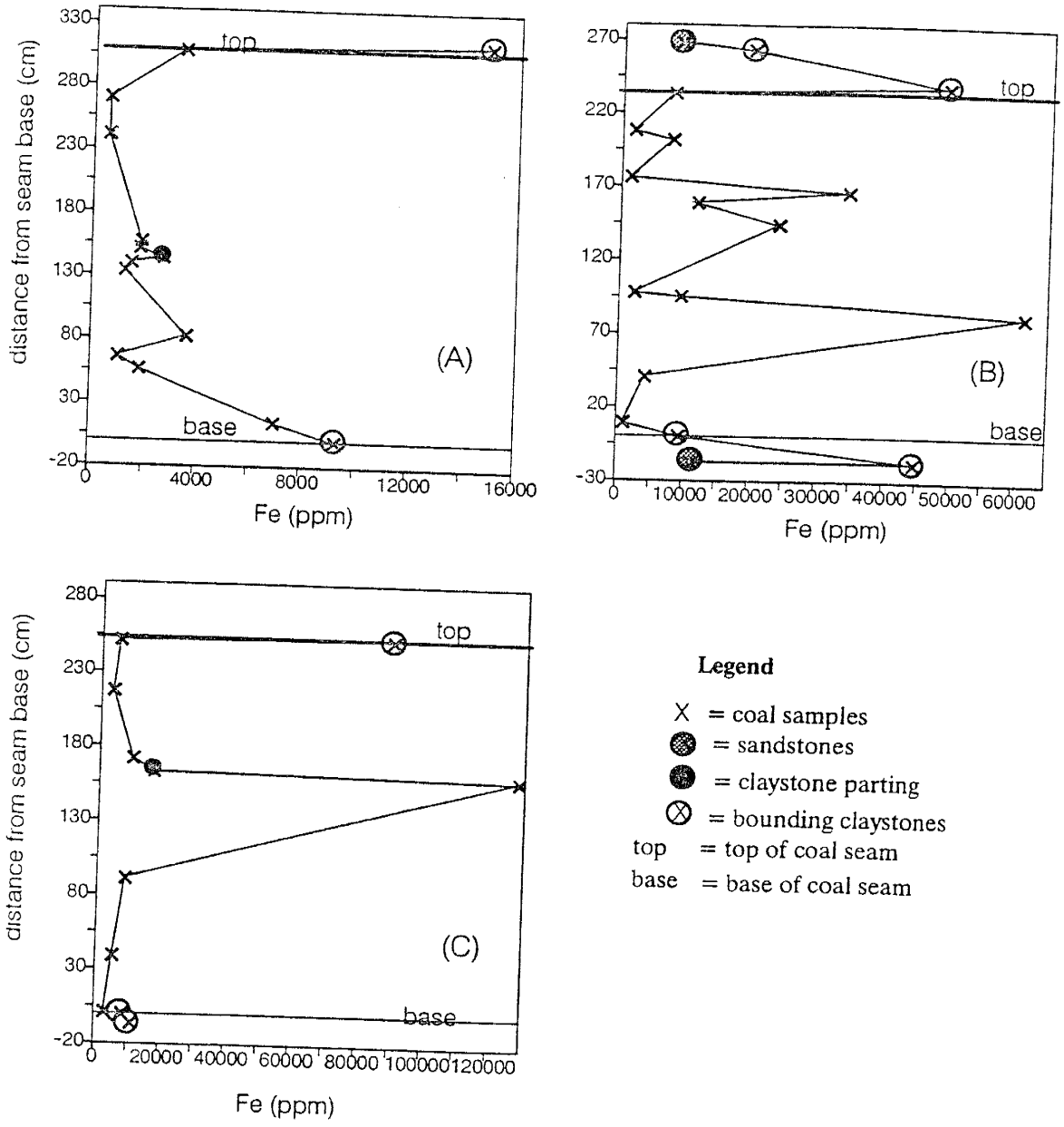

Figure. A4-8. Vertical distribution of iron in the BB seam; (A) in DHS1, (B) in DHS2, and (C) in DHS3.

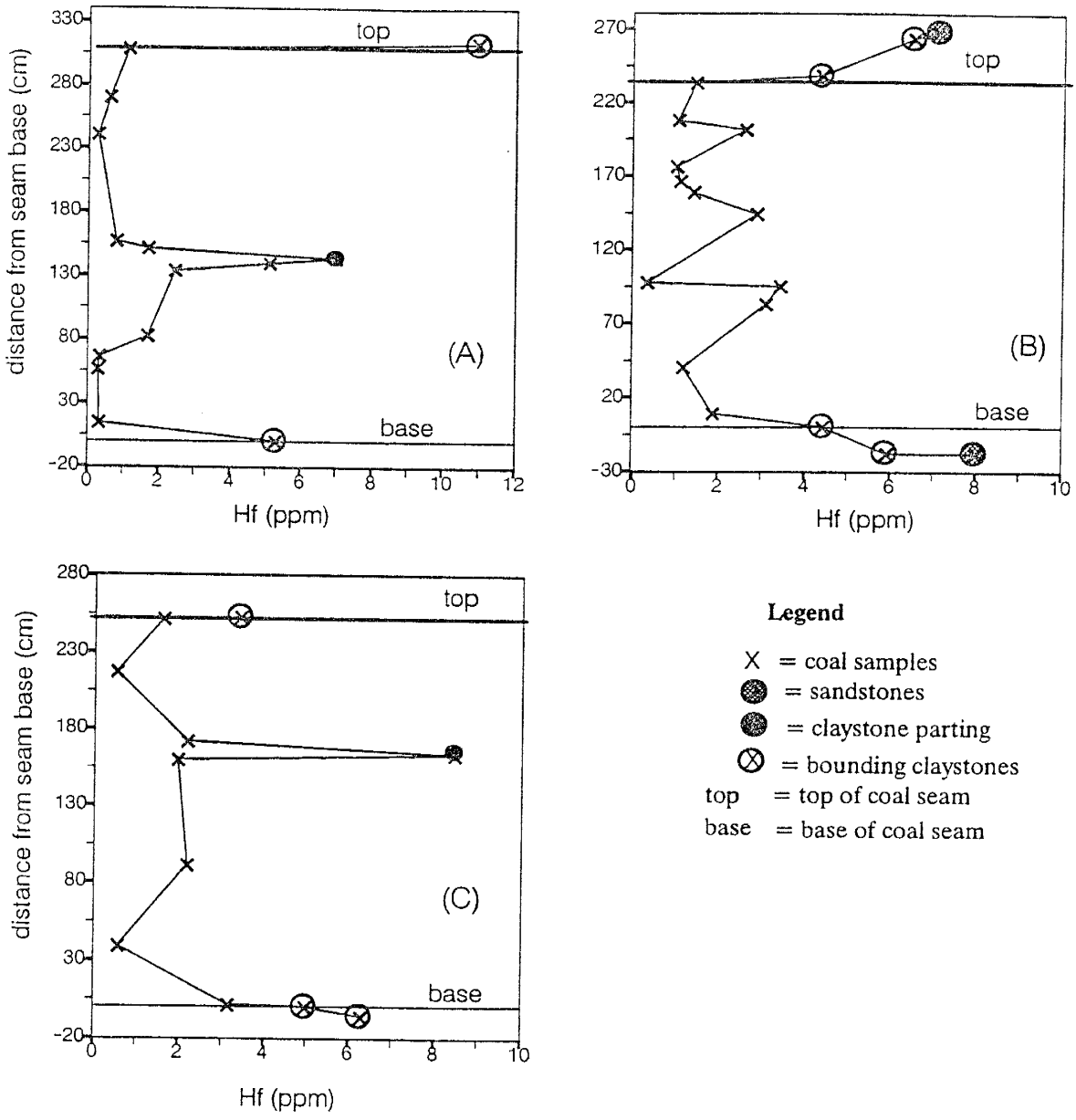

Figure A4-9. Vertical distribution of hafnium in the BB seam; (A) in DHS1, (B) in DHS2, and (C) in DHS3.

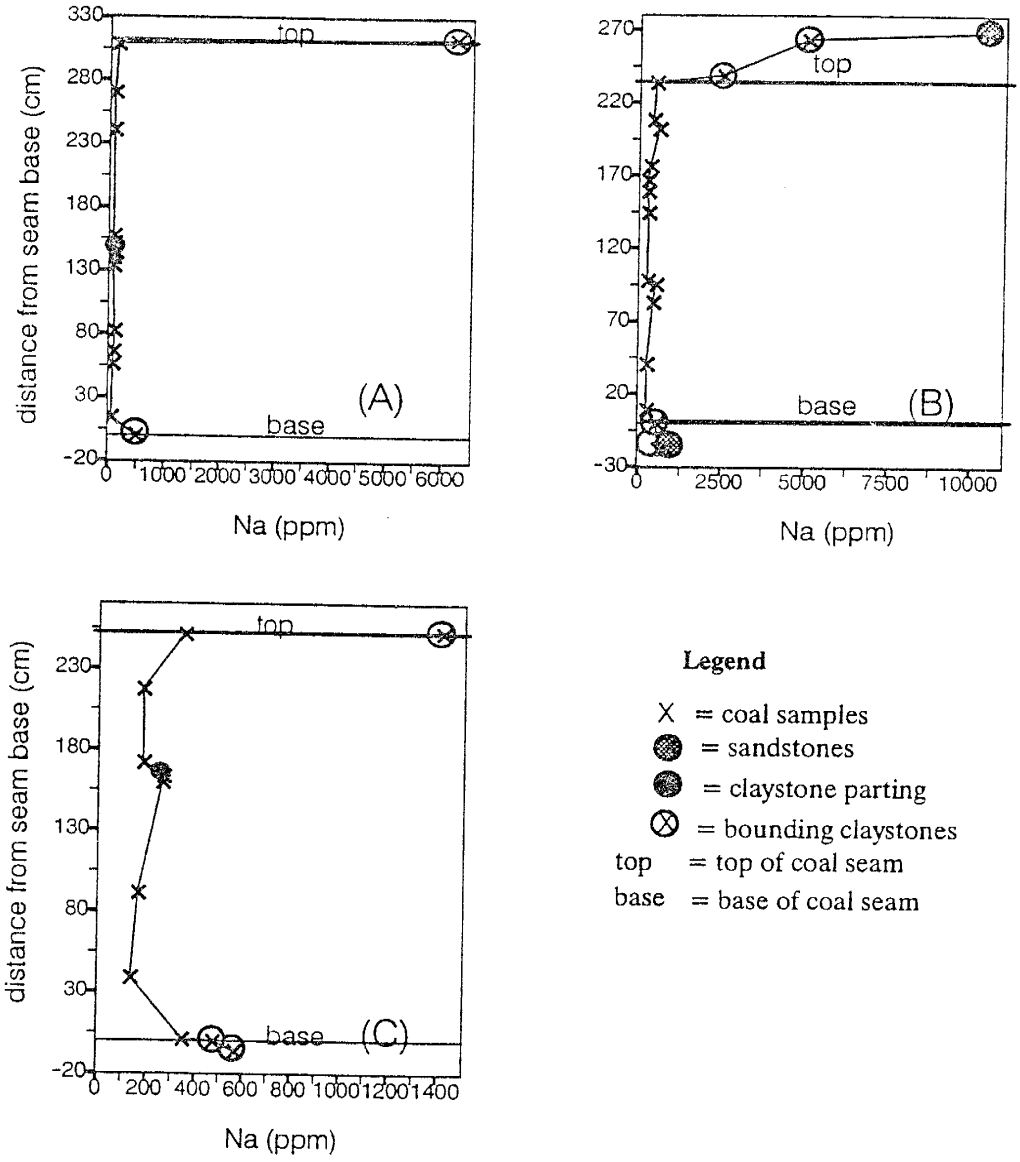

Figure A4-10. Vertical distribution of sodium in the BB seam; (A) in DHS1, (B) in DHS2, and (C) in DHS3.

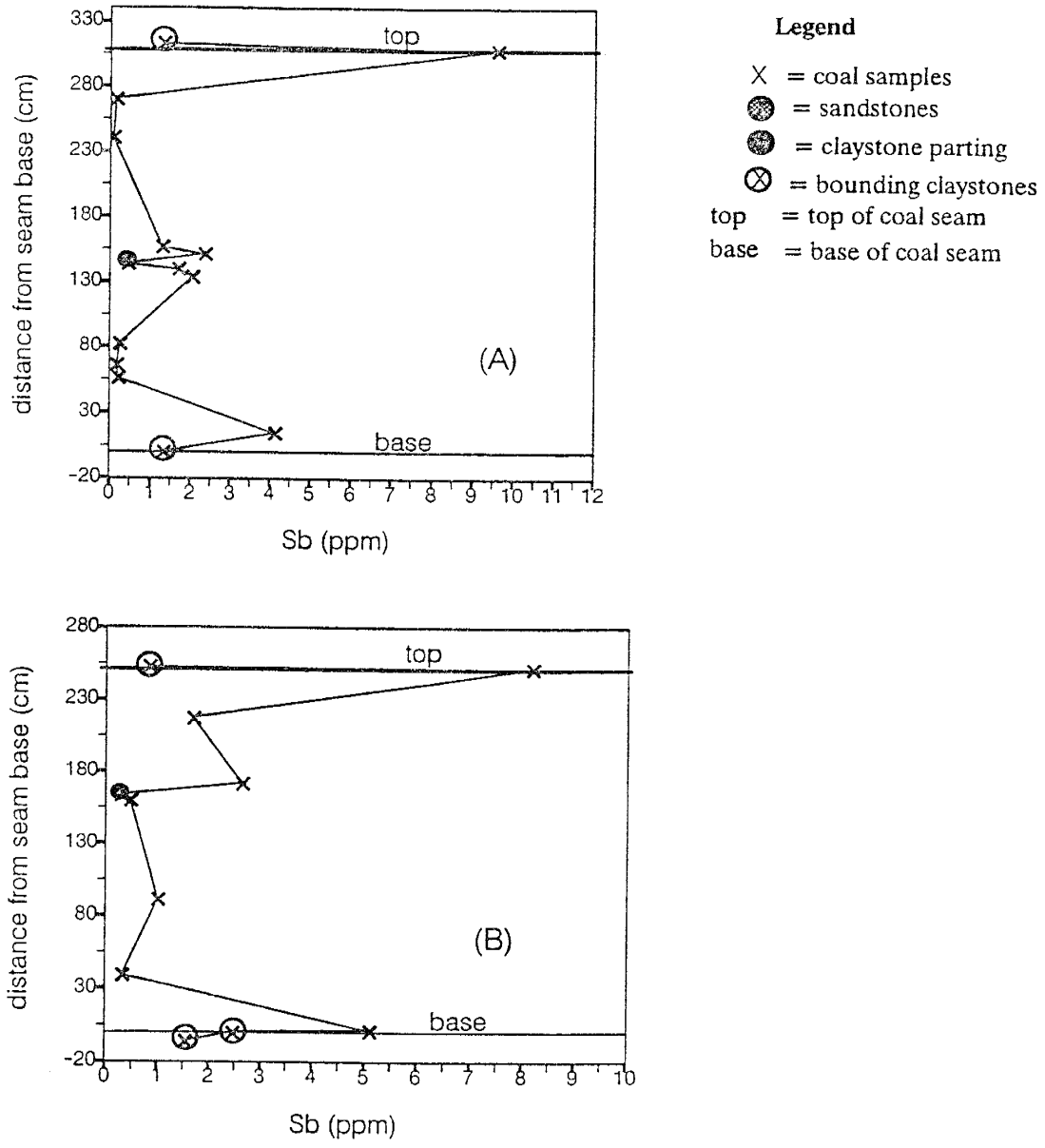

Figure A4-11. Vertical distribution of antimony in the BB seam; (A) in DHS1, and (B) in DHS3.

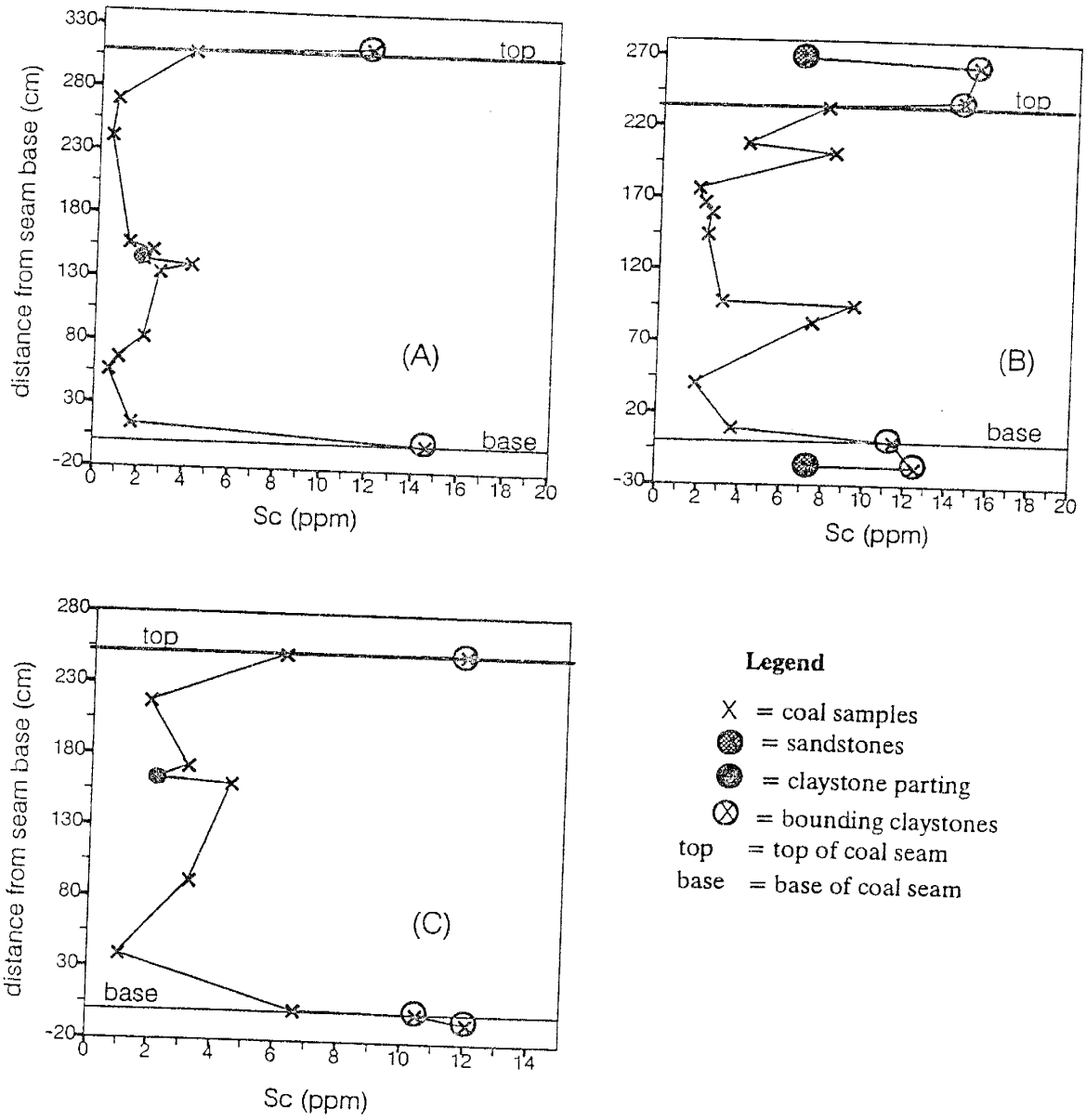

Figure A4-12. Vertical distribution of scandium in the BB seam; (A) in DHS1, (B) in DHS2, and (C) in DHS3.

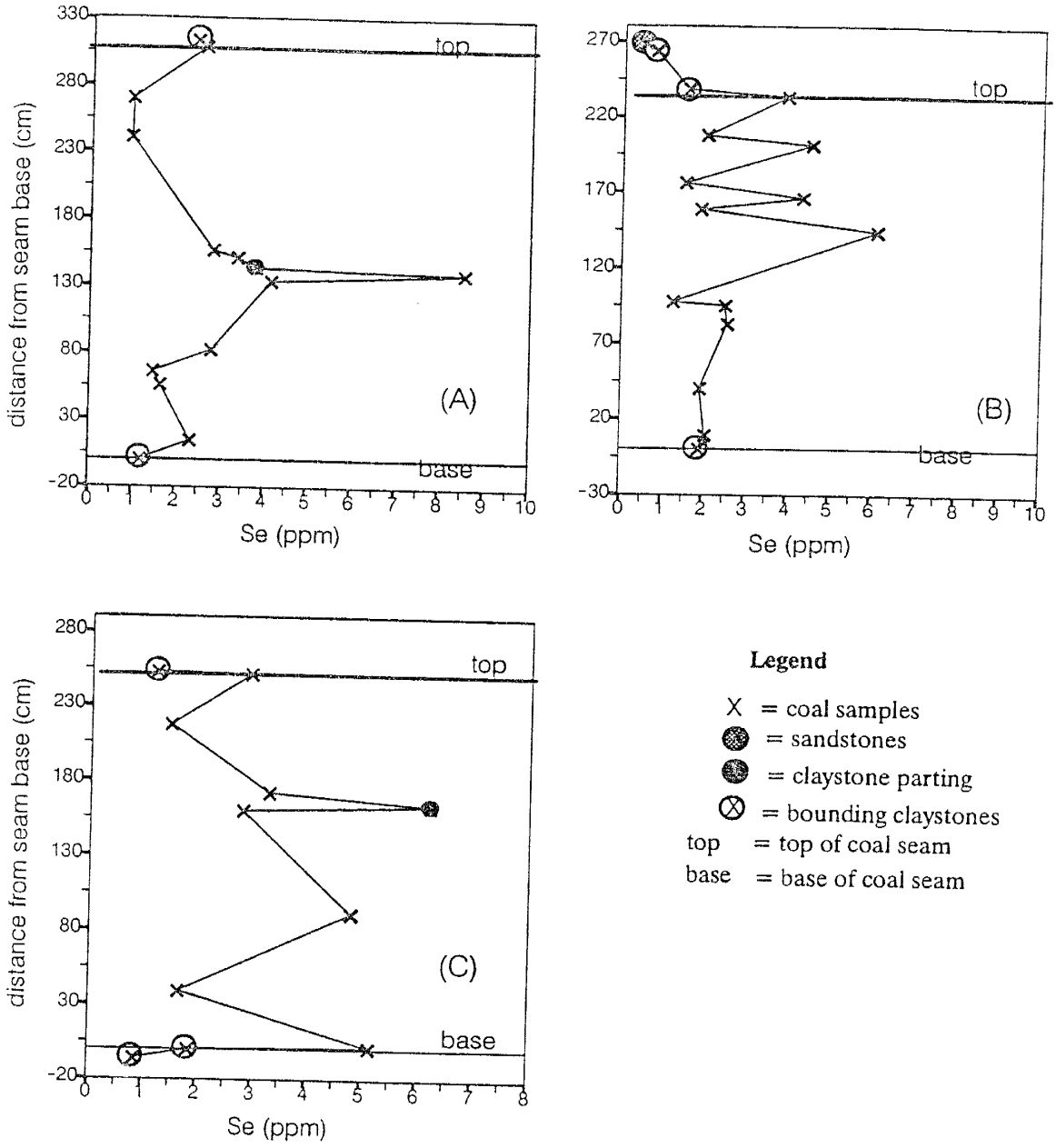

Figure A4-13. Vertical distribution of selenium in the BB seam; (A) in DHS1, (B) in DHS2, and (C) in DHS3.

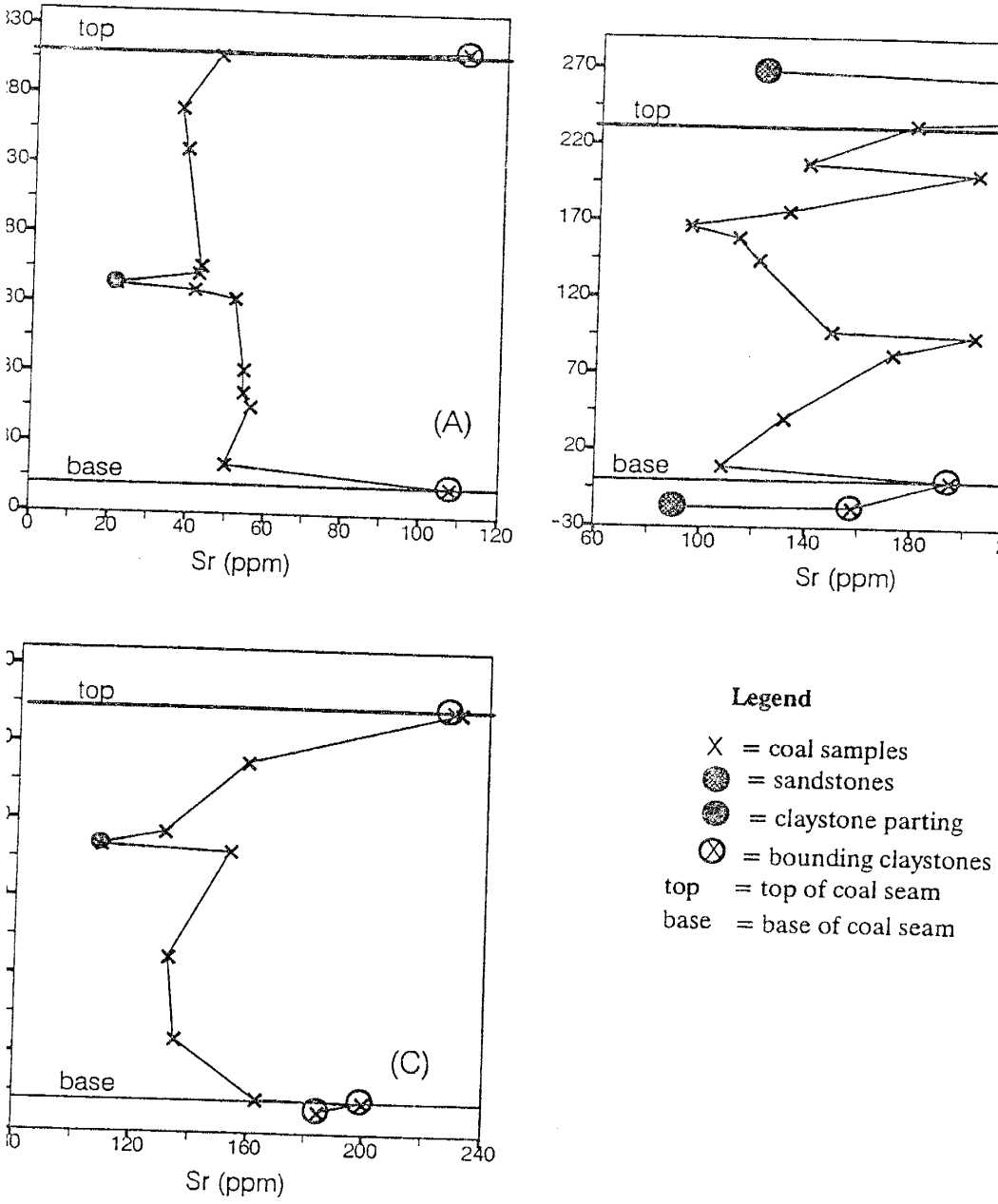

e A4-14. Vertical distrbution of strontium in the BB seam; (A) in DHS1, (B) in DHS2, and (C) in DHS3.

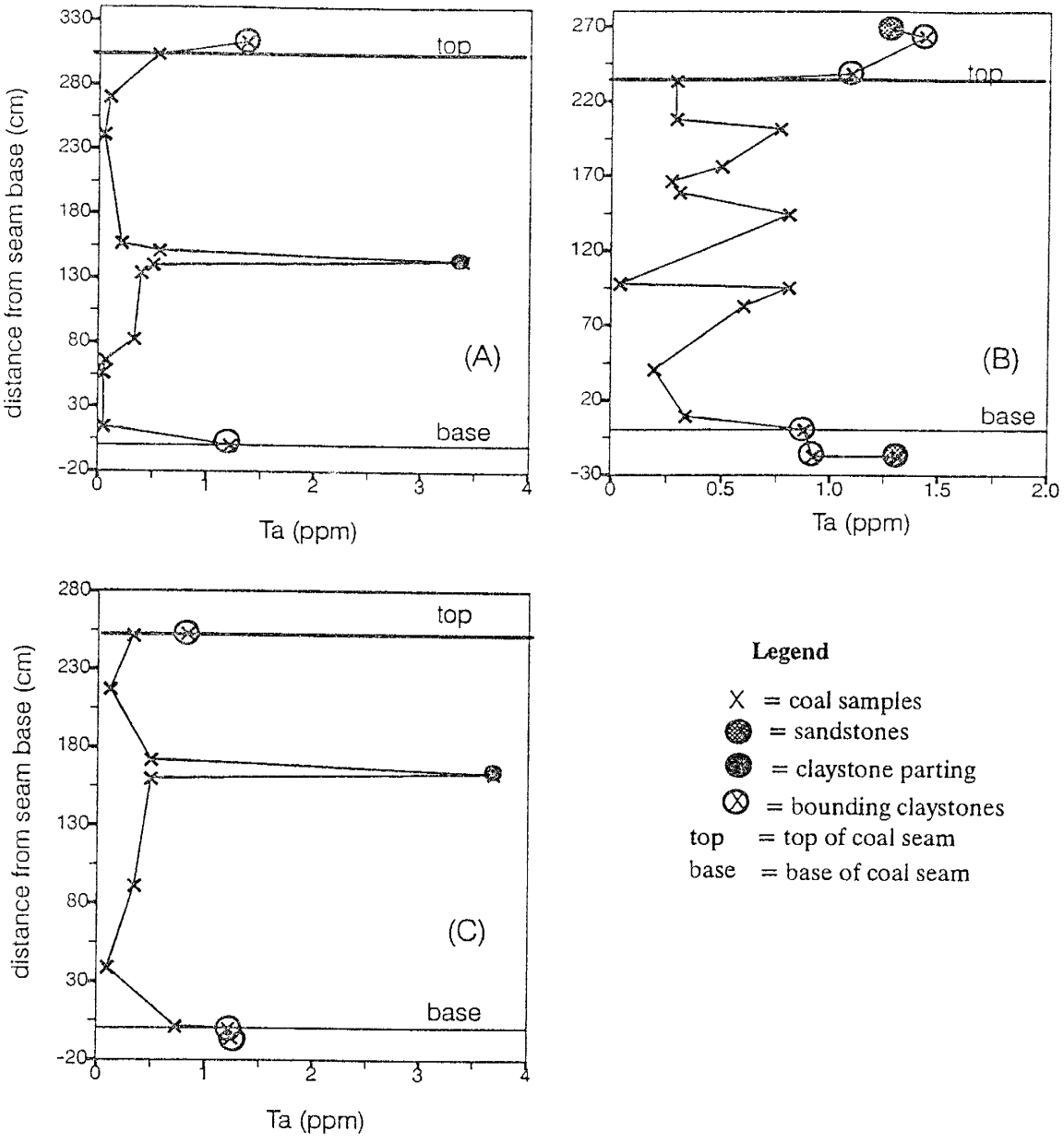

Figure A4-15. Vertical distribution of tantalum in the BB seam; (A) in DHS1, (B) in DHS2, and (C) in DHS3.

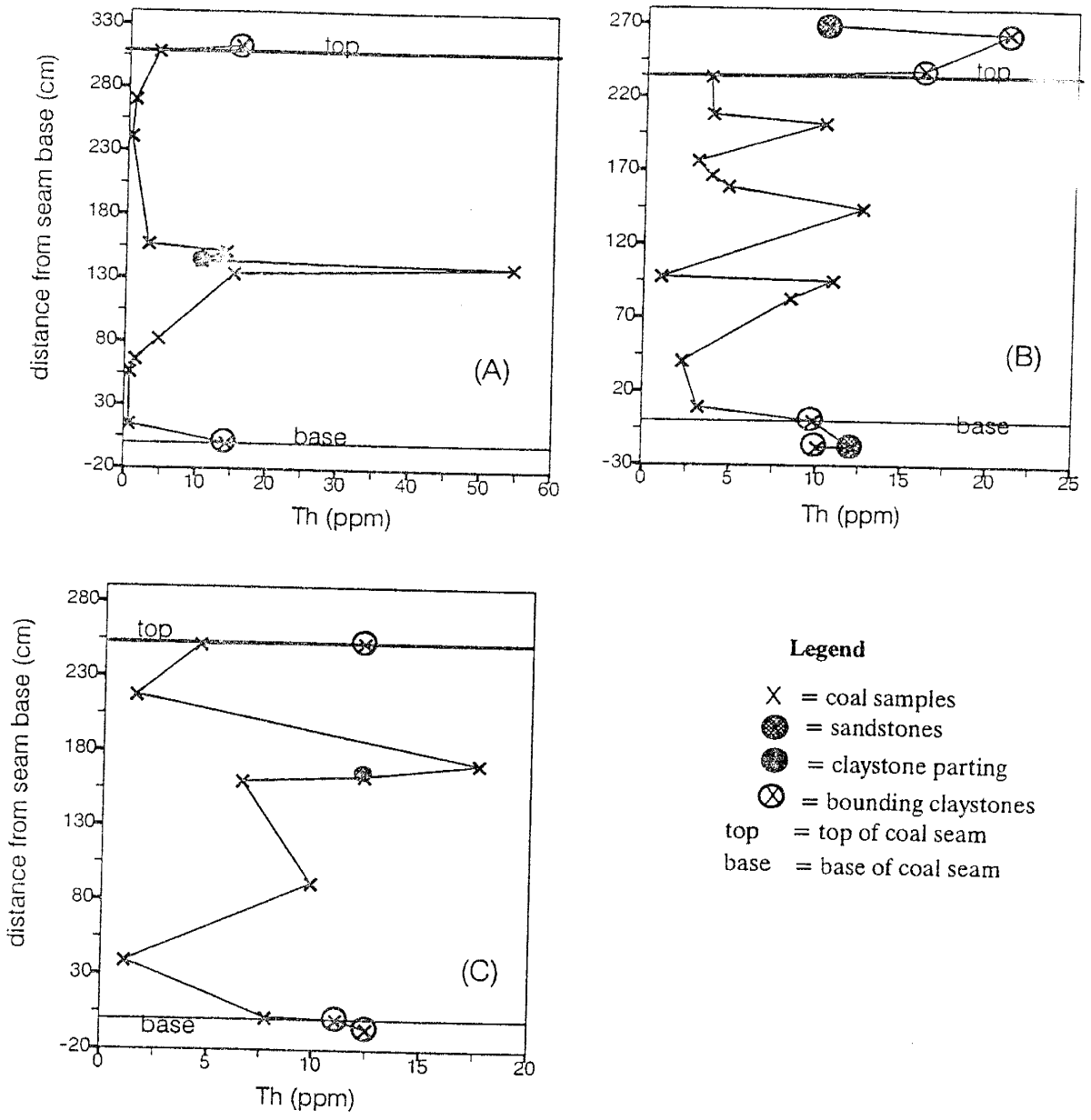

Figure A4-16. Vertical distribution of thorium in the BB seam; (A) in DHS1, (B) in DHS2, and (C) in DHS3.

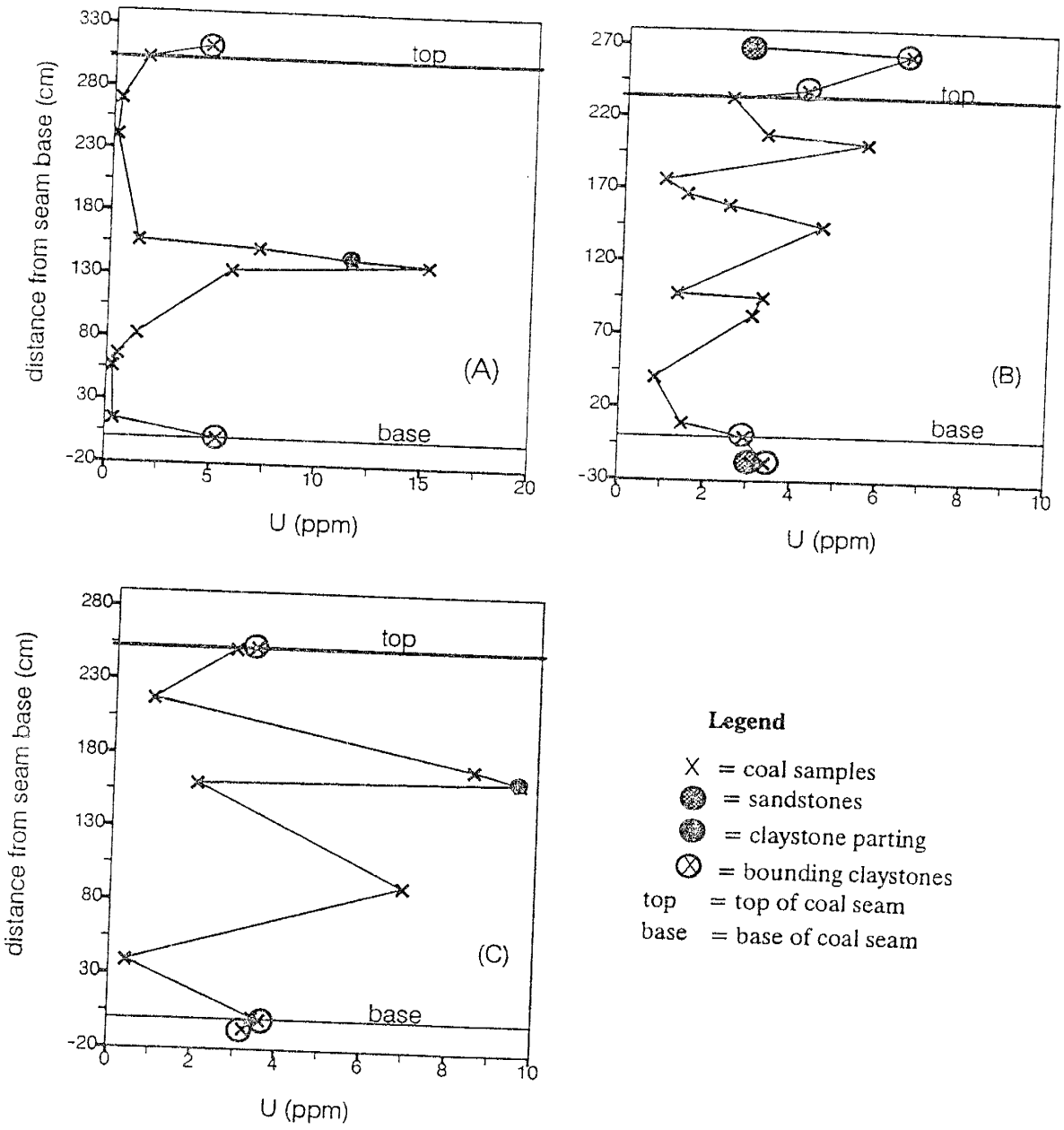

Figure A4-17. Vertical distribution of uranium in the BB seam; (A) in DHS1, (B) in DHS2, and (C) in DHS3.

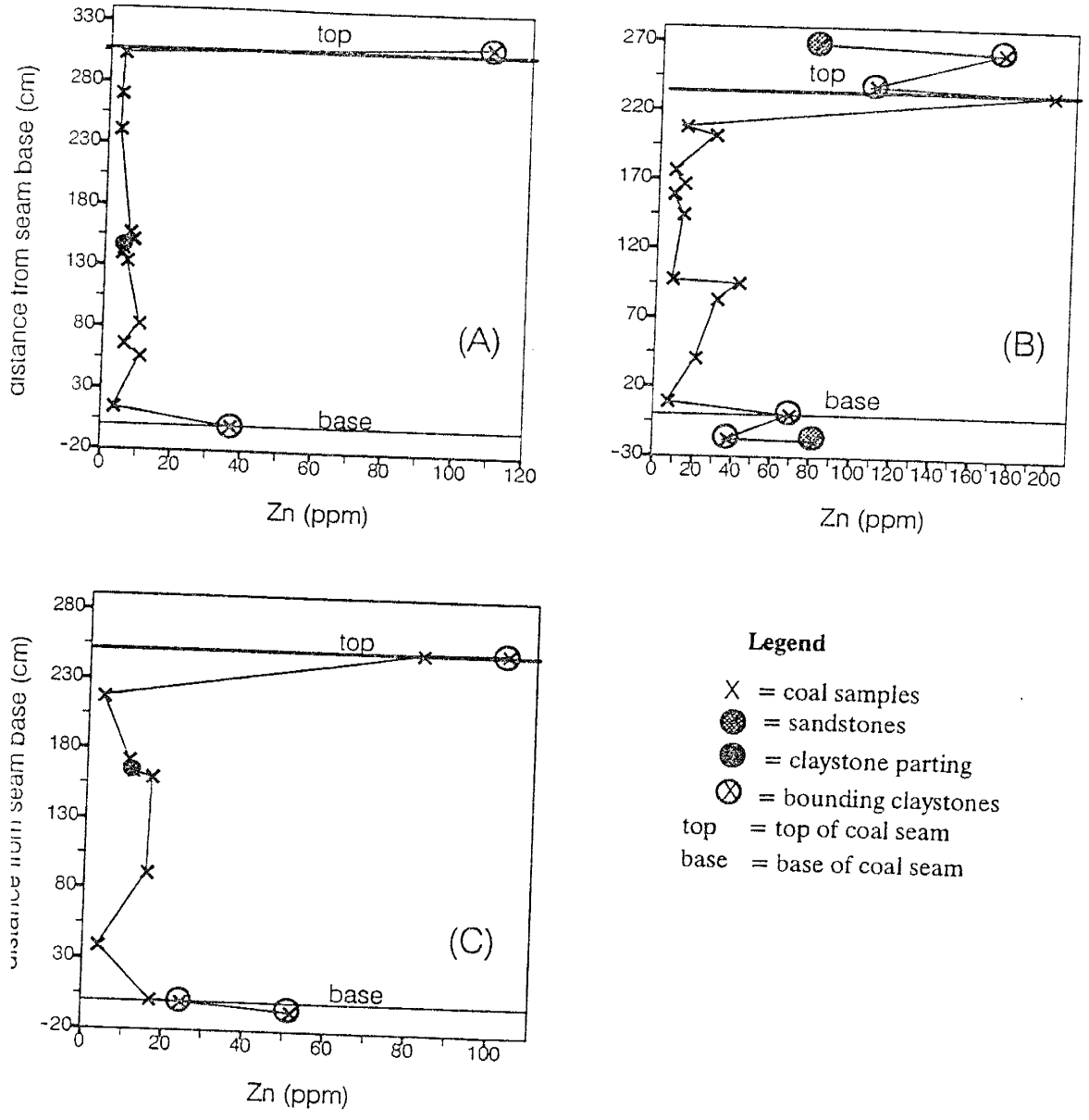

Figure A4-18. Vertical distribution of zinc in the BB seam; (A) in DHS1, (B) in DHS2, and (C) in DHS3.

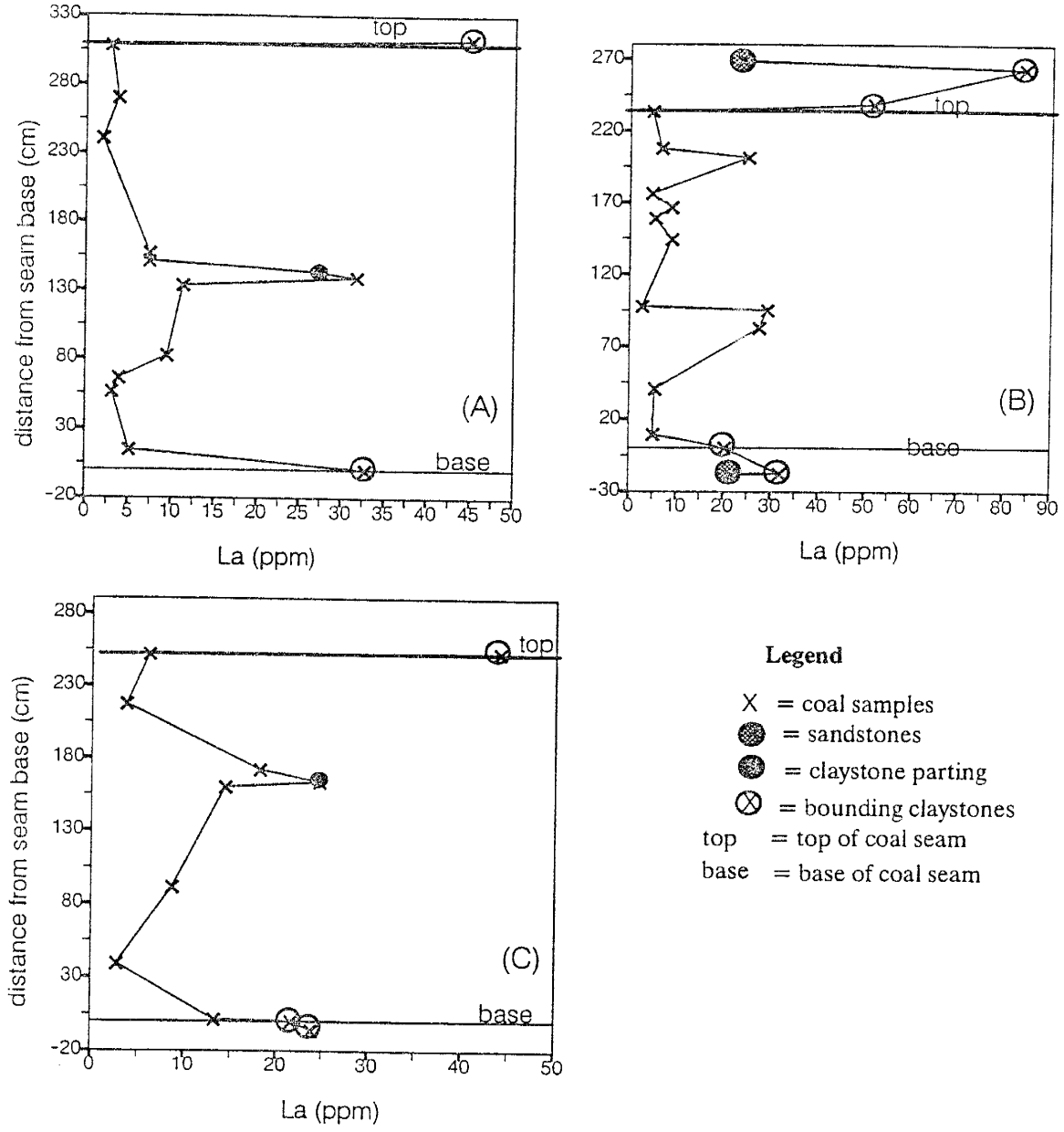

Figure A4-19. Vertical distribution of lanthanum in the BB seam; (A) in DHS1, (B) in DHS2, and (C) DHS3.

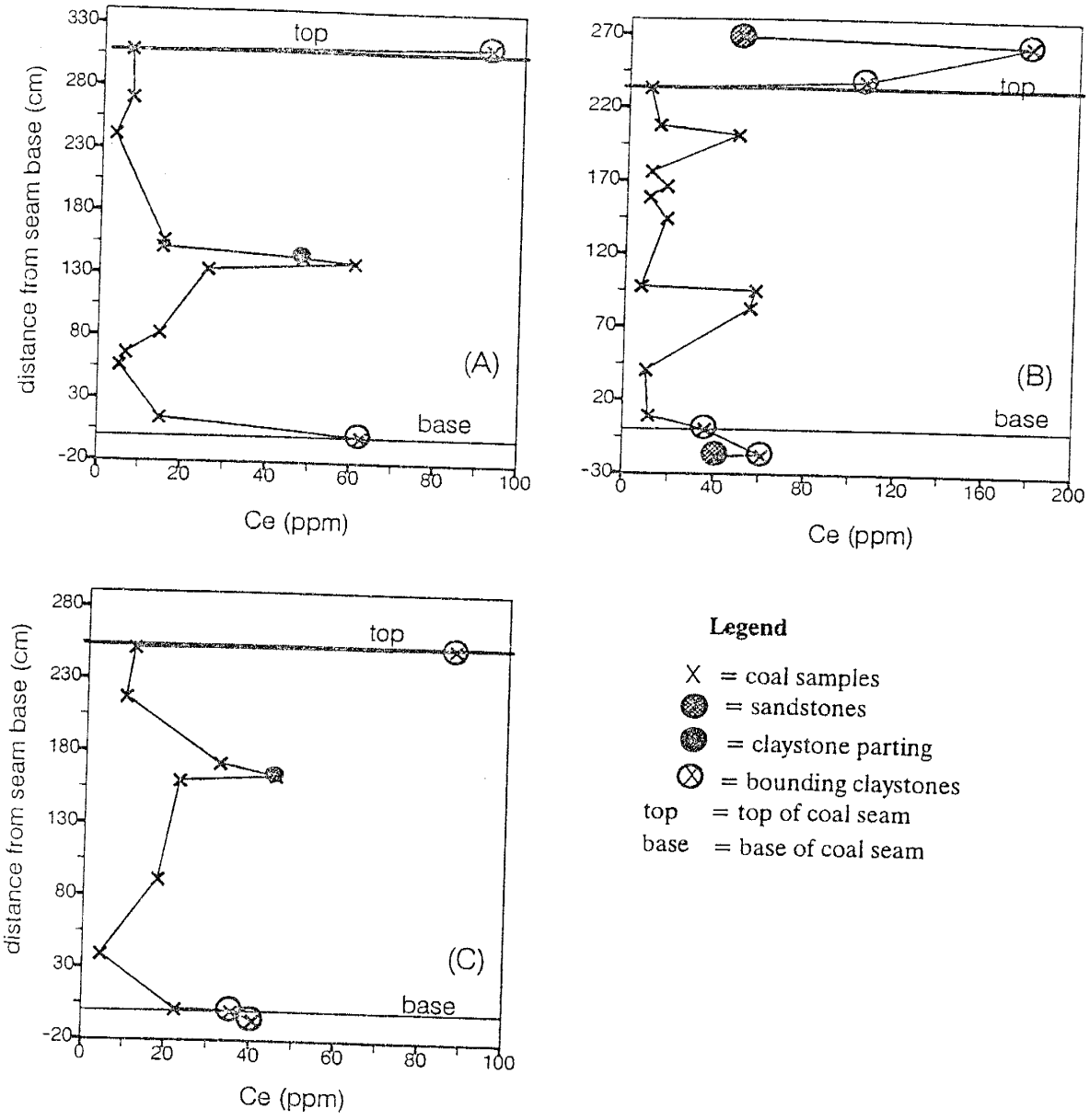

Figure A4-20. Vertical distribution of cerium in the BB seam; (A) in DHS1, (B) in DHS2, and (C) in DHS3.

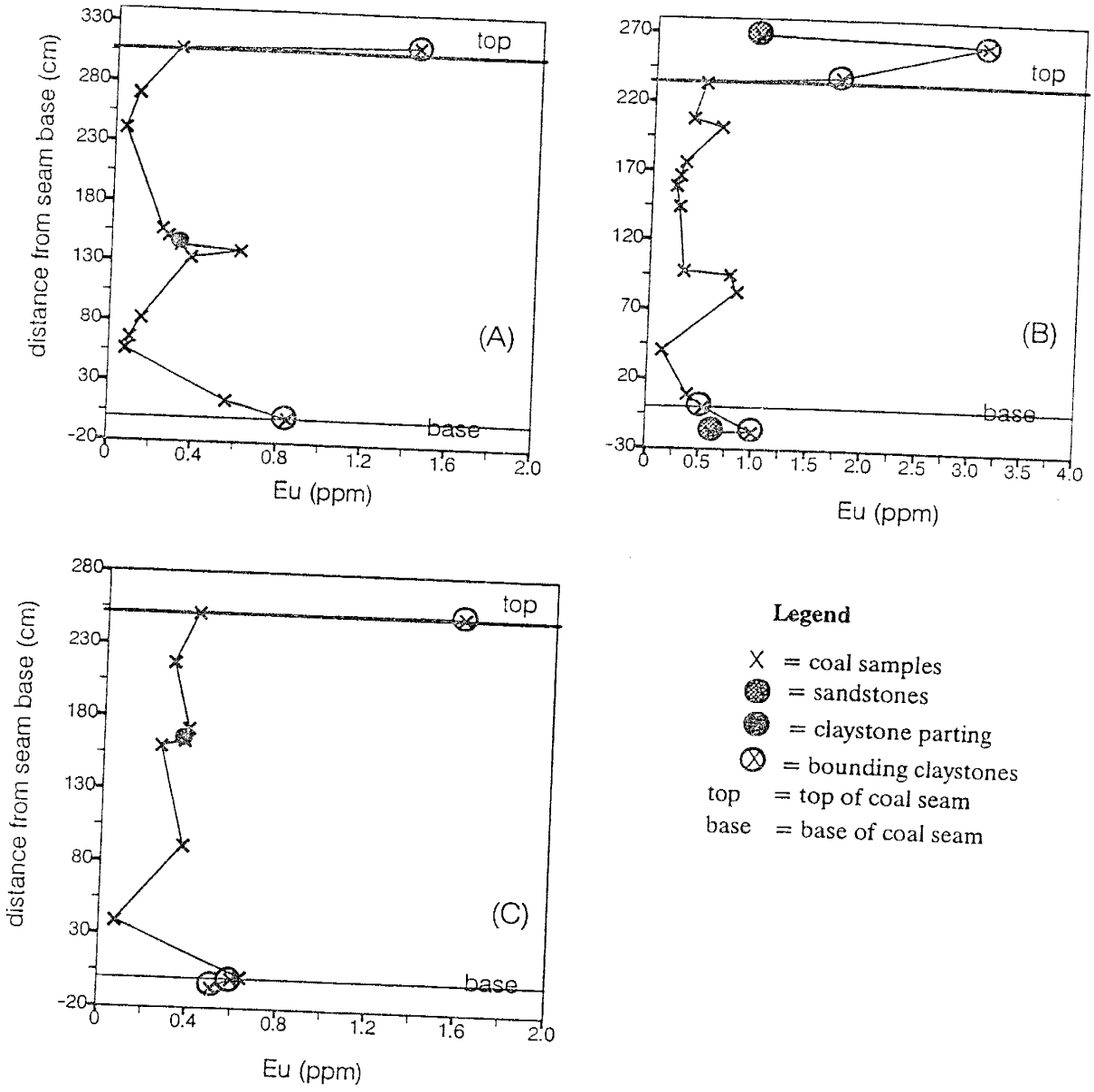

Figure A4-21. Vertical distribution of europium in the BB seam; (A) in DHS1, (B) in DHS2, and DHS3.

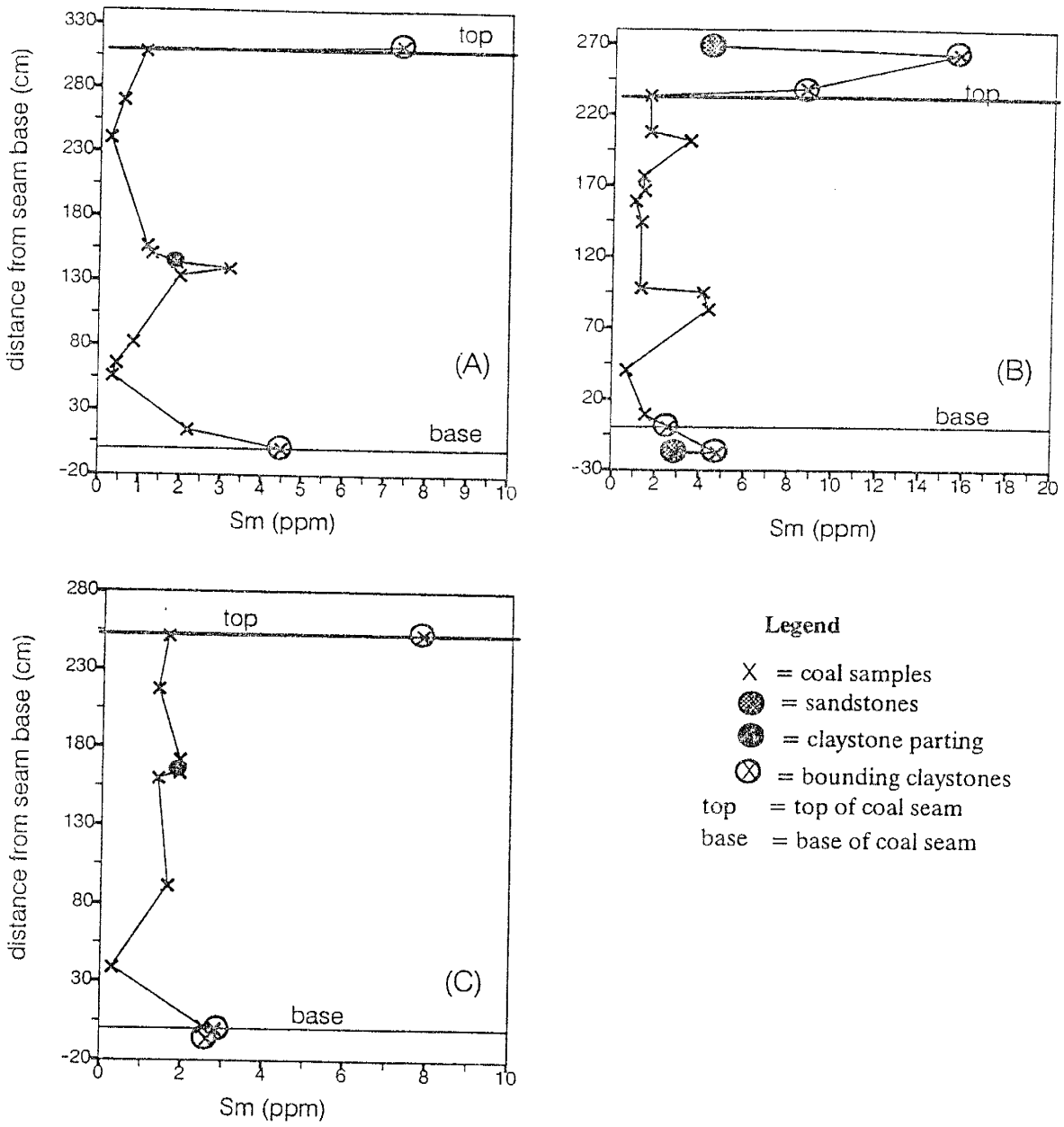

Figure A4-22. Vertical distribution of samarium in the BB seam; (A) in DHS1, (B) in DHS2, and (C) in DHS3.

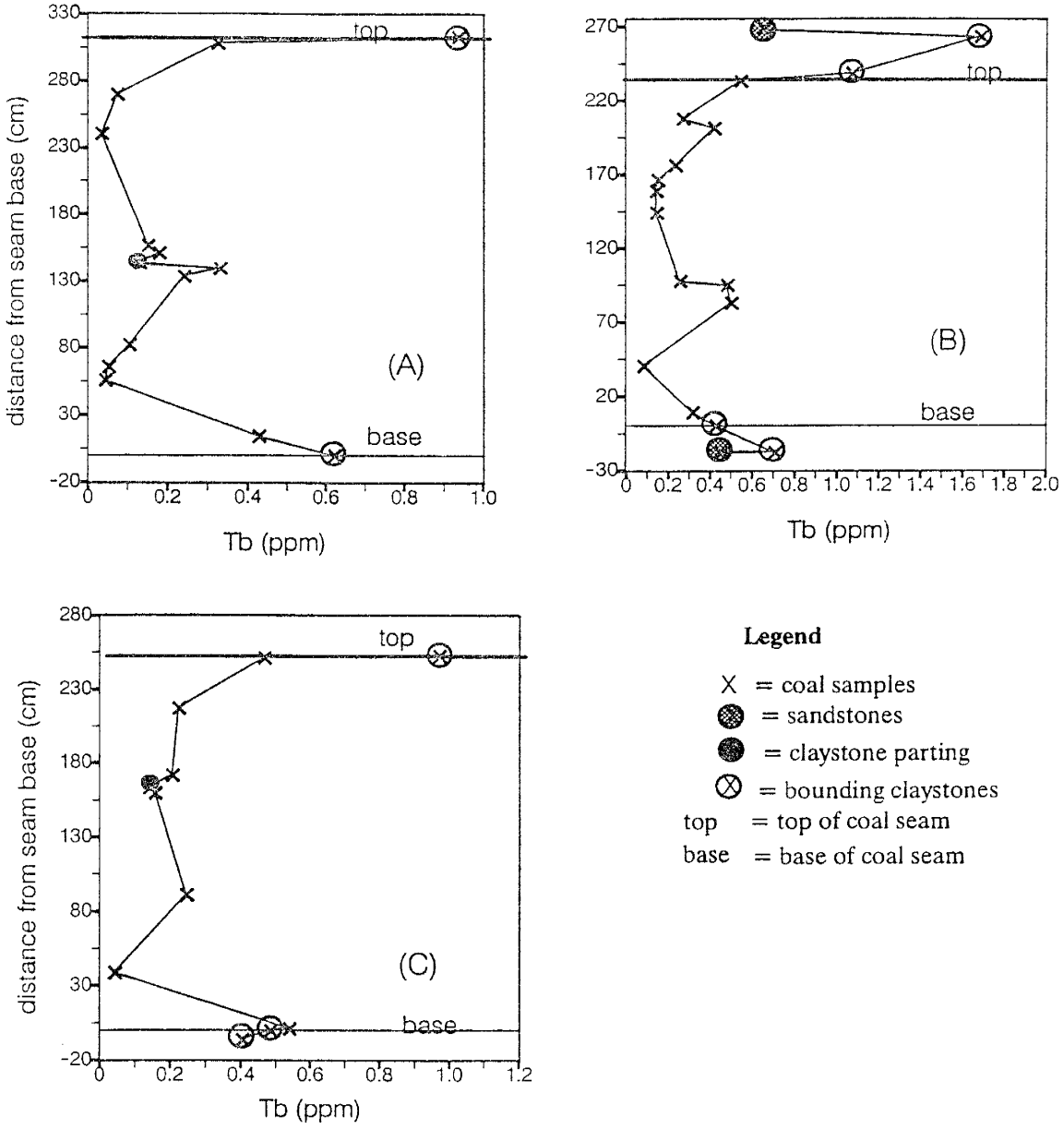

Figure A4-23. Vertical distribution of terbium in the BB seam; (A) in DHS1, (B) in DHS2, and (C) in DHS3.

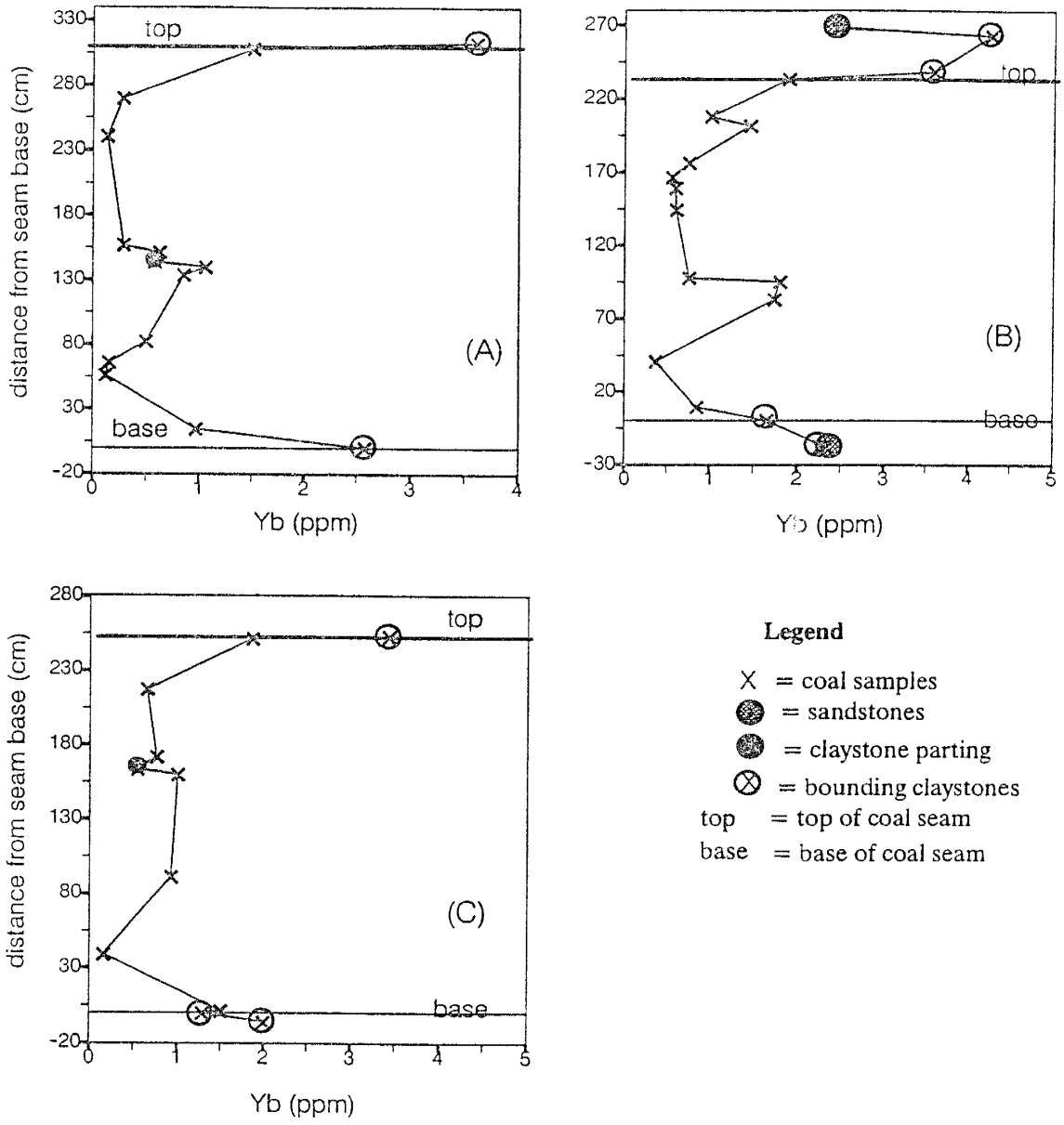

Figure A4-24. Vertical distribution of ytterbium in the BB seam; (A) in DHS1, (B) in DHS2, and (C) in DHS3.

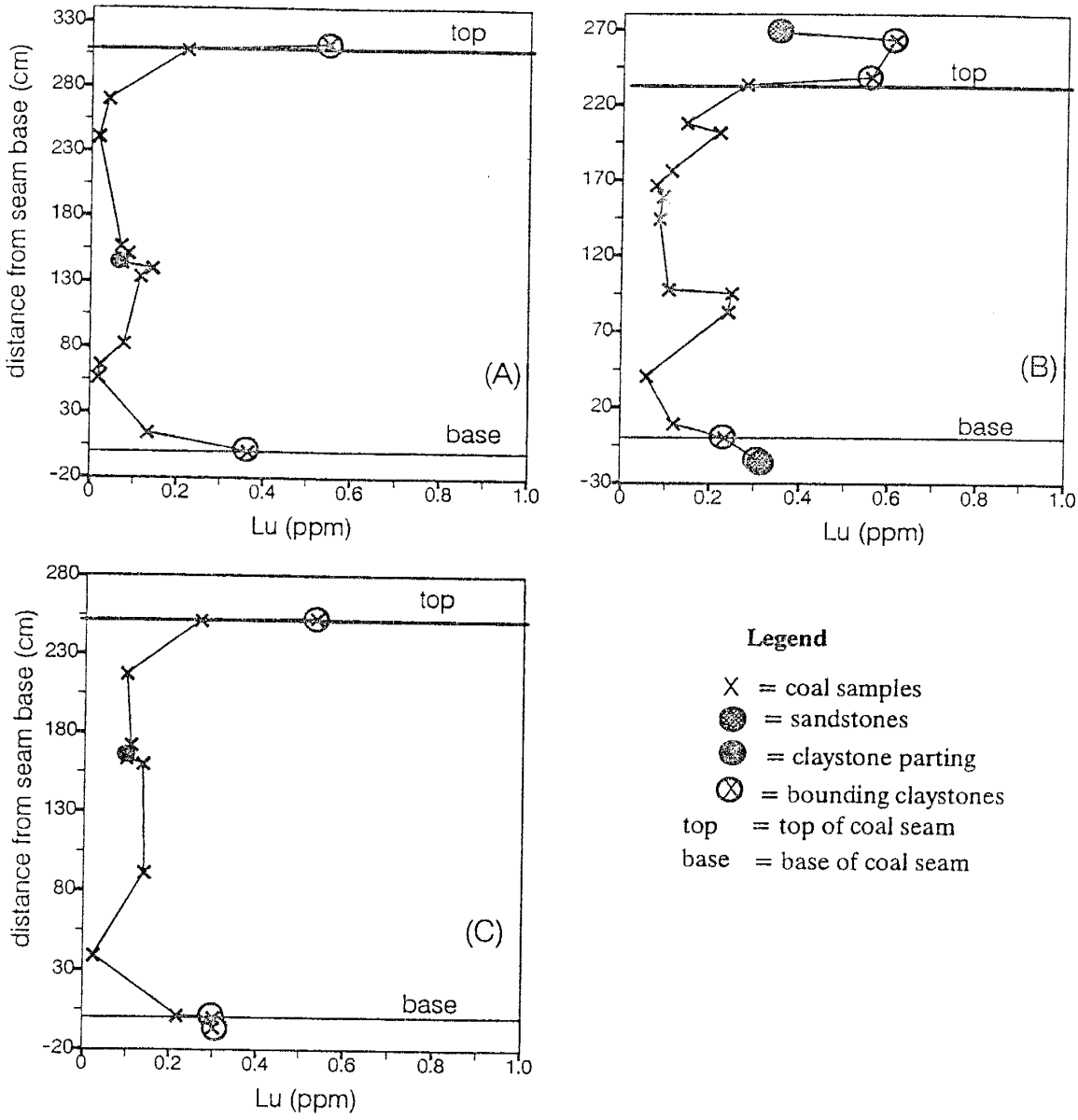

Figure A4-25. Vertical distribution of lutetium in the BB seam; (A) in DHS1, (B) in DHS2, and (C) in DHS3.

Appendix 5. Correlation analysis results

27 Apr 93 SPSS Release 4.0 for Sun 4
13:38:57 Tech Computer Center SPSS 4.0 Sun-4 SunOS 4.1.1

- - Correlation Coefficients - -

	CR	BA	FE	SC	NA	CO	ZN	AS	SE	SR	LA
CR	1.0000 (30) P= .	.3334 (30) P= .072	.4579 (30) P= .011	.8582 (30) P= .000	.7433 (30) P= .000	.1807 (30) P= .339	.7430 (30) P= .000	.2618 (30) P= .162	.4738 (30) P= .008	.6539 (30) P= .000	.6182 (30) P= .000
BA	.3334 (30) P= .072	1.0000 (30) P= .	.1816 (30) P= .337	.4026 (30) P= .027	.2394 (30) P= .203	.2338 (30) P= .214	.6072 (30) P= .000	.1884 (30) P= .319	.4095 (30) P= .025	.3160 (30) P= .089	.2510 (30) P= .181
FE	.4579 (30) P= .011	.1816 (30) P= .337	1.0000 (30) P= .	.4638 (30) P= .010	.4788 (30) P= .007	.0129 (30) P= .946	.4496 (30) P= .013	.6390 (30) P= .000	.4013 (30) P= .028	.5457 (30) P= .002	.4732 (30) P= .008
SC	.8582 (30) P= .000	.4026 (30) P= .027	.4638 (30) P= .010	1.0000 (30) P= .	.7251 (30) P= .000	.4832 (30) P= .007	.6772 (30) P= .000	.2319 (30) P= .218	.5903 (30) P= .001	.6200 (30) P= .000	.6669 (30) P= .000
NA	.7433 (30) P= .000	.2394 (30) P= .203	.4788 (30) P= .007	.7251 (30) P= .000	1.0000 (30) P= .	.3541 (30) P= .055	.7308 (30) P= .000	.4608 (30) P= .010	.1890 (30) P= .317	.8852 (30) P= .000	.5560 (30) P= .054
CO	.1807 (30) P= .339	.2338 (30) P= .214	.0129 (30) P= .946	.4832 (30) P= .007	.3541 (30) P= .055	1.0000 (30) P= .	.1724 (30) P= .362	.0573 (30) P= .764	.2852 (30) P= .127	.3030 (30) P= .104	.1584 (30) P= .403
ZN	.7430 (30) P= .000	.6072 (30) P= .000	.4496 (30) P= .013	.6772 (30) P= .000	.7308 (30) P= .000	.1724 (30) P= .362	1.0000 (30) P= .	.4427 (30) P= .014	.3713 (30) P= .043	.6592 (30) P= .000	.3855 (30) P= .035
AS	.2618 (30) P= .162	.1884 (30) P= .319	.6390 (30) P= .000	.2319 (30) P= .218	.4608 (30) P= .010	.0573 (30) P= .764	.4427 (30) P= .014	1.0000 (30) P= .	.4030 (30) P= .027	.3801 (30) P= .038	.2571 (30) P= .170
SE	.4738 (30) P= .008	.4095 (30) P= .025	.4013 (30) P= .028	.5903 (30) P= .001	.1890 (30) P= .317	.2852 (30) P= .127	.3713 (30) P= .043	.4030 (30) P= .027	1.0000 (30) P= .	.1408 (30) P= .458	.7045 (30) P= .000
SR	.6539 (30) P= .000	.3160 (30) P= .089	.5457 (30) P= .002	.6200 (30) P= .000	.8852 (30) P= .000	.3030 (30) P= .104	.6592 (30) P= .000	.3801 (30) P= .038	.1408 (30) P= .458	1.0000 (30) P= .	.2792 (30) P= .135
LA	.6182 (30) P= .000	.2510 (30) P= .181	.4732 (30) P= .008	.6669 (30) P= .000	.5560 (30) P= .054	.1584 (30) P= .403	.3855 (30) P= .035	.2571 (30) P= .170	.7045 (30) P= .000	.2792 (30) P= .135	1.0000 (30) P= .
CE	.5736 (30) P= .001	.2391 (30) P= .203	.4506 (30) P= .012	.6995 (30) P= .000	.3500 (30) P= .058	.2671 (30) P= .154	.3445 (30) P= .062	.2220 (30) P= .238	.7025 (30) P= .000	.2677 (30) P= .153	.9796 (30) P= .000

(Coefficient / (Cases) / 2-tailed Sig) " . " is printed if a coefficient cannot be computed

Table APP5-1. Correlation matrix for trace elements, ash, and forms of sulfur in BB seam coals. OS = organic sulfur; PS = pyritic sulfur; TS = total sulfur.

27 Apr 93 SPSS Release 4.0 for Sun 4
13:39:00 Tech Computer Center SPSS 4.0 Sun-4 SunOS 4.1.1

- - Correlation Coefficients - -

	CR	BA	FE	SC	NA	CO	ZN	AS	SE	SR	LA
SM	-.6240	-.2846	-.4016	-.8527	-.5078	-.5385	-.4229	.1800	-.6265	-.4148	-.7900
	(30)	(30)	(30)	(30)	(30)	(30)	(30)	(30)	(30)	(30)	(30)
	P= .000	P= .127	P= .028	P= .000	P= .004	P= .002	P= .020	P= .341	P= .000	P= .023	P= .000
EU	-.6228	-.3295	-.3652	-.3733	-.5236	-.6196	-.4421	-.1412	-.6035	-.4467	-.6895
	(30)	(30)	(30)	(30)	(30)	(30)	(30)	(30)	(30)	(30)	(30)
	P= .000	P= .075	P= .045	P= .000	P= .003	P= .000	P= .014	P= .457	P= .000	P= .013	P= .000
YB	-.7143	-.3027	-.4206	-.9340	-.5219	-.6257	-.5501	-.1895	-.5434	-.5264	-.5655
	(30)	(30)	(30)	(30)	(30)	(30)	(30)	(30)	(30)	(30)	(30)
	P= .000	P= .104	P= .021	P= .000	P= .000	P= .000	P= .002	P= .316	P= .002	P= .003	P= .001
LU	-.7276	-.2997	-.4056	-.9319	-.6333	-.5698	-.5835	-.1764	-.5032	-.5354	-.6085
	(30)	(30)	(30)	(30)	(30)	(30)	(30)	(30)	(30)	(30)	(30)
	P= .000	P= .108	P= .026	P= .000	P= .000	P= .001	P= .001	P= .351	P= .005	P= .002	P= .000
HF	-.6935	-.2440	-.4038	-.7556	-.4568	-.2982	-.4521	-.3190	-.7818	-.3463	-.8363
	(30)	(30)	(30)	(30)	(30)	(30)	(30)	(30)	(30)	(30)	(30)
	P= .000	P= .194	P= .027	P= .000	P= .011	P= .109	P= .012	P= .086	P= .000	P= .061	P= .000
TA	-.6152	-.1577	-.4056	-.7227	-.5102	-.3596	-.4248	-.3305	-.6997	-.3605	-.7350
	(30)	(30)	(30)	(30)	(30)	(30)	(30)	(30)	(30)	(30)	(30)
	P= .000	P= .405	P= .026	P= .000	P= .004	P= .051	P= .019	P= .074	P= .000	P= .066	P= .000
TH	-.4944	-.2976	-.3283	-.6649	-.2780	-.2931	-.3198	-.2615	-.6289	-.1842	-.8501
	(30)	(30)	(30)	(30)	(30)	(30)	(30)	(30)	(30)	(30)	(30)
	P= .005	P= .110	P= .076	P= .000	P= .137	P= .116	P= .085	P= .163	P= .000	P= .330	P= .000
U	-.5035	-.3455	-.3162	-.7390	-.3571	-.3440	-.3809	-.2534	-.8079	-.2949	-.7517
	(30)	(30)	(30)	(30)	(30)	(30)	(30)	(30)	(30)	(30)	(30)
	P= .004	P= .061	P= .091	P= .000	P= .053	P= .063	P= .038	P= .177	P= .000	P= .114	P= .000
ASH	-.8024	-.2007	-.5755	-.8506	-.7557	-.5572	-.6464	-.4159	-.6105	-.6758	-.7017
	(30)	(30)	(30)	(30)	(30)	(30)	(30)	(30)	(30)	(30)	(30)
	P= .000	P= .288	P= .001	P= .000	P= .000	P= .053	P= .000	P= .022	P= .000	P= .000	P= .000
OS	-.3398	-.1070	-.1485	-.2686	-.1001	.0614	-.2114	-.2497	-.0701	-.2063	-.3686
	(28)	(28)	(28)	(28)	(28)	(28)	(28)	(28)	(28)	(28)	(28)
	P= .060	P= .588	P= .451	P= .167	P= .612	P= .756	P= .280	P= .200	P= .723	P= .292	P= .054
PS	-.2092	-.0757	-.4524	-.0474	.0121	.0531	-.0359	-.6707	-.2646	-.0156	-.0643
	(28)	(28)	(28)	(28)	(28)	(28)	(28)	(28)	(28)	(28)	(28)
	P= .285	P= .702	P= .016	P= .811	P= .951	P= .789	P= .856	P= .000	P= .174	P= .937	P= .745
TS	-.3005	.0071	-.2487	-.2051	-.0176	.0170	-.1116	-.6681	-.1546	-.0947	-.2409
	(28)	(28)	(28)	(28)	(28)	(28)	(28)	(28)	(28)	(28)	(28)
	P= .120	P= .971	P= .202	P= .300	P= .929	P= .932	P= .572	P= .000	P= .432	P= .632	P= .217

(Coefficient / (Cases) / 2-tailed Sig) " . " is printed if a coefficient cannot be computed

Table APP5-1. continued

27 Apr 93 SPSS Release 4.0 for Sun 4
13:39:00 Tech Computer Center SPSS 4.0 Sun-4 SunOS 4.1.1

Correlation Coefficients

	CR	BA	FE	SC	NA	CO	ZN	AS	SE	SR	LA
SB	.3125 (23) P= .147	.3283 (23) P= .126	.1601 (23) P= .466	.6787 (23) P= .000	.3044 (23) P= .158	.7995 (23) P= .000	.1979 (23) P= .365	.0773 (23) P= .726	.5310 (23) P= .009	.2742 (23) P= .205	.2461 (23) P= .258
RB	.7453 (17) P= .001	.3492 (17) P= .170	.3357 (17) P= .196	.6697 (17) P= .003	.6759 (17) P= .003	.0629 (17) P= .810	.6941 (17) P= .002	.0079 (17) P= .976	.2625 (17) P= .309	.5964 (17) P= .012	.6490 (17) P= .005
CS	.7700 (18) P= .000	.3501 (18) P= .154	.3824 (18) P= .117	.6966 (18) P= .001	.5122 (18) P= .007	.2441 (18) P= .329	.6496 (18) P= .004	.0254 (18) P= .920	.3049 (18) P= .219	.5755 (18) P= .012	.6953 (18) P= .001
TB	.6371 (30) P= .000	.3151 (30) P= .090	.2928 (30) P= .116	.8395 (30) P= .000	.5850 (30) P= .001	.6530 (30) P= .000	.5608 (30) P= .002	.0768 (30) P= .687	.4821 (30) P= .007	.5062 (30) P= .004	.5009 (30) P= .005

(Coefficient / (Cases) / 2-tailed Sig) " . " is printed if a coefficient cannot be computed

Table APP5-1. continued

27 Apr 93 SPSS Release 4.0 for Sun 4
13:39:00 Tech Computer Center SPSS 4.0 Sun-4 SunOS 4.1.1

Correlation Coefficients

	CE	SM	EU	YB	LU	HF	TA	TH	U	ASH	OS
CR	-.5736	-.6240	-.6228	-.7143	-.7276	-.6983	-.6152	-.4944	-.5085	-.8024	-.3598
	(30)	(30)	(30)	(30)	(30)	(30)	(30)	(30)	(30)	(30)	(28)
	P= .001	P= .000	P= .000	P= .000	P= .000	P= .000	P= .000	P= .005	P= .004	P= .000	P= .060
BA	-.2391	-.2346	-.3295	-.3027	-.2997	-.2440	-.1577	-.2976	-.3455	-.2007	-.1070
	(30)	(30)	(30)	(30)	(30)	(30)	(30)	(30)	(30)	(30)	(28)
	P= .203	P= .127	P= .075	P= .104	P= .108	P= .194	P= .405	P= .110	P= .061	P= .288	P= .588
FE	-.4506	-.4016	-.3682	-.4206	-.4056	-.4038	-.4056	-.3283	-.3142	-.5755	-.1485
	(30)	(30)	(30)	(30)	(30)	(30)	(30)	(30)	(30)	(30)	(28)
	P= .012	P= .028	P= .045	P= .021	P= .026	P= .027	P= .026	P= .076	P= .091	P= .001	P= .451
SC	-.8996	-.8529	-.8730	-.9340	-.9319	-.7556	-.7227	-.6649	-.7380	-.8304	-.2684
	(30)	(30)	(30)	(30)	(30)	(30)	(30)	(30)	(30)	(30)	(28)
	P= .000	P= .000	P= .000	P= .000	P= .000	P= .000	P= .000	P= .000	P= .000	P= .000	P= .167
NA	-.3500	-.5078	-.5256	-.6219	-.6383	-.4568	-.5102	-.2780	-.3571	-.7357	-.1001
	(30)	(30)	(30)	(30)	(30)	(30)	(30)	(30)	(30)	(30)	(28)
	P= .058	P= .004	P= .003	P= .000	P= .000	P= .011	P= .004	P= .137	P= .053	P= .000	P= .612
CO	-.2671	-.5385	-.6196	-.6257	-.5698	-.2982	-.3596	-.2931	-.3440	-.3572	-.0614
	(30)	(30)	(30)	(30)	(30)	(30)	(30)	(30)	(30)	(30)	(28)
	P= .154	P= .002	P= .000	P= .000	P= .001	P= .109	P= .051	P= .116	P= .063	P= .053	P= .756
ZN	-.3445	-.4229	-.4421	-.5501	-.5835	-.4521	-.4268	-.3198	-.3809	-.6464	-.2114
	(30)	(30)	(30)	(30)	(30)	(30)	(30)	(30)	(30)	(30)	(28)
	P= .062	P= .020	P= .014	P= .002	P= .001	P= .012	P= .019	P= .085	P= .038	P= .000	P= .280
AS	-.2220	-.1800	-.1412	-.1895	-.1764	-.3190	-.3305	-.2615	-.2534	-.4159	-.2497
	(30)	(30)	(30)	(30)	(30)	(30)	(30)	(30)	(30)	(30)	(28)
	P= .238	P= .341	P= .457	P= .316	P= .351	P= .086	P= .074	P= .163	P= .177	P= .022	P= .200
SE	-.7023	-.6265	-.6035	-.5434	-.5032	-.7818	-.6997	-.6289	-.6079	-.6105	-.0701
	(30)	(30)	(30)	(30)	(30)	(30)	(30)	(30)	(30)	(30)	(28)
	P= .000	P= .000	P= .000	P= .002	P= .005	P= .000	P= .000	P= .000	P= .000	P= .000	P= .723
SR	-.2677	-.4148	-.4467	-.5264	-.5354	-.3463	-.3483	-.1842	-.2949	-.6758	-.2005
	(30)	(30)	(30)	(30)	(30)	(30)	(30)	(30)	(30)	(30)	(28)
	P= .153	P= .023	P= .013	P= .003	P= .002	P= .061	P= .060	P= .330	P= .114	P= .000	P= .292
LA	-.9796	-.7900	-.6895	-.5655	-.6085	-.8363	-.7350	-.8301	-.7517	-.7017	-.3686
	(30)	(30)	(30)	(30)	(30)	(30)	(30)	(30)	(30)	(30)	(28)
	P= .000	P= .000	P= .000	P= .001	P= .000	P= .000	P= .000	P= .000	P= .000	P= .000	P= .054
CE	1.0000	.8779	.7895	.6463	.6832	.8117	.7178	.8165	.7665	.6946	.3497
	(30)	(30)	(30)	(30)	(30)	(30)	(30)	(30)	(30)	(30)	(28)
	P= .	P= .000	P= .000	P= .000	P= .000	P= .000	P= .000	P= .000	P= .000	P= .000	P= .068

(Coefficient / (Cases) / 2-tailed Sig) " . " is printed if a coefficient cannot be computed

Table APP5-1. continued

27 Apr 93 SPSS Release 4.0 for Sun 4
13:39:00 Tech Computer Center SPSS 4.0 Sun-4 SunOS 4.1.1

Correlation Coefficients

	CE	SM	EU	YB	LU	MF	TA	TH	U	ASH	OS
SM	.8779 (30) P= .000	1.0000 (30) P= .	.9827 (30) P= .000	.8869 (30) P= .000	.8886 (30) P= .000	.7199 (30) P= .000	.6654 (30) P= .000	.6900 (30) P= .000	.7442 (30) P= .000	.7316 (30) P= .000	-.2841 (28) P= .143
EU	.7893 (30) P= .000	.9827 (30) P= .000	1.0000 (30) P= .	.9241 (30) P= .000	.9130 (30) P= .000	.6665 (30) P= .000	.6224 (30) P= .000	.6280 (30) P= .000	.7111 (30) P= .000	.7200 (30) P= .000	-.2583 (28) P= .184
YB	.6463 (30) P= .000	.8869 (30) P= .000	.9241 (30) P= .000	1.0000 (30) P= .	.9598 (30) P= .000	.6790 (30) P= .000	.6712 (30) P= .000	.5924 (30) P= .001	.6792 (30) P= .000	.7450 (30) P= .000	-.1981 (28) P= .312
LU	.6832 (30) P= .000	.8886 (30) P= .000	.9130 (30) P= .000	.9598 (30) P= .000	1.0000 (30) P= .	.6769 (30) P= .000	.6769 (30) P= .000	.5825 (30) P= .001	.6470 (30) P= .000	.7718 (30) P= .000	-.2757 (28) P= .156
MF	.8117 (30) P= .000	.7199 (30) P= .000	.6665 (30) P= .000	.6790 (30) P= .000	.6769 (30) P= .000	1.0000 (30) P= .	.9282 (30) P= .000	.9323 (30) P= .000	.8651 (30) P= .000	.7971 (30) P= .000	-.2190 (28) P= .263
TA	.7178 (30) P= .000	.6654 (30) P= .000	.6224 (30) P= .000	.6712 (30) P= .000	.6769 (30) P= .000	.9282 (30) P= .000	1.0000 (30) P= .	.8725 (30) P= .000	.7931 (30) P= .000	.7755 (30) P= .000	-.1055 (28) P= .593
TH	.8155 (30) P= .000	.6900 (30) P= .000	.6280 (30) P= .000	.5924 (30) P= .001	.5825 (30) P= .001	.9323 (30) P= .000	.8725 (30) P= .000	1.0000 (30) P= .	.9501 (30) P= .000	.6580 (30) P= .000	-.1395 (28) P= .479
U	.7665 (30) P= .000	.7442 (30) P= .000	.7111 (30) P= .000	.6792 (30) P= .000	.6470 (30) P= .000	.8651 (30) P= .000	.7931 (30) P= .000	.9501 (30) P= .000	1.0000 (30) P= .	.6778 (30) P= .000	-.1561 (28) P= .428
ASH	.6946 (30) P= .000	.7316 (30) P= .000	.7200 (30) P= .000	.7450 (30) P= .000	.7718 (30) P= .000	.7971 (30) P= .000	.7755 (30) P= .000	.6580 (30) P= .000	.6778 (30) P= .000	1.0000 (30) P= .	-.4991 (28) P= .007
OS	-.3497 (28) P= .068	-.2841 (28) P= .143	-.2583 (28) P= .184	-.1981 (28) P= .312	-.2757 (28) P= .156	-.2190 (28) P= .263	-.1055 (28) P= .593	-.1395 (28) P= .479	-.1561 (28) P= .428	-.4991 (28) P= .007	1.0000 (28) P= .
PS	-.0286 (28) P= .885	-.0193 (28) P= .922	-.0200 (28) P= .920	-.0021 (28) P= .992	-.0129 (28) P= .948	-.0417 (28) P= .833	-.0022 (28) P= .991	.0338 (28) P= .864	.0595 (28) P= .764	-.0088 (28) P= .965	.3788 (28) P= .047
TS	-.2122 (28) P= .278	-.1665 (28) P= .398	-.1387 (28) P= .420	-.1220 (28) P= .536	-.1858 (28) P= .344	-.1446 (28) P= .463	-.0645 (28) P= .745	-.0840 (28) P= .671	-.0800 (28) P= .686	-.2148 (28) P= .272	.7505 (28) P= .000

(Coefficient / (Cases) / 2-tailed Sig) " . " is printed if a coefficient cannot be computed

Table APP5-1. continued

27 Apr 93 SPSS Release 4.0 for Sun 4
13:39:00 Tech Computer Center SPSS 4.0 Sun-4 SunOS 4.1.1

Correlation Coefficients

	CE	SM	EU	YB	LU	HF	TA	TH	U	ASH	OS
SB	-.3695 (23) P= .083	-.6761 (23) P= .000	-.7691 (23) P= .000	-.7748 (23) P= .000	-.7058 (23) P= .000	-.4123 (23) P= .051	-.4612 (23) P= .027	-.4222 (23) P= .045	-.5580 (23) P= .006	-.4267 (23) P= .042	-.0555 (22) P= .806
RB	-.5821 (17) P= .014	-.4522 (17) P= .068	-.3803 (17) P= .132	-.5236 (17) P= .031	-.5569 (17) P= .020	-.5410 (17) P= .025	-.5289 (17) P= .029	-.3918 (17) P= .120	-.1881 (17) P= .470	-.5181 (17) P= .033	-.3247 (15) P= .238
CS	-.6288 (18) P= .005	-.4815 (18) P= .043	-.4022 (18) P= .098	-.5074 (18) P= .032	-.5485 (18) P= .018	-.5719 (18) P= .013	-.4709 (18) P= .049	-.4278 (18) P= .077	-.2742 (18) P= .271	-.5235 (18) P= .026	-.3423 (16) P= .194
TB	-.5956 (30) P= .001	-.8604 (30) P= .000	-.8836 (30) P= .000	-.8960 (30) P= .000	-.8761 (30) P= .000	-.5822 (30) P= .001	-.5435 (30) P= .002	-.4765 (30) P= .008	-.5711 (30) P= .001	-.6472 (30) P= .000	-.1683 (28) P= .392

(Coefficient / (Cases) / 2-tailed Sig) " . " is printed if a coefficient cannot be computed

Table APP5-1. continued

27 Apr 93 SPSS Release 4.0 for Sun 4
13:39:00 Tech Computer Center SPSS 4.0 Sun-4 SunOS 4.1.1

Correlation Coefficients

	PS	TS	SB	BB	CS	TS
CK	-.2092 (28) P= .285	-.3005 (28) P= .120	-.3125 (23) P= .147	.7453 (17) P= .001	.7700 (18) P= .000	.6371 (30) P= .000
BA	.0757 (28) P= .702	-.0071 (28) P= .971	-.3283 (23) P= .126	-.3492 (17) P= .170	-.3501 (18) P= .154	-.3151 (30) P= .090
FE	-.4524 (28) P= .016	-.2487 (28) P= .202	-.1601 (23) P= .466	-.3367 (17) P= .186	-.3824 (18) P= .117	-.2928 (30) P= .116
SC	-.0476 (23) P= .811	-.2031 (29) P= .300	-.6757 (23) P= .000	-.6697 (17) P= .003	-.6966 (18) P= .001	-.8395 (30) P= .000
NA	-.0121 (28) P= .951	-.0176 (28) P= .929	-.3044 (23) P= .158	.6759 (17) P= .003	.6122 (18) P= .007	.5850 (30) P= .001
CU	.0531 (28) P= .789	.0170 (29) P= .932	-.7995 (23) P= .000	-.0629 (17) P= .810	-.2441 (18) P= .329	-.6530 (30) P= .000
ZN	-.0359 (28) P= .856	-.1116 (28) P= .572	-.1979 (23) P= .365	.6941 (17) P= .002	.5496 (18) P= .004	.5408 (30) P= .002
AS	.6707 (28) P= .000	.6681 (28) P= .000	.0773 (23) P= .726	-.0079 (17) P= .976	.0254 (18) P= .920	.0768 (30) P= .687
SE	.2646 (28) P= .174	.1546 (28) P= .432	.5310 (23) P= .009	.2625 (17) P= .309	.3049 (18) P= .219	.4821 (30) P= .007
SR	.0156 (28) P= .937	-.0947 (28) P= .632	.2742 (23) P= .205	.5964 (17) P= .012	.5755 (18) P= .012	.5062 (30) P= .004
LA	.0643 (28) P= .745	-.2409 (28) P= .217	-.2451 (23) P= .258	.6490 (17) P= .005	.6953 (18) P= .001	.5009 (30) P= .005
CE	-.0286 (28) P= .885	-.2122 (29) P= .278	-.3695 (23) P= .083	.5821 (17) P= .014	.6288 (18) P= .005	.5966 (30) P= .001

(Coefficient / (Cases) / 2-tailed Sig) " . " is printed if a coefficient cannot be computed

Table APP5-1. continued

27 Apr 93 SPSS Release 4.0 for Sun 4
13:39:00 Tech Computer Center SPSS 4.0 Sun-4 SunOS 4.1.1

Correlation Coefficients

	PS	TS	SB	RB	CS	TB
SM	-.0193	-.1563	.6761	.4522	.4815	.8404
	(28)	(28)	(23)	(17)	(18)	(30)
	P= .922	P= .398	P= .000	P= .069	P= .043	P= .000
EU	-.0200	-.1587	.7691	.3803	.4022	.8836
	(28)	(28)	(23)	(17)	(18)	(30)
	P= .920	P= .420	P= .000	P= .132	P= .098	P= .000
YB	-.0021	-.1220	.7748	.5236	.5074	.8960
	(28)	(28)	(23)	(17)	(18)	(30)
	P= .992	P= .536	P= .000	P= .031	P= .032	P= .000
LU	-.0129	-.1338	.7058	.5569	.5485	.8761
	(28)	(28)	(23)	(17)	(19)	(30)
	P= .948	P= .344	P= .000	P= .020	P= .018	P= .000
HI	-.0417	-.1446	.4123	.5410	.5719	.5822
	(28)	(28)	(23)	(17)	(18)	(30)
	P= .833	P= .463	P= .051	P= .025	P= .013	P= .001
TA	-.0022	-.0643	.4612	.5289	.4709	.5435
	(28)	(28)	(23)	(17)	(18)	(30)
	P= .991	P= .745	P= .027	P= .029	P= .049	P= .002
TM	.0338	-.0840	.4222	.3918	.4278	.4765
	(28)	(28)	(23)	(17)	(18)	(30)
	P= .864	P= .671	P= .045	P= .120	P= .077	P= .008
U	.0593	-.0800	.5590	.1881	.2742	.5711
	(28)	(28)	(23)	(17)	(18)	(30)
	P= .764	P= .686	P= .006	P= .470	P= .271	P= .001
ASH	.0088	-.2148	.4267	.5181	.5235	.6472
	(28)	(28)	(23)	(17)	(18)	(30)
	P= .965	P= .272	P= .042	P= .033	P= .026	P= .000
OS	-.3788	.7505	.0555	-.3247	-.3423	-.1683
	(28)	(28)	(22)	(15)	(16)	(28)
	P= .047	P= .000	P= .806	P= .238	P= .194	P= .392
PS	1.0000	.8343	.0976	-.3272	-.3037	-.0509
	(28)	(28)	(22)	(15)	(16)	(28)
	P= .	P= .000	P= .666	P= .234	P= .253	P= .797
TS	.8343	1.0000	.0946	-.4175	-.4073	-.1494
	(28)	(28)	(22)	(15)	(16)	(28)
	P= .000	P= .	P= .675	P= .122	P= .117	P= .448

(Coefficient / (Cases) / 2-tailed Sig) " . " is printed if a coefficient cannot be computed

Table APP5-1. continued

27 Apr 93 SPSS Release 4.0 for Sun 4
13:39:01 Tech Computer Center SPSS 4.0 Sun-4 SunOS 4.1.1

Correlation Coefficients

	PS	TS	SB	RB	CS	TB
SB	-.0970	-.0946	1.0000	-.3371	-.3055	.7538
	(22)	(22)	(23)	(11)	(11)	(23)
	P= .666	P= .675	P= .	P= .311	P= .361	P= .000
RB	-.3272	-.4175	-.3371	1.0000	.9919	.6275
	(15)	(15)	(11)	(17)	(17)	(17)
	P= .234	P= .122	P= .311	P= .	P= .000	P= .007
CS	-.3037	-.4073	-.3055	.9919	1.0000	.6206
	(16)	(16)	(11)	(17)	(18)	(18)
	P= .253	P= .117	P= .361	P= .000	P= .	P= .006
TB	-.0509	-.1494	.7538	.6275	.6206	1.0000
	(28)	(28)	(23)	(17)	(18)	(30)
	P= .797	P= .448	P= .000	P= .007	P= .006	P= .

(Coefficient / (Cases) / 2-tailed Sig) " . " is printed if a coefficient cannot be computed

Table APP5-1. continued

Appendix 6 - Analytical and Statistical methods

Analytical methods

- Proximate analyses

Proximate analyses cover the determination of moisture, ash, and volatile matter and the calculation of fixed carbon. These tests were done in the NM Bureau of Mines and Mineral Resources (NMBM&MR) coal lab in accordance with ASTM standard methods for coal analysis (ASTM, 1990). Brief summaries of the methods used are given below.

1 Equilibrium moisture

As there was some time lapse between sampling and analysis, equilibrium moisture was determined as an estimate of the coal bed moisture following STM procedure D-1412 instead of ASTM procedure D-3173 which requires that e analysis be done within a relatively short time after sampling. ASTM ocedure D-1412 covers the determination of equilibrium moisture of coal in an mosphere over a saturated solution of potassium sulfate at 30 °C and relative midity of 96 to 97%. Coal that had been ground to pass a 16 mesh size sieve is used. More finely ground coal may be used, but the procedure will take ich more time (Verploegh, 1990 personal comm.).

Ash

The determination of the inorganic residue as ash in the samples was ie in accordance with ASTM procedure D-3174. Ash was determined by ghing the residue remaining after burning the coal at high temperatures 0°C) a Sybron thermodyne muffle furnace. Samples ground to pass a 60 sh size sieve were used in this test.

1.3 Volatile matter

Volatile matter was determined by establishing the loss in weight resulting from heating a coal sample in a vertical electric furnace which has a temperature maintained at 950 ^{o}C (+/- 20 ^{o}C). This test was done in accordance with ASTM procedure D-3175.

Fixed carbon was calculated as described in ASTM procedure D-3172. The fixed carbon value is the resultant of the summation of percentage moisture, ash, and volatile matter subtracted from 100. Ash, and volatile matter are both on the equilibrium moisture reference base.

2 - Calorific value (BTU)

The determination of the gross calorific value of coal samples was done according to the ASTM procedure D-2015. The calorific value was determined by burning a weighed sample, in oxygen, in a calibrated adiabatic bomb calorimeter. The calorific value of the sample was calculated from temperature observations made before, during and after combustion, making proper allowances for heat contributed by other processes, and for thermometer and thermochemical corrections.

3 - Petrography

Coal briquettes or pellets for petrographic study were prepared in accordance with ASTM procedure D-2797. A representative sample was crushed to pass a 20 mesh (850 mm) size sieve, air dried, mixed with a binder, and pressed in a mold into a briquette. In this study, a mixture of APCO resin 2410A and catalyst 2183B was used as a binder.

Grinding of the pressed pellets (or briquettes) was done on 240, 400, and finally 600 grits. Polishing was then carried out on 5 μm, 1 μm, 0.3 μm, and finally 0.05 μm alpha alumina powder.

Polished petrographic pellets were examined under oil immersion using a Nikon reflected light microscope at varying magnifications. Maceral composition analysis was done by point counting approximately 200 to 250 points on each duplicate sample under a 20X oil immersion objective using 10X oculars. A swift automated point counter was used.

4 - Forms of sulfur

The determination of sulfur forms was done in accordance with ASTM procedures D-2492 and D-3177, with slight modifications in total and sulfate sulfur determinations.

According to ASTM procedure D-2492, sulfate sulfur was extracted from the sample with dilute hydrochloric acid and determined gravimetrically by precipitating it as $BaSO_4$. In this study the extracted sulfate sulfur was determined as sulfate ion with a Dionex series 4000i ion chromatograph fitted with a conductivity detector that uses suppressed conductivity. The amount of soluble sulfate in coal was then reported as percent sulfate sulfur using the following conversion:

$$\frac{(\text{ppm } SO_4^{=})\ (L)\ (0.333)\ 100}{\text{weight}} = \%\ \text{sulfate sulfur}$$

where ppm $SO_4^{=}$ is the sulfate ion concentration from ion chromatograph reading, L is the volume of sulfate solution in liters, weight refers to sample weight in milligrams, and 0.333 is the $S/SO_4^{=}$ gravimetric factor.

Total sulfur was determined using the bomb washing method (ASTM procedure D-3177). A weighed sample of coal was placed in a Parr bomb calorimeter with about 1 mL of 100X $CO_3^{=}$/ HCO_3^{-} eluant in the bottom. Maintaining the pressure in the bomb at approximately 25 atm. of oxygen, the bomb was ignited to burn the coal inside. The assumption behind this method is that all the various forms of reduced sulfur in the coal sample will be transformed into the sulfate form. The total sulfur in the washings was then determined as sulfate ions using the ion chromatograph. The percent total sulfur was computed using the formula applied in the determination of percent sulfate sulfur above.

Total sulfur and sulfate determination using ion chromatograph is currently being developed by the NMBM&MR coal laboratory. The main advantage of using ion chromatography is that it has a lower detection limit than the gravimetric method (Verploegh, 1992 personal comm.).

Pyritic sulfur was determined in accordance with ASTM procedure D-2492. This form of sulfur was calculated as stoichiometric combination with iron. Pyritic iron was determined by a model 857 IL AA/AE spectrophotometer.

Organic sulfur was obtained by subtracting the sum of the percentages of sulfate sulfur and pyritic sulfur from the percentage of total sulfur.

5 - Instrumental neutron activation analysis

5.1 - Experimental procedures

Approximately 60 to 100 mg per sample, quality assurance and calibration standards were weighed to the nearest 0.01 mg, placed in clean ultra-pure silica vials and sealed. The vials were then re-cleaned and re-weighed for identification purposes and placed in aluminum foil, formed into a tube, and placed inside an irradiation cylinder. This method of sample preparation is a modification of that described by Jacobs et al., (1977).

National Institute of Standard and Technology (NIST) standard reference material (SRM) 1633a (coal fly-ash) was used as a calibration standard. NIST SRM 1632B and 1635 were used as quality assurance standards.

Samples were irradiated in the 10 MW research reactor facility at the University of Missouri for 48 hours at a neutron flux of 2.5×10^{13} n cm^{-2} sec^{-2}, with a cadmium ratio of 17. The irradiation cylinder was rotated during irradiation to allow equal exposure to the neutron flux. Irradiation containers were flooded with reactor water to cool the samples and thus prevent combustion.

The counting scheme used here follows the one outlined by Kendrick et al. (1988). After a decay interval of about 3-4 days, the samples were returned to the New Mexico Institute of Mining and Technology neutron activation laboratory for counting. The laboratory is equipped with a Vaxstation (model 3100) linked by ethernet with two high-purity germanium detectors and their associated electronics. Energy resolution on both detectors was about 1.8 KeV (FWHM) at 1332 KeV, and the detector efficiencies were 26% and 18% for detectors 2 and 3 respectively.

Irradiated samples were counted three times: after 5 days decay (early count), 7 days after the irradiation (short count), and 30 days following the irradiation (long count). The samples were counted for 45 minutes during the early count , and for 3 hours each during the short and the third long counts. Calibration standards were counted for six hours during each of the count schedules. Quality assurance samples were treated as unknown samples.

Elemental abundances were calculated using the computer software package TEABAGS (Lindstrom and Korotev, 1982). TEABAGS (Trace Element Analysis By Automated Gamma Ray Spectrometry), is a set of computer programs used for acquisition and reduction of gamma-ray spectral data acquired during instrumental neutron activation analysis of geochemical samples. These

sets of programs are designed to monitor the status of all spectra obtained from samples and comparison standards irradiated together and to do all calculations.

5.2 - Precision and accuracy

The precision of the analytical technique was estimated by running replicate analyses on aliquots of some of the samples. Three analyses each were made on samples S2-21 and S3-6 (both coal samples), and two analysis were run on aliquots of sample S3-18 (a claystone). The coefficient of variation is used as an estimate of the analytical precision. Results of precision analyses are given in Table1 APP6 -1.

As a measure of the relative accuracy of the technique,NIST SRMs1632B and 1635 were analyzed as unknowns together with the other samples. The results are compared with NIST and/or literature recommended (consensus values) and listed in Tables APP6 -2 and APP6 -3.

Table APP4-1 shows that for sample S2-21 the precision is relatively good, with most elements having a coefficient of variation of less than 10%. Cesium, strontium, hafnium, and rubidium have coefficients of variation between 10 and 15%. In S3-6, all elements except barium (coefficient of variation = 12.29%) have coefficients of variation of less than 10%. All elements, except for arsenic (12.97%) and ytterbium (40.29%), have coefficients of variation of less than 10% in sample S3-18.

Table APP6-2 shows that all the analyzed elements show good agreement with NIST and/or consensus values. Sodium, Sc, Fe, Co, As, Sr, Sb, La, Sm, Hf, and Th in the samples have concentrations lower than the literature values. The concentrations of Cr, Zn, Se, Rb, Cs, Ba, Ce, Eu, and U in the samples are higher relative to the consensus values. In general, when the

uncertainity on the NIST values are taken into account, much of the data overlaps with the standards.

For NIST SRM 1635 (Table APP6-3), all the elements show lower concentrations compared to consensus values. Zn, Rb, Ba, and U show the highest variations. The consistently low values may be due to weighing error.

Table APP6-1. Sample replicate analyses summary (all values in ppm unless noted otherwise).

	S2-21 (n=3)			S3-6 (n=3)			S3-18 (n=2)		
Element	mean*	S.D	C.V.%	mean	S.D.	C.V.%	mean	S.D.	C.V.%
Na	283.19	7.52	2.65	349.3	4.53	1.3	266.5	5.4	2.03
Sc	2.262	0.018	0.8	6.12	0.026	0.42	2.13	0.0	0.0
Cr	7.33	0.28	3.82	19.13	0.5	2.61	3.85	0.03	0.78
Fe	2.398%	0.055	2.31	.547%	.0163	3.0	1.67%	.0201	1.21
Co	1.683	0.016	0.95	8.07	0.055	0.68	1.881	0.027	1.43
Zn	12.5	1.22	9.76	82.4	4.47	5.42	11.32	0.318	2.81
As	34.34	0.752	2.19	5.29	0.31	5.86	0.848	0.11	12.97
Se	6.08	0.19	3.12	2.92	0.19	6.51	6.212	0.05	0.8
Rb	2.08	0.32	15.38	19.42	0.058	0.3	8.77	0.035	0.4
Sr	120.69	6.61	5.48	230.5	21.15	9.17	108.7	10.87	10.0
Sb	n.d	n.d	n.d	8.19	0.11	1.34	0.301	0.03	9.97
Cs	0.284	0.029	10.21	2.394	0.07	2.92	1.609	0.038	2.36
Ba	105.83	5.01	4.73	2028.	655	32.29	60.75	1.06	1.75
a	8.75	0.21	2.4	6.09	0.08	1.31	24.61	0.14	0.57
e	17.28	0.37	2.14	11.18	0.27	2.41	45.0	1.48	3.29
m	1.26	0.15	11.9	1.59	0.009	0.57	1.889	0.041	2.32
u	0.253	0.005	1.98	0.411	0.004	0.97	0.363	0.005	1.38
b	0.603	0.037	6.13	1.86	0.017	0.91	0.546	0.22	40.29
I	0.084	0.003	3.57	0.266	0.002	0.75	0.096	0.006	6.25
	2.87	0.43	14.98	1.615	0.01	0.62	8.455	0.7	8.28
t	0.804	0.015	1.86	0.326	0.007	2.15	3.68	0.056	1.52
	0.145	0.001	0.69	0.467	0.008	1.71	0.142	0.004	2.82
	12.56	0.1	0.8	4.417	0.065	1.47	12.26	0.27	2.2
	4.59	0.15	3.27	2.815	0.11	3.91	9.6	0.11	1.14

* = arthimetic mean; C.V% = percent coefficient of variationn.d. = not determined (below threshold value); S.D. = standard deviation

Table APP6-2. Analysis of NIST coal standard SRM 1632B (all values are in ppm unless noted otherwise).

Element	mean* (n = 2)	S.D	NIST**
Na	491.29	0.79	515 (11)***
Sc	1.856	0.013	1.9
Cr	11.07	0.042	11.0
Fe	7306	255.26	7590 (450)
Co	2.11	0.058	2.29 (0.17)
Zn	11.97	0.46	11.89 (0.78)
As	3.54	0.28	3.72 (0.09)
Se	1.37	0.18	1.29 (0.11)
Rb	5.27	0.11	5.05 (0.11)
Sr	97	0.71	102
Sb	0.212	0.003	0.24
Cs	0.458	0.011	0.44
Ba	68	1.18	67.5 (2.1)
La	4.06	0.014	5.1
Ce	9.14	0.071	9.0
Sm	0.797	0.011	0.87
Eu	0.173	0.0007	0.17
Tb	0.106	0.003	n.a
Yb	0.346	0.0007	n.a
Lu	0.0511	0.0001	n.a
Hf	0.423	0.011	0.43
Ta	0.12	0.008	n.a.
Th	1.238	0.023	1.342 (0.036)
U	0.44	0.013	0.436 (0.012)

* = mean element concentration of NIST SRM 1632B this study (based on duplicate analyses); ** = NIST and /or consensus values used as "true values" from Gladney et al., (1982); *** = numbers in parenthesis refer to standrad deviations of NIST values; S.D = Standard deviation between measurements (of NIST SRM 1632B); n = number of samples; n.a. = information not available;

Table APP6-3. Analysis of NIST coal standard SRM 1635 (all values in ppm unless noted otherwise).

Element	mean* (n=2)	S.D	1635 **	NIST***
Na	2031.55	7.87	2420	2400
Sc	0.501	0.002	0.598	0.63
Cr	2.392	0.43	2.47	2.5 (0.3)****
Fe	1907.0	23.33	2230	2390 (50)
Co	0.516	0.009	0.64	0.65
Zn	3.0	0.8	n.a	4.7 (0.5)
As	0.37	0.085	0.44	0.42 (0.15)
Se	0.84	0.003	0.90	0.9 (0.3)
Rb	0.5	0.11	< 1	0.85 (0.1)
Sr	107	0.707	135	121 (19)
Sb	0.103	0.008	0.148	0.14
Cs	0.046	0.004	0.048	0.053 (0.007)
Ba	49.0	0.707	84	73 (5)
La	1.482	0.021	1.81	1.8 (0.3)
Ce	2.807	0.053	3.32	3.6
Sm	0.229	0.005	0.28	0.29 (0.04)
Eu	0.052	0.001	0.059	0.06
Tb	0.039	0.002	0.045	0.042
Yb	0.151	0.006	0.169	0.165 (0.016)
Lu	0.0223	0.001	0.028	0.028 (0.009)
Hf	0.224	0.003	0.28	0.29
Ta	0.04	0.001	0.049	0.0458 (0.002)
Th	0.487	0.003	0.58	0.62 (0.04)
U	0.17	0.025	0.24	0.24 (0.02)

= mean element concentration of NIST SRM 1635 this study (based on duplicate analyses); ** = mean alues of NIST SRM 1635 from Kendrick et al. (1988); 1635= NBS coal standard reference material; *** = IIST and /or consensus values used as "true values" from Gladney et al (1982); **** = numbers in arenthesis refer to standard deviations for NIST values; S.D= standard deviation between measurements of NIST SRM 1635); n = number of samples; n.a. = information not available

6 - Electron microprobe analysis

Electron microprobe analyses were done by Dr. Michael Spilde and carried out on the JEOL 733 Super probe in the Electron Microbeam Facility at the Institute of Meteoritics/Department of Geology, University of New Mexico. The fully automated 733 utilizes 5 wavelength spectrometers and a Tracor Northern TN2000 energy dispersive system, controlled by Sandia TASK 8C software (Chambers and Doyle, 1990). Polished petrographic coal samples containing pyrite and/or carbonate minerals were vacuum dried and carbon coated prior to analysis.

Pyrite analysis. Pyrite was analyzed at 20 kV and 100 nA beam current with a beam diameter of 1-2 μm. Counting times on detectable elements were adjusted according to a graphical counting scheme from Mack and Spielberg (1958) to give approximately 5% error in counting at a desired confidence level of 95%. Actual detection limits were determined and ZAF corrections were calculated on line by Sandia TASK. The detection limits and standards used are listed in Table APP6-4.

The local background in the vicinity of the Pb Mα line slopes upward toward the very strong S Kα peak, and in measuring trace levels of Pb, the background is overwhelmed by the slope of the tail of the S Kα peak. Attempts were made to set backgrounds avoiding this slope but always resulted in an apparent content of around 0.1 wt. % Pb in pyrite standards containing no Pb. Therefore the Pb Lα line was selected for analysis, even though it resulted in higher limits of detection and necessitated longer counting time.

Table APP6- 4. Standards and detection limits used in electron microprobe analyses of iron sulfides.

Element	Standard	Concentration	Counting Time	Detection limit*
S	Nat. Pyrite	53.45 wt.%	20 sec	0.005 wt%
Fe	Nat. Pyrite	46.55	20	0.005
Ni	Ni metal	pure metal	100	0.0025
Cu	Nat. chalcopyrite	34.63	100	0.004
Zn	Nat. sphalerite	67.09	200	0.0035
Mn	Nat. spessartine	40.50	150	0.0025
As	Syn. InAs	39.49	200	0.005
Co	Nat. Karnacite	0.89	200	0.0025
Se	Syn. CdSe	41.26	250	0.005
Sr	Syn. SrF_2	69.75	200	0.02
Cd	Nat. CdSe	58.74	200	0.004
Pb	Nat. galena	86.60	250	0.02

* = at 95% confidence level

Likewise, the local background in the vicinity of the Co Kα is dominated by the Fe Kβ line, producing systematic errors in Co that were 0.04 wt.% too high. To avoid this error, the Co peak and background were measured on a meteoritic Kamacite (Fe-Ni metal) which duplicated the local sloping background present in pyrite at the Co peak position.

Carbonate analysis The carbonates were analyzed at 15 kV and 20 nA, using a 5-10 µm beam to avoid CO_2 volatilization. Corrections were done using the Bence-Albee (1968) procedure, with CO_3 calculated by difference. Natural siderite (USNM R-2460), dolomite (USNM 10057), calcite (USNM 136321) and celestite were used as standards; the use of such standards close to the unknown composition results in very small corrections.

X-ray fluorescence analysis

Major element analysis on coal ash and non-coal samples was done following the Norrish and Hutton (1969) fusion method.

A Rigaku 3064 wavelength dispersive sequential spectrometer was used for major element analysis. X-ray fluorescence analysis was done at the New Mexico Bureau of Mines and Mineral Resources, Socorro, New Mexico.

X-ray diffraction analysis

X-ray diffraction analysis was done at the New Mexico Bureau of Mines and Mineral Resources, Socorro, New Mexico.

Coal and non-coal samples were analyzed using a Rigaku DMAXA diffractometer controlled by a PDP 11/23 computer. Manufacturer's supplied software was used to identify, search, and match peaks. The diffractometer has

a copper, long fine focus tube and graphite monochromator. It uses a scintillation counter for the detector. The following instrumental settings were used:

- 40 kV and 25 mA
- divergent slit = 1^0
- scattered slit = 1^0
- receiving slit = 0.3 mm
- monochromator slit = 0.3 mm

Low -temperature-ashed (LTA) coal samples and very finely ground non-coal samples were packed into well-mounts and scanned from 3 to 75^0 2θ at 2^0 / minute. Before XRD analysis the coal samples were ashed at low temperatures (< 150^0 C) using a LFE Corp. model 504 Electronic Low Temperature Asher. Low temperature ashing was done at the Los Alamos National Laboratory, Los Alamos, New Mexico.

Statistical analyses

1 - Descriptive statistics

A set of statistical analyses were performed on the data to describe and characterize distribution patterns and to illustrate interrelationships and variations between variables.

Descriptive statistics used include the arithmetic mean, geometric mean, minimum and maximum values, standard deviation, and coefficient of variation. The mean is defined as the sum of all observations divided by the number of observations. The geometric mean is the Nth root of the products of N observations or equivalently, the arithmetic mean of the logarithms of the observations. Geometric means are preferred to arithmetic means when comparing samples because extremely high values, often the result of epigenetic mineralization within the coal, influence the geometric mean less than the

arithmetic mean (Gluskoter et al., 1977; Davis, 1986). The standard deviation is a measure of dispersion or spread of data around the mean. The coefficient of variation, which is the standard deviation divided by the mean, is a more useful quantity than the standard deviation or variance (the square of the standard deviation) in describing the relative variability of dissimilar things or different populations (Renton and Hidalgo, 1975).

As the reliability of many statistical procedures is dependent on the nature of the distribution of the population, element data were plotted as histograms with linear coordinates to decide whether the distributions are normal or log-normal. In normal distributions the histogram is symmetrical, and the median, arithmetic mean, and mode of the data coincide. If the histogram is asymmetric with a pronounced skew, it is possible that a normal distribution will be obtained if the logarithms of the elemental concentrations are used. In such circumstances, the original distribution is termed log-normal. In log-normal distributions, the median of the data corresponds to the geometric mean. The most important reason for deciding whether data are normally or log-normally distributed is that the most sensitive statistical procedures assume that the data are normally distributed. If the data are log-normally distributed, the statistical procedures should be applied to the logarithms of the elemental concentrations (Reeves and Brooks, 1978; Davis, 1986).

2 - Comparative statistics

Parametric and nonparametric statistical methods were used to treat the data in this study. Parametric methods of statistical analysis are often only valid if the data are normally distributed , whereas nonparametric methods do not depend on the data being normally distributed. The following statistical methods

were used in this study: (1) Correlation analysis, (2) Mann-Whitney U Test, (3) Analysis of Variance (ANOVA), (4) Cluster analysis, and (5) Factor analysis.

When comparing sample parameters between bright and dull coals, and between drill holes, for example, the null hypothesis used is that, $H_0 : m_1 = m_2$, the mean of the population from which the samples in one group was drawn is the same as the mean of the parent population of the second group, or simply there is no significant difference between the two means and that both groups are derived from the same population. The probability that this hypothesis is true is then determined (Reeves and Brooks, 1978; Davis, 1986). Geologists and geochemists deal with circumstances of great uncertainties and thus as a general rule, the null hypothesis is rejected only if there is less than a 10% probability ($P <$ or equal to 0.1) of its being true (Reeves and Brooks, 1978; Davis, 1986). The evel of significance is a matter of decision by the researcher and could be set at any level, however, more stringent levels of significance could lead to accepting he null hypothesis almost all the time and may require greater amounts of data o reject it. A list of generally accepted levels and divisions for tests of ignificance has been outlined by Brookes et al (1966) and is given in Table PP6-5 .

The following summary of the various parametric and nonparametric tatistical procedures used in this study and listed above is compiled from Siegel 956), Brooks et al (1966), Duran and Odell (1974), Green (1978), Kim and lueller (1978a, 1978b), Reeves and Brooks (1978), Augustithis (1983), Davis 986), and Elifson et al (1990). The reader is referred to these publications for ore detailed description of the statistical methods.

Table APP6-5. List of levels and divisions for tests of significance (after Brookes et al., 1966).

Probability (P)	Conclusion
> 0.1	not significant
0.1 - 0.05	Possibly significant, some doubt cast on H_0
0.05 - 0.01	Significant, H_0 is rejected though with reservations
0.01 - 0.001	Highly significant, H_0 confidently rejected
< 0.001	Very highly significant, H_0 very confidently rejected

2.1 - Correlation analysis

Correlation analysis tests the strength of the association between random variables. It measures the linear relationship between two variables and helps to show how the variation in one is linked to the variation in the other. The most common approach to estimating the degree of association is through the calculation of the Pearson product moment correlation coefficient r.

The correlation coefficient , r, can vary between +1 and -1, positive values indicating a direct relationship and negative values implying an inverse relationship between the variables. The closer the value of r is to +1 or -1, the closer the linear relationship.

In this study some elements show log-normal distributions. As the Pearson correlation coefficient provides an estimate of the association between two variables only if the data are approximately normally distributed, r values were calculated using log-transformed data. Pearson correlation coefficients were calculated using the SPSS and StatView SE+ Graphics computer software packages (Feldman et al., 1988).

2.2 - Mann-Whitney U Test

The Mann-Whitney U Test was used as a nonparametric substitute for the t-Test as a test of the equality of the means of two samples. This test does not depend on the distribution of the data and helps the researcher avoid the assumptions of the parametric t-Test. The Mann-Whitney U Test was done using the StatView SE + Graphics software package.

2.3 - Analysis of Variance (ANOVA)

Sample values in general differ somewhat. One problem is to determine whether the observed sample differences signify differences among populations

or whether they are merely the chance variations that are to be expected among random samples from the same population.

Analysis of variance was used to compare variations in sample characteristics from the three drill holes between samples grouped into different categories (for example bright versus dull coals). This test was also used in an attempt to compositionally differentiate various morphologically different pyrite grains.

ANOVA was performed on log-transformed data. The null hypothesis that we wish to test is that all the populations from which the samples are taken have identical distributions. The alternative hypothesis is that at least one of the populations has a different central value. ANOVA tests were performed using the StatView SE + Graphics computer software package.

2.4 - Cluster analysis

Cluster analysis is a technique used for classifying objects into related groups or sub groups. The simplest way of correlating multi-element data is to generate a matrix that contains the correlations between all possible pairs of elements considered. Such a matrix may, however, be difficult to interpret and impossible to plot meaningfully upon a map. With the use of cluster analysis, however, it is possible to group variables according to their mutual correlations, taking into account all possible combinations of the given elements.

Most clustering methods may be grouped into four general types: (1) partitioning methods, (2) arbitrary origin methods, (3) mutual similarity procedures, and (4) hierarchical clustering. The last clustering method is widely applied in the earth sciences. Hierarchical clustering techniques join the most similar observations, then successively connect the next most similar observation to these. The process is iterated until the similarity matrix is reduced to 2X2. A

dendrogram (or a tree-like diagram) is then constructed from the levels of similarity at which observations are merged.

Clustering procedures commonly involve the following steps:

1) raw data matrix of the type nXm (n objects or samples and m characteristics such as element concentrations),

2) standardization of the raw data matrix,

3) computation of resemblance or similarity measures, and

4) clustering and construction of a dendrogram.

Hierarchical clustering was used in this study. This procedure was done using the computer software package SYSTAT (Wilkinson, 1989) using log-transformed and standardized data. The clustering options used were the average linkage method and the (squared) Euclidean distance measurement.

Prior to computing distance measurements, the data matrix is commonly standardized to mean zero and unit standard deviation. Standardization ensures that each variable is weighted equally. Otherwise, the distance will be influenced most strongly by the variable which has the greatest magnitude.

The Euclidean distance is a distance-type measure of resemblance or similarity between a pair of objects. A low distance indicates that two objects are similar or "close together," whereas a large distance indicates dissimilarity.

The average linkage option of clustering starts out by finding the two points with the shortest distance. These are placed in the first cluster. At the next stage a third point joins the already-formed cluster of two if its shortest distance to the members of the cluster is smaller than the two closest unclustered points. Otherwise, the two closest unclustered points are placed in a cluster. This process is repeated until all points end up in one cluster. The distance

between two clusters is the average distance from points in the first cluster to points in the second cluster.

2.5 - Factor analysis

Factor analysis refers to a variety of statistical techniques used in the interpretation of relationships between variables in a multivariate collection of data. The common objective of these techniques is to represent a set of variables in terms of a small number of hypothetical variables. Kim and Mueller (1978a, 1978b) give a relatively simplified introduction to factor analysis and examples of applications. The reader is referred to these publications for additional information on factor analysis.

The fundamental assumption in factor analysis is that some underlying factors, which are smaller in number than the number of observed variables, are responsible for the covariation among the observed variables.

Four basic steps are involved in applying factor analysis to raw data: (1) preparation of relevant covariance or correlation matrix, (2) the extraction of initial factors, (3) rotation to a terminal solution and interpretation, and (4) construction of scales and their use in further analysis. Factor methods can be divided into two broad classes, R-mode and Q-mode techniques. The first is concerned with interrelations between variables, and operates by extracting eigenvalues and eigenvectors from a covariance or correlation matrix. Q-mode techniques are concerned with the relationship between objects.

Factor analysis has become a generic term that includes a wide variety of separate procedures for effecting the desired dimensional reduction. One of the most popular approaches to factor analysis is Principal Component Analysis (PCA). In this study, the PCA factor procedure was used and computation of factors was done using the computer software package StatView SE + Graphics.

Log-transformed data of element concentrations was input into the factor analysis program and the PCA method of obtaining the initial solution employed. The eigenvalue criterion was used to determine the number of initial factors. This method considers only those eigenvalues greater than or equal to 1. Using the default option available in the StatView SE + Graphics program gives essentially the same results as the eigenvalue criterion.

In obtaining an initial solution the following restrictions are imposed: (1) there are a certain number of common factors that account for the covariation among a large number of variables, (2) underlying factors are orthogonal to each other, and (3) the first factor accounts for as much variance as possible, the second factor accounts for as much of the residual variance left unexplained by the first factor, and so on, with the last factor explaining the residual variance left unexplained by all the other factors. The first restriction, although its adequacy can be partially tested in certain methods of initial factoring and can be modified in subsequent factor analysis, remains in effect throughout a given factor analysis. The last two restrictions are considered arbitrary and one or both are removed in the rotation stage in order to obtain simpler and more readily interpretable results.

The orthotran/varimax transformation method was used to simplify initial solutions. This method is an operation through which a simple structure is sought under the restriction that factors be orthogonal (or uncorrelated) and by maximizing the variance of a column of the pattern matrix.

a copper, long fine focus tube and graphite monochromator. It uses a scintillation counter for the detector. The following instrumental settings were used:

- 40 kV and 25 mA
- divergent slit = 1^0
- scattered slit = 1^0
- receiving slit = 0.3 mm
- monochromator slit = 0.3 mm

Low -temperature-ashed (LTA) coal samples and very finely ground non-coal samples were packed into well-mounts and scanned from 3 to 75^0 2θ at 2^0 / minute. Before XRD analysis the coal samples were ashed at low temperatures (< 150^0 C) using a LFE Corp. model 504 Electronic Low Temperature Asher. Low temperature ashing was done at the Los Alamos National Laboratory, Los Alamos, New Mexico.

Statistical analyses

1 - Descriptive statistics

A set of statistical analyses were performed on the data to describe and characterize distribution patterns and to illustrate interrelationships and variations between variables.

Descriptive statistics used include the arithmetic mean, geometric mean, minimum and maximum values, standard deviation, and coefficient of variation. The mean is defined as the sum of all observations divided by the number of observations. The geometric mean is the Nth root of the products of N observations or equivalently, the arithmetic mean of the logarithms of the observations. Geometric means are preferred to arithmetic means when comparing samples because extremely high values, often the result of epigenetic mineralization within the coal, influence the geometric mean less than the